



Journal of Applicable Chemistry

2015, 4(3): 637-800

(International Peer Reviewed Journal)



Perspective Review

Computational Quantum Chemistry (CQC)

Part 1: Evolution of a computational tool into an instrumental probe

K RamaKrishna¹, Ch. V. Kameswara Rao² and R. Sambasiva Rao^{3*}

1. Department of Chemistry, Gitam Institute of Science, Gitam University, Visakhapatnam, 530 017

2. Department of Chemistry, Basic sciences and Humanities, GMRIT, Rajam 532 127, AP

3. School of Chemistry, Andhra University, Visakhapatnam 530 003, **INDIA**

Email: karipeddirk@gmail.com, kamesh.chembolu@gmail.com, rsr.chem@gmail.com

Accepted on 13th May 2015

(Dedicated to Smt. R. Adi lakshmi, mother of RSR, on her ninetieth birth anniversary)

CONSPECTUS

Background: In conventional experimental science, human senses and/or instrumental probes observe/make direct or indirect measurements on an existential object or its response under perturbed environment. This is to grasp scientific force driving it as well as manifested characteristics. In simulation, a mathematical/statistical model generates data about a process, object with the same goals of experiments. Animation, emulation etc. are add-ons to get a real feel of the realistic scenario through the model. Theoretical models are arrived for a real life task based on fundamental principles of a disciplines and mathematical frame is deemed to reproduce the behavior of system in real time. Computational science brings forth the numerical solution of mathematical equations and software/hardware are only high performance supportive tools pushing away the drudgery of number crunching and ensuring reproducibility of even thousands of man-hours of time in a fraction of second. The quantum mechanics, the core of quantum chemistry now spread its wings in functional form to make a mark itself as probe alike hyphenated instruments.

In basic quantum mechanics, the system considered consists of electrons revolving around nucleus and the physical model relates the energy of the system with a function of electron density in the Eigen frame. Schrodinger wave equation (SWE) is a second order partial differential equation in XYZ co-ordinates connecting energy with ψ . The mathematical solution is exact for hydrogen atom in ground state, the primary output being a tensor of second order (matrix) of orbitals and corresponding electronic energies with dimensions of $2 \times \text{number_of_orbitals}$.

Computational methods: For multi-electron atoms or molecules even in gas phase and in absence of environment, the exchange/correlation phenomenon renders the solution of SWE impracticable. This led to approximation of exact equations starting with complete neglect of differential overlap (CNDO), the pioneering contribution of Pople. The battery of SEMO methods from this school and Dewar is a novel admixture of employing already available experimental data for chemical species to develop parametric methods in QC. The description of electron density profile is through STO, GTO and plane waves etc. The basis sets simplifying the picture of discriminating valence and core electrons, diffusion and polarization contributions improve accuracy of computational quantum chemistry (CQC). For metal ions, special basis sets are developed. DFT with functionals is an alternate paradigm for the same applications but consuming comparatively lesser CPU time. The interest in first stage to explain electronic spectra, NMR, ESR, photochemistry resulted in considering the effects in Hamiltonian operator. Now, the field is at a mature level and transformed CQC into experimental probe without employing half century aged

electronic instruments. The next venture in QC was extending the applications to solutes in solvent, solvent mixtures, solid surfaces, interfaces and inside macro-molecules/ nano-structures. The hybrid paradigms with MM, QC, and

DFT paved way for viable investigation of large systems at different levels of theory based on reactive site/ reaction center and remaining bulk moiety. Thus, wave function is fundamental quantity relating the energy of multi-electron atomic/ molecular system. Statistical experimental design in choosing functionals/basis sets and neural networks for interpolating electron density are new directions in quantum chemistry computations. The derived parameters from primary output of CQC with varying factors output many chemically significant descriptors.

Software: The research in CQC is with a wide variety of packages and wide used ones are Gaussian 09, GAMESS, SCHRODINGER, Hyperchem, ADF etc. The range of hardware is QUAD core laptops, blade architectures to super computers and the sizes of molecule are 20 to thousands of atoms through hundreds.

Applications: The typical tasks in CQC are optimization of geometry, frequency analysis for stable chemical structure/TS/higher order saddle points, IRC, DRC, spectra, characteristic properties, thermodynamic quantities, solute-solvent optimized geometric structures. The significant characteristics derived from energy, its first and second derivatives are IP, charges, multi-pole moments, polarizabilities, microwave constants and Fukui/ softness/ hardness parameters. The systems studied pervade almost all disciplines of science and engineering. The select chemical systems reviewed here include molecules in aqueous solution/organic solvent/mixture of aquo-organic mixtures, pKas, transition state (TSs) in chemical kinetics, bio-molecules, nano-structures, drugs, reactions including hydrogen atom, hydride transfer and NLO materials. The advanced applications of CQC are using peta scale hardware for proteins, enzymes and reactions at interfaces. Another phase in CQC is in ab initio DFT modeling of plasmas, superconductivity, mixtures of fermions and bosons.

Keywords: Ab initio, DFT, Semi-empirical, Hybrid, Conceptual-QC, Software, Thermodynamics, Solvents, Electron density, ESP, Excited states, Exotic molecules, Descriptors, Optimized geometry, Experimental concurrence.

Contents of Comput. Quant. Chem. (CQC)	
1.	Introduction
1.1	Chemistry and physics of atoms
1.2	Mathematical Chemistry
1.3	Chemoinformatics
1.4	Chemometrics
1.5	Computational quantum chemistry
2.	MethodBase_CQC (MB.CQC)
2.1	☞ Semi Empirical Molecular Orbital (SEMO)
2.2	Ab initio approach
	☞ HF approximation
	☞ TimeDependent_HF
	☞ Post-HF methods
	☞ DFT
2.3	Molecular mechanics

2.4 ONIOM(QM:MM)

2.5 Hybrid methods

2.6 Gn models

2.7 Solvent models

3. Tasks in CQC

- ☞ Geometry optimization
- ☞ Vibrational frequency analysis
- ☞ Transition state

4. CQC in action

- ☞ Species in a solvent and mixture of solvents
- ☞ Interfaces
- ☞ Biomolecules
- ☞ pKa of ligands
- ☞ Acid ionization
- ☞ Hydrogen bonds
- ☞ Stacking interactions

- ☞ Chemical reactions
- ☞ Ion-electron interaction
- ☞ Chemical kinetics
- ☞ NLO materials

4.2 Comparison of CQC output with experimental results

4.3 Molecular Dynamics

4.4 QM-MM applications

4.5 NLO materials

5. Characteristic Properties

- ▶ Ionization potential (IP)
- ▶ Electron affinity (EA) and Electrophilicity

- ▶ Charges on atoms of the molecule
 - 🔔 Mullikan_charge
 - 🔔 CHelpG charge
 - 🔔 Atomic charges
 - 🔔 QC_descriptor charges

<ul style="list-style-type: none"> ▶ Multi-pole moments <ul style="list-style-type: none"> 🔔 Dipole moment 🔔 Quadrupole moment 🔔 Octupole moment ▶ Polarisabilities <ul style="list-style-type: none"> → Linear (First order) polarisability ⚡ Non-linear <ul style="list-style-type: none"> ↕ Second order hyperpolarisability ↕ Third order hyperpolarisability ▶ Derived NLO characteristics ○ Chemically significant descriptors derived from CQC <ul style="list-style-type: none"> 🔔 Fuki Descriptors 🔔 Softness and hardness
<ul style="list-style-type: none"> 6. I/O of CQC (ICO) <ul style="list-style-type: none"> 6.1 Input 6.2 output
<ul style="list-style-type: none"> 7. Software and Hardware 8. State-of-knowledge-of-CQC 9. Future outlook of CQC
<p style="text-align: center; color: #800000; margin: 0;">Appendices</p> <ul style="list-style-type: none"> 01 QM evolving into an instrumental probe through CQC 02 SEMO-methods 03 Post-HF methods 04 DFT 05 Basis functions 06 Gn models 07 IO files 08 Exchange correlation

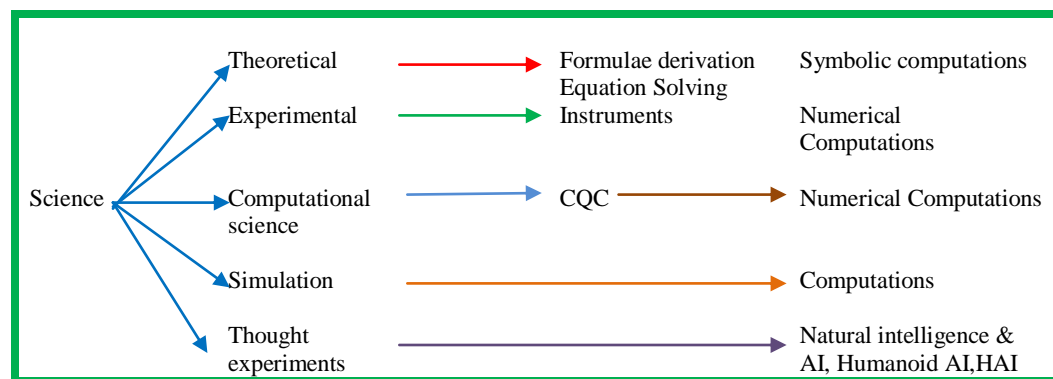
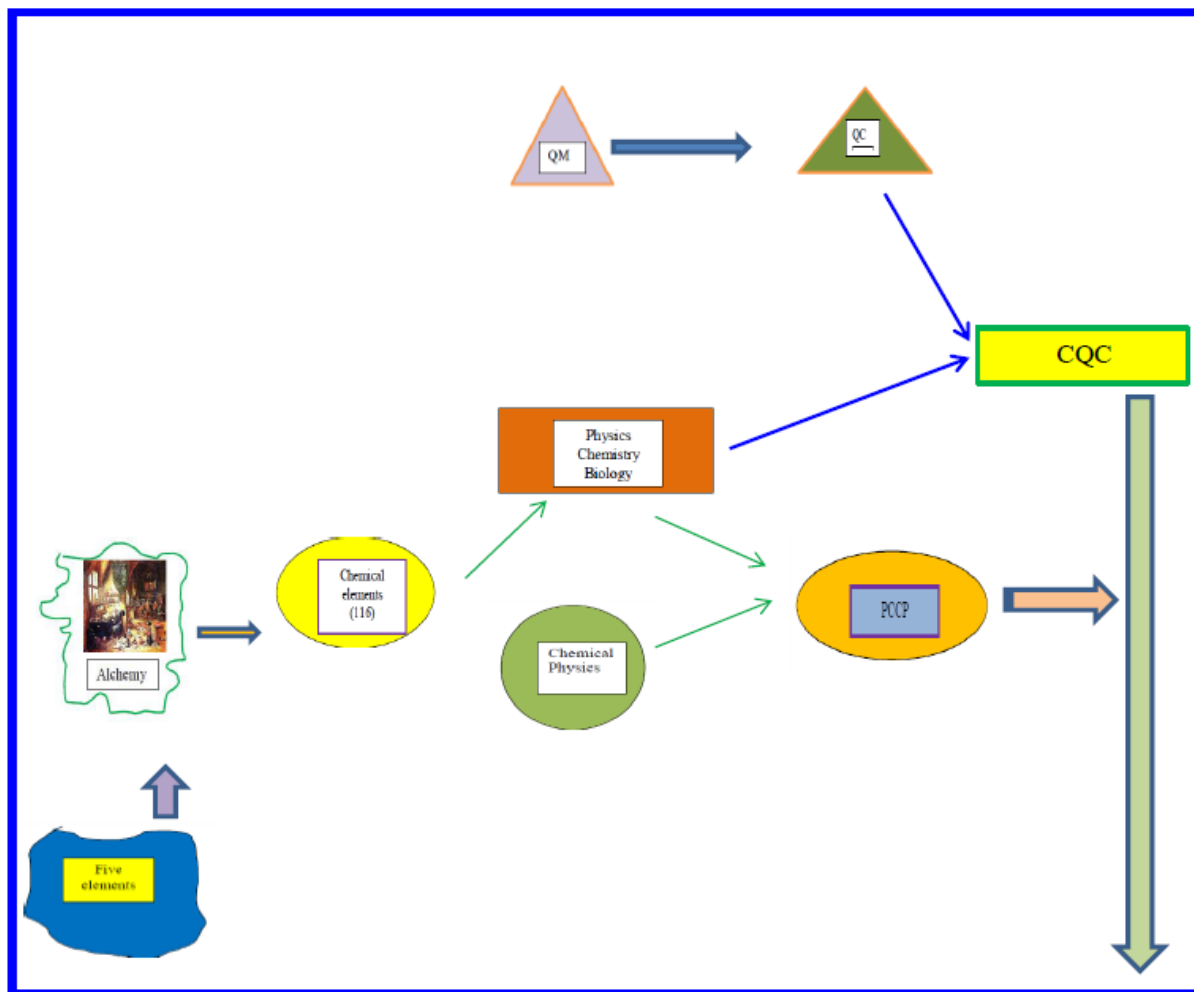
INTRODUCTION

The earth from mantle to surface with engulfing environment is a nature's chemical factory. It is much bigger than ever man made one in the world functioning also under extreme temperatures and pressures. The evolutionary outcome of life from flatworms to human beings is a biochemical industry producing, consuming and destroying exponential number of chemical species from diatomic to macro-molecules in an energy efficient manner over wide time scales (pico- to minutes) on need basis. Their roles include fighting against invaders viz. bacteria, viruses and undesired products of normal/wayward bio-processes/extraneous sources/ consequences of accidents. The multitude of complicated network of just twisting of poly atomic molecules to multi-step biosynthesis without the concern of the species is to

sustain life, pass on the legacy to progeny with a scope of retaining essential characteristics and at the same time adapting to the changing environment and furthering capabilities over a longer period of time/larger number of generations.

The universe started as dense packed energy (radiation) exploding into larger and larger volumes generating protons, neutrons, atoms, molecules, galaxies, stars, solar system, earth, moons, water, air, soil, micro-life, phytoplankton, marine-species, animals, birds, homosapeons and humans of present era. In this long history of nearly 13.7 billion years, evolution has witnessed the dinosaurs, viruses and newer emanations. The ants have been continuing since **mid-Cretaceous period** i.e. 110-130 million years. The science based on human intellect/ observation is a tiny hole compared to the size and complexity of universe in four dimensions. Yet, the science of Science is a promotor of better living of future generations too ([chart 1](#)). Quantum mechanics in general, quantum chemistry in particular is a complimentary tool to experimental domain/theoretical science/ simulations on one hand probing into many of these subsystems of systems (vide supra) to a worth noting stage. Computational quantum chemistry (CQC) is black box for application oriented starters and is a white-box-see-through-device (like Barreleye, a fish with transparent cranium) for an expert.

Chart 1: Sub-disciplines of science (SDS)



<table border="1"> <tr><td colspan="2">Computational Quantum Science</td></tr> <tr><td> </td><td> </td></tr> <tr><td colspan="2">Computational Quantum \$\$\$</td></tr> <tr><td>Organic</td><td rowspan="4">chemistry</td></tr> <tr><td>Physical</td></tr> <tr><td>Inorganic</td></tr> <tr><td>Nanomaterials</td></tr> <tr><td> </td><td> </td></tr> </table>	Computational Quantum Science				Computational Quantum \$\$\$		Organic	chemistry	Physical	Inorganic	Nanomaterials			<table border="1"> <tr><td colspan="2">ComputationalQuantum \$\$\$ Physics</td></tr> <tr><td>Chemical</td></tr> <tr><td>Liquid state</td></tr> <tr><td>Solid state</td></tr> <tr><td>Nuclear</td></tr> <tr><td>Subatomic particle</td></tr> <tr><td colspan="2">ComputationalQuantum \$\$\$</td></tr> <tr><td> </td><td>Biology</td></tr> <tr><td> </td><td>Proteomics</td></tr> <tr><td> </td><td>Genetics</td></tr> <tr><td> </td><td>Geology</td></tr> </table>	ComputationalQuantum \$\$\$ Physics		Chemical	Liquid state	Solid state	Nuclear	Subatomic particle	ComputationalQuantum \$\$\$			Biology		Proteomics		Genetics		Geology	<table border="1"> <tr><td colspan="2">Hybrid paradigms</td></tr> <tr><td> </td><td> </td></tr> <tr><td>CQC + NN</td></tr> <tr><td>CQC + ED</td></tr> <tr><td>MM + CQC</td></tr> <tr><td>Empirical + CQC</td></tr> <tr><td>Conceptual + CQC</td></tr> </table>	Hybrid paradigms				CQC + NN	CQC + ED	MM + CQC	Empirical + CQC	Conceptual + CQC
Computational Quantum Science																																									
Computational Quantum \$\$\$																																									
Organic	chemistry																																								
Physical																																									
Inorganic																																									
Nanomaterials																																									
ComputationalQuantum \$\$\$ Physics																																									
Chemical																																									
Liquid state																																									
Solid state																																									
Nuclear																																									
Subatomic particle																																									
ComputationalQuantum \$\$\$																																									
	Biology																																								
	Proteomics																																								
	Genetics																																								
	Geology																																								
Hybrid paradigms																																									
CQC + NN																																									
CQC + ED																																									
MM + CQC																																									
Empirical + CQC																																									
Conceptual + CQC																																									
<table border="1"> <tr><td colspan="2">EscQC</td></tr> <tr><td> </td><td> </td></tr> <tr><td>ESCQC</td><td>Evolving science of computational quantum chemistry</td></tr> <tr><td>ES CQC</td><td>Expert system computational chemistry</td></tr> <tr><td>Esc QC</td><td>Escape Quantum chemistry</td></tr> <tr><td> </td><td>Pronounced as (Esq C) esquire chemistry</td></tr> <tr><td>NN</td><td>Neural networks</td></tr> <tr><td>ED</td><td>Statistical experimental design</td></tr> </table>			EscQC				ESCQC	Evolving science of computational quantum chemistry	ES CQC	Expert system computational chemistry	Esc QC	Escape Quantum chemistry		Pronounced as (Esq C) esquire chemistry	NN	Neural networks	ED	Statistical experimental design																							
EscQC																																									
ESCQC	Evolving science of computational quantum chemistry																																								
ES CQC	Expert system computational chemistry																																								
Esc QC	Escape Quantum chemistry																																								
	Pronounced as (Esq C) esquire chemistry																																								
NN	Neural networks																																								
ED	Statistical experimental design																																								

The recent sparkles in quantum chemical methodology and applications in chemical sciences are reviewed [1-225] here, in continuation of our studies in speciation, kinetometrics, quantitation employing Chemometrics, neural networks, nature inspired optimization algorithms and CQC probes[217-225].

Nature-Science-Technology Laboratory (NSTL)

The findings are scientific if they have observable consequences with rational evidence supporting them, although, imaginable or foreseeable applications are not in vision even by far off future. The technology and applications of science are completely different entities than science itself. Over selling as well as underselling of scientific bits are malicious and pernicious. The true science perceiver is unbiased and affirms only when a proof to accept or reject the proposition becomes available.

1.1 Chemistry and physics of atoms

An atom consists of a nucleus and one (for hydrogen) and many electrons for all other chemical elements. The nucleus has (unit positive charged) protons equal to atomic number and neutral neutrons corresponding to the difference between mass number and atomic number. A molecule is formed from two to large number of atoms (hydrogen, HCl, H₂O, CH₄) and thus number of electrons going to hundreds to thousands. This frame leaves aside the particle physics, fundamental forces, dark matter and dark energy.

Theoretical Science

1.2 Mathematical Chemistry: It models the structure of the compounds from non-quantum chemical framework viz. connectivity, geometric and electrostatic properties. The molecular descriptors like molecular weight, Kier shape index, number of H-bond donors/acceptors/aromatic rings/rotatable bonds are used in the analysis of the databases with 15,000 drugs and 15,00,000 of presumed non drugs. Even one descriptor results in predictive capability and increase in number of descriptors may not result in improvement in predictability. For instance Wiener index which encodes information about Vander Waal's interaction between two parts of the molecule and mean external contact area, still finds use to sort out similar structure from a large pool of (virtual combinational) library.

1.3 Chemoinformatics: It started with management of bibliographic (chemical Abstracts) information, now encompasses 2D and 3D structure of fragments, theoretically computed electron density, ESP maps and chemical knowledge. Recently bibliometrics with state-of-art-search techniques grew and available for research and pedagogic purposes from science journal publishers (Elsevier, ACS, Royal society etc.) and commercial as well as non-profit making organizations/search engines (Google, Scholarpedia, EPA etc.).

1.4 Chemometrics: The prospective aim was to obtain maximum information from a limited number of statistically designed experiments. The impact of advanced chemometric tools in computational chemistry has very recently been endorsed as a necessity, but not an add-on-flavor. Many other –metrics and –mics are cited earlier [217-224] while discussing the evolution of omnimetrics and their impact on science and technology of inter disciplinary research and training.

1.5 Computational quantum chemistry: The life force of ‘Quantum chemistry’ is Schrodinger wave equation. The evolved DNA_quantum chemistry over last ninety years with many noble prize awarded core sparkling contributions won laurels in almost all scientific materialistic world from hydrogen atom/proton to life/life-sustaining/life-saving/ life-threatening as well as inanimate realm with buzz words ‘ab initio, semi-empirical, density function and instrumental probe’.

Quantum chemistry (QC) goes around the motion of electrons under the influence of electromagnetic forces of nuclear (protons) charges. The energetics of electrons in molecules is quantified based on QM principles. It is the heart of geometric structures of conformers, isomerization process, chemical reactions in all the phases and organic photo-/electro-/radiation- chemistries. It also explains spectroscopy and physico-chemical properties. Classical quantum chemistry could not even deal with hetero atoms and metal ions' electronic spectra. The efforts during the last three decades render QC into a powerful paradigm. Yet, the limitation is in dealing with stacking interactions, Van der waal forces, low energy H-bonding and low-energy solvent-solvent interactions. The historical progress of this coveted discipline is briefed in [appendix-1](#).

2. MethodBase_CQC (MB.CQC)

The category of data bases brings to the memory of even a common man the trivial dynamic sources of personal characteristics, telephone numbers, business details, inventory etc. with a short active shelf life. In core scientific disciplines, databases and knowledge_bases entered later and are now value added ones in research/teaching. We introduced method_bases in chemical sciences in nineteen nineties in a series of publications emphasizing the object oriented capsules of algorithms, necessary condition, failure situations and partial remedial measures, of course not with software engineering details. The number of procedures in CQC increased over time and a highlight of some of typical ones follow.

☺ Semi Empirical Molecular Orbital (SEMO)

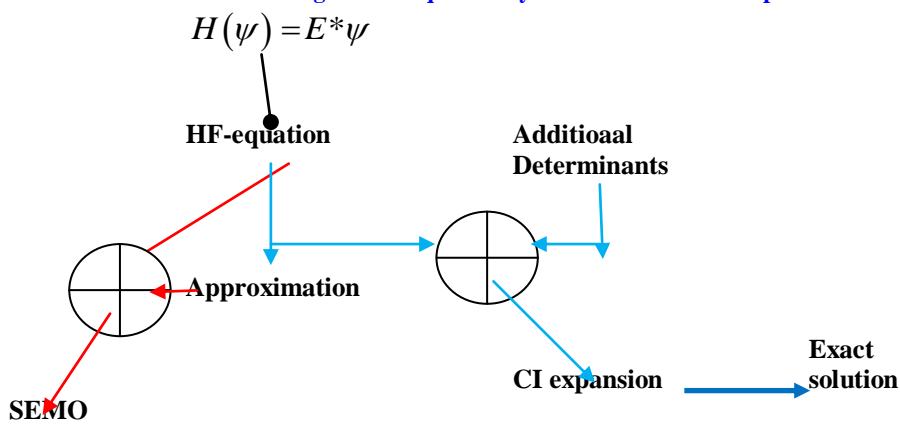
Seminal contributions of Pople and Dewar resulted in a battery of semi empirical procedures. CNDO available in G03 is the first member of the series. SEMO methods are categorized broadly as MNDO series, AM1 /PM3/PM6 and SAM1. The state of art of these procedures along with the quality of the properties derived from QC output is instrumental in interpretation. SEMO methods, although are not rigorous, are the first indispensable tool in optimization of the geometry of a conformer.

The core of SEMO calculations uses experimental data base of enthalpies, dipole moments, heats of formation etc. of chemical compounds. They are fitted in multi parametric equation and the success is astounding for some similar compounds, but fails for compounds with dissimilar characteristics compared to those present in the database. The experience of a large number of users of SEMO-CQC packages and perseverance of experts resulted in SAM1 and PM6 models with functionality comparable with ab initio methods, no doubt in a limited sense.

Solution of electronic Schrödinger wave equation of even small molecules (multi-electron systems) is not pragmatic (chart 2). This led to different approaches viz. exact solution of an approximate equation or approximate solution of an exact equation. SEMO methods are grouped into three broad categories, namely MNDO series, AM1, PM3 and SAM1 (appendix -02).

The interaction of electrons by virtue of their charge, distance between them, motion, isolation of a group even in absence of external field is complicated for multi-electron systems and quantum chemists imbibed most of it in most of current models over half a century. Still it is not whole but a dense mesh with many holes, patches, loose filling and momentary contentment.

Chart 2: Solution of Schrodinger wave equation by different levels of computation



Ab initio Approach

The ab initio (HF to post HF), DFT, TD-DFT and prefixed set of encapsulated (Gn: G3, G3B3, G4 etc.) procedures rendered the dream of last century quantum chemists in solving Schrödinger wave equation for chemical moieties into a reality. Kohn and Sham brought out DFT as an alternate tool to ab initio methods as a fast (CPU) solution finder without loss of accuracy (appendices 03-09). The basis of the two methods is mathematically significant ψ (in ab initio) and physics-originated ψ^2 (in DFT). The solution of Schrodinger wave equation is obtained by several procedures like employing approximate methods for exact form or exact solution for approximate equation. Hartree Fock self consistent field (HF-SCF) model involves iterative refinement of initial guess of ψ of the $H(\psi) = E * \psi$. To overcome the limitations of HF method, post-Hartree Fock procedures viz. configuration interaction (CI), Moller Plesset (MPn) and multi configuration SCF (MCSCF), complete active space SCF (CAS-SCF) have been in use. They account for correlation energy between electrons, which is important for chemical interactions in spite of its small magnitude. These correlation corrected solution methods are implemented in HYPERCHEM, GUASSIAN 03/09 and ADF.

Now, theoretical computation of electronic/thermal energies, physico-chemical properties and spectra up to 100 atoms for almost all elements in the periodic table is feasible. The improvements in modeling electron density in the molecule through Slater and Gaussian functions to represent molecular orbitals, exchange/correlation contributions to energy and diffuse/ polarization functions resulted in reliable optimized geometries, quantum chemical derived physico-chemical quantities agreeing with (accurate) experimental values, chemical/quadrupole shifts of H-NMR and oscillator strengths of electronic spectra. Accurate energies indispensable for rotamers are now a reality with CBS and GX (G1, G2, G3, G3B3, G3MP2, G4, G4MP2, G4MP3).

HF approximation

It is the oldest and simplest approximation (KB-1).

Electrons are identical and molecular orbital describes an electron such that $\psi_i^2(r) dr$ at a point r describes the probability of electron being in a small volume around that point. The total probability of

finding the electrons is $\int \psi_i^2(r) dr = 1$. The interaction between electrons is considered as an average

effect rather than as an individual contribution. The assumption that each electron sees all others as an average field or metaphorically, every electron experiences a 'sea' of all other electrons is a great boon for wide spread application of HF approach.

The wave function for a multi-electron system is developed by occupation of lowest possible energy orbitals. Lowest energy eigenvalue is lower than E_{HF} . Here, the ground state $\psi^{electron}$ is the determinant of single particle states i.e. Slater determinant

$$\Psi_0^e(\mathbf{r}_1\sigma_1, \dots, \mathbf{r}_N\sigma_N) \approx \Phi_{1\dots N}(\mathbf{r}_1\sigma_1, \dots, \mathbf{r}_N\sigma_N)$$

$$\Phi_{i_1\dots i_N}(\mathbf{r}_1\sigma_1, \dots, \mathbf{r}_N\sigma_N) = \frac{1}{\sqrt{N!}} \det \begin{pmatrix} \phi_{i_1}(\mathbf{r}_1\sigma_1) & \dots & \phi_{i_N}(\mathbf{r}_1\sigma_1) \\ \vdots & & \vdots \\ \phi_{i_1}(\mathbf{r}_N\sigma_N) & \dots & \phi_{i_N}(\mathbf{r}_N\sigma_N) \end{pmatrix}$$

KB-1: Heuristics, pros and cons of Hartree-Fock energy

If Ground state of stable organic molecule is singlet electronic state

Then Use restricted HF (RHF)

If Multiplicity > singlet

Then Use unrestricted HF (UHF)

DO's UHF can be used even if, multiplicity = 1 (singlet)
Consequence → Results of UHF and RHF are same

If At. No. > 1

Then Relative PE between electrons is intractable!! & Solution not possible

☞ **Remedy:** Hartree Fock (HF)

If At No > 2

Then Restricted HF energy $H_{SCF}(\psi) = H_{SCF}(\psi) * (\psi)$

If Poly atomic molecules

Then Roothan-Hall Equation

Hartree-Fock model

- + Predicts ground state energy for Helium atom
- + HF equation has similar structure of ordinary single particle SWE
- + For isodermic reactions the errors due to correlation cancel. HF energy (although in error) is useful to compare a set of chemical systems
- + HF orbitals do satisfy 'Bruener theorem', while KS orbitals do not.

$$HF_{total_single_particle_potential} = Hartree(direct_Coulomb)_potential + Exchange_potential$$

- Fails for excited state energy
- It over emphasizes occupation of bonding electrons. The predicted bond lengths are too short. The effect increases as one proceeds towards saturated BSs
- HF orbitals are not complete (true/perfect) due to inherent approximation
 - ☞ **Remedy:** A complete remedial measure is also difficult, but improvement to be nearer to truth is proposed. Different Slater determinants are formed from any occupation of HF orbitals to themselves in a basis set. It is used to calculate an improved many-electron wave function.
- It does not account for other configuration
 - ☞ **Remedy:** Configuration interaction (CI)

⌘ TimeDependent_HF (TD_HF)

The solution of time-dependent Schrodinger equation with HF approximation constraint is referred as TD_HF. The HF procedure with coupled perturbation is called CPHF. RPA is the random-phase approximation and multi-configuration RPA is equivalent to time-dependent MCSCF using the time-dependent gauge invariant approach (TDGI). Thus, the static calculations of course are at the limit of frequency tending to zero.

⌘ Post-HF methods

Although ab initio is popular for ψ based on CQC, a recent contention is DFT based on $\rho(=\psi^2)$ also fits into ab initio framework. Simple HF approximation does not account for correlation and exchange energies. In ab initio CQC, post HF methods viz. configuration interaction (CI), coupled-cluster (CC) and perturbation theory (PT) (appendix-03) are developed to correct for (recover) the electron correlation (chart 3). DFT embeds both exchange correlations in the variety of functionals (B3LYP)(appendix-08).

▢ DFT

The origin of DFT can be traced to the proposition of Dirac that exchange energy of an uniform electron gas can be calculated from charge density alone. The basis of current DFT is Kohn-Sham approach accounting for electron exchange correlation energy by involving fictitious particles in a field of effective electric potential(appendix-04). The failure of local density approximation (LDA) for ionization energy and optical response functions is not the failure of DFT. The generalized gradient approximation is more accurate compared to LDA for peptides in water or protein in nano-tubes. Many effective pure exchange, correlation and hybrid functionals render DFT faster than ab initio methods. B3LYP is one of the most popular hybrid functionals accounting for both exchange and correlation usually yielding values nearer to experimental ones. However, DFT developed for ground states of atoms and molecules is extended to excited states in recent times. Further, it does not produce reliable results in presence of inter molecular interactions like nucleic acid base stacking. Self-consistent_charge-density_functional tight binding (SCC-TB) and hybrid DFT are recent additions to the arsenal of DFT describing Van der Waals complexes.

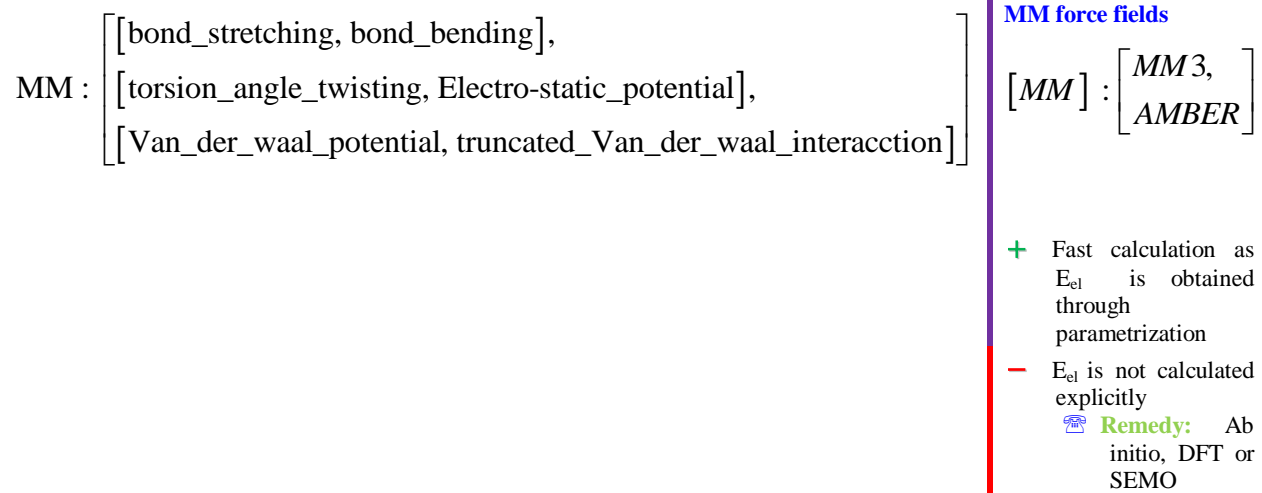
Chart 3: Corrections for electronic energy by typical method to approximate accurate (true) energy from Schrodinger wave equation

BS	HF	MPn	QCISD(T)	Full CI
Minimal	STO-3G			
Split				
Polarisability				
Diffusion	6-311++G**			
High angular momentum				
.....	
∞	HF_limit			SWE

2.3 Molecular mechanics

The energetics and geometry of macro molecules of biological/industrial importance and of even small molecules in condensed phase are indispensable. Molecular mechanics employing Hooks and Newton's second law is feasible. And, quantum chemical calculations with full swing are impracticable with even today's hardware speeds. In molecular mechanics, a force field which implicitly represents electronic energy (E_{el}) is calculated. Thus, the output is approximate geometry and energy of the system. The progress of molecular mechanics is briefly described in chart 4 and appendix-05.

Chart 4: Evolution of molecular mechanics paradigm



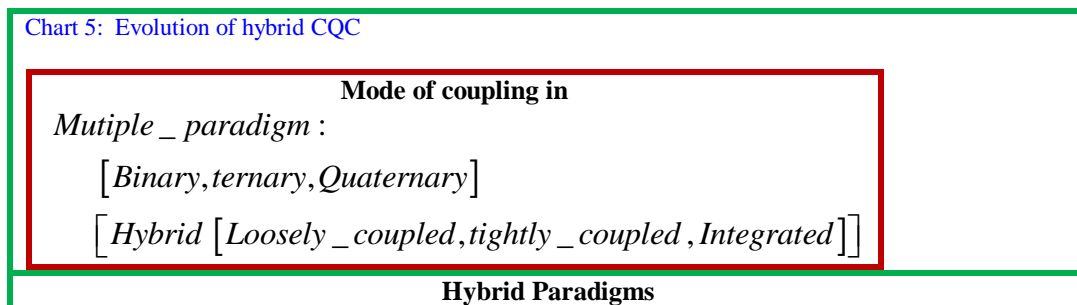
2.4 ONIOM (QM:MM)

Diels-Alder cycloaddition ONIOM model: The energies of cycloaddition of 2,5-dimethylfuran (DMF) and ethylene with H-Y zeolite catalyst in n-heptane are calculated along the reaction path way by a three-layer ONIOM approach. The orders of reactions are in agreement with experimental observations.

2.5 Hybrid methods

Although SEMO, ab initio (HF, post-HF, DFT) and MM force field methods were developed in their own trait, the hybridization these paradigms (Chart 5) pushed the field to the cost (CPU time) optimization for a variety of molecules. QM/MM is a revolutionary approach of considering a small part of the molecule at quantum chemical level and the rest with molecular mechanics paradigm. The subject area of quantum chemistry is a culmination of advances in computational science, quantum mechanics, chemical knowledge and computer hardware. Even with work stations or multi-node computers, the latest quantum chemical techniques available are QM/MM (quantum mechanics/molecular mechanics) or ONIOM models for large bio-molecules, polymers or aqueous salt solutions. Even with projected CPU speed in the next decade, it would not be possible to adopt ab initio and DFT procedures due to requirement of several years of computer time for computations.

Chart 5: Evolution of hybrid CQC



Hybrid	:	$\begin{bmatrix} SEMO + MM, \\ SEMO + ab_initio, \\ DFT + ab_initio, DFT + Dispersion \end{bmatrix}$
[SEMO + MM]	:	[PM3MM]
	Ex:	[PM3 + MM]
[SEMO + ab_initio]	:	[SAM1]
	Ex:	[PM3 + ab_initio]
[DFT + ab_initio,]	:	[Gn]
[DFT + Dispersion]	:	[Empirical]

2.6 Gn models

Pople and his school proposed a series of smart modules (popularly known as Gn theoretical models) (appendix 6) based on approximation theory for calculating more exact energies of molecules of several types. The test data sets used for Gn series of models employed experimental values for IP, EA, PA, ΔH and energies. The size of the data sets grew from 61 to 454 atomic/molecular species.

Accurate energies for many small molecules with hetero atoms (O, S, N and P) are calculated with G03 package. The results for water are presented in table 1, which serves for pedagogical purpose. The computing power of Dell-INSPIRON_1525 is not sufficient for molecules with 20 to 30 atoms like isopropyl derivatives of hydrazides.

Table1: Evolution of Gn models of Pople

G(aussian) n : [G1 G2 G3 G4]	
G1	[G1]
G2	[G2 G2_MP2]
G3	[G3 G3_B3LYP G3_MP2 G3_MP2_B3LYP]
G3X	[G3X_MP3 G3X_MP2 G3SX G3SX_MP3 G3SX_MP2]
G4	[G4 G4_MP2 G4_MP3]

2.7 Solvent models in CQC

The chemistry and physics of many processes in solvents especially in water are germane in environment, pharma industry and synthesis. The inclusion of dielectric properties of the medium in non-linear Hamiltonian was the turning point of application of CQC in presence of solvent. Continuum models of increasing accuracy have become available. The wave function of the solute is obtained by solving the effective Schrödinger equation (PCM) (Eqn.1). The QC/MM approach also contributed to the advances of this field. The solute is described at the QC level and solvent in terms of polarizable non-polarizable framework. The shape of cavity from spherical, ellipsoidal to oblique (molecular shape) form enabled realistic approach to solute-solvent systems. CQC successfully spread its wings into energetics and spectral response of species and reactions in a solvent and binary mixture. Recent surge is in water and aquo-organic mixtures. A gist of solvent models and references are depicted in chart 6.

Eqn.1: Schrodinger equation for a solute in a solvent

$$\hat{H}_{\text{eff}} |\Psi\rangle = [\hat{H}^0 + \hat{V}_\sigma] |\Psi\rangle = E^{\text{GS}} |\Psi\rangle$$

H_0	Hamiltonian for the isolated system.
V_σ	Solute-solvent interaction operator V depends on electronic charge distribution of the solvent.
H_{eff}	Effective Hamiltonian for the solute ground state wave function :
$ \Psi\rangle$	Contains all the relevant information about the solvent effect on the solute

6: Solvent models

Chart 6a: Solvation approaches:

- ☞ [SES: Seperable Equilibrium Solvation
- ☞ ESP: Equilibrium Solvation Path
- ☞ NES: Non-Equilibrium Solvation
- ☞ SZP: Secondary-Zone Potential
- ☞ ESZ: Equilibrium Secondary Zone
- ☞ Solvent_Models: [Explicit,implicit]

- PCM : [PCM, isodensity-PCM]
- PCM : polarizable continuum method
- ☞ COSMO : Conductor like screening model]
- ☞ [SM_x]

Chart 6b : Typical water models

1990	Aquist
1992-	Dang
2002	
2006	JJ
2006	LR
2006	JC_TIP3P
2008	JC_SPCE
2008	JC_TIP4PEW
2009	HMN-5
2009	HMN-5a
2009	HMN-5b
2010	YWHLVAMR
2012	DVH/2014_RDVH
2012	PCSND
2014	HFE_TIP3P
2014	HFE_SPCE
2014	HFE_TIP4PEW
2014	IOD
2014	12-6-4-TIP3P
2014	12-6-4-SPCE
2014	12-6-4-TIP4PEW

Chart 6c : SM_x models

M5.0	No quantal Hamiltonian
SM5.2	AM1, PM3, MNDO, MNDO/d
SM5.4	AM1, PM3
SM5.42	INDO/S or S2 DFT or HF
SM5.43	DFT or HF
SM5C	AM1, PM3, MNDO/d
SM6	DFT or HF
SM8	DFT or HF
SM8AD	DFT or HF
SM8T	DFT or HF
SMD	any method
VEM42	INDO/S or S2

Chart 6d:Typical software packages with solvent models

- ☞ Gaussian 09/03
- ☞ GAMESS (10, version)
- ☞ AMM
- ☞ DGSOL
- ☞ Makolab
- ☞ MN-GSM
- ☞ Homepage
- ☞ Jaguar 7.0;
- ☞ Schrodinger, Inc.
- ☞ Spartan 02
- ☞ Q-Chem (4.0)

Chart 6e: References_Solvent_Models

Output of om_ref_JAVATYP.m

C. J. Cramer and D. G. Truhlar, in *Reviews in Computational Chemistry*, Vol. 6, edited by K. B. Lipkowitz and D. B. Boyd (VCH Publishers, New York, 1995), pp. 1-72.

- ▶ [Continuum Solvation Models: Classical and Quantum Mechanical Implementation](#)

C. J. Cramer and D. G. Truhlar, in *Quantitative Treatments of Solute/Solvent Interactions*, edited by P. Politzer and J. S. Murray (Elsevier, Amsterdam, 1994), pp. 9-54. [Theor. Comp. Chem. **2**, 9-54 (1994).]

- ▶ [Development and Biological Applications of Quantum Mechanical Continuum Solvation Models](#)

C. J. Cramer and D. G. Truhlar, in *Structure and Reactivity in Aqueous Solution: Characterization of Chemical and Biological Systems*, edited by C. J. Cramer and D. G. Truhlar (American Chemical Society, Symposium Series 568, Washington, DC, 1994), pp. 1-9

- ▶ [Structure and Reactivity in Aqueous Solutions: An Overview](#)

J. W. Storer, D. J. Giesen, G. D. Hawkins, G. C. Lynch, C. J. Cramer, D. G. Truhlar, and D. A. Liotard, in

Structure, Energetics, and Reactivity in Aqueous Solution: Characterization of Chemical and Biological Systems, *ibid.*, pp. 24-49.

- ▶ [Solvation Modeling in Aqueous and Nonaqueous Solvents: New Techniques and a Re-examination of the Claisen Rearrangement](#)

C. J. Cramer and D. G. Truhlar, in *Solvent Effects and Chemical Reactivity*, edited by O. Tapia and J. Bertrán (Kluwer, Dordrecht, 1996), pp. 1-80. [Understanding Chem. React. **17**, 1-80 (1996).]

- ▶ [Continuum Solvation Models](#),

D. J. Giesen, C. C. Chambers, G. D. Hawkins, C. J. Cramer, and D. G. Truhlar, in *Computational Thermochemistry*, edited by K. Irikura and D. J. Frurip (American Chemical Society, Symposium Series 677, Washington, DC), pp. 285-300 (1998).

- ▶ [Modeling Free Energies of Solvation and Transfer](#)

C. C. Chambers, D. J. Giesen, G. D. Hawkins, W. H. J. Vaes, C. J. Cramer, and D. G. Truhlar, in *Rational Drug Design*, edited by D. G. Truhlar, W. J. Howe, A. J. Hopfinger, J. M. Blaney, and R. A. Dammkoehler (Springer, New York, 1999), pp. 51-72. [IMA Vol. Math. Its Appl. **108**, 51-72 (1999).]

- ▶ [Modeling the Effect of Solvation on Structure, Reactivity, and Partitioning of Organic Solutes: Utility in Drug Design](#),

G. D. Hawkins, J. Li, T. Zhu, C. C. Chambers, D. J. Giesen, D. A. Liotard, C. J. Cramer, and D. G. Truhlar, in *Rational Drug Design*, edited by A. L. Parrill and M. R. Reddy (American Chemical Society, Symposium Series Volume 719, Washington, DC, 1999), pp. 121-140

- ▶ [New Tools for Rational Drug Design](#),

G. D. Hawkins, T. Zhu, J. Li, C. C. Chambers, D. J. Giesen, D. A. Liotard, C. J. Cramer, and D. G. D. G. Truhlar, in *Combined Quantum Mechanical and Molecular Mechanical Methods*, edited by J. Gao and M. A. Thompson (American Chemical Society, Symposium Series Volume 712, Washington, DC, 1998), pp. 201-219.

- ▶ [Universal Solvation Models](#),

C. J. Cramer and D. G. Truhlar, *Chemical Reviews* **99**, 2161-2200 (1999).

- ▶ [Implicit Solvation Models: Equilibria, Structure, Spectra, and Dynamics](#),

C. J. Cramer and D. G. Truhlar, in *Free Energy Calculations in Rational Drug Design*, edited by M. R. Reddy and M. D. Erion (Kluwer Academic/Plenum, New York, 2001), pp. 63-95.

- ▶ [Solvation Thermodynamics and the Treatment of Equilibrium and Nonequilibrium Solvation Effects by Models Based on Collective Solvent Coordinates](#),

D. G. Truhlar, in *First International conference on Foundations of Molecular Modeling and Simulation*, edited by P. T. Cummings, P. R. Westmoreland, and B. Carnahan (American Institute of Chemical Engineers, Symposium Series Vol. 97, New York, 2001), pp. 71-83.

- ▶ [Molecular-Scale Modeling of Reactions and Solvation](#),

C. J. Cramer and D. G. Truhlar, in *Trends and Perspectives in Modern Computational Science*, Lecture Series on Computer and Computational Sciences, Vol. 6, edited by G. Maroulis and T.E. Simos (Brill/VSP, Leiden, 2006), pp. 112-139.

- ▶ [SMx Continuum Models for Condensed Phases](#),

D. G. Truhlar and J. R. Pliego Jr., in *Continuum Solvation Models in Chemical Physics: Theory and Application*, edited by B. Mennucci and R. Cammi (Wiley, Chichester, 2007), pp. 339-366.

- ▶ [Transition State Theory and Chemical Reaction Dynamics in Solution](#),

C. J. Cramer and D. G. Truhlar, *Accounts of Chemical Research*, **41**, 760-768 (2008).

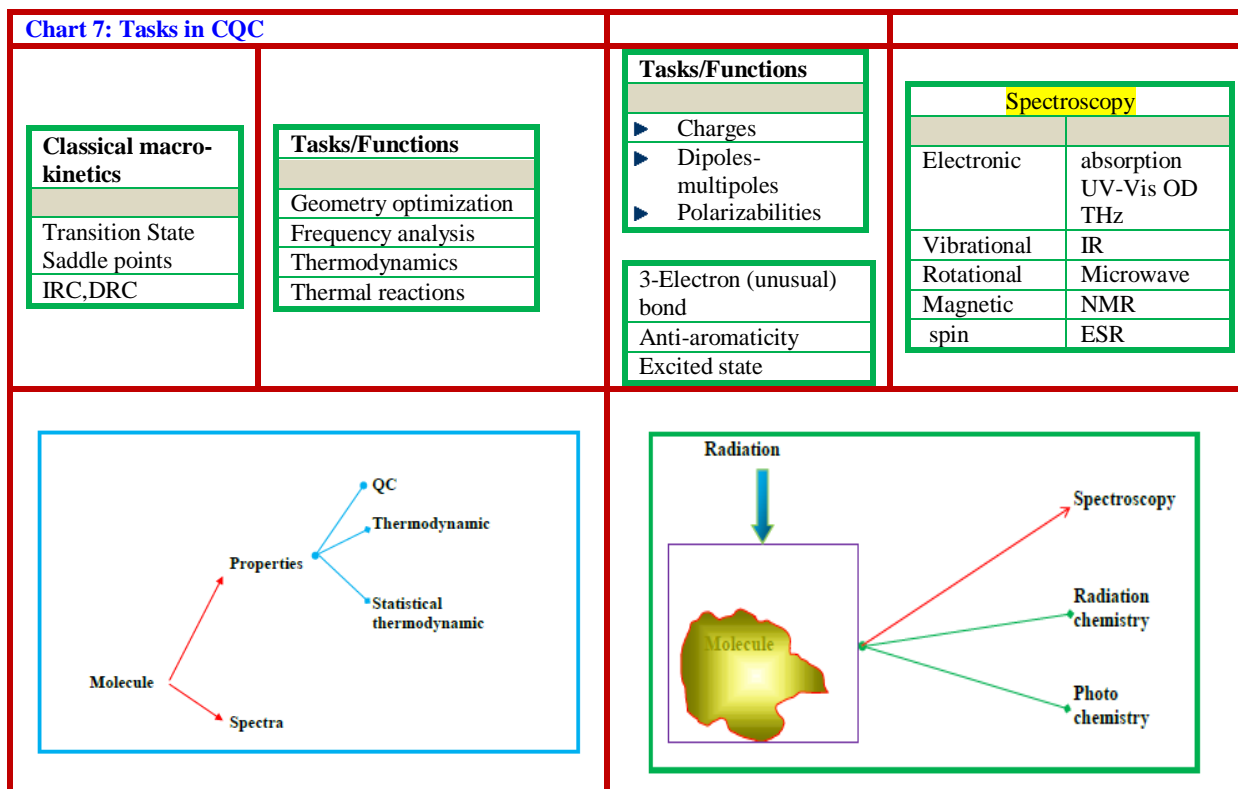
- ▶ [A Universal Approach to Solvation Modeling](#),

A. V. Marenich, C. J. Cramer, and D. G. Truhlar, *Journal of Chemical Theory and Computation*, 2008. (Perspective article)

- ▶ [Perspective on Foundations of Solvation Modeling: The Electrostatic Contribution to the Free Energy of Solvation](#)

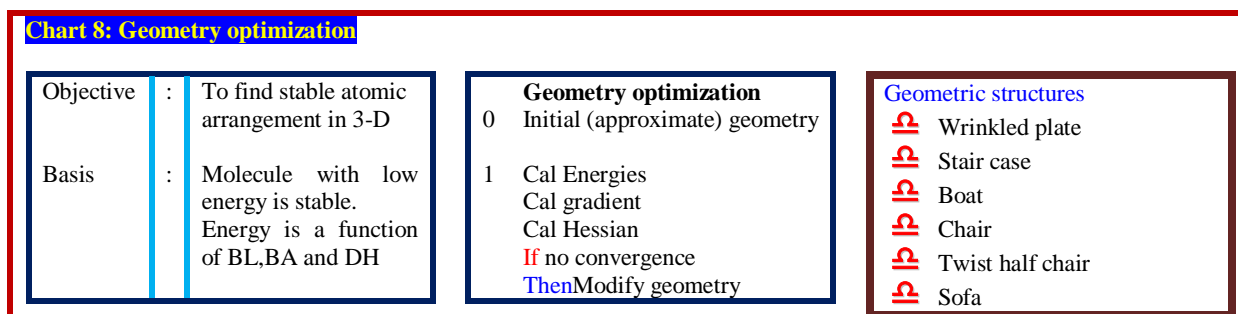
3. Tasks in CQC

Optimised geometry and vibrational spectra are obtained based only on quantum chemical postulates and requires only fundamental constants ([chart 7](#)). Thus, solution of Schrodinger wave equation here is popularly known as ab initio approach. But, the list of chemical tasks tackled by CQC is ever increasing competing with accuracy of many state-of-art techniques. The results are deterministic and hence concept of precision does not arise as no stochastic method is used in solution of SWE. The accuracy of CQC methods of course depend upon components (functionals, basis sets, implicit/explicit approximations/assumptions) of a method.



3.1 Geometry optimization

The geometry of a molecule from x-ray diffraction or NMR-studies is vitiated by the cohesive forces in the solid state or by influence of the solvent. Quantum chemical (electronic) energy minimization on potential energy surface (chart 8), on the other hand, results in an optimized 3-D geometry of an isolated (gaseous) molecule in vacuum. But, the optimization of geometry is a complex problem being a function of the level of theory, Hamiltonian, basis sets, functionals, optimization algorithms and convergence criteria. There are no explicit databases for the choice of the procedures based on the class of the compounds, form (ionic, zwitter ionic, radical etc.) and spin state. So far it has been practiced more like a craft rather than a science. A perusal of the literature shows hit and trial procedures, no doubt depending upon the objectives on hand deal with some structure reinvestigation with progress in QC jargon. Bery's optimization algorithm using redundant internal coordinates in HF, post-HF and DFT paradigms is in use. The hybrid technology (MM and QC) and ONIOM is employed depending upon trade off of accuracy vs computational time. The results differ at different levels of QC theory and basis sets (appendix-05). Ab-initio calculations with different basis sets at MP2 to MP4 levels and DFT/TD_DFT approach with hybrid functions account for exchange and correlation energies. G4 and G3 approaches compute more exact single point (SP) energies of select moieties. A programmed search of geometry optimization and generation of ASCII files for output are described in appendix-07.



Approach : minimum of Energy on PES using HF method

go to 1
else
minimum energy

Envelope
Molecule_rotation_through_dihedral_angle

Geometry optimization

- Post HF method is correlated with basis sets
- SVWN basis set extremely under estimates O-O
- If H-bonding complexes, the inter molecular distance is under estimated

3.2 Vibrational frequency analysis

The optimized geometry corresponds to a realistic (not hypothetical) 3-D picture of a moiety adhering to the rules of chemical bonding (valence and accepted bond types). It is indicated by zero number of imaginary frequencies (in other words zero/low first six vibrational frequencies), in the vibrational analysis of the optimized geometry(Chart 9,Alg.1). Only after arriving at a valid chemical structure for a chemical species/moiety, properties (now popular as descriptors exceeding 5000 in number) viz. physical/chemical/physico-chemical/spectroscopic are calculated. The object function in vibrational analysis is a multi-dimensional complex surface in normal coordinates of the atoms of species.

Chart 9: Frequency Analysis in CQC

Objectives of frequency calculation

Cal first six vibrational frequencies

- ↑ Stable geometric structures/conformer
- ↑ Transition state (TS)
- ↑ Saddle point or higher order saddle point

Meta rules in frequency

Output : [optimized geometry, {energy,MO}]

- If Stationary point
- Then Perform frequency analysis
- If Number of imaginary Eigen values is zero
- Then Chemically valid geometry
- If Chemically valid geometry
- Then Calculate properties
- If Dihedral angle
- Then Search for isomers

KB for Frequency_analysis_of_AMPAC

- If Gnorm < max
- Then Do frequency analysis
- If Gnorm > max
- Then Ignore g-norm test & perform frequency analysis

Alg. 1: Frequency Analysis

Input Structure
Step : 0 Calculate gradient norm (gnorm) of input geometry
If gnorm < 3
Then do frequency analysis

Identification of stable geometries from vibrational frequency analysis

- If No imaginary frequencies (NIMAG = 0)
- Then Stable structure (local/global) with minimum energy
- If One imaginary frequency (NIMAG = 1)
- Then Transition State (TS)
- If More than one imaginary frequencies (NIMAG >1)
- If NIMAG == 2
- Then saddle point
- else Higher order saddle point
- end
- endif

```

Else if gnorm test required then stop
else end

```

```

Step : 1 Calculation of Hessian
Step : 2 Diagonalize Hessian – force constant
      Cal matrix weighted values for
      isotopic masses
Step : 3 Calculate vibrational frequencies
      from F
Step : 4 If Hessian & Thermo
      Then calculates thermodynamic
      parameters

```

```

J. W. McIra Jr., A. Komornicki,
J. Am. Chem. Soc., 96(1974)5798

```

```

File Name: bah-isop-HF-6-311G-Geo-Freq
# opt freq=noraman rhf/6-311G geom=connectivity % G03

```

```

Molecular mass: 178.11061 amu.
Principal axes and moments of inertia in atomic
units:

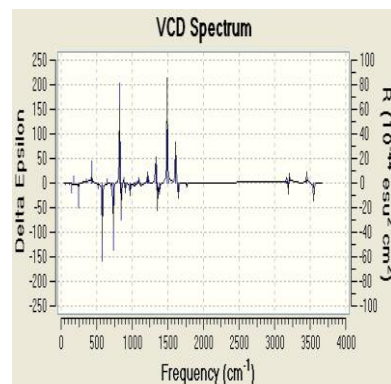
```

	1	2	3
EIGENVALUES --	821.445664927	2.245515509	50804
X	0.99999	0.00331	-0.00341
Y	-0.00335	0.99995	-0.00972
Z	0.00338	0.00973	0.99995

```

This molecule is an asymmetric top.
Rotational symmetry number 1.

```



The prime aim of is to find whether stationary point on PES represents a chemically valid structure or transition state. The fundamental vibrational frequencies, IR intensities (equal to the product of square of transition dipole and vibrational frequency), normal modes for an optimised geometry, zero point energy (to correct the frozen nuclei energy) and anharmonic frequencies are also calculated. The calculated vibrational frequencies are used in calculation of thermodynamic properties. The (default) thermodynamic output is at 298.15° and 1.0 atmosphere pressure and for most abundant isotope. The gradient or first derivative with respect to geometric parameters is calculated analytically or by numerical differentiation using finite difference method. The study second derivatives (Hessian) with respect to nuclear coordinates are referred as harmonic vibrational frequency analysis. The co-ordinates are calculated to mass weighted ones. The force constants, vibrational frequencies, pre-resonance Raman, IR, polarized/ depolarized, NMR, VCD, ROA, UV-Visible form part of the output.

3.3 Transition state

The geometries of TS structures are not readily available from experiments. However, it is possible to detect it from CQC. Transition state has only one imaginary frequency required by McIves –Komornicki criteria. For a saddle point, potential energy is maximum along one direction (of reaction coordinates) and minimum in all other directions.

State-of-the-art-of_CQC

From abstract physics point of view, the two fundamental particles are bosons (symmetrical under exchange) and fermions (antisymmetric under exchange). The electrons being fermions from particle physics perspective, there exists a relation between quantum molecular tasks and abstract physics tools too. At the rock bottom level, universe can also be viewed of consisting of bosons and fermions only. Also it is true to the naked eye that the world around us is made up of matter of different forms in different phases which are only an artifact.

Quantum chemistry (QC) computations for small to large size organic molecules and small inorganic species can be considered as the first phase. The feasibility of chemical reactions in presence/absence of single catalyst, detection/conformation of TS/intermediates is in the second phase. Simulation of all types of spectra, chemical parameters for known molecules of increasing complexity is the third wave. The effect of water/solvent/mixed solvent/solid state supports/interfaces on QM parameters/chemically derived quantities/spectra/reaction profile, different forms of energy are successfully obtained with the state of the art QC methods with application of software/hardware. The references are given in methodology and introduction immediately after the topic to increase readability.

4. CQC in action

Our solar system over time made available an array of diverse natural compounds ranging hydrogen, oxygen, water, CO₂, methane, nitrogen, ammonia, glucose, amino-acids, nucleotides, DNA and many many tiny entities. They range from life, food to even poisonous (to whom is a pertinent question) moieties through enormous modifications. Synthetic organic chemistry, purely a man-made creative mimic (tool), during the last century supplemented with nature in supplying these molecules for greedy needs. The activity in this direction resulted in newer technologies. But, environmental pollution and economy of synthesis posed a challenge.

The study of eco-balance, climate change, environment pollution and ill effects on human health require the stability, transport dynamics of chemical species in gaseous/solvent media, formation of new species, decomposition into stable/meta-stable/unstable moieties in the three states of matter and also at interfaces (air-water, water-solid, gas-solid). Another approach is to design simplified molecules which are better in function and through simpler synthetic route. Function oriented synthesis (FOS) offers access to novel structure not found in nature and paves way to solve riddles in the science of synthesis. Synthetic chemistry brought renaissance in food, clothing, shelter, medicine, culture and even art to an unimaginable extent. It endorses that there is no medicine without synthesis and synthesis without quantum chemical information. An intelligent eye sees most of current drug discovery strategies find precedence in nature. An organism screens the environment around, selects chemicals for synthesizing food and use for evolutionary advantage. Bryozoans use a chemical produced by symbiosis to protect their progeny from predation. Bacteria putatively employ chemicals to wage war against other bacteria for control of their ecological niche. Some of the animals use natural materials for self-medication. Ants use chemicals for communication. The electronic structure and localization of FMOs in conjugated compounds functioning as molecular devices--wire, diode, switch etc. is of interest. The efforts in the preparation of organic non-linear optical compounds (substituted diphenyl penta dienes) with high second order hyper polarizabilities drew attention over years. Manufacture of materials with desired characteristics for health, food and comfort involve synthesis, structure elucidation and reactivity at molecular level. The synthesis and isolation of organic molecules in purest and desired chiral form is the prime concern of research, apart from inorganic and electronic materials.

The literature on CQC applications grew exponentially and a typical search with keys words 'DFT OR Ab initio OR CHARMM' in Science Direct and ACS from the year 2000 in research are shown in [chart 10](#). Now, it is humanly out of scope to go through even abstracts, leaving aside the full papers. Very few publications deal with rememberable knowledge bits to carry torch of the method or tune to changing sub-goals, systems and environment.

Chart 10a: Online search of number of research papers during 2000-2015 in CQC with keywords 'DFT OR Ab initio OR CHARMM'

Science Direct Search results on 5-5-2015
16,590 results found for pub-date > 1999
 and TITLE-ABSTR-KEY(DFT OR Ab initio
 OR CHARMM)

Journal	#	Year	#
---------	---	------	---

ACS Search results on 5-5-2015: DFT OR ab initio OR CHARMM
 OR TDDFT: **27025**

 Acc. Chem. Res.	124	 J. Org. Chem.	1506
---	-----	---	------

















Chemical Physics Letters	1,910	2015	622	 ACS Catal.	156	 J. Phys. Chem. A	8013
Journal of Molecular Structure: THEOCHEM	1,698	2014	1,058	 ACS Nano	148	 J. Phys. Chem. B	3143
Journal of Molecular Structure	1,014	2013	1,063	 ACS Symposium Series ACS Book Series	193	 J. J. Phys. Chem. C	5636
Chemical Physics	826	2012	999	 Inorg. Chem.	2381	 J. Phys. Chem. Lett.	323
Spectrochimica Acta Part A: Molecular and Biom...	782	2011	979	 J. Am. Chem. Soc.	3655	 Langmuir	280
...	 J. Chem. Inf. Model.	140	 Nano Lett.	200
				 J. Chem. Theory Comput.	1019	 Org. Lett.	284
				 Organometallics	1812	 Macromolecules	260
			

Chart 10b: Chemical systems investigated with CQC

Systems amenable for CQC

Chemical_system : [solute, environment]

Solute_phase : [gas, liquid, [solid [crystal, layer, amorphous]], plasma]

Solute_size : [small, medium, large, very_large]

Solute : [atom, molecule[neutral, ion [cation, anion], radical], complex]

Molecule : [[inorganic, organic][homo,hetero] [diatomic, triatomic,polyatomic]]

Complex : [molecular_complex, metal-ligand_complex]

Environment : [vacuum, condensed_phase, electric/magnetic field]






Condensed_phase : [[liquid, liquid_mixture], micelle, cell, interface[binary, ternary], solid]

Chemical reaction : [Molecule1 + Molecule2 -> Product]

Molecule + solvent : [ionization, solute_solvent_complex]

Product : [isomerization, Molecule3]

Atoms, molecules & clusters (CAM)

 Solute in solvent(s) Molecule in Matrix Molecule in solid phase Molecule in macromolecule Solute (molecule) in interfaces

Species in a solvent and mixture of solvents

Chemistry and CQC in condensed phases

The real life phenomena require a knowledge of a molecule (with substituents), ions in solvents/cells and lipid media (chart 10b).

Heavy water: Bankura et al. [172] found hybrid CQC results on heavy water are very nearer to experimental outcome (Chart 11).

Chart 11 : Hybrid ab initio, DFT and empirical vdW for H-bond network in (heavy) water	
<p>First-principles</p> <ul style="list-style-type: none"> ▪ Born–Oppenheimer-MD (BOMD) 	<p style="text-align: center;">+</p> <ul style="list-style-type: none"> ▪ DFD (BLYP) ▪ Empirical van der Waals (vdW) corrections <ul style="list-style-type: none"> ◆ DRSSL-PBE, DRSSL-optB88) ▪ Semilocal (vdW) exchange <ul style="list-style-type: none"> ◆ BLYP-D2, BLYP-D3, PBE-D3, revPBE-D3 ▪ correlation functionals <ul style="list-style-type: none"> ◆ modified B88

Gaussian electrostatics model (GEM): GEM means Gaussian electrostatics model based on pure density of Ca(II)–H₂O system and takes into account of short-range quantum behavior of electric fields. It thus introduces non-classical effects. Chaudret et al. [107] used GEM for accurate representation of first hydration shell and CQC of HIV-1 NCp7-Zn(II) metalloprotein Hg(II) water complexes (chart 12). This hybrid MM²/MM polarizable FF is possible only because of transferability of ab initio pseudopotentials.

Chart 12: Hybrid MM ² /MM polarizable force field
<ul style="list-style-type: none"> ● Advanced electrostatics (GEM) <ul style="list-style-type: none"> ▪ Non-bonded interactions by fitted electronic densities ● SIBFA (sum of interactions between fragments ab initio computed), which resorts to distributed multipoles.
<p>GEM</p> <ul style="list-style-type: none"> → two point dipole polarizable force fields + It includes overlap-dependent exchange-polarization repulsive contribution through Gaussian damping function + Made it possible to incorporate explicit scalar relativistic effects in to molecular mechanics + NO need of an extensive parametrization. Yet, nonambiguous short-range quantum effects within any point-dipole are introduced. + Reproduces ab initio total (induction, polarization, and charge-transfer) interaction energies for closed-shell metal complexes

S/G-1

- + models accurately polarization up to quadrupolar response level
- + accurately reproduce ab initio total interaction energies within closed-shell metal complexes regarding each individual contribution including the separate contributions of induction, polarization, and charge-transfer

COSMO in GAUSSIAN94

- + Cavities are modeled on the molecular shape, using recently optimized parameters
- + Electrostatic and non-electrostatic contributions to energies and gradients are considered

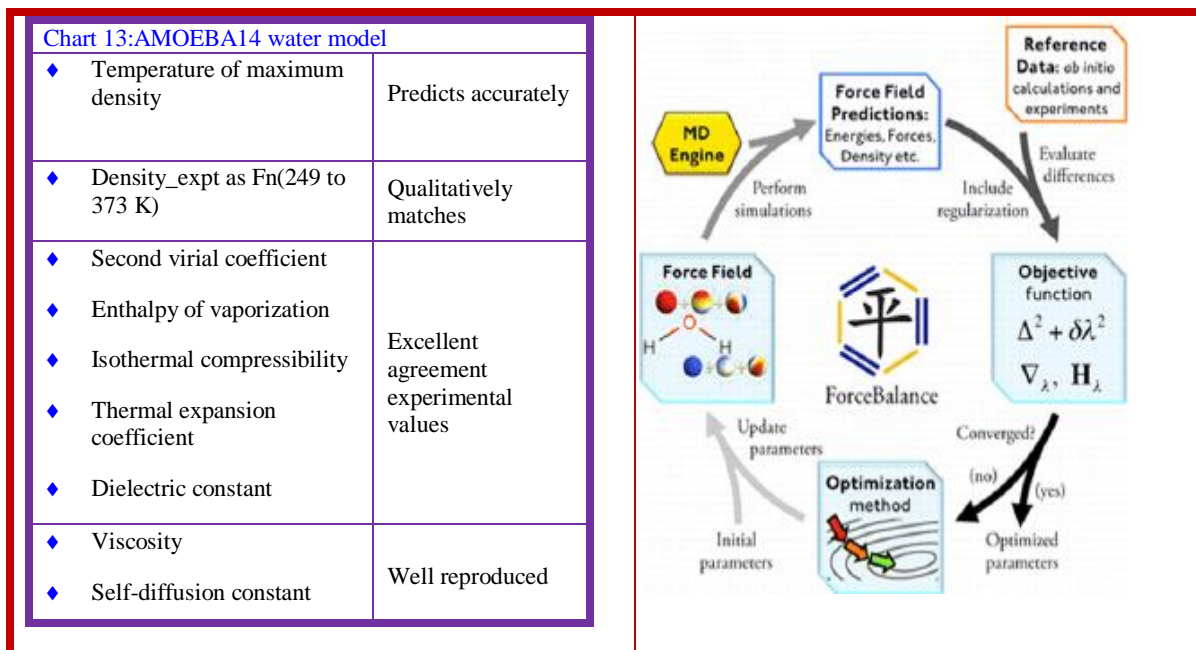
Macroscopic quantum electrodynamics based continuum model: Duignan et al. [157] proposed a model based on frequency dependent multi- (di-, quadru-, octu-) pole polarizabilities to account for dispersion component of interaction of solute with water molecules. A bulk dielectric susceptibility of the solvent and spherical cavity for the solute is assumed. The additivity of electrostatic and dispersion (quantum mechanical) interactions are valid as the model is similar to Born. In the case of fluoride in water, 50% of the dispersion solvation energy is from higher order multipole moments.

Lennard-Jones (LJ) nonbonded model: Li et al. [57] reoptimized 12–6 LJ parameters for 15 monovalent ions (11 positive and 4 negative ions) for the water models (TIP3P, SPC/E, and TIP4PEW).

- + Agrees closely with QC-calculated VDW radii
- + transferable to ion-pair solutions

AMOEBA14 water model

Laury et al. [143] employed force balance to adjust parameters for the AMOEBA polarizable atomic multipole water model (chart 13). This reduces discrepancy between ab initio and experimental properties (over a wide range of temperatures) for water clusters and it is a promising tool of futuristic scientific (polarizable) water model in multi-process-covalent and non-covalent interactions.



<ul style="list-style-type: none"> ◆ Surface tension <p style="text-align: center;">Inf.Bits.</p> <p>AMOEBA14 model (for 2–20 water molecules) yields results similar to AMOEBA03 and the direct polarization iAMOEBA model high-level <i>ab initio</i> results</p>	<p>Method. 99: Car–Parrinello ab initio MD</p> <p>Classical water models</p> <ul style="list-style-type: none"> ◆ SPC/E ◆ TIP3P ◆ TIP4P ◆ TIP4P/2005 <p>Bulk water at $T = 330$</p> <ul style="list-style-type: none"> ◆ Car–Parrinello ab initio MD
---	---

TIP4P/2005 model for liquid water: Calero et al. [140] found that the temperature-dependence of ^1H NMR-nuclear spin relaxation times (T1 and T2) of liquid water by TIP4P/2005 is in good agreement with experimental quantities.

TIP4P-QDP: Bauer et al. [67] highlighted a new water force field, TIP4P-QDP. It explicitly incorporates the terms responsible for differences in polarizability between vapor and liquid phases and parametrized to accurately reproduce properties in gas phase and select ones in liquid form (table 2).

Table 2: TIP4P-QDP force field

Property	Gas (high level ab initio)	KB
Polarizability	1.40 Å ³	CQC Excellent agreement with Expt
Dipole moment	1.85 Debye	
Liquid density	Liquid (TIP4P-QDP) 0.9954 (± 0.0002) g/cm ³ at 298 K and 1 atm	
Enthalpy of vaporization	10.55 (± 0.12) kcal/mol.	

Property (liquid)	TIP4P-QDP	KB
Dielectric constant	85.8 ± 1.0	10% > exptal
Dipole moment	2.641 (± 0.001) Debye	0.02 Debye > TIP4P-FQ & within the range of values currently surmised for the bulk liquid.

Evolution of electron solvation: Iglev et al. [179] probed into recombination of excess electrons produced by high-energy irradiation of water or alcohols by (two-and three- pulse) femtosecond spectroscopy and ab initio-CQC. The activation energy (12 kJ/mol) in the early stage of electron solvation increases to (44 kJ/mol) at full aquation.

Evolution of electron solvation: Fritsch et al. [63] studied nuclear quantum effects in liquid water from ab initio simulations with FFs (Alg. 2).

Hydrated electron/water/vapor interface: Uhlig et al. [105] obtained optical spectrum of hydrated electron in bulk water, water/vapor interface by DFT, TD-DFT and ab initio methods and found to be similar. The detection, monitoring and study of properties are through optical spectral probe only.

Solvated electron in 32 water molecules: Marsalek [2] reported electrons solvated in water 32 water molecules by ab initio molecular dynamics simulations. It is reported that electron localizes into a cavity close to surface of the cluster at ambient conditions. But, the cavity is more flexible and accessible to water molecules compared to negatively charged ions (Fig. 1).

Alg.2: Nuclear quantum effects

- ◆ MD from first-principles
- ◆ Force-matching technique: Cal effective force field for bulk liquid water
- ◆ Validation: Reproduction of structural/dynamic properties of reference system
- ◆ Role of nuclear quantum effects on bulk water
- ◆ Perform path integral simulations
- ◆ Probe into radial distribution functions, vibrational spectra, H-bond fluctuations

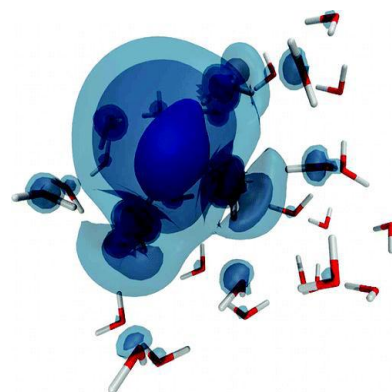
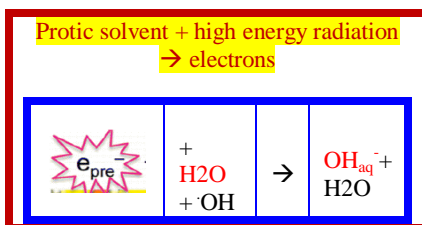
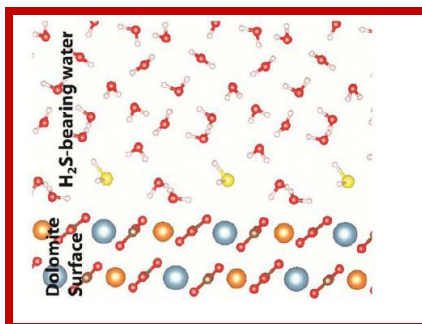
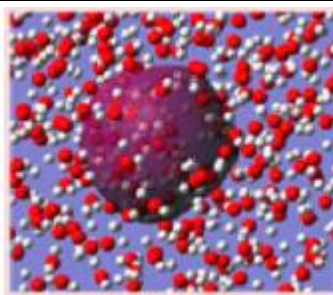


Fig. 1: electron solvated in 32 water molecules
Courtesy of Ref [2]

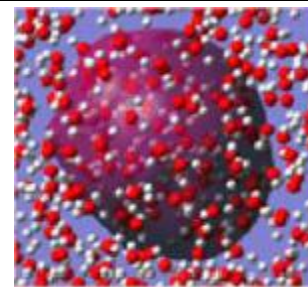
Cavity based model for hydrated electrons in water clusters: Turi [68] reported that physical properties of the cluster based on cavity pseudopotential models explain experimental data on three electron–water molecule better than non-cavity structures (KB.1).

KB.1: Models of Hydrated Electrons in Water Clusters

- ◆ Larsen–Glover–Schwartz (LGS), modified version
 - + Predicts noncavity hydrated electron structure in clusters at room temperature
 - Inconsistent with the size dependence of the experimental data
 - Ab initio calculations indicate weak stabilization of the excess electron in regions where LGS potential strongly binds the electron



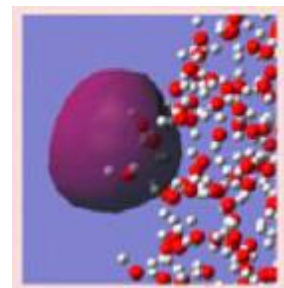
Cavity



Non-cavity

Courtesy from Ref [68]

- ◆ cavity-preferring Turi–Borgis (TB) model
 - + Predicts interior-state/surface-state cluster isomer
 - + Qualitatively correct tendencies
 - + TB calculations give stabilization energies in line with the ab initio



Surface

Hydration

The function of water as a structure maker or structure breaker in presence of ions/molecules is a familiar concept in solution processes. Protein-folding in aqueous solution is one of the major fields of applications. However, the mechanism of this process is not fully clear. The dipole moments of water molecules in the first hydration shell are instrumental to probe into the hydrogen bond strength of water molecules in the next hydration shells. Hydroxyl groups form roughly two H-bonds viz. one weaker acceptor H-bonds and one stronger H-bond. The chemical environment of the groups influences the variation. A detailed analysis in this direction was missing during the last 50 years.

Hydration of ions, material surfaces, chemical reactions in aqueous/organic liquid/binary mixtures/ternary mixtures of solvent are of great importance in science and technology. Water molecules in the vicinity of biomolecules play a key role in bio-physico-chemical energetics. It may have a beneficial effect or sometimes leads to catastrophic effect at molecular/functional level of a few processes.

The discrimination of carcinogenic compounds from non-carcinogenic one is recently explained from energies of FMOS and their contribution from local density of states (LDOS). This will be illustrated with estrone, estradiol and their derivatives. QC derived parameters like Fukui functions, local/global hardness/softness etc. find relevance in chemical reactions of synthetic importance and biological response. The interface as well as the transfer of ions/neutral molecules between two phases is crucial in environment/synthetic chemistry/drug transport in the human body and even for the safety of brain from myriad of chemical species. Momoh studied hydration of phenyl acetylene cation in gas phase using mass-selected ion mobility spectrometer. The ΔH was calculated using equilibrium measurements in an ion mobility drift cell. CQC energies are calculated with MP2//ROHF/6-311+G** and ROHF/6-311+G**. Phenyl acetylene forms a trimer (triphenyl benzene). It interacts weakly with H₂O molecules, due to steric hindrance. Thus no additional water molecules are observed.

The interaction energy between water and dipeptide G-Tyr is 2-3 Kcal mol⁻¹ larger than for G..H₂O (Noguera,2009). The additional strength arises from co-operative interplay between stacking and H-bond forces. The removal of damaged nucleobase from DNA by BER glycosylases is influenced by – stacking interactions between the side chain of tyrosine and neutral and protonated guanine.

Binding energy of MP2 (-30.5) is compared with experimental one (-31.4 KJ/mol). Experimental data is based on high resolution rotational spectral analysis. The proton transfer from phosphonic acid to proton accepting groups (H₂O or NH₃) is energetically favourable to generate anions. alpha-fluorination significantly stabilizes anion. The significant change of bioactivity phosphatase inhibitors with substitution is correlation with pK_a values.

The apparent failure of earlier QC was due to ignoring the hydration (solvation) effects viz., dispersion, weak H-bonds and other non-electrostatic contributions. With refinement in polarized models (chart), cavity size by shape contribution and newer functionals. The state of art of CQC-Solv model results in reasonable values of pK_a/ΔG for a good number of different functional groups. Yet, it is a far off vision to accept CQC as equivalent/dependable alternative for equilibrium/rate constants in presence of a solvent. The generalized Born model underwent renaissance during the last three decades within the purview of QC, to enable CQC as an alternate tool to the experimental physical chemistry/chemical physics. The internal hydration of BPTI is studied with NMR and MD. The first three water molecules are strongly interactive, while the fourth is in a hydrophobic protein cavity with lower affinity.

Protein is viewed as a dielectric continuum (Andrei). Electrostatic contribution calculated from Poisson equation. Non-polar part and interaction energy and binding entropy change are assumed to be summed for every bound water molecule.

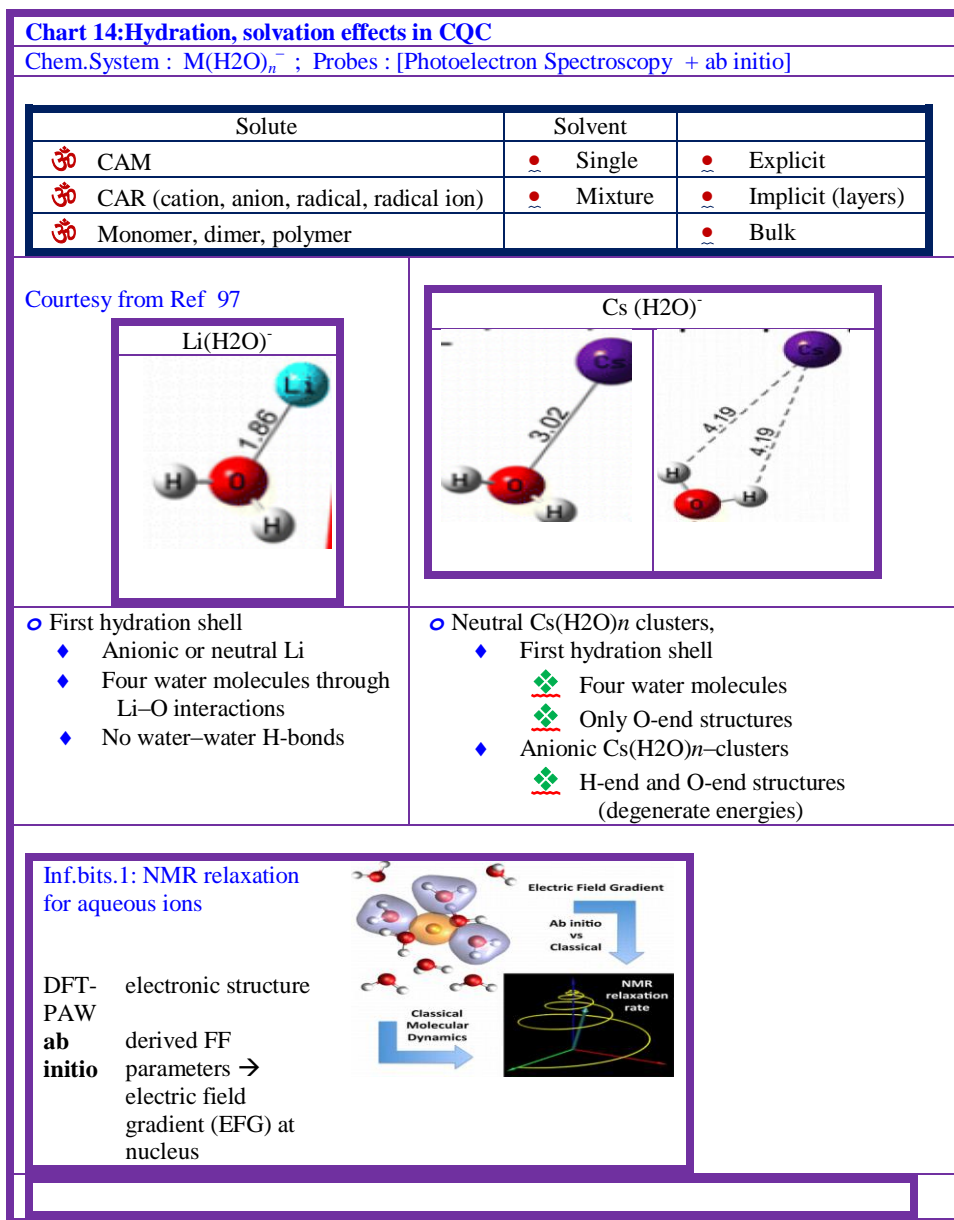
The dissolution of hydrophobic molecule in water results in decrease of both entropy and enthalpy. It also reduces the mobility of water molecule (14-31 of PCCP 2006-8-737-743). It was attributed to structure formation of water around hydrophobic moiety and this concept was used to explain thermodynamics. Further, it was assumed the hydration shell is strengthened like crystalline hydrate which prevails diffusion motion of water. Yamaguchi [208] reported electrostatic interaction and number density fluctuation resulted from cavity formation by the solute in a region for slowing down of solvent water.

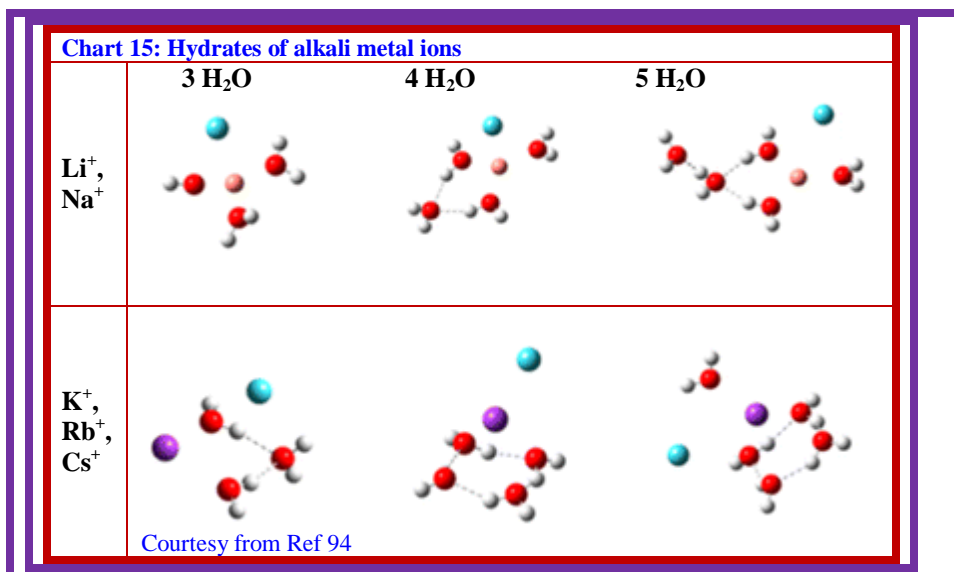
Four water molecules detected by NMR in solution phase is retained as deeply buried ones. The three water molecules (w111, w112, w113) are located in large cleft and form H-bonded cluster and strongly interactive. They are hydrogen-bonded to PR08, Tyr, Asn43, Lys41 and Asn44. The fourth water molecule w122 is located in a small hydrophobic protein cavity and H-bonded to cys38, cys14 and thr11 with lower affinity. The difference between calculated hydrated free energies and those calculated from mass spectra is about 0.5 Kcal mol⁻¹.

Hydration of metal ions

Many proteins contain metal ions and are play a role in electron transfer reactions of metabolic processes. Also, they are responsible for structural stability and modifications and catalysis of bio-chemical reactions.

Li and Cs in H₂O: Zeng et al. [97] ascribed the different hydration nature of ions of Li and Cs to the delicate balance between the alkali-metal-water and the water-water interactions as well as the effect of excess electron. It is inferred that Cs sticks on the surface of water-water H-bonds network (chart 14).





Metals ions in water

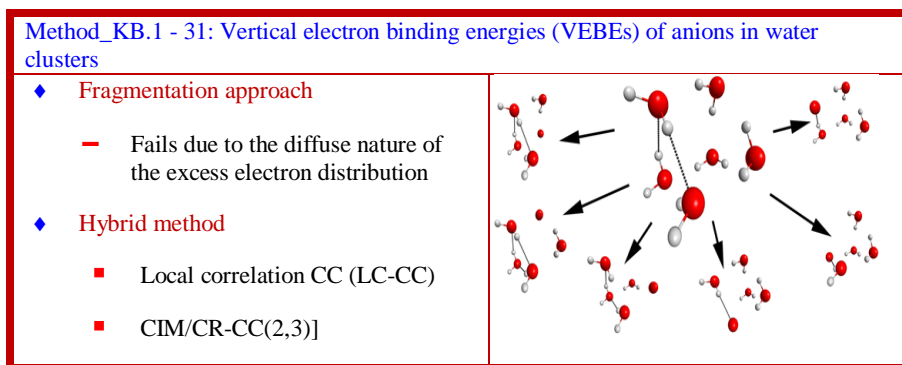
Alkaline and alkaline earth cations in water: Carof[148] obtained NMR relaxation rate from classical MD, electric field gradient (EFG) at the nucleus, and longtime sampling of trajectories. The CQC and experimental results for aqueous alkaline and alkaline earth cations are in good agreement (Inf.Bits. 1, chart 15).



Hydrated alkali metal ions: Ke et al. [94] found that a number of structural isomers result with water molecules in the first hydration shell alkali metal ions (Li⁺, Na⁺, and K⁺). The IR action spectra with argon as a messenger for alkali metal ions with five water molecules are instrumental in probing into these isomers. The competing noncovalent interactions are mirror of microscopic details of macroscopic competition between enthalpy–entropy reflecting structural variation with energy.

The movement of hydrated ions from aqueous to biological system is interesting and multiple types of processes. The movement at entrance of ion channel is dictated by intermolecular forces between ion–water and water–water.



Hydration of Gd by Born–Oppenheimer MD: Carmona-Pichardo et al. [18] studied hydration of Gd and interaction of [Gd(H₂O)₈ or ₉]³⁺ with Ptn (n = 3–7) clusters using Born–Oppenheimer MD (BOMD). The activation of Pt–H bond (2.55 Å) is responsible for absorption of Gd (H₂O)₈³⁺ on the Pt cluster.

Hydrated anions: Xu and Gordon [106] employed CIM/CR-CC(2,3) for anionic water clusters of small-to-intermediate-size (Method_KB-1).



 Cluster-in-molecule (CIM)	Courtesy from Ref [106]
 Completely renormalized CR-CC(2,3) method	

Aqueous hydroperoxide anion: Ma et al. [155] studied (HOO^-) at 300 K by ab initio MD (chart 15). The CQC procedures support co-existence of classical Lewis-picture of H-bonding at the middle oxygen and non-Lewis behavior at the terminal oxygen in HCOO^- in water. In H-bonding to water, H of HOO^- is always a donor.

Chart 15: MD for hydroperoxide anion		
Time scale	Structure	Keynote
<ul style="list-style-type: none"> 25 ps NVT run at 300 K 	 Two solvation structures account for 90%	<ul style="list-style-type: none"> Four H- bond donors to the terminal oxygen atom of HOO^- One or two hydrogen bond donors to its middle oxygen atom
<ul style="list-style-type: none"> 74 ps v 	 Time spent in each type of solvation pattern varies	<ul style="list-style-type: none"> Mean lifetimes : 54 to 109 fs,

Protactinium (V) is probably the natural actinide chemical species, the chemistry being little known (5). The aqueous ions have not been experimentally identified. NPA derived charges are reported using NBO 5.0, which includes 6d in the valence space is suitable for actinides. MPA is sensitive to BSs when diffusion function is present (table 3).

PJH-CF2, a flexible model is favored to any rigid water models. It ensures compatibility and smooth transition when a water molecule moves from QM region with its full flexibility of ligand molecules to the MM region. Russo performed elastic and quasi elastic neutron scattering experiments to probe into H-bonding network dynamics of hydration water on hydrophilic and hydrophobic sites of peptides (N-acetyl-leucine-methylamide (NALMA), and N-acetyl-glycine-methylamide (NAGMA)). The vibrational spectra were investigated with 7-60% hydration level. $[\text{K}(\text{aq})]^+$ ion has a role in transmitting electrical impulses along the nerve. It plays a key role in many cellular processes. Simulation studies indicated that six water molecules are within the initial minimum at infinite dilution. Quasi chemical theory showed four water molecules which are considered as theoretical innershell. The fifth and sixth water molecules appeared as a distinct should on the principle maximum of $g_{\text{kO}}(r)$. $[\text{Na}(\text{aq})]^+$ template was used an initial configuration.

Gas phase clusters cannot give reliable values of energy of aqueous complexes. What is required is long range solvation of complex. To define solution composition one can think of explicitly surrounding a complex with 100 to 1000 water molecules together with other species. For example, solvation of copper chloride complex in 1.017 NaCl can be modeled by CuCl_2 surrounded by 555 water molecules, 10 Na^+ ions and 10 Cl^- ions. As CQC calculation of this size are not possible, semi classical models of solvation field that have been implemented in QC codes. COSMO implemented in ADF package is used.

Table 3a: Spectra of Cu(II) complexes				
Ru	UV-Vis	TD-DFT	B3LYP	3-21G*
			LAN L2Dz	
			LAN L2Dz hybrid	6-31G*
Cu(II)	Synthesis	DFT	B3LYP	6-31G**

x-ray IR Geo_opt Vibr_freq				6-311G* 6-31++G**
Raman (G03)	HF	MPW1PW91		Mixed BSs (Gen) 6-311+G* for cu atom 6-31G** for all other atoms

Table 3b: Hydration of cations and anions

Protactinium (V)	Hydrolysis [PaF5]hH2O h = 8,18	DFT	Gradient corrected hybrid B3LYP		G03	[194]
Chloride, fluoride		Ab initio	MD PJH-CF2	20,000 to 40 000 time steps	D95- V+ 6-31+G	[209]
K+	Inner shell hydration		ΔG	Quasi-chemical theory MD Statistical Mech.	PW91 VASP	[200]
K+, Cl-, HCOO-	Rigid water		Ab initio MD (AIMD) SHAKE	PBE : Perdew–Burke–Ernzerhof functional		[207]

Water molecules in second hydration sphere: Souza et al. [31] performed DFT computations to Simulate twist of aqua ligand induced by the water molecules in the second solvation layer (chart 16).

Chart 16: *trans*-[RuIII(NH3)4(4-pic)(H2O)](CF3SO3)3

<ul style="list-style-type: none"> ◆ EPR ◆ UV–vis 	→ aqua ligand interaction in this low-spin ruthenium(III) complex
<ul style="list-style-type: none"> ◆ DFT 	→ explicit water solvent effect
<ul style="list-style-type: none"> ◆ UV–vis broad- and low-intensity absorption band ◆ 28 500 cm⁻¹ ($\epsilon \approx 500 \text{ M}^{-1} \text{ cm}^{-1}$) 	→ charge-transfer (CT) transition from the equatorial ligands to the Ru β -4dxy orbital (β -LUMO) using DFT calculations
<ul style="list-style-type: none"> ◆ Electronic reflectance spectrum ◆ Broad and intense absorption band around 25 500 cm⁻¹ 	→ CT transition from 4-picoline to the Ru β -4dxzorbital (β -LUMO)

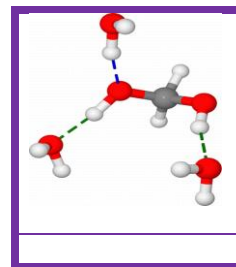
Solvation in aquo-organic mixtures

Mancera [201] investigated hydrophobic and hydrophilic hydration characteristics of DMSO-H2O at different temperatures using MD-simulations. A linear hydrogen bond is formed around O- of DMSO. It increases the life time of H2O-H2O hydrogen bonds in the vicinity of oxygen/sulphur groups. There is a formation of an ordered hydration shells around methyl groups of DMSO (table 4) reflecting hydrophobic hydration, but there is no evidence for temperature dependence.

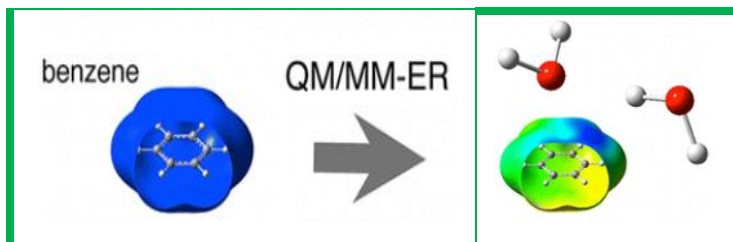
Table 4: CQC of Ice and aquo-organic mixture

DMSO	Water	MD-NVT (MOLDY software)	TIP-4P	[201]
Ice XI		MP2 Vibrational spectra Post-HF	CRYSCOR	[214]

Benzene in water: Takahashiet al.[51] for the first time quantified the contribution of fluctuation of π electrons in benzene to be responsible for affinity of benzene to water (FactBase. 1). Further, the substituent effects of electron donating groups and delocalization effect on hydration of phenyl methyl ether and 1,3-butadiene respectively.

**FactBase. 1:**

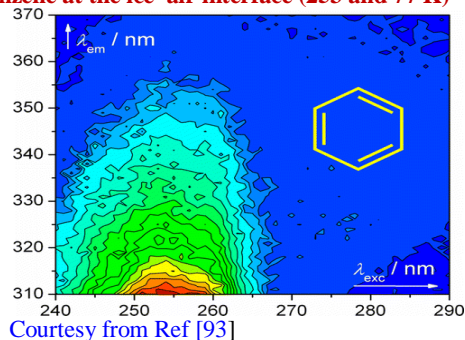
- Benzene -- nonpolar organic liquid
- Solvation free energy of molecule of benzene in ambient water: -0.87 kcal/mol



- Free energy $\delta\mu$ is decomposed based on QM/MM + theory of solutions

$$\delta\mu = \delta\mu_{\pi} + \delta\mu_{\sigma}$$

- $\delta\mu =$ contributions from π electrons + σ electrons of π -conjugated systems
- Free energy $\delta\mu_{\pi}$ arising from the fluctuation of π electrons in benzene was obtained as -0.94 kcal/mol

Benzene at the ice-air interface (253 and 77 K)

- ▶ MD, ground-state DFT
 - 🔔 Benzene associates
- ▶ No bathochromic shift in absorption spectrum
 - 🔔 Benzene interactions with the water molecules of ice
 - 🔔 Dimers microcrystals at the air-ice interface
- ▶ Application
 - 🔔 Predictions and modeling of chemical processes occurring in polar regions

Argon clusters: Pruitt [25] studied water and argon hexamers with HF, CC, EFP, DFT methods with and without dispersion correction (chart 17). The energy contributions for argon cluster are mainly due to dispersion, while that from many body contributions are small.

Chart 17: Performance of EFP, DFT-D, HF-D methods

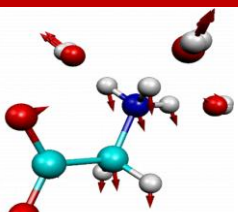
EFP	HF-D
+ Computationally inexpensive	+ HF-D performs well.
+ Captures high-level CC binding energy	+ HF-D method does not rely on such error cancellation
	DFT-D

<p>+ Better than DFT-D</p> <p>Reason: captures both two-body and many-body contributions to the water hexamer very well</p>	<p>+ Reasonable performance</p> <p>+ Reason: fortuitous off-setting cancellation of errors in binding energy due to two-body and many-body contributions</p>
HF-D	: HF corrected for dispersion
DFD-D	: Corrected for dispersion

Methanediol in water: Delcroix et al. [95] studied H-bond interactions of methanediol in water (PCM) by ab initio CQC and Car-Parrinello MD. The symmetric and antisymmetric CO stretching modes at 1050 cm^{-1} are probed with QC results

Creatine in water: Braun et al. [27] reported that CQC found three polymorphs and monohydrate of creatine and also their stability order. The experimental data of heat of hydration corroborate these results.

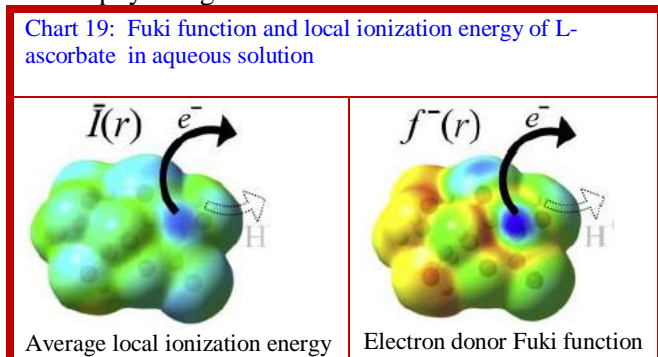
Glycine in H₂O and D₂O: Sun et al. [44] employed THz-absorption spectra and ab initio-MD in elaborating solute-solvent interactions including hydrogen-bond of glycine in H₂O and D₂O (Chart 18).

<p>Chart 18: Typical components of molecular motion in THz absorption spectra</p> <ul style="list-style-type: none"> ◆ Intramolecular vibrations ◆ Rigid-body-like ◆ Rotational motion ◆ Translational motion ◆ Specific couplings to interfacial water molecules 	 <p>Courtesy from Ref [44]</p>
--	---

Dipeptide in water-cluster: Fatehi and Steele [53] made a MD simulations of sarcosine/glycine dipeptide embedded in a 19-water cluster by HF and B3LPY using a multiple-time step scheme based on varying two electron integral screening method.

Emulsions of water with scCO₂: Liu et al. [6] studied solubility of VTfBu/vinyl acetate statistical copolymers in scCO₂ by ab initio CQC, surface tension and glass transition temperatures. These CO₂-philic polymers having appreciable chemical stability will be macromolecular surfactants of next generation for emulsions of water and scCO₂.

L-ascorbate in aqueous solution: Brala al. [14] described electron donor reactive sites of L-ascorbate level under physiological conditions in terms of local reactivity descriptors derived from DFT (chart 19).



Inform.Bits

- $\bar{I}(r)$ and $f^-(r)$ identify same reactive site toward electrophiles on ascorbate molecule.
- Side chain conformations or intramolecular H-bonding have no significant contributions to reactive site position in ascorbate molecule
- Intramolecular H-bonding could play a role in modulation of antioxidant reactivity of ascorbate
- Electron donor reactive site is different from proton donor reactive site for ascorbate

◆ Leaving H(9) proton of hydroxyl group

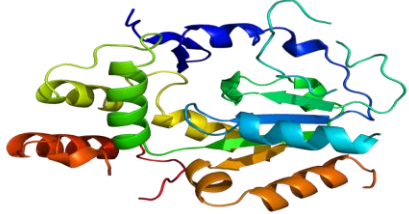
⌋ $f^-(r)$ values are not large



⌋ HOMO orbital

Implies →




- ◆ Proton and electron from ascorbate are transferred through different orbital set

Implicit solvation- SULT1A3 enzyme active site: Bigler et al. [13] reported CQC of dopaminergic ligands in the SULT1A3 enzyme active site with MP2 and DFT (chart 20).

Chart 20: Sulfotransferase 1A3/1A4 is an enzymethat in humans encoded by SULT1A3 gene	
◆ Resveratrol	→ MP2
◆ SULT1A3 active site	→ DFT-M062X_6-311+G*
◆ Structures for the nine ligands bound in the active site	→ Implicit water solvation M062X/6-31G
<p style="text-align: center;">Inform.Bits</p> <p>⌋ 6-carboxydopamine is strongest binding ligand interaction energy > 100 kcal/mol</p> <p style="text-align: center;">+ Nearest neighbor</p> <p>⌋ Four non-dopamine ligands interact with SULT1A3 more strongly than dopamine in the solvated-relaxed model.</p>	
<p style="text-align: center;">Optimization of ligands bound in active site</p> <ul style="list-style-type: none"> ✓ Vacuum ✓ With rigid amino acid residue side chains ✓ Implicit solvation by water with <ul style="list-style-type: none"> ○ Rigid amino acid residue side chains ○ relaxed amino acid residue side chains 	
 <p style="text-align: center;">SULT1A3</p> <p>Sulfotransferase family, cytosolic, 1A, phenol-preferring, member 3 Courtesy of Ref [13]</p>	

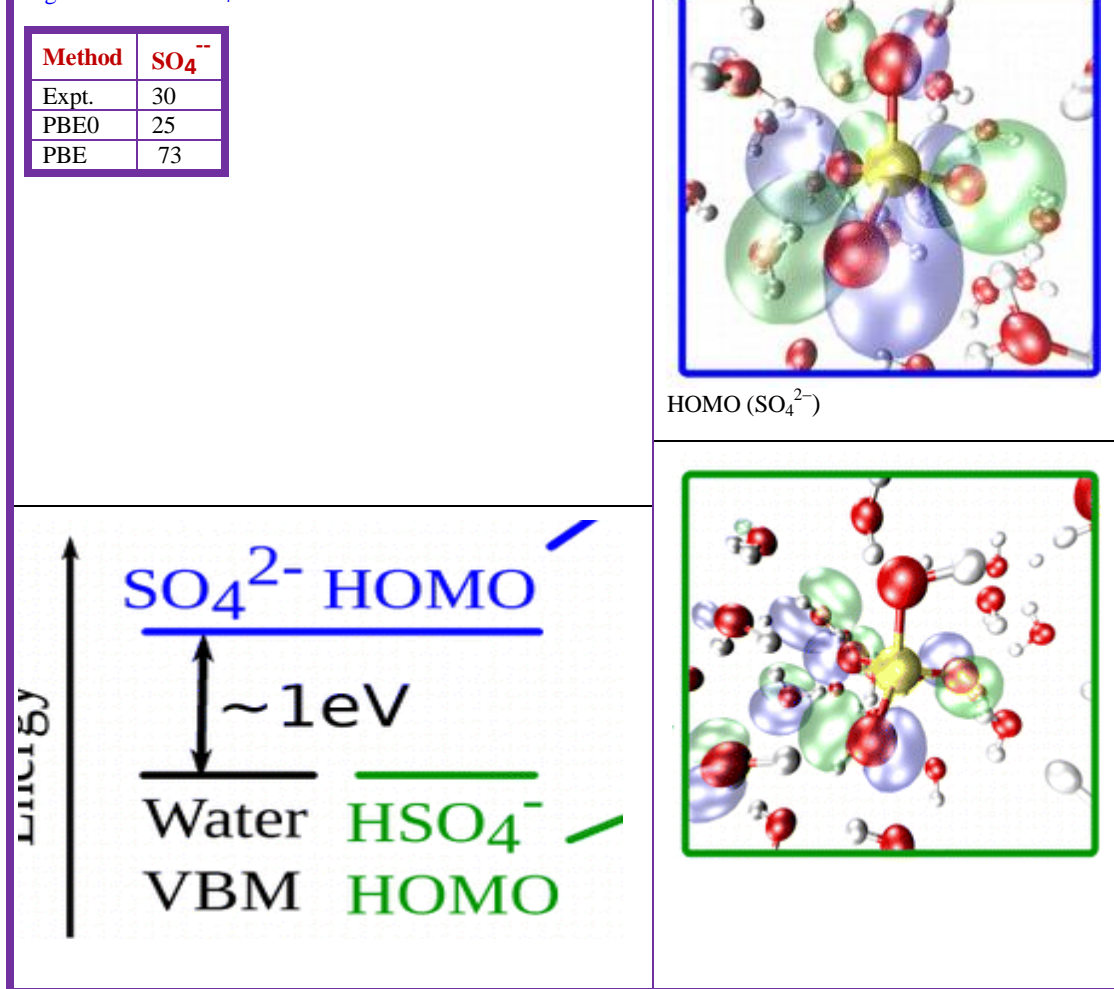
Pt[X ₆] ²⁻ X:Cl, Br	Hydration	¹⁹⁵ Pt NMR	DFT MD	COSMO	[29]
Be	[Be(OH ₂) _h] ⁺⁺ h: 4,8,12	Raman spectra	HF	STO-3G 3-31G* 6-31+G*	[28]
			MP2	6-31G* 6-31+G*	
			B3LYP	6-31G*	
Guanidinium hydrochloride Aqueous solution	Hydration dynamics of water	of	 Steady-state absorption / emission / UV-VIS  Temperature dependent femtosecond-resolved fluorescence		[197]

Flavonoids in benzene and water by DFT + PCM: Vagánek al. [16] computed OH bond dissociation enthalpies, ionization potentials, proton dissociation enthalpies, proton affinities and electron transfer enthalpies of apigenin, luteolin, fisetin, kaempferol, quercetin, epicatechin, taxifolin, tricetin, tricin and cyanidin in benzene and water by DFT and PCM (IEF-PCM B3LYP/6-311++G**) (chart 21).

Chart 21: phenolic chain-breaking antioxidants mechanisms of Flavonoids in benzene and water by DFT and PCM	
<p>Objectives</p> <ul style="list-style-type: none"> → Thermodynamically preferred mechanism → Solvent effect on the homolytic and heterolytic cleavage of OH groups 	<p>Mechanisms for phenolic chain-breaking antioxidants</p> <ul style="list-style-type: none">  Hydrogen atom transfer (HAT)  Single Electron Transfer-Proton Transfer (SET-PT)  Sequential Proton-Loss Electron-Transfer SPLET

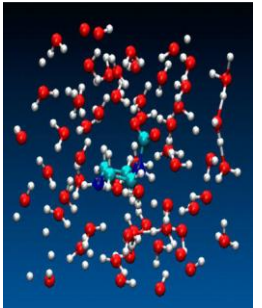
1M sulfuric acid solution: Wan et al. [182] performed ab initio and hybrid DFT computations on 1M aqueous sulphuric acid (Inf.bits. 2, Fig.2).

Inf.Bits. 2:Aqous H ₂ SO ₄	
<ul style="list-style-type: none"> ○ PBE: Semilocal functional <ul style="list-style-type: none"> - Overestimates degree of dissociation of HSO₄⁻ ○ PBE0: hybrid functional <ul style="list-style-type: none"> + CQC is in qualitative agreement with Raman measurements ○ HOMO_ SO₄²⁻ anion is above water valence band maximum → SO₄²⁻ kinetically favored to HSO₄⁻ 	

Fig. 2 HOMO of SO_4^{2-} 

Carbamate zwitterions in aqueous solution: The ab initio MD simulations (chart 22) on deprotonation of aqueous carbamate zwitterions R1R2NHCOO^\pm by bulk water upto 210 ps were studied [180].

Chart 22: Species detected in MD-simulation		
H+-bridging complexes	[water-H+·water] ⁺ ; Zundel ions	
Neutral carbamate complexes	[carbamate-H+·water],	
Carbamic acid structures	R1R2NCOOH	
Typical systems relevant inter and intra disciplinary research		
System	Relevance	
CO ₂ + amine reaction	CO ₂ capture	MD



Courtesy from Ref [180]

Glucose with explicit water molecules and enclosed by implicit solvent: Momany and Schnupf [21] reported low energy conformers of glucose with ten explicit molecules of water and the hydrated molecule enclosed in implicit bulk water by DFT, AMB06C/TIP3P and COSMO models (chart 23, KB. 2).

Chart. 23: Glucose in ten explicit water molecules

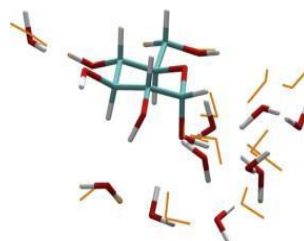
- 21 starting configurations
- Opt: AMB06C/TIP3P force field,
- Opt2: (B3LYP/4-31G) on the sugar carbon atoms
- Larger B3LYP/6-31+G* on all other atom
- Caln. lifetimes of water molecule contact with glucose by DFT-MD

Conformations –
Glucose hydroxymethyl

- | | |
|-------|---------------------|
| → gg, | → counter clockwise |
| → gt, | → clockwise |
| → tg | |

KB.2 Super-molecule (water–water, water–glucose) complex

- ↑ Water molecules migrate off and move around glucose in picoseconds scale
- ↑ Any water molecule does not remain at any one specific site around glucose for a significant time
- ↑ Hydrated configurations with gg-r and gg-c are low energy conformers



Courtesy of Ref [91]78

Trehalose in vacuum, aqueous NaCl: Kan et al. [92] employed MD and DFT in probing into conformational changes of α , α -trehalose in vacuum, water and 0–20 wt % aqueous NaCl solutions (Alg. 3).

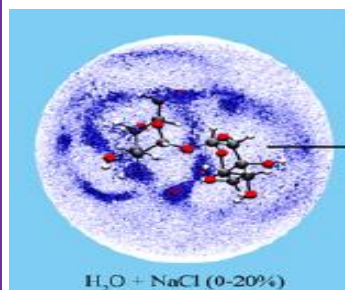
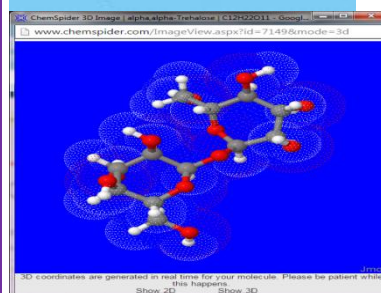
Alg.3: Hydration of trehalose

- ⇒ energy calculation and MD simulation with Polarizable FF
- ⇒ **DFT** + FF parameters : update trehalose every 2 ps
- ⇒ Water molecules around the trehalose are in asymmetry position
- ⇒ Trehalose has stronger tendency for water molecules than Na^+ and Cl^- ions.

If Trehalose concentration is increased (3.26 to 6.31 wt %)

Then Two trehalose molecules approach each other in a nearly anhydrate state & leave a way to keep the favorable hydration structure with the mean trehalose–trehalose distance of 8.6 Å.

- ⇒ The similarity between solvated dimer packing styles (shoulder-by-shoulder or head-to-head) and crystal stacking useful for extrapolation to higher sugar concentrations

 α -D-Glucopyranosyl α -D-glucopyranoside $\text{H}_2\text{O} + \text{NaCl}$ (0–20%)**DFT-based *ab initio* MD simulation**

- + Increased thermodynamic stability of trehalose
- + Formation of intercycle and/or intracycle H-bonds
- + Some thermodynamically unfavorable



Liu et al.[62] reported that in aqueous solution, glucose molecules penetrate into water structure forming voids around the solute (Fig.3). These results in favoring excess electron (EE) to be localized efficiently in the cavity-shaped state in aqueous glucose solution (AGS) compared to that in water.

Decomposition of H_2CO_3 in water of different cluster sizes ([6 to 9] and [10 to 45]): Galib and Hanna[153] reported a concerted mechanism for decomposition of H_2CO_3 in water of small (<10) clusters and stepwise path in bulk water (even 10-45 clusters of water molecules) (KB. 3).

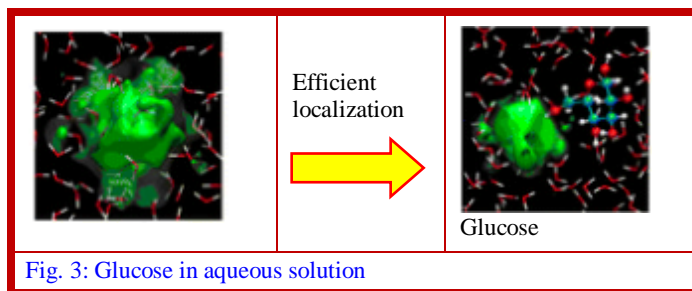


Fig. 3: Glucose in aqueous solution

KB.3: decomposition of H_2CO_3 in water by ab initio metadynamics

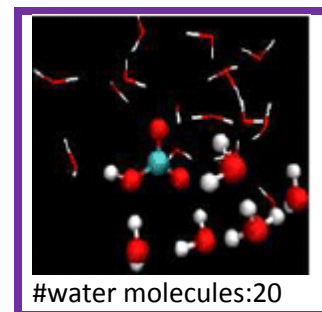
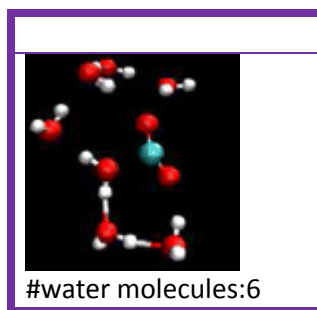
If Range of water clusters is [6 to 9]
Then cyclic transition state \rightarrow concerted proton shuttle mechanism

If Range of water clusters is [10,20 to 45]
Then two-step mechanism

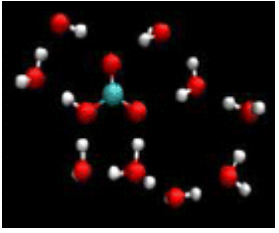
Intermediate: Energetically favorable solvent-separated meta stable ion pair $[\text{HCO}_3^- \text{ [H}_2\text{O]}_x \text{H}_3\text{O}^+]$ \rightarrow prevents formation of the cyclic transition state (sequential route)

If size of cluster increases
Then number of **water** molecules hydrogen bonded to H_3O^+

Clusters of (H_2O)



intermediate increases & concerted \rightarrow stepwise mechanism



#water molecules:9

Courtesy from Ref [153]

Aqueous N-methyl-6-oxyquinolinium betaine: Musto et al. [154] studied electrostatic interactions, spectral profiles of aqueous solution of N-methyl-6-oxyquinolinium betaine by combining Classical/Dynamical and Quantum/Static approaches (chart 24).

Pyridine-water: Liu et al. [108] reported ab initio ADC(2), CASPT2 results of PES of the triplet excited states of the pyridine-water complex (chart 25).

Chart 24: DFT-PCM for solute-solvent interaction

- \rightarrow Explicit solvent models
- \rightarrow (DFT)/(MM)
- \rightarrow DFT-(PCM clusters)

\rightarrow (CIMD), spectrum

Franck-Condon principle, dispersion of TD-DFT vertical transitions

\rightarrow Cluster model (Qst)

Spectrum simulation through quantum vibronic structure, state-specific TD-DFT/PCM

- Solute vibrational modes
- Solute-bulk solvent
 - ◆ Electrostatic interaction
 - ◆ Vibrations
- Quantum broadening effect of the spectra in water
- Vibronic progressions along the solute/solvent H-bonds

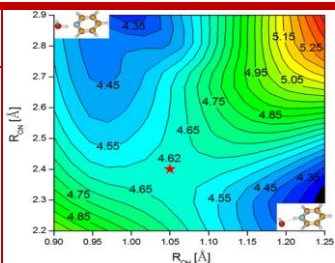
Chart 25: Pyridine-water complex

Low-lying dark charge-separated singlet excited states of $n\pi^*$ and $\pi\pi^*$

Hydrogen-bonded pyridine-water complex

$n\pi^*$
 $\pi\pi^*$

Excited states of the pyridine chromophore



Inf.Bits. 3: of TCBQ in water

- \rightarrow geometry of TCBQ has little effect by explicit water molecules
- \rightarrow After capturing an electron, water has influence on geometry
- KB**
- \rightarrow TCBQ is a good electron acceptor in various environmental media

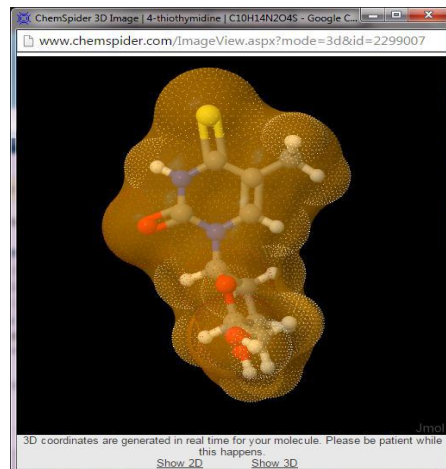
Li et al. [22] calculated electron affinity of tetrachloro-p-benzoquinone in aqueous solution by polarizable continuum model (Inf.Bits.. 3).

4-thiothymidine in aqueous solution: Cui and Thiel[183] performed optimization and calculated SP energy in hybrid paradigm for 4-thiothymidine in aqueous solution (chart 26) and the CQC results will guide development of newer photosensitizers for photodynamic therapy in the coming years.

Benzoporphyrin in aqueous medium: Tessaro et al. [23] applied B3LYP for protolytic species of B-ring benzoporphyrin derivative in aqueous solution (chart 27). The low dipole moment explains the poor solubility in water and also formation of self-aggregates. TD-DFT output of excitation energies and oscillator strengths explain experimental spectral data of dicationic species. The earlier

Gouterman model failed to account for the absorption spectra.

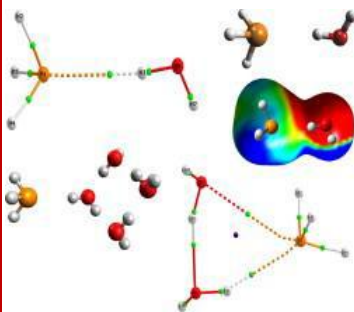
	Method
4-Thiothymine	<ul style="list-style-type: none"> ● CASSCF ● CASPT2 ● QM
Ribose	<ul style="list-style-type: none"> ● CHARMM
Solvent water	<ul style="list-style-type: none"> ● TIP3P
Opt. five lowest electronic states (S0, S1, S2, T1, and T2) and six minimum-energy intersections	<ul style="list-style-type: none"> ● QM(CASSCF)/MM
Single-point Energies	<ul style="list-style-type: none"> ● QM(CASPT2)/MM ● CASPT2



Courtesy from Ref [183]

Chart 27: DFT and MPx models for solvated phosphine with one to six H2O

- Isomers
- Relative stability
- Dissociation energies



Courtesy of Ref [23]

- ◆ CC
- ◆ MPx
- ◆ (DFT)
- ✓ 6-311++G(2df, 2pd),
- ✓ 6-311++G(3df, 3pd)
- ✓ aug-cc-pVTZ]
- ✓ (GGA), hybrid-GGA, meta-hybrid-GGA,
- ✓ meta-GGA, double-hybrid-GGA, empirical London dispersion correction

- Different population methodologies

- ⌋ QAIM,
- ⌋ Chelp,
- ⌋ ChelpG,
- ⌋ MK,
- ⌋ NPA,
- ⌋ GAPT
- ⌋ (QAIM)
- ⌋ NBO

Inform.Bits.PopAnal

- Most of the population analysis failed to determine the phosphorous charge

Hydration of phosphine with post-HF and DFT: Viana and da Silva [11] investigated the interaction of phosphine and $(\text{H}_2\text{O})_h$ [$h = 1: 6$] with MPx, CC and DFT.

CO₂ and H⁺ in aqueous solution: Cuny and Hassanali [150] used ab initio MD in the reaction of proton with CO_3^{2-} . The penultimate micro step is correlated behavior of the transferred protons mediated by the water wires decorating the carbonate (Fig. 4).

Donor-bridge-acceptor system in water: Rivard et al. [185] considered donor-bridge (single water molecule)-acceptor system in aqueous solution. Ab initio MD showed a sub-picosecond charge-transfer pathway through bridge to be dominant. The bridge adapts to an Eigen-like (hydronium) structure. However, it is not possible to describe the multidimensional reaction coordinate only in terms of local coordinated solvent structure and/or structural parameters of the donor-bridge-acceptor system.

Tyrosine/tryptophan complexes in aqueous medium: Kowalska-Baron [12] reported DFT(B3LYP-CAM)/6-31+G(d,p)/PCM results on complexes of Na^+ , K^+ , Mg^{++} , Ca^{++} with zwitterionic tyrosine/tryptophan in aqueous solution. The salt bridged structures contain bidentate coordination of metal cation.

2,4-Dinitrophenyl ethyl phosphate aminolysis in aqueous and gaseous phases : Ferreira [19] studied aminolysis of anion of 2,4-dinitrophenyl ethyl phosphate (2,4-DNPEP) promoted by methylamine in gas and aqueous phases by B3LYP and EFP procedures (chart 28).

Chart 28: 2,4-DNPEP in gaseous and aqueous phases		
B3LYP/6-31++G(d,p)	Gas phase	<ul style="list-style-type: none"> ⊙ Concerted mechanism ⊙ One step ⊙ Activation free energy: 39 kcal/mol
B3LYP/6-31++G(d,p)/EFP	Aqueous Medium	Two-step associative mechanism

Two-step associative mechanism

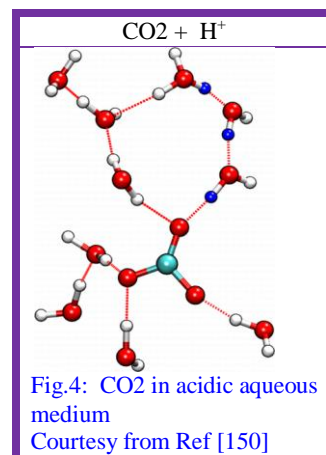
Step 1: Formation of the P-NHMe bond

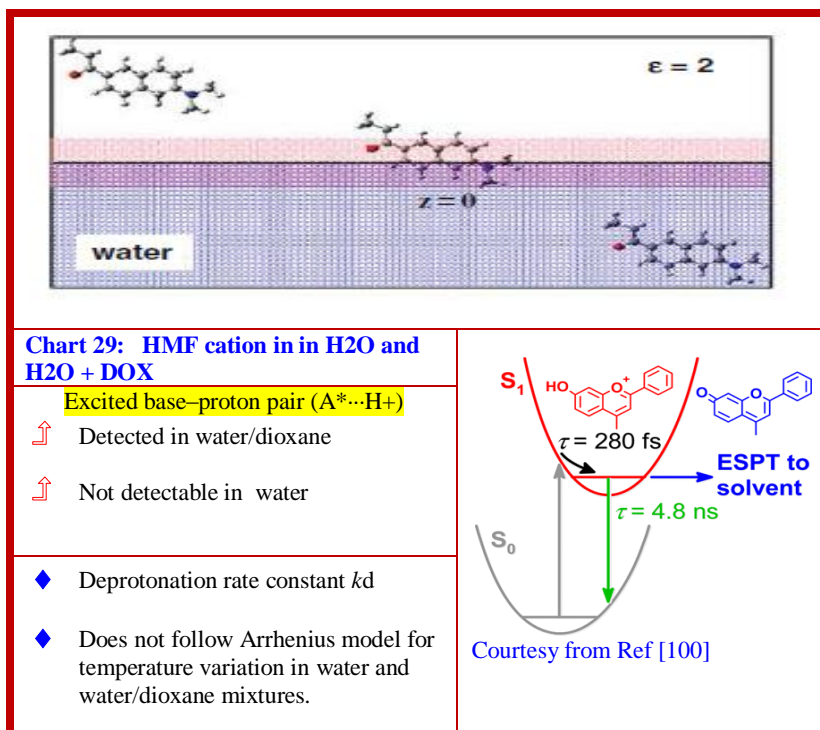
Step 2: Concerted proton transfer
Cleavage of P-O(2,4-dinitrophenolate)

Hydridotetraminecobalt(III) complexes with implicit and explicit solvent molecules: Bhattacharjee et al. [152] employed DFT for hydridotetraminecobalt(III) complexes with implicit solvent and adaptive-DFT/MM-MD simulations for explicit solvent systems. The results are compared with experimental data from spectroscopy.

Acetonitrile-water system: Wang et al. [110] investigated $\text{CH}_3\text{CN}-(\text{H}_2\text{O})_{40}$ cluster with an excess electron (EE) injected vertically using ab initio-MD. The time scale for proton transfer processes.

Excited-state protonwater/1,4-dioxane transfer : Freitas et al. [100] studied excited-state proton transfer (ESPT) of 7-hydroxy-4-methylflavylium (HMF) cation in water and in binary water/1,4-dioxane mixtures (chart 29).

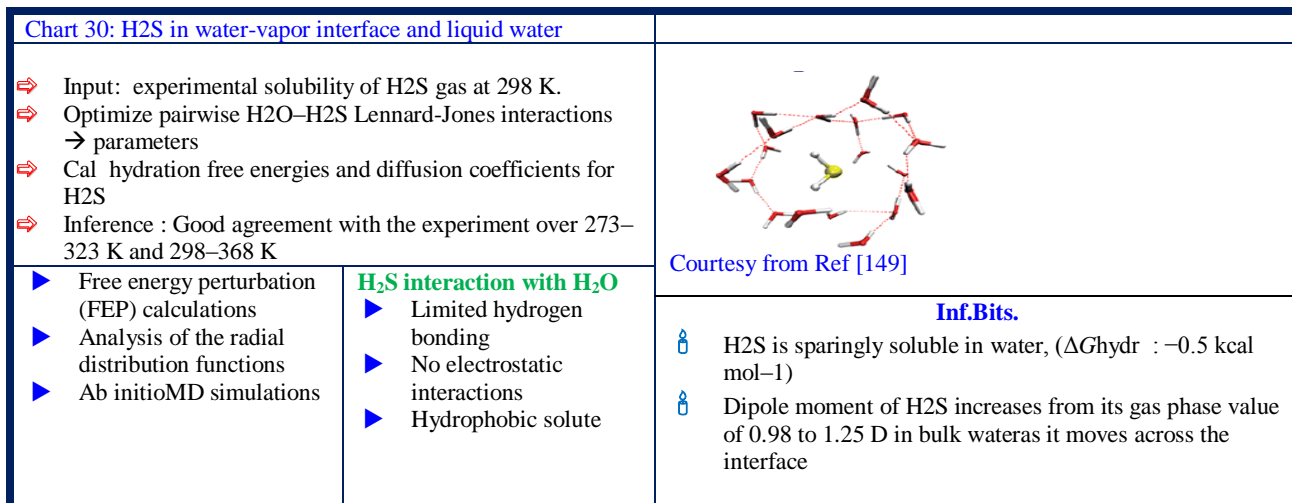




🌀 Interfaces

The common boundary between two different phases of matter (viz. two immiscible liquids, a liquid and insoluble gas, liquid and vacuum, or insoluble solid and liquid) is called an interface. The greater the value of area/volume, the more effective opportunity for surface phenomena and thus the importance of interface processes increases.

H₂S in water–Vapor Interface: Riahi and Rowley [149] studied H₂S in bulk water and at water–vapor interface by MD and polarizable force field (chart 30).



TiO₂ water interface: Cheng et al. [174] applied ab initio MD based on hybrid DFT in the study of [TiO₂(110)] water interface.

Proton transfer in water–ZnO interface: Tocci and Michaelides [186] used ab initio-MD to probe into interfacial water structure and proton transfer in water–ZnO(101□0) interface. The increase in proton-transfer rate at the surface is an influencing factor in going from adsorbed single layer water into multilayer. The non-covalent interactions have consequence in chemical reactivity of wet oxide interfaces. Thus, a complete picture of dynamics of proton transfer at interfaces is still a fertile area of research.

Chemical reactions at metal–water interfaces: Faheem and Andreas Heyden [61] proposed QM/MM- free energy perturbation to model chemical reactions at metal–water interfaces (Alg. 4, chart 31). It is compared with ab initio QM and applied for C–C cleavage in double-dehydrogenated ethylene glycol on a Pt (111) model surface (≈ 8000 atoms).

Alg. 4: QM/MM-FEP method for metal-water interfaces	
⇒ QM/MM: Cal potential of mean force(PMF) of the reaction system	Chart 31: Hybrid CQC for free energy of Complex metal–water system Planewave- DFT Periodic electrostatic embedded cluster (PEEC) method with GTOs MD-simulations
⇒ Input: fixed-size, finite ensemble of MM conformations precise evaluation of the PMF of QM coordinates with its gradient defined within this ensemble	
⇒ QM/MM-FEP method: Cal approximate reaction coordinate using a number of interpolated states	
⇒ Cal free energy difference between adjacent states	
+ Computational speedup of multiple orders of magnitude + Avoids on-the-fly QM calculations + Circumvents challenges associated with statistical averaging during MD sampling	

Metal–Organic Frameworks at the Air–Water Interface: Koitz et al. [163] applied ab initio MD for tris-terpyridine-derived molecule (TTPB) on a water surface. The properties and reaction of TTPB with Zn ions from aqueous phase showed conformational flexibility permitting dynamic rearrangement and chemical interactions (Fig. 5). The polypyrrole nanoparticles split water at the interfaces assisting in keeping electrons and holes apart.

H₂S and H₂O adsorption on dolomite surface: Shen et al. [63] employed DFT and ab initio CQC to understand thermodynamics of competitive adsorption of H₂S and H₂O on dolomite (104) surfaces. The adsorption energy in vacuum and aqueous solution are –13.6 kJ/mol and –12.8 kJ/mol respectively.

Membranes: Savage and Voth [184] found benzene is attached to two water molecules symmetrically through hydrogen bond (chart 32). IR spectrum is in better agreement with Eigen isomer, when Ar-tagged. These results throw light on behavior of protons on water/organic-phase interfaces.

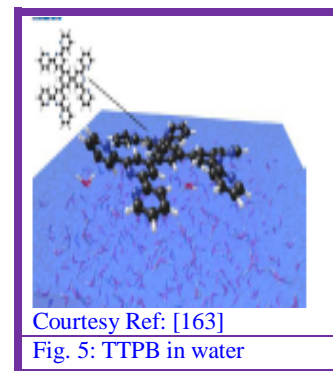
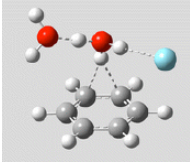
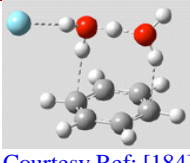


Chart 32: H-bonding between protonated water and neutral benzene

Chart 33: All-atomistic force field (AAFF) for a new class

Standing Eigen" isomer	Contains hydronium core		of halogen-free chelated orthoborate-phosphonium ionic liquids → Basis_AAFF: AMBER framework → Caln. of force field parameters for phosphorus and boron atoms → FF parameters
Crouching Zundel" isomer	Attaches to benzene ring symmetrically via both of its water molecules	 Courtesy Ref. [184]	→ BL → BA → DH → Validation
Protonated water dimer ("Zundel ion") on benzene	Asymmetric binding of protonated water dimer to benzene ring through a single water molecule	Normal-mode analysis using DFT corrected for Dispersion functionals	<ul style="list-style-type: none"> ✦ Vibration frequency data <ul style="list-style-type: none"> ○ Expts. ○ Ab initio calculations ✦ Torsion energy profiles deduced from ab initio calculations ✦ 12 Ionic liquids <ul style="list-style-type: none"> ◆ Tetraalkylphosphonium cations ◆ Chelated orthoborate anions

PES for water dimer: Jankowski et al. [99] developed a PES for water dimer with ab initio CQC for varying monomer coordinates. The quarter million points in the 12-dimensional configurational space from previously published interaction energies are fitted into a model. The minimum and saddle-point structures of the potential surface were nearer to ab initio CQC results. The computed second virial coefficients agreed well with experimental values.

Water-amorphous silica nanoparticle (NP) interface: Brown et al. [170] investigated optimum geometric structure at water-amorphous silica nanoparticle (NP) interface using solid-state NMR, X-ray photoelectron spectroscopy from a liquid microjet and DFT. The (de)protonated silanol species established by DFT could not be directly identified with NMR.

The applications of silica nanostructures in drug delivery, catalysis and composites made a mark. But, a detailed picture of the surface chemistry, aqueous interfaces, and recognition of biomolecules is still obscure with spectroscopic/ imaging probes.

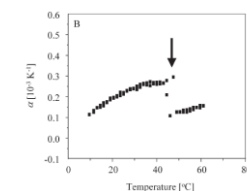
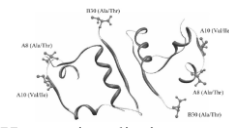
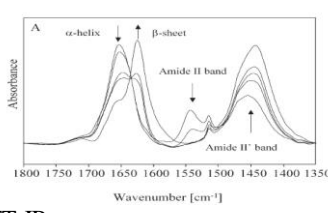
Water physi-sorption on carbon nanotubes (CNT): Stein et al. [7] reported that wet (CNTs) array mass is 200% more than that of dry CNTs at ambient conditions. The presence of water layer of thickness greater than 5 nm on the outer CNT surface is inferred from CQC.

All-atomistic force field for ionic liquids: Wang et al. [156] proposed and validated a new force field for ionic liquids (chart 33).

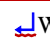
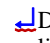
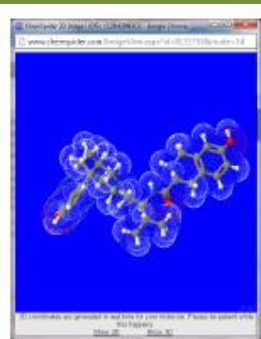
🌀 Biomolecules

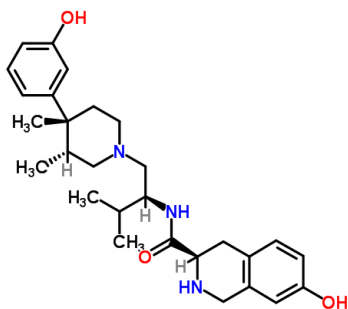
In bio-systems, involuntary inhalation of pollutants, metal vapors in industry, petrol vapor at filling stations are a few professional hazards. The oral/intravenous/dermis/implant mode of administration pharmaceutical preparation and (risky) addiction to drugs and adulterated/misuse addiction to drugs and adulterated/misuse of medicines or contaminated/state/rotten food are the sources of miscreants into the human (bio) system from external environment. The mal functioning/disease and aging fuel the deterioration of health, sometimes leading to fatal condition. Table 5 incorporates the spectra with CQC.

Table 5: Spectra of biomolecules by CQC

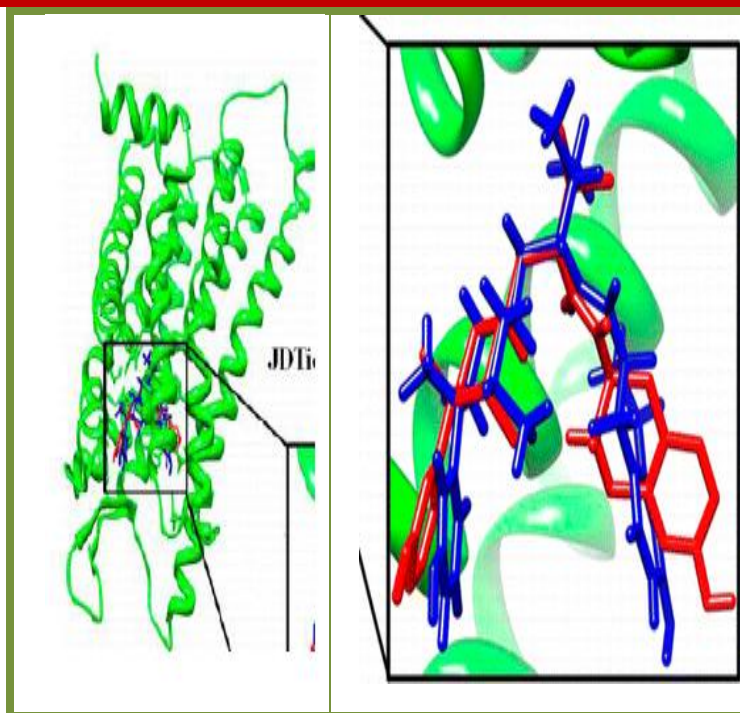
Insulin (monomer/ dimer)	 PPC PM3-D	 Human insulin in dimeric state 1GUJ.pdb	 FT-IR		
First generation dendron	Built from cyclotriphosphazene core	IR Raman	DFT PBE (TZ2P) polarising functions	PRIRODA SHRINK	[77]

Human κ -opioid receptor: Leonis et al. [49] reported results of MD, free energy, and *ab initio* computations using crystal structure of the human κ -opioid receptor (κ -OR) to probe into binding mechanism in complexes with antagonist JDTC and agonist SalA (chart 34).

Chart 34: Modeling of antagonist JDTC in water											
		Method									
→ Antagonist JDTC	 Water	Effect of membrane upon conformational dynamics.									
→ Agonist SalA	 DPPC lipid bilayers										
<table border="1" data-bbox="186 1134 470 1281"> <thead> <tr> <th></th> <th>CQC</th> <th>Expt</th> </tr> </thead> <tbody> <tr> <td>ΔG JDTC</td> <td>-31.</td> <td>-14.4</td> </tr> <tr> <td>ΔG SalA</td> <td>-9.8</td> <td>-10.8</td> </tr> </tbody> </table>		CQC	Expt	ΔG JDTC	-31.	-14.4	ΔG SalA	-9.8	-10.8	Inference.Bits ΔG s are in qualitative agreement	 JDTC <p>Two conformations “V-shape” (water-mediated) intramolecular interaction → stabilization Extended conformation → enough suppleness for binding effectively</p>
	CQC	Expt									
ΔG JDTC	-31.	-14.4									
ΔG SalA	-9.8	-10.8									
Unique Inform.Bits		<ul style="list-style-type: none"> + Unattainable information on the dynamics of human κ-OR earlier now possible + Rational design of drugs with desirable pharmacological properties 									

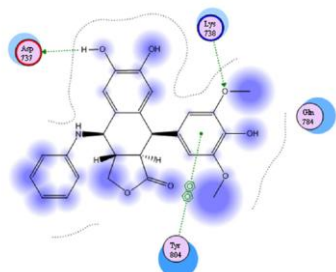
**IUPAC Name**

(3R)-7-Hydroxy-N-[(2S)-1-[(3R,4R)-4-(3-hydroxyphenyl)-3,4-dimethylpiperidin-1-yl]-3-methylbutan-2-yl]-1,2,3,4-tetrahydroisoquinoline-3-carboxamide

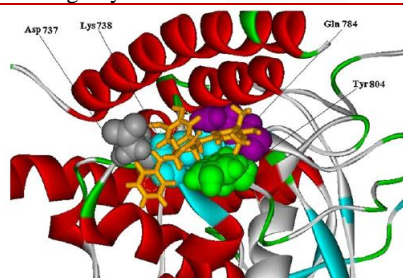


Courtesy from Ref [49]

Molecular Formula: $C_{28}H_{39}N_3O_3$
 Average mass: 465.628 Da
 CAS Registry Number : 361444-66-8



Human-TP II α -epidodophyllotoxin binding site



Epidodophyllotoxin

Implicit water; Generalized Born model
 Macro model V9.1(eMBrAcE)

Unfolding

Hydrophobic interaction has a pivotal role in protein chemistry mainly because of their influence on the functional characteristics and tertiary structure.

Partial unfolding and subsequent refolding into aggregated β strands refer to conformational events. Hydrophobic interaction drives aggregation of insulin.

It involves rearrangement of hydrophobic side chain amino acid residue that leads to overall reduction in number of unfavorable protein-water contacts. Ramraj [73] et al. compared DFT-dispersion with

Glucose Fructose	Toluene 3-Me indole p-OH toluene	DFT-dispersion	MO6	GLYCAM06 MM3 force fields	[73]
Phosphonic Fosfomycin	Raman NMR 2D-correlation Spectra	DFT B3LYP	6-311++ G(2df,p)	GIAO NMR PCM-IEF ^{31}P NMR ^1H NMR ^{13}C NMR	[87]

CCSD(T). PM3-dispersion and GLYCAM06 yield interaction energies with one Kcal mole⁻¹ of the DFT-D values. MM3 differs by more than 2 Kcal mole⁻¹ in carbohydrate–aromatic interactions. B3LYP and BLYP fail to accurately derive dispersive interactions. M06 family of functional proposed by Truhlar successfully describes short range dispersive interaction.

Drugs

The incidence of morbidity and mortality is still significant due to carcinoma, HIV/AIDS, cardiovascular disorder and tuberculosis. The popular anti tubercular drug (1) of 1970s contain the active ingredient isonicotinic acid hydrazide in the pharmaceutical formulations (Isoniazid, isonex etc.). Recent world health organization (WHO) studies predict that in the coming two decades, the number of infected patients and the death rate will supercede even those suffering with other fatal diseases. Mycobacterium tuberculosis (MTB) bacillus causes tuberculosis and now TB strains resistant even to multi drug therapy have been detected. Further, TB now is an opportunistic infection for patients suffering from haemodialysis, immuno deficiency including HIV/AIDS or for women in productive age group.

This led to the surge in probing into detailed mechanistic study in-vitro/ in-vivo / in-silico and sorting out new lead structures. Bachi et al (2) recently reported a QSAR model for the variation of reciprocal of minimum inhibitory concentration (MC) of substituted INH with a few molecular (topological) descriptors. The five parametric MLR model explained the biological response very well compared to lower (two-, three-) parametric models. Dias et al (3) proposed a series of biflavonoids to model the active and inactive ones for tubercular bacilli. The explanatory parameters –hydration energy, heat of formation and log P – are obtained from semi empirical level of theory employing PM3 Hamiltonian making use of AMPAC. In continuation of our efforts in the study of solution equilibria/quantitation of drugs (4-7), calculation of molecular descriptors, interactions between small molecules(8-11), predictive modeling with PCR, PLS and NNs/GAs, we have taken up the study of hydrazides with computational quantum chemistry. The objectives of the current project are (1) static electronic structure of various conformers of aliphatic, aromatic (five- and six- membered) hydrazides, mono- and di- substituted ones and derivatives, (2) effect of 1 to 6 molecules/bulk of solvent for typical compounds, (3) complexes with copper(II), cobalt(II) etc., (4) molecular dynamic studies to calculate realistic average energies (5) selection of best set of compounds using docking, COMFA, COSIMA and (6) energetics of reaction of hydrazides with bio-molecules/model compounds

☞ Conformers

The complete (exhaustive) search even for small molecules with multiple chiral centers or in hetero atoms optimization becomes a hard problem. The optimized geometry of a conformer is refined at various levels of theory. Under each frame of theory, the complexity of BS is increased.

The energy is calculated at different dihedral angles of four atoms (A, B, X, C) keeping all other at a fixed value. The guidelines are literature reports, stable conformers or an educated guess value. The increments are generally 30° resulting in cis-, gauche, persp- and trans- forms.

An increment of 15° and 2° give rise to mathematically better optimum conformers (chart 8). With increase in number of asymmetric centers, the conformers grow. Testing at different levels of theory is a herculean task. Statistical experimental design (uniform, CCD) may be a via media between one variable at a time (OVAT) resulting in unrealistic/wrong results and exhaustive search, which is time prohibitive even on work stations of today. Rotation around a bond or varying angles for important substructures of the fragment is in practice, which throws light on the energy of conformers.

The initial geometry of a moiety (molecule/atom) can be given in any of the coordinate systems available. It is trivial to convert to all other coordinate systems. The question arises which is the best system from computational point of view and quality of refined geometry? The best choice for Q-Chem is delocalized internal coordinate system. G03 uses internal co-ordinates in computations. It is not strange that different geometries are obtained with different packages. The main reason is the type of co-ordinate system used and also optimization algorithm/convergence criteria and number and type of object functions. If the input geometry is far away from the optimum, a stepwise refinement using different models of

SEMO, STO-3G of ab initio is a short cut. Although, not necessarily, trial and error method for optimization is a part of routine housekeeping in CQC jargon. The heuristics generally followed are accumulated success stories for similar compounds, and meta-rules from continuous progress of the field and the expertise of the school. The general practice is to start with an inexpensive lower method and progressively moving upward for a typical compound under study and then skipping some of them for rest of species.

Now, the differences in bond length, dihedral angles from CQC and experiments are less than the experimental precision and accuracy. The algorithm for geometry optimization of a molecule in AMPAC involves hierarchical and multiple convergence tests. In the first phase, electronic energy and diagonal elements of density matrix are tested. In the second level of hierarchical testing, multiple criteria for convergence of geometry are attempted. It is followed by nearness of heat of formation (HoF) in successive iterations. In case of divergence of geometry within a prefixed number (3 to 5) of cycles, the job is aborted with an error message that 'further iterations are not justified.'

Nagy[112] detailed the conformers for 2-halo (F, Cl) substituted ethyl alcohol or phenol in CCl_4 or water by CQC (table 6).

Table 6: Halo substituted ethanol and phenol in CCl_4 and H_2O	
<p>Geo.opt.gas</p> <ul style="list-style-type: none"> ⇒ DFT/B97D/aug-cc-pvtz ⇒ ab initio MP2/aug-cc-pvt ✓ Coincide with exptal values 	<p>Inf.Bits.</p> <ul style="list-style-type: none"> ▶ OCCF gauche/trans ratio for 2F-ethanol by CQC \approx experimental compositions ▶ In CCl_4 predominant gauche has intramolecular hydrogen bond ▶ In H_2O, gauche conformers with HB \approx NoHB ▶ For 2X-phenol species, CBS internal free energies, IEF-PCM and FEP/MCsolvation free energies show predominant internally hydrogen-bonded conformer <p style="text-align: center;">Gas or CCl_4</p>
<p>Solvent</p> <ul style="list-style-type: none"> ⇒ Continuum solvent method ⇒ Explicit solvent + Monte Carlo using free energy perturbation 	
<p>relative internal free energies</p> <ul style="list-style-type: none"> ⇒ CBS 	

The sampling of conformational space of a peptide is carried out through a topographical exploration of potential energy methods (SAA) (9) or in the configurational space (Monte Carlo) or MD. Twelve lowest energy conformers for each diastereomer of sulfinyl dilactones using DFT method of G03 package are reported (table 7). ^1H NMR spectrum was computed quantum mechanically at B3LYP level using 6-31G(d,p) functional and GIAO method. Relative Energies, relative Gibbs free energies, population fractions, absolute optical rotations, weighted optical rotations and total optical rotatory power for diastereo-isomers are reported.

+ Sampling in configurational space. convergence is achieved where a Maxwell Boltzman weighted ensemble is obtained

– Local minima in conformational energy space

Table 7: Spectra by CQC

► Synthesis ► Absolute configurations	Sulfinyl dilactones	<ul style="list-style-type: none"> ▪ ^1H NMR ▪ Optical (Vacuum) rotations 	<ul style="list-style-type: none"> ❖ DFT ❖ MM 	B3LYP 6-31G (d, p) G03 MMFF94	[80]
			EtOH	DFT/PCM	
► Conformational analysis	Benzyl acetoacetate	<ul style="list-style-type: none"> ▪ IR ▪ Raman ▪ NMR <ul style="list-style-type: none"> ○ ^{13}C ○ ^1H 	<ul style="list-style-type: none"> ❖ DFT Gas phase	B3LYP/6311++G*// B3LYP/6-311++G* ► GIAO_NMR	
			CH3CN	PCM	
conformational stability trans gauche	ethanol	• Mid_IR (gas)	4000-300 cm^{-1}	MP2(full)/6-31G(d) G03	[82]
		• Raman gas			
		• Ar_matrix, Xe_solution			

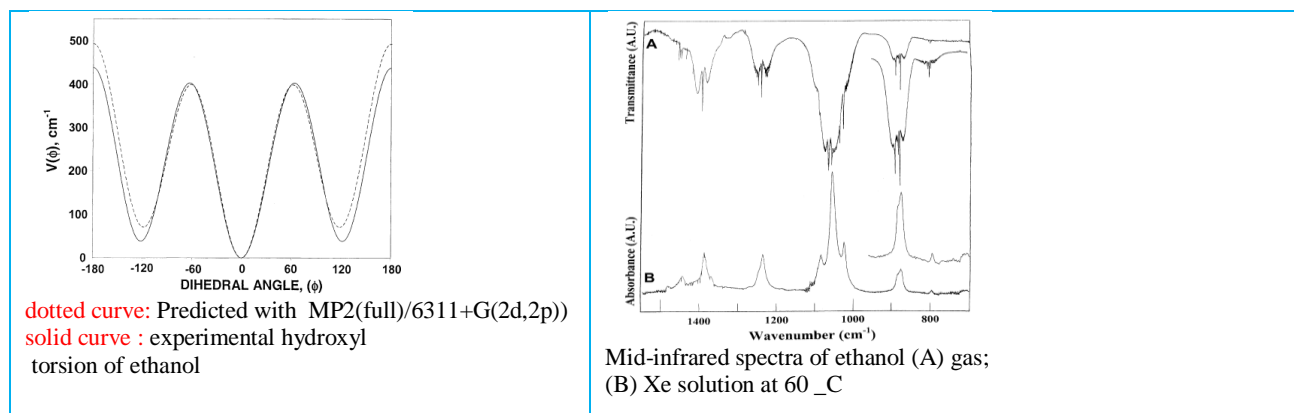


Chart 35: Absorption and emission spectra of anionic p-coumaric methyl ester in gas and water phases

Geometry opt	<ul style="list-style-type: none"> ✓ CASSCF ✓ CASPT2
→ Ground state	
→ Bright excited state	DFT
	<ul style="list-style-type: none"> ✓ B3LYP ✓ CAM-B3LYP ✓ PBE0
Inform.Bits	
○ Average # water molecules	
○ Decreases around the phenolic oxygen	
○ Increases around the carbonyl oxygen.	
Absorption spectra	
○ Charge flux from phenolic towards carboxylic	

Spectra

Absorption and emission spectra of p-coumaric methyl ester: Frutos-Puerto al. [15] reported absorption and emission spectra of anionic p-coumaric methyl ester in gas and aqueous solutions by CQC (chart 35).

Emission spectra

Charge flux from carboxylic toward phenolic



Fluxes are similar in gas and water phase

pK_a of ligands

pK_a of acids/bases is a century old task approached by experimental methods. The measurements of activity of Hydrogen ion with hydrogen electrode/GE, UV-visible absorbance/¹H NMR propelled the accuracy and simple graphical to non-linear statistical parametric algorithms joined the band wagon. Information based criteria, sophistication of instruments/reputation of research school was considered to pick up the so called critical/reliable constants in 1970's. Later, Merck and other industries repeated the experimental measurements for a select set of thousands of compounds of relevance in pharma research. The prediction of pK_a for a number in a homologous series was appraised with success in 1980's.

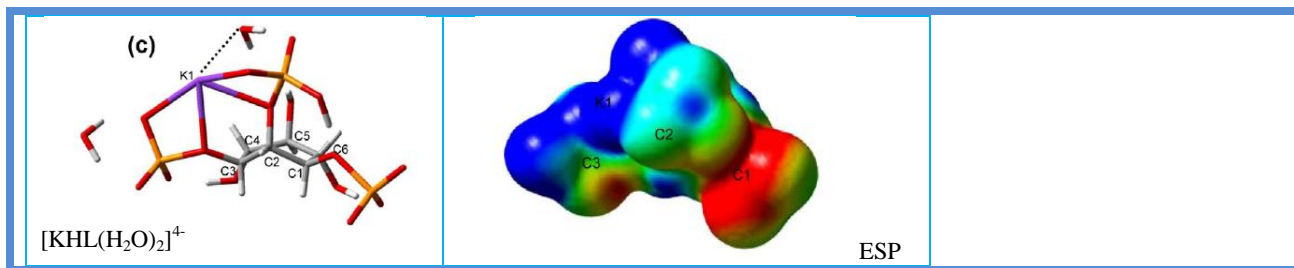
The earliest attempts of quantum chemists to compute pK_as (table 8) was with a little success for a few simple compounds, but with a large error (> 2 to 4 log units) for di-/tri- basic acids. This was compromised viewing from a correlation window and proposing QC computed value can be projected on to the experimental scale.

Table 8: pK_a by CQC and comparison with experimental values

pK _a	H ₂ O	Benzo-quinuclidine series		B3LYP/6-31+G(d) geometric optimization/frequency/no symmetry constraint
		UAHF	UAKS	pKa (exp.)
I	11.25	11.25	10.58	CPCM B3LYP 6-311++G (2df, 2p) [10] Radii of UAHF, UAKS, Pauling, Bondi and KLAMT
II	7.98	7.84	7.79	
III	4.17	4.05	4.46	
IV	2.25	2.25	2.10	
MAD	0.40	0.39	–	

Table 8b: pK_a by experimental and CQC methods

	water	pK _a	Resorcinol	UV-vis	HF/6-31 + G(d) B3LYP/6-31 + G(d)	[211]
			Gaussian	MP2 PCM		
EtOH	water	pK _a	Chrysin	UV-Vis	HF/6-31G(d) HF/6-31 + G(d)	[210]
MeOH DMSO	4-halo(Cl, Br) pyridine N-oxide	pK _a	Potentiometry – STOICHIO for pK _a	RHF	6-31++G** GAMESS	[69]
				Tomasi G98 Rev A9		
Protonation K ⁺ -interaction	inositol 1,2,3-trisphosphate	³¹ P NMR	RHF/3-21 + G*	G03		



Charmet et al. [113] compared CQC generated IR spectra and pKa values of indole in aqueous phase with experimental values (chart 36). Castro used Tomasi method for inter molecular H-bonds between 7(O⁻) chrysinate anion and H₂O molecules. The pKa values from QC coincide with experimental ones.

The accuracy of results of CPCM model predominantly depends upon cavity models. Yu reported a mean absolute deviation of 0.40 pKa units for CPCM solvent model using different types of radii (UAHF, UAKS, Pauling, Bondi and KLAMT) from experimental values. It is opined that pKa s of large substituted ammonium ions in water.

Geom. opt.	<ul style="list-style-type: none"> ▶ DFT ▶ MP2 							
IR	<ul style="list-style-type: none"> ▶ B3LYP ▶ B97-1 	<p style="text-align: center;">pK_a</p> <table border="1"> <tr> <td>⇒ Gas phase basicity</td> <td> <ul style="list-style-type: none"> ▪ G3 , G4 ▪ CBS extrapolation of Petersson ▪ DFT </td> </tr> <tr> <td>⇒ Proton affinity</td> <td> <ul style="list-style-type: none"> ▪ Implicit Solvation models ▶ SMD and SM8 </td> </tr> <tr> <td>⇒ Aqueous</td> <td> <ul style="list-style-type: none"> ▪ Hybrid ▪ SP energy (MP2) ▪ CCSD(T) </td> </tr> </table>	⇒ Gas phase basicity	<ul style="list-style-type: none"> ▪ G3 , G4 ▪ CBS extrapolation of Petersson ▪ DFT 	⇒ Proton affinity	<ul style="list-style-type: none"> ▪ Implicit Solvation models ▶ SMD and SM8 	⇒ Aqueous	<ul style="list-style-type: none"> ▪ Hybrid ▪ SP energy (MP2) ▪ CCSD(T)
	⇒ Gas phase basicity		<ul style="list-style-type: none"> ▪ G3 , G4 ▪ CBS extrapolation of Petersson ▪ DFT 					
	⇒ Proton affinity		<ul style="list-style-type: none"> ▪ Implicit Solvation models ▶ SMD and SM8 					
⇒ Aqueous	<ul style="list-style-type: none"> ▪ Hybrid ▪ SP energy (MP2) ▪ CCSD(T) 							
hybrid approach ▶ B3LYP ▶ N07D basis set								
error in cm ⁻¹								
	mean unsigned	RMS						
	5.1	7.2						

🌀 Acid ionization on ice quasi-liquid layer

Riikonen et al. [102] probed into ionization of deuterated hydrogen iodide (DI) and nitric acid (DNO₃) on QLL, where water molecular species with weakly bonded hydrogen-bond single-acceptor double-donor are available abundantly. The ice_QLL forms below the bulk ice melting temperature and it is modelled with empirical FF at nanosecond time scale and chemical reactivity by ab initio MD. These studies shed light on atmospheric (upper troposphere and lower stratosphere) chemistry viz. acid ionization and proton transfer.

Proton transport in hydrated perfluorosulfonic acid membranes: Savage and. Voth [184] showed Proton transport in hydrated perfluorosulfonic acid (PFSA) in picosecond time scales and exhibits caging effects around nano second intervals (chart 37)

Hydrogen bonds (Fig. 6)

Hao-Hong[81] reported seven hydrogen bonds in APHEN-H⁺ cations of which five hydrogen bonds are shown in 2-D layer. The remaining two serve to the formation of 3-D network. In spite of the fact,

Chart 37a: Pico and nano second scale Proton transport

Proton transport in hydrated perfluorosulfonic acid membranes

- Subdiffusive for several hundred picoseconds
- Extent of sub-diffusive nature depends upon water conc.
- Caging effects up to at least 1 ns for excess proton
- For complete picture
 - Multiple detailed nanosecond trajectories
 - ✦ Far away from current ab initio MD capabilities

CAH...I hydrogen bonds are relatively weak; they play a key role to hold together the overall crystal frame. The neighboring $[\text{Ag}_2\text{I}_4]_n^{2-}$ polyanion chains act as “cavities” wherein APHEN-H⁺ cations lie sandwiched between two adjacent chains.

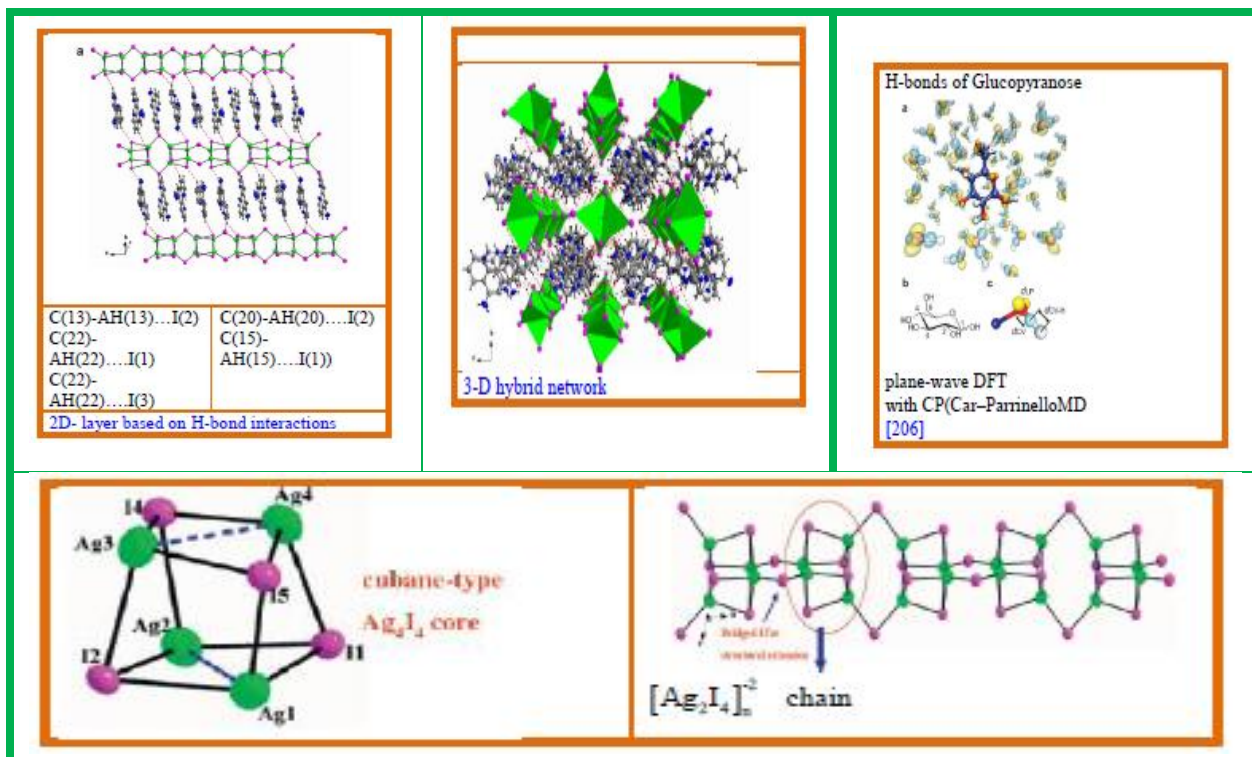
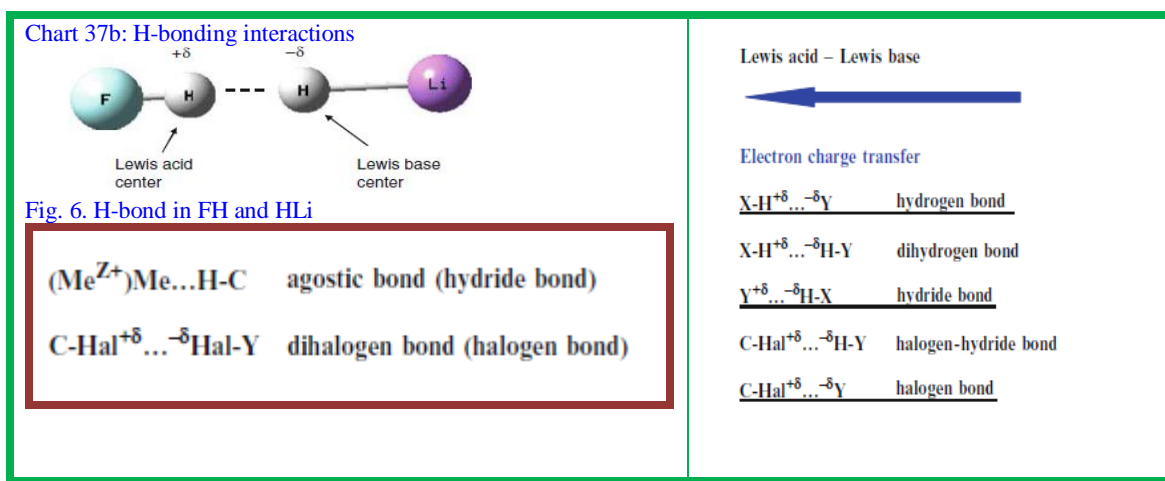
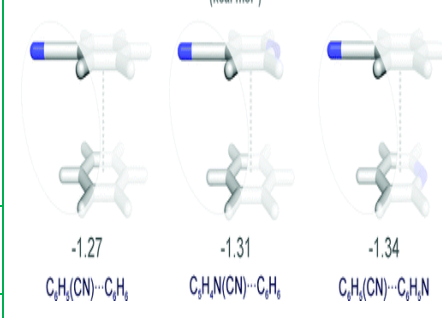


Table 9 summarizes the DFT application in study of NMR spectra along with synthesis.

			DFT		
Pyrimidine derivatives	Synthesis NMR	^{15}N NMR ^1H NMR ^{13}C NMR	B3LYP	6-311++G(d,p)	(G03)

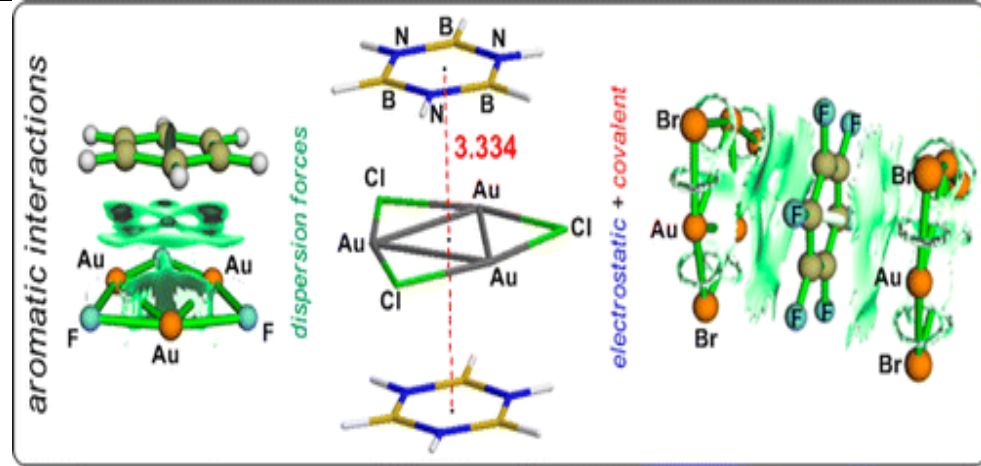
Hybrid iodoargentate [(APHEN-H) ₂ (Ag ₄ I ₆)] _n (1) APHEN : 5-amino-1,10-phenanthroline	XRD UV-vis Optical diffuse-reflectance FT-IR		PW-91 GGA	CASTEP code	Effect of CN Substituents on Stacking Interactions (kcal mol ⁻¹) 
Maquinox	Synthesis NMR	NMR-GIAO			
Indole derivatives		NMR-GIAO (G03) FT-IR	B3LYP PW91	6-311G(d,p)	

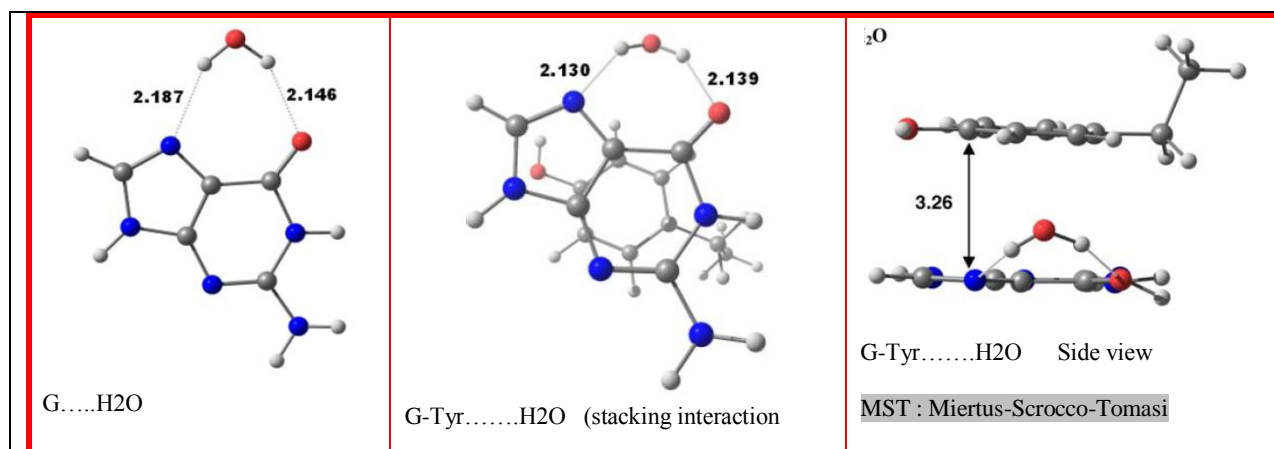
Stacking interactions

Substituent effects: Wheeler [45] used DFD-D and CCSD (T) results to explain substituent effects through direct interaction model (chart 38). The sign of ESP above the face of an aromatic ring or molecular quadrupole moment are useful to probe into stacking interactions in fluorinated benzenes and protein-RNA complexes on the regiochemistry of fluorinated base analogues.

In yesteryears, substituent effects in π -stacking interactions are around induced changes in the aryl π -system, which are inadequate to explain high level CQC descriptors. Tsipis and Stalikas [35] inferred that stacking interactions arise from dispersion and electrostatic forces in supra molecular assemblies of $\{[c\text{-Au}_3(\mu\text{-X})_3](\text{C}_6\text{H}_6)\}_\infty$, $\{[c\text{-Au}_3(\mu\text{-X})_3]_2(\text{C}_6\text{F}_6)\}_\infty$, and $\{[c\text{-723 Au}_3(\mu\text{-X})_3](\text{B}_3\text{N}_3\text{H}_6)_2\}_\infty$. The contribution of covalent bonding is small here. A linear correlation has been found between interaction energy ΔE_{int} (ΔE_{disp} , ΔE_{elstat} , ΔE_{orb} , ΔE_{Pauli}) with physical properties.

Chart 38: Stacking interactions using quantum chemical calculations

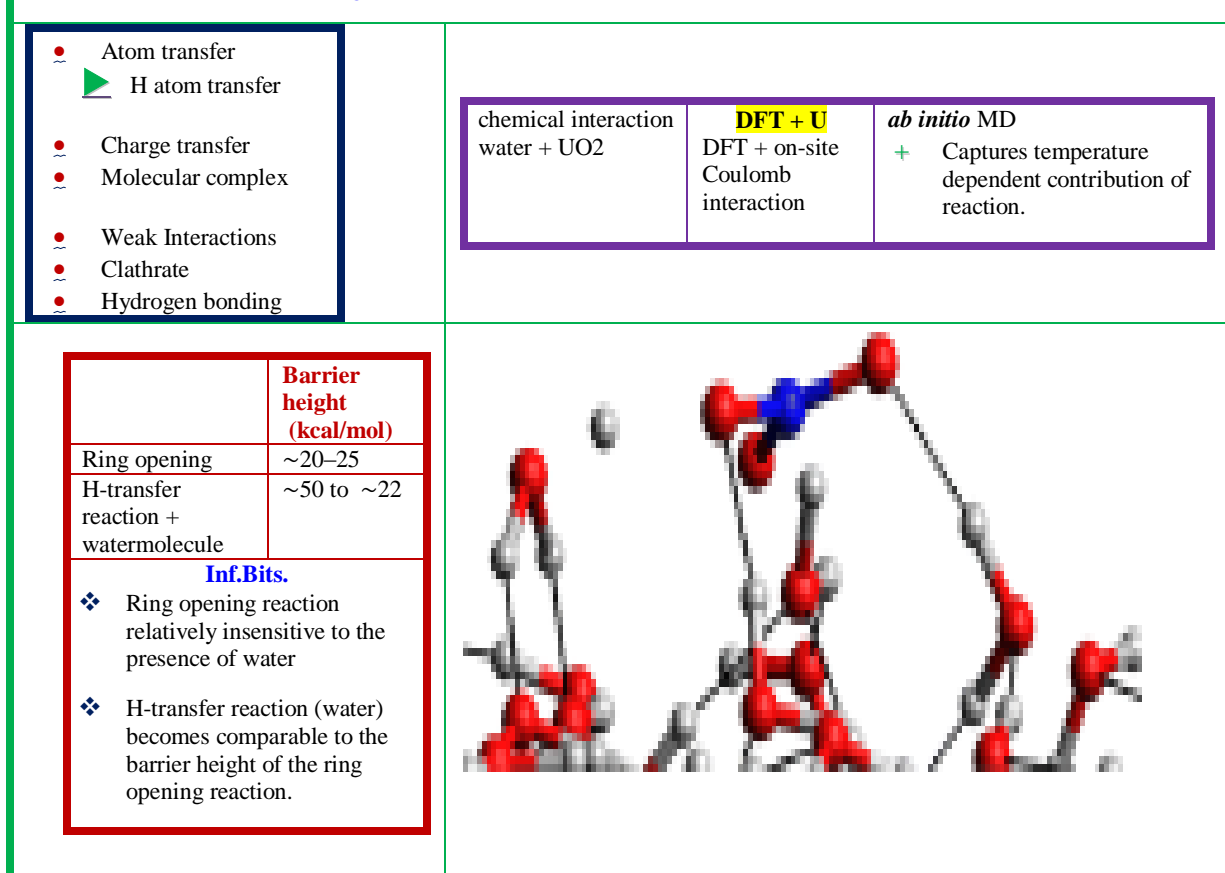
Weak interactions Stacking $\sigma - \sigma$ $\sigma - \pi$ $\pi - \pi$ H-bond Strong Medium Weak Ion-dipole Dispersion Van der wall			
Neutral solutes	Water octanol	Enthalpy of solvation	Continuum solvent MST model PCM-IEF
Guanine of tyrosine	Water	B3LYP-D, MP2 M05-2X	[212]



🌀 Chemical reactions

The chemical reactions are a tiny rearrangement (including sharing) of electrons of at least two atoms, each belonging to a different moiety/species/molecule (chart 39).

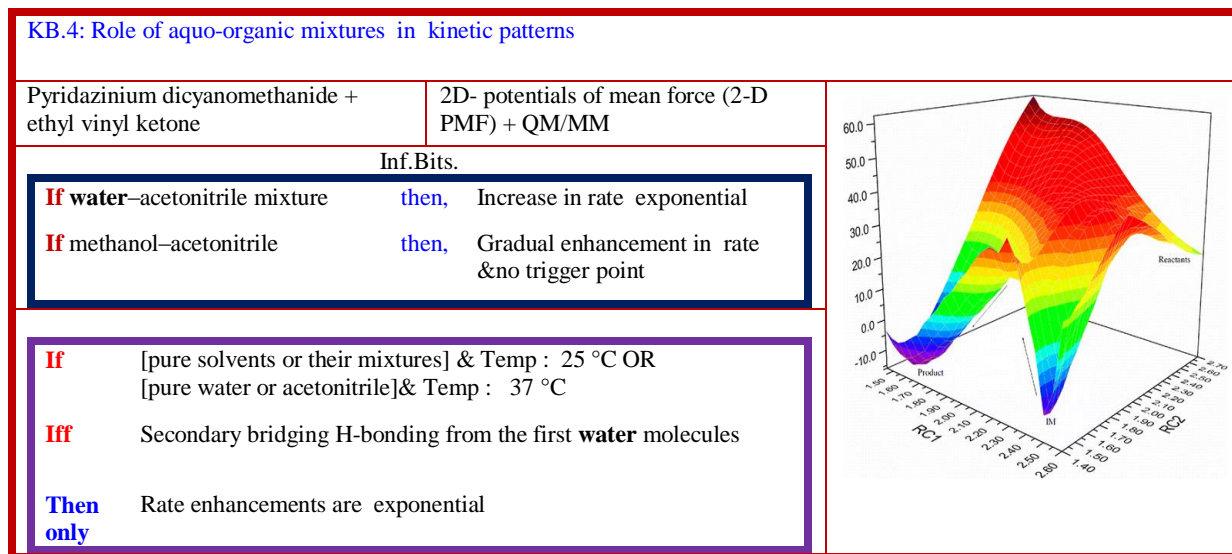
Chart 39: Chemical reactions using CQC



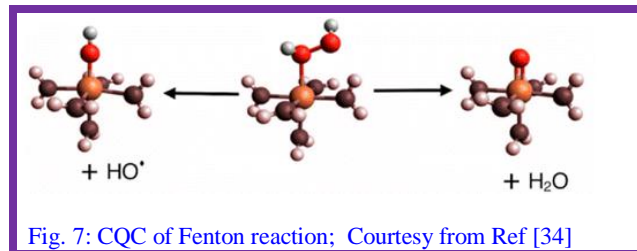
Maldonado et al. [176] found from *ab initio* and DFT computations that water reacts with UO₂ surfaces even at room temperature and pressure resulting in dissociation of water (chart 39).

Ring opening and hydrogen transfer reactions: Chaban et al. [96] from NASA Ames Research Center, studied attack of OH radical on DNA base guanine resulting in ring opening and hydrogen transfer reactions.

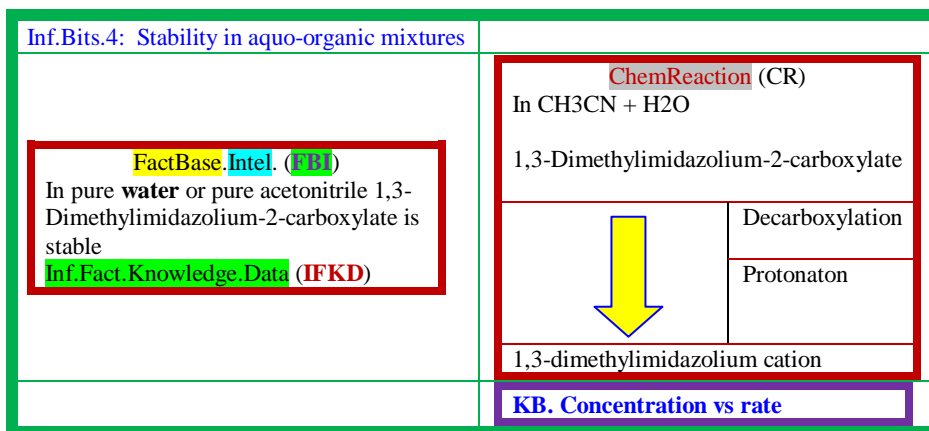
Cycloaddition reaction in gas, water, water_miscible solvents and aquo_organic_mixtures: found stepwise mechanism of 1,3-dipolar cycloaddition in presence of solvent(s) while it is a concerted one in gas phase KB. 4.



Fenton reaction: Petit et al. [34] found DFT validated by accurate ab initio correlated electronic structure theory based CQC concludes that Fe(III) + OH formation is favored at low pH in the famous Fenton reaction (fig.7).



Stability of 1,3-Dimethylimidazolium-2-carboxylate in water, acetonitrile and their mixtures: From DFT computations and kinetic experiments, Denning and Falvey [89] reported that 1,3 dimethylimidazolium-2-carboxylate forms 1,3-dimethylimidazolium cation in acetonitrile-water mixtures (Inf.Bits.4).



<p style="text-align: center;">Data (DB)</p> <p>Barrier energy of decarboxylation [gas phase to (SMD-simulated) water] = ca. 20 kcal/mol</p> <p style="text-align: center;">Information</p> <p>Polarity of the solvent influences length and strength of the C-C bond between imidazolium ring and the carboxylate group</p>	<table border="1"> <tr> <td style="color: red;">If</td> <td>Low concentrations</td> </tr> <tr> <td style="color: blue;">Then</td> <td>Provides a proton source for the trapping of the carbene and accelerates decomposition</td> </tr> <tr> <td style="color: red;">If</td> <td>Higher concentrations</td> </tr> <tr> <td style="color: blue;">Then</td> <td>Increases the polarity of the medium. Slowing down decarboxylation process and likewise the overall decomposition rate</td> </tr> </table>	If	Low concentrations	Then	Provides a proton source for the trapping of the carbene and accelerates decomposition	If	Higher concentrations	Then	Increases the polarity of the medium. Slowing down decarboxylation process and likewise the overall decomposition rate
If	Low concentrations								
Then	Provides a proton source for the trapping of the carbene and accelerates decomposition								
If	Higher concentrations								
Then	Increases the polarity of the medium. Slowing down decarboxylation process and likewise the overall decomposition rate								

Chart 40: Ionization of 2-aminopyrimidine in water and gas phases

Gas phase {DFT(B3LYP)/6-311+G(d,p)}		Water phase {PCM(water)//DFT(B3LYP)/6-311+G(d,p)}					
Gas	< 0.01 %	100 %	IP 8.5 eV	100 %	EA -0.4 eV	0.5 %	99.5 %
Water	38 %	62 %	6.3 eV	100 %	1.8 eV	2 %	98 %

DFT and PCM for 2-aminopyrimidine characteristics in water and gas phase: Raczyńska [20] reported ionization of 2-aminopyrimidine in the gas phase and in water solution by DFT and PCM (chart 40). The change in adiabatic IP and EA from transferring 2-aminopyrimidine from gas to water is ca. 2 eV.

Inf.Bits.Method.1: CQC

- ✓ GGA functionals output accurate geometries & frequencies for uranium fluorides & oxofluorides (UF₆ and UO₂F₂) in gas
- ✓ Hybrid -DFT functionals are superior for energetics
- MP2 is erratic
- ✓ CCSD(T) gives the most accurate results
- ✓ Relativistic methods, small-core effective core potentials (SC-ECP), ZORA, all-electron scalar, yield comparable results
- Earlier large-core ECP (LC-ECP) is consistently worse
- ✓ Actinyl aquo complexes [AnO₂(OH₂)₅]ⁿ⁺, (An = U, Np, or Pu and n = 1 or 2)
- ✓ If first coordination sphere of the metal

Lanthanide chemistry: Li et al. studied [1] the effect of choice of approximate electron–electron correlation method and basis sets (model chemistry), approximate relativistic method, solvent (condensed phase) modeling and choice of suitable models on the accuracy of properties of compounds of lanthanides (Inf.Bits.Method1). In this review, it is highlighted that molecules with more than 100 atoms containing actinide elements are amenable for chemical queries with advanced DFT-functionals. The experimentally observed Ac(V) by 18-crown-6 ligands and screening of positive charge of the ion from the polarizable solvent by macrocycles are explained by CQC.

included explicitly
 Then continuum solvation models reliable
 ◆ Inclusion of second coordination sphere has no clear advantage
 → If Spin-orbit effects included,
 Then trend in An(VI)/An(V) reduction potentials realized

Electrochemistry of Triazole fungicides: Han et al. [30] combined CQC (by DFT) of electrochemical degradation of Triazole fungicides in aqueous solution at TiO₂-NTs/SnO₂-Sb/PbO₂ anode and GC-MS, LC-(ESI)-MS/MS results to understand molecular structure and process chemistry. DFT calculations led to atomic charge and active sites of the ligands.

Water sorption with ab initio, FT-IR etc.: Musto et al. [154] made an intensive study of water sorption of poly(ϵ -caprolactone) by ab initio, thermodynamic, spectroscopic and gravimetric techniques. It is inferred that of self- and cross-HBs which compare favorably with FT-IR information (Inf.Bits. 5).

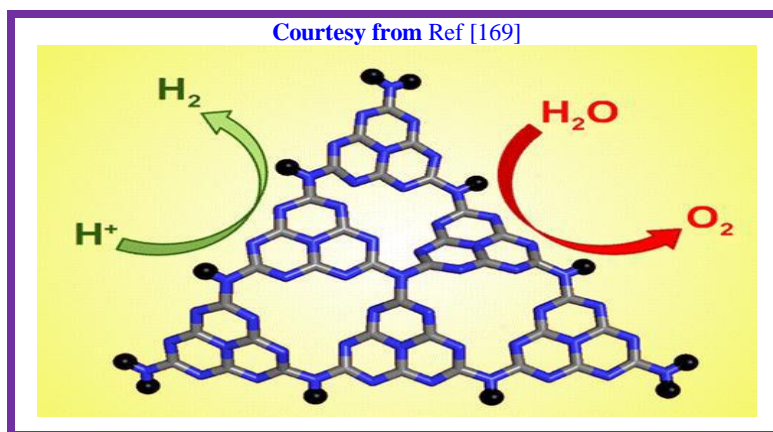
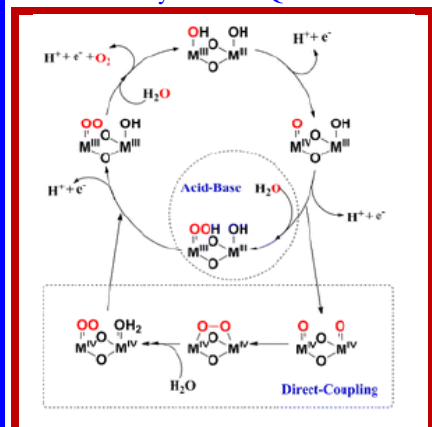
Ion-electron interaction

Hao-Hong [81] employed plane wave basis set and the spin polarized version of the PW-91 DFT level. GGA was employed for the exchange–correlation functional in the CASTEP code [191] for Electronic structure elucidation. The electron–ion interactions are modelled using highly efficient ultrasoft pseudopotentials. The linear optical properties are described in terms of complex dielectric function ($D = D_1 + i^*D_2$).

Covalent molecules + ion clusters

Sommerfeld et al. [104] used CC method to probe into the interaction of covalent molecules with ion clusters having large quadrupoles, but vanishing dipole moments. There is no correlation between the vertical attachment energy and quadrupole moment values.

Chart 41: Catalysis with CQC



Alg. 5: Photocatalysts by CQC

- **TD-DFT**

→ Absorption spectra of the different cluster models

→ Compare CQC spectra with Exptal

- **DFT and TD-DFT**

→ Calculate the reduction potentials of the free electron, free hole, exciton

→ Predict thermodynamically feasible carbon nitride structures which reduce protons and oxidize water

Decarboxylation	Tetrahydrocannabinol	B3LYP 6-31G*	TS IRC	SPARTAN 06	[89]
Wittig reaction ⇒ vacuum ⇒ THF	2,4-dimethyl-3-pyrrol-1-ylpentanal and triphenyl-phosphonium ylide		DFT-B3P86 G03	6-31G*	[215]

⚗ Chemical kinetics

Mavros et al. [33] reviewed current state-of-art-of-DFT in role of transition metal oxidecatalysts in water splitting, a crucial process in generation of hydrogen gas as an alternate fuel. One of the wings of DFT is in thermochemical computations in condensed phases at 300°K, modeling solvent, derived chemical descriptors, electro-chemical over potentials, kinetic mechanisms and thermodynamic path ways of catalytic reactions etc. (chart 41,Alg. 5).

Triazine- and heptazines in water splitting: Butchosa et al. [169] investigated carbon nitride materials as photo-catalysts in water splitting by TD-DFT.

Transition state in chemical reactions

The focus is on the intermediates of reaction especially those cannot be observed spectroscopically IEF-PCM for THF solvent. The transition state found in vacuo became vanishingly small in THF. George Witting was awarded Nobel Prize in 1979 for the conversion of C=O into C=C using phosphorus ylide (or phosphorane). The mechanism however is under debate. The cavity surrounding the solute is used to formulate the basic electrostatic equation reflecting solute-solvent interactions.

Inf.Bits,5: Ab initio calculations, macroscopic thermodynamics modeling, and relevant features emerging from spectroscopic and gravimetric measurements on poly(ϵ -caprolactone)-water system

FTIR

→ Difference spectroscopy

- 2D-correlation spectroscopy
- LS- curve-fitting analysis

Multicomponent $\nu(\text{OH})$ band representative of absorbed water interpreted with ab initio CQC

Gravimetry

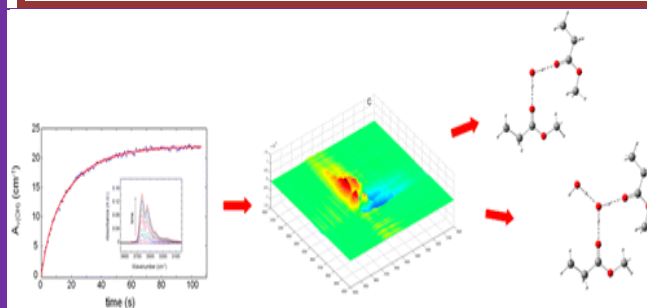
gravimetric determination of water sorption isotherm

the molecular interactions between the polymer and the penetrant.

Inf. Bits

First-shell and second-shell layers -- two spectroscopically discernible water species

- | | |
|------|---|
| If | relative humidity of water vapor < 0.65 |
| Then | dimers of water molecules within equilibrated polymer |
| If | relative humidity of water vapor > higher |
| Then | clustering of water molecules sorbed starts |

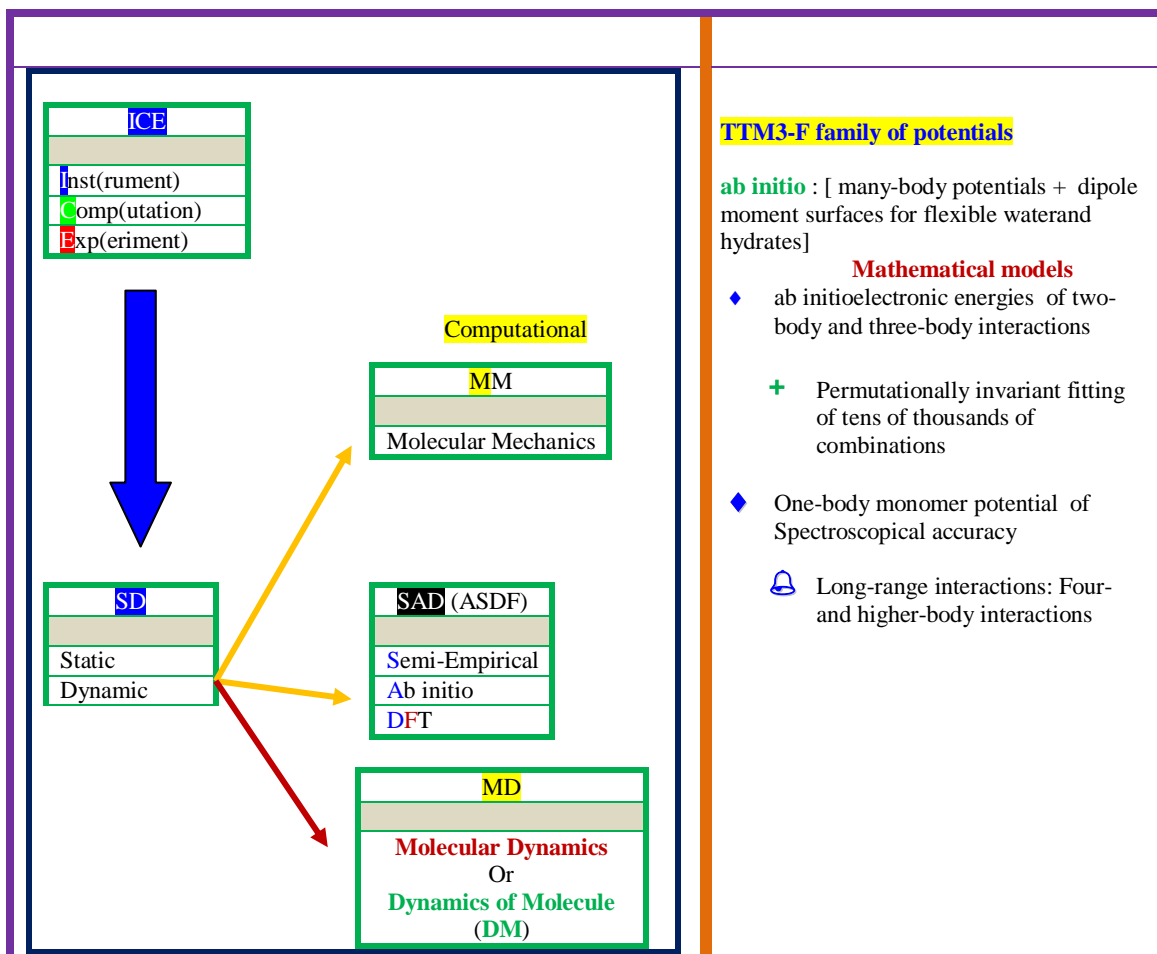


4.2. Comparison of CQC output with experimental results

CQC deals with molecules in static mode, or in other words equivalent to perform calculations at 0°K. But, many man-made experiments (save CERN, NASA etc.) are performed at 300°K and 1atmosphere pressures. In oceanography an ionic strength is around 0.37N NaCl and biological systems 37°C (310°K) and 0.1N ionic strength. On the other hand, Mother Nature used very high pressures, temperature, radiation, electrical/magnetic fields, gravity, enzymes etc. in evolving from Big-Bang stage to today's universe (chart 42).

Chart 42: Independent and mutual evolution of Experimental and CQC probes - pros and cons

Method	Material	Instrument	Output
Experiment	ॐ Real	• Real	↓ Direct/indirect
Fails	ॐ Virtual	• Real	
CQC	ॐ Virtual	• Virtual	
CQC	ॐ Real	• Virtual	↓ Derived
Thought Experiment/ in vivo computation	ॐ No	• No	↓ Sparkles Awaiting realization/ mathematical proof/ time tested validity



Similar output results of Experiments and CQC

b-cyclodextrin	NMR	Conformers ESP	B3LYP/6-31G(d)	Gaussian 03	[203]
			B3LYP/6-311++G(d,p)		
			MD	NAMD2.6	
Aqueous Diazole(pyrazole)	X-ray	DFT	B3LYP 6-311++G**	G03	[202]
		(H ₂ O) _n n=1,2,3,6,11	MD	GROWMACS V3.3.3	
Calcite 1.5 nm	X-ray		MD	Water 300K	[71]
LiH, BeH ₂ , CO ₂	HF	Topological featus	[216]		
HF, H ₂ O		Z3-AO basis of Benkova			

Z3-AO basis of Benkova is designed specifically for the polarizability calculation. The method is applied to HF and H₂O. Due to reduced size reasonable full CI expansion is possible. Huang and Rodgers [130] found the agreement between CQC and experimental energy values is excellent for Na⁺ and K⁺ complexes of pyrrole/ pyrazole (table 10).

M	L	Geo.opt.	SPE
⇒ Li+	○ Pyrrole	MP2(full)/6-31G*	MP2(full)/6-311+G(2d2p)
⇒ Na+	○ 1-methylpyrrole pyrazole		
⇒ K+	○ 1-methylpyrazole		
	○ 1-methylimidazole		

InfBits

- CQC bond dissociation energies of Li-complexes are systematically low compared to experimental values

Wu et al. [133] studied solid-state ^{17}O NMR study of the ^{17}O electric field gradient (EFG) and chemical shielding (CS) tensors of oxonium ion (H_3O^+) in *p*-toluenesulfonic acid monohydrate (TAM) by both experimental and CQCs Table 11.

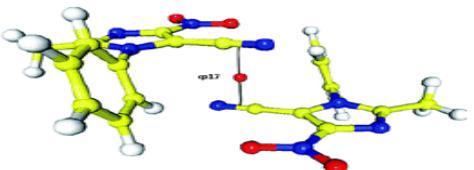
^{17}O	Expt GIAO	CQC
Quadrupole coupling constant(QuadCC)	7.05 ± 0.02 MHz	⇒ RHF
Chemical shift anisotropy	87 ± 5 ppm	⇒ MP2
	+7.382 MHz,	⇒ DFT

Inf.Bits. 6

Strong hydrogen-bonding: In H_3O^+ ion in TAM is stronger than in isolated H_3O^+ by 3 mhz
 Calculated ^{17}O isotropic chemical shifts by CQC = Expt values
 CQC values with different basis sets differ by 20 ppm

Computation	SCS-RI-MP2-F12
Expt charge density distribution	Hansen-Coppens multipole model

Courtesy from Ref [115]



Bulanin and Lobo [162] found that FT-IR spectra at 77K of diatomic molecules N_2 , O_2 , and D_2 adsorbed on the dehydrated LiX, NaLiX, and NaX zeolites match with results ab initio values.

Lo Presti et al. [161] compared total experimental electron density $\rho(r)$, its Laplacian $\nabla^2\rho(r)$, electrostatic potential $\phi(r)$, intermolecular interaction energies and molecular dipole moment from set of single-crystal X-ray diffraction studies and on DFT computations on isolated fungal secondary metabolite Austdiol. The crystallization results in significant charge rearrangement and mutual cooperation of hydrogen bonds evident from dipole moments. Spackman approach using promolecular charge density to calculate penetration component of intermolecular electrostatic energies predicts relative electrostatic interaction energies of most of molecules.

Paul et al. [115] calculated electro-static energy from CQC and compared with experimental and theoretical methods (table 12).

Avramopoulos [160] calculated electrostatic interactions in liquid acetonitrile using multipolar expansion up to hexa-decipoles.

Different force fields take care of partial charges to varying extents. Thus, refractive index and dielectric constant, or third-harmonic generation (THG), electric field induced second-harmonic (EFISH) generation, bulk density are in good agreement with experimental or high level CQC but not all.

Depending on the partial charges describing the Coulomb interactions of the force field employed, either the linear properties (refractive index and dielectric constant) were reproduced in good agreement

with experiment or the nonlinear properties [third-harmonic generation (THG) and electric field induced second-harmonic (EFISH) generation] and the bulk density but never both sets of properties together. Thus new generation methods are the need of hour to take care of long-range electrostatic interactions and also collective behavior more precisely.

IR spectra of water and HCl + H₂O by TTM3-F: Bowman et al. [178] reported IR using WHBB potential dipole transition moment. The vibrational energies and dipole transition moments are calculated with local monomer quantum method. This approach is applied to IR of water and hydrates like small HCl–H₂O clusters.

The calculated potential function for hydroxyl torsion angle of ethanol overlaps and compared the IR experimental results with CQC. Sudha [78] reported that QC computed IR and Raman spectra are in good agreement with experimental one (NBO), TD-DFT is used to calculate energy and oscillator strength.













Bryce [46] showed that ⁴³Ca solid-state NMR at 21.1T is a complementary tool to X-ray crystallography. The combined experimental and CQC and gauge-including projector-augmented-wave (GIPAW) DFT to probe into vaterite polymorph of calcium carbonate.

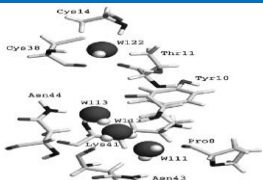
Karimi-Jafari and AliMaghari [124] computed PES of F₂ dimer at MP4/aug-cc-pVTZ level with three minima. The first one corresponds to a stable structure (table 13) and potential is in agreement with experimental value. The remaining two represent canted and X-shaped configurations.

R	6.82 au	Configuration	Meh
θa	12.9°	Canted	-596
θb	76.0°	X-shaped	-629
φ	180°	well depth	716 μEh

4.3 Molecular Dynamics

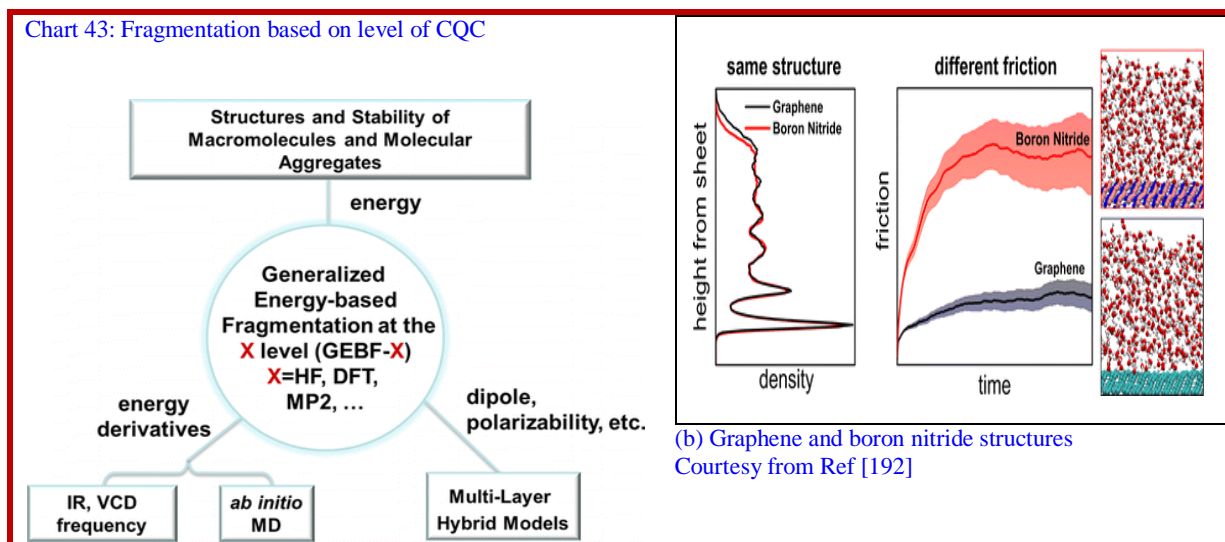
Ramondo [202] studied molecular dynamics of aqueous pyrazole using GROWMACS package. The solute is described by GAFF (general atom force field). A cubic box containing 240 pyrazole and 1131 water molecules is considered. Four nano-seconds trajectories using 2-femto second time steps. The model for water molecule is TIP-5P. Table 14 describes the role of chemical moieties in real life tasks and thus their study with CQC is highly rewarding from scientific as well as higher level human life and endeavors.

Moiety	Role	Ref
Hydroperoxide anion (HOO ⁻) in water	 Biological systems & industrial processes Dynamics of HOO–  its solvation shell are unknown	[155]
Opioid G protein-coupled receptors	 Modulating pain, addiction, psychotomimesis, mood and memory	[49]
Synthetic flavylum salts	 Water-soluble pigments in the plant kingdom	[100]
Hydrated electrons	 Detected by pulse radiolysis of water in 1962	[2]
Actinide chemistry	 Nuclear waste problem  5f contributions to bonding	[3]
Triazole fungicides	 Toxic and bio-refractory contaminants  Spread in environment	[30]
<i>p</i> -coumaric methyl ester,	 Model for the chromophore of the photoactive yellow protein	[15]
L-ascorbate	 Main reactive form of vitamin C for antioxidant reactions in water medium	[14]
Flavonoids	 Scavenging of free radicals in biological systems	[16]

ATP E. coli Hfq	binding site, Na ⁺ , Cl ⁻	MD	GROMACS package AMBER99 TIP3PFF	[72]			
Bombesin	Conformational profile NMR peptide in trifluoro-EtOH + H ₂ O	MD Solvent model Berendsen's versus Langevin's thermostat	Solvent model ➤ Onufriev, Bashford ➤ Case implementation of Generalized Born				
BPTI (bovine pancreatic trypsin inhibitor)	Internal hydration		MD MM	TIP3P CHARMM	ΔG Crystal structure from PDP	MEAD Pressure perturbation calorimetry (PPC)	[198]

Devereux et al. [118] applied ab initio CQC and Molecular Dynamics (MD) simulations for vibrational frequency shifts of CO and H₂ in uniform as well as inhomogeneous electric fields. CCSD(T) computations for H₂ (with no permanent dipole moment) showed bond-weakening effects importance in force fields when inhomogeneous electric field is applied. It paves way in interpreting Stark spectroscopic data of protein active sites.

MD in friction of water: Tocci et al. [192] used ab initio MD for relating structure of nanoscale water with friction for liquid water in contact with hexagonal boron nitride and graphene (chart 43). These results have impetus on transport of water at nanoscale and future desalination membrane.



Ab initio and Auger spectra: Unger et al. [171] identified the transfer of proton between core-ionized hydrogen peroxide and water molecules which is an ultrafast electronic relaxation processes by Auger-electron spectroscopy. Ab initio MD results compliment the experimental Auger spectral data. Further, it is possible to discriminate species from variation of (H₂O₂/D₂O₂) isotope effect on Auger spectra.

Auger-electron spectra of water: Slaviček et al. [43] compared ab initio and quantum dynamical simulated spectra of oxygen 1s Auger-electron spectra of H₂O and D₂O with experimental results.

Ab initio MD computed IR spectra of methylacetamide-calcium complex: Pluhařová et al. [181] applied ab initio MD in computing IR shifts when sodium or calcium ions bind methylacetamide. A significant shift in IR compared to *N*-methylacetamide in pure water infers strong binding of calcium.

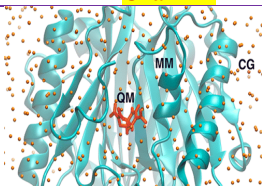
THz spectra and MD of dye: Petrone et al. [41] probed into specific molecular motions of *N*-methyl-6-oxyquinolinium betaine by far IR, THz frequency spectra, ab-initio MD and wavelet-based time-dependent frequency analysis of nonstationary signals. After electronic excitation, approximately 1.5 water molecules move from the first solvation shell into the bulk solvent structure. The collective solvent motions in THz and IR regions indicate restructuring of micro-solvation regions.

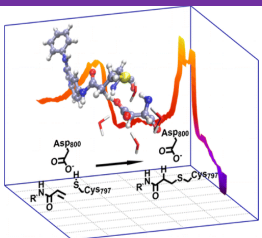
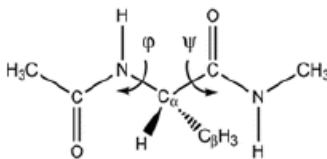
Mössbauer Spectra (^{57}Fe): Sinnecker et al. [37] compared the results of nonrelativistic_DFT and quasi-relativistic_DFT within the zero-order regular approximation (ZORA). The electric and magnetic hyperfine parameters in ^{57}Fe Mössbauer Spectra were predicted.

Generalized energy-based fragmentation (GEBF): Here, ground-state energies of various small moieties are calculated from “electrostatically embedded” subsystems by *HF*, *DFT* etc. From this, the ground-state energy or properties of a large system are computed for hundreds to thousands of atoms on workstations. Li et al. [1] observed the conformational dynamics of two peptides by GEBF-based AIMD are different from those obtained with classical FF-MD procedure.

4.4 QM-MM applications

It is well accepted that even small changes in ligand structure leads to major alteration in activity. QM,MM and X-ray/NMR structural information paved way to probe into molecular level details [74] (table 15).

Solute		Solvent/macromolecule		Ref	CHARMM
	FF		Solv. Model		
500 neutral molecules	AMBER		TIP3P	[02]	0.96 and 1.04 kcal/mol difference in comparison with the experimental and simulation data
Cellulose	CHARMM36	Supercritical H ₂ O Density : [0.2 to 0.7 ; 1.0]	TIP3P	[07]	
4-Thiothymidine	CASSCF CASPT2	Ribose	CHARMM	[04]	
		Water	TIP3P		
Solute		FF		Ref	Charmm
Chorismate mutase (CM) <i>p</i> -hydroxybenzoate hydroxylase		Active-site biomolecular environment solvent QM MM CG Martini-FF + polarizable (pol-CG) water		[05]	

Alkylation of Cys797 by the prototypical covalent inhibitor N-(4-anilinoquinazolin-6-yl) acrylamide.	QM/MM	[22]	
Hydrogen abstraction of the androstenedione (ASD) substrate catalyzed by the cytochrome P450 aromatase enzyme	Bonding evolution theory (BET)	[18]	
Retinylidene chromophore in rhodopsin	<ul style="list-style-type: none"> ☞ QM/MM ☞ DFT/MM ☞ Coupled Perturbed DFT 	[24]	
Folded protein	Coincide with coupling, chemical shifts secondary structure populations	[14]	
Solute: Hemicellulose polysaccharides Solvent: Water	CHARMM36 TIP3P, GROMOS56A6_CARBO SPC, GLYCAM06h TIP3P, GLYCAM06 TIP5P	[58]	

Bonding evolution theory (BET): The electron localization function (ELF) and Thom's catastrophe theory (CT), have been combined and coupled with QM/MM [56].

+ Includes polarization of charges in wave function
→ Realistic & accurate picture chemical process

A comparison of functioning of FFs for anthracene (polyaromatic hydrocarbons) with ab initio methods is made by Grancic [26].

Hartree-Fock_Heitler-London (HF-HL) method: It belongs [125] to ab initio paradigm and variationally combines HF and HL, approximations. The application is in modeling dissociation products.

Protein + DNA with TIP3P+AMBER: The potentials of mean force (PMF) for all 105 pairs of interacting components in DNA/protein system are calculated by hybrid UNRES+NARES-2P force field (chart 44).

Chart 44: Categories of mean-field interactions between a protein and a DNA											
<ul style="list-style-type: none"> ✓ Nonpolar side chain-DNA base ✓ Polar uncharged side chain-DNA base ✓ Charged side chain-DNA base ✓ Peptide group-phosphate group ✓ Peptide group-DNA base ✓ Nonpolar side chain-phosphate group ✓ Polar uncharged side chain-phosphate group ✓ Charged side chain-phosphate group 	<table border="1"> <thead> <tr> <th colspan="2">Performance</th> </tr> </thead> <tbody> <tr> <td>✓</td> <td>Good</td> </tr> <tr> <td>✓</td> <td>BMM2, BMM3, W99 and isoPAHAP</td> </tr> <tr> <td>-</td> <td>Fails</td> </tr> <tr> <td>-</td> <td>AMBER, Bordat, Dreiding, DRESP, MM2 and MM3</td> </tr> </tbody> </table>	Performance		✓	Good	✓	BMM2, BMM3, W99 and isoPAHAP	-	Fails	-	AMBER, Bordat, Dreiding, DRESP, MM2 and MM3
Performance											
✓	Good										
✓	BMM2, BMM3, W99 and isoPAHAP										
-	Fails										
-	AMBER, Bordat, Dreiding, DRESP, MM2 and MM3										

Kemp elimination of a designed enzyme, HG3.17 α -phosphate and Asp554 as the catalytic bases	Hybrid QM/MM MD QM/MM Car-Parrinello molecular dynamics	[4] [146]
Excited-state relaxation dynamics of thymine and thymidine in aqueous solution neutral molecules in water	COSMO in GAUSSIAN94	[135]
Cobalt-substituted homoprotocatechuate 2,3-dioxygenase (Co-HPCD) with electron-rich substrate homoprotocatechuate (HPCA) and electron-poor substrate 4- nitrocatechol (4NC)	FF	
Mono- and dithiolated azobenzenes chemisorbed on a gold surface		[54]
Mono- and dithiolated azobenzenes chemisorbed on a gold surface		[164]
Vertical absorption spectrum of cytosine in water		[55]

Hermane cation + DNA: Etienne et al. [17] used TD-DFT and PCM for emission spectrum of aqueous Hermane cation and its interaction with DNA. The explicit water molecules around solute through hybrid QM-MM-MD account for shifts in absorption and emission maxima through dynamic effects. Two stable modes have been identified in the interaction of this cation with DNA.









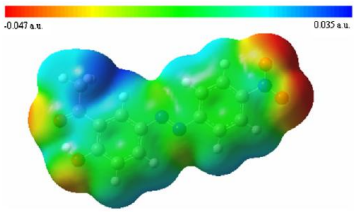
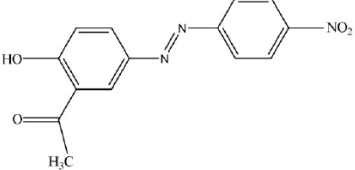
SHG imaging of hydrated starch: Cisek et al. [151] reported the results of ab initio and polarization-in, polarization-out (PIPO) second harmonic generation microscopy of maize starch and potato starch granules. It is shown that major contribution to SHG arises due to ordered hydroxide and hydrogen bond network. Nandi et al. [120] reported hyperpolarizabilities of indigo derivatives with DFT (table 16).

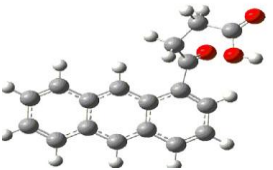
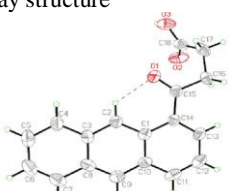
NLO properties	Fn ([ground-state electric moments, linear polarizability (α), and second-order polarizability (β)])	Inf.Bits. 7 SHG imaging
	Inf.Bits. 8	<ul style="list-style-type: none"> ◆ Fully hydrated starch granules have highest SHG intensity ◆ Dried starch granules (by) PIPO SHG imaging have a much higher NLO susceptibility component ratio than fully hydrated granules ◆ Deuterated starch granules showed a smaller susceptibility component ratio ◆ In maize granules amount of aligned water was higher
	<ul style="list-style-type: none"> ⇒ Pyramidalization of the NH₂ group decreases third-order polarizability ⇒ Explanation: the two-state model <ul style="list-style-type: none"> ↓ Decrease of dipole moment difference ↑ Increase of transition energy 	

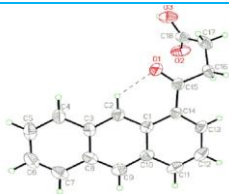
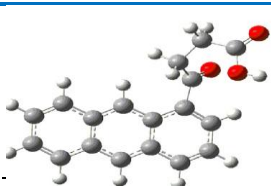
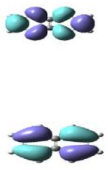
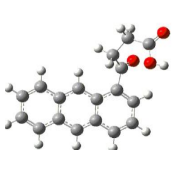
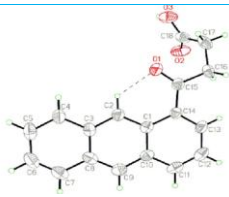
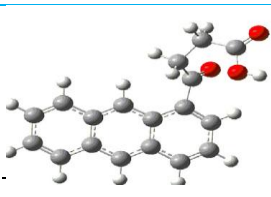
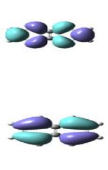
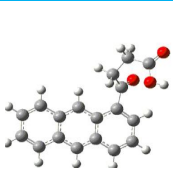

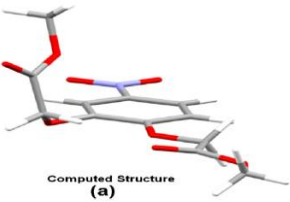
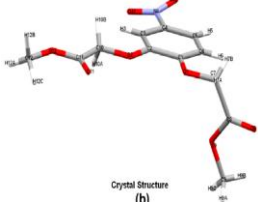
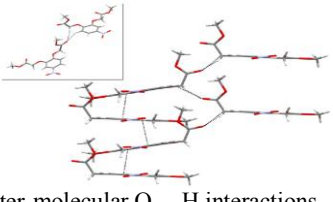
4.5 NLO materials

Kariduraganavar [79] studied second harmonic measurements with a Mode-Locked Nd:YAG laser which is used as a fundamental light source. The second harmonic signal generated by the p-polarized fundamental wavelength (1064 nm) was detected by fast photodiode (FDS010, rise time 0.9 ns, Thorlabs) and an oscilloscope (Tektronix TDS 724D, Digital Phosphor Oscilloscope) with a frequency of 500 MHz.

Mn(II)	2-(3,5-dimethyl-1H-pyrazol-1-yl)-1,10-phenanthroline)	Synthesis Xray	DFT	[76]
Polyurethanes	<ul style="list-style-type: none"> ▶ Synthesis ▶ TGA ▶ DSC ▶ SHG 	<ul style="list-style-type: none"> □ 1H NMR □ FT-IR □ GPC □ DSC □ TGA 		[79]

Poly-nuclear lithium –substituted (Me, t-butyl, phenyl, ph-NO ₂ , phNH ₂)	Electronic spectra	Hyperpolarizability : 262.55 to 16336.35 × 10 ⁻³³ esu	DFT MP2	 B3LYP,  CAM-B3LYP  LC-BLYP,  BHandHLYP  MX-05	6-311G* G 09		
	electronic transition energy, oscillator strength transition character		TD-DFT				
2-amino-4-chlorobenzonitrile	FT-IR FT-Raman	 DFT  TD-DFT  NBO	B3LYP method with 6-311++G (d,p)	[78]			
Substituted phenol		IR UV XRD	NLO	DFT	B3LYP	6-311G (d,p)	[86]
							

4-(naphthalen-2-yl)-4-oxobutanoic acid (I) 4-(anthracen-1-yl)-4-oxobutanoic acid hapten for PAHs		<p>(First Excited State)</p> <p>E_{LUMO} = 0.103 a. u.</p> <p>ΔE = 0.389 a. u.</p> <p>E_{HOMO} = -0.286 a. u.</p> <p>Homo Plot (Ground State)</p>
X-ray structure		<ul style="list-style-type: none"> ▶ Synthesis ▶ IR ▶ HNMR ▶ X-ray ▶ HOMO LUMO ▶ ESP-charges <p>[83]</p>

						<p>(First Excited State)</p> <p>$E_{LUMO} = 0.103 \text{ a. u.}$</p> <p>$\Delta E = 0.389 \text{ a. u.}$</p> <p>$E_{HOMO} = -0.286 \text{ a. u.}$</p> <p>Homo Plot (Ground State)</p>					
						<p>(First Excited State)</p> <p>$E_{LUMO} = 0.103 \text{ a. u.}$</p> <p>$\Delta E = 0.389 \text{ a. u.}$</p> <p>$E_{HOMO} = -0.286 \text{ a. u.}$</p> <p>Homo Plot (Ground State)</p>					
2,20-[(4-nitro-1,2-phenylene)bis(oxy)]diacetate (I)		Synthesis		 IR, Raman X-ray		B3LYP		6-31++G		G03 [85]	
		PE distribution		VEDA4							
 <p>Computed Structure (a)</p>		 <p>Crystal Structure (b)</p>		 <p>inter-molecular O...H interactions</p>							

The nonlinear optical materials are chemical compounds in solid phase but not available on the lap of Mother Nature for use. The chemical processes viz. redox, protonation and photocyclisation result in desirable NLO properties. Thus, the synthesis is the key step in this pursuit. Due to impracticability of exploring a large number of compounds, resort to computational study is indispensable. Till today, CQC procedures are mature only for gaseous molecules. The insurmountable gap between computed values of a single molecule in gas phase, experimental figures for a bundle of molecules (material) in solid phase is bridged through scaling methods. But yet, it is not a true solution and only iterative cycle of CQC, synthesis, experimental measurement keeping in view of the multiple conflicting objectives of a rational material design (RMD) akin to Rational Drug design(RDD)/D³ (Drug discovery and Design) leads to the best of best set of NLO start up compounds for devices. There is an exponential growth of reported NLO compounds, but the upper limits of second order optical nonlinearities of organic crystals have not been reached yet. The research in science and technology of NLO is perennial due to their multifaceted applications in optical computers, electro-optics (EO), optical rectification (OR), optical communication, second harmonic generation(SHG), optical parametric oscillation(OPO), electro-optic modulation and terahertz (THz)/quintivalent (QHz) wave generation, medical imaging and smart materials that repair themselves. This gives impetus to ever demanding research with rational design protocols for newer organic moieties in the infinitely (10^{100}) wide chemical playground.

The industrial production of materials with non-linear optical (NLO) properties is the prototype technological outcome. The science in it is the interaction of light (single or multiple photons), a part of electromagnetic radiation with electrons of atoms of material and medium (solvent, bulk, cells etc.). The interaction induces polarization of the local distribution. It results in charges of the atoms of the moieties to oscillate. The strength and amount of induced polarization depends upon the nature of electronic

structure of the materials. The net interaction of electromagnetic radiation with the environment and of the material produces a change in frequency, phase, amplitude and many other optical characteristics of the incident light. These results throw light on microscopic properties of system. Alternatively, the materials can be designed to harness light for useful applications. This demands that the material is to be first synthesized, followed by assignment of its crystal structure, measurement of classical optical properties, effects in magnetic/electric fields, measurement of second order and non-linear polarisabilities. This is a natural cycle demanding huge amount of finances like drug industry, man-years of basic science/engineering research and technological pursuits. The computational i.e. quantum chemical study of virtual library of molecules based on basic skeleton of well proven moieties is relatively less expensive in terms of CPU time/experts' expertise/skilled persons' schedule hours. It no doubt reduces chemical space to probe into more prospective materials. In a nutshell, these/any predictive approaches mostly helpful to eliminate unfruitful areas. Yet, the predicted area exactly may not coincide with the real molecular space (which of course is unknown). But, the iterative cycle of theoretical prediction, experimental synthesis, followed by measurement, projecting into new space, computational prediction, experiment etc. is indispensable. However, at the end of day, this repetitive effort gives rise to more desirable materials than otherwise with random/intuitive/contented probes. This can be summarized as, instead of performing a billion/trillion experiments (like Mother Nature), a thousand trials are adequate. Scaling down, a couple of hundreds of experiments result in 3σ level rather than a thousand or so.

Considering the material (single crystal to polymer), a susceptibility tensor is in vogue. Taking into consideration of molecular orientation, weighted averages of the molecular values result in the susceptibility tensors. But, NLO properties are cumulative effects of oscillating electric field component of the incident light. The discrepancy between experimental and computed ones is rationalized proposing a correction factor.

If high intensity monochromatic light interacts with a single (non-linear) molecule, the optical electric field induces linear (α) and non-linear (β , γ , ...) polarisabilities. The mathematical model of change of energy with electric field is expressed as a Taylor's infinite series. The polarization can be expressed as the sum of the linear polarization and nonlinear polarization terms. Here, a static electric field is considered and thus polarizabilities are known as static. But, now TD ab initio/ DFT calculations opened new vistas to compute NLO values with varying electric field strength of course with high price.











The ability of NLO material to double the frequency of laser light passing through them, is called second harmonic generation (SHG). The continual interest in the field is due to production of laser light of higher energy than that of the source for high utility devices. The advancement in the lasers, particularly in the deep-UV/far IR/Tera hertz (THz)/quintivalent hertz (QHz) spectral regions generate intense monochromatic light sources to render tenable compounds to exhibit (second and third order) hyperpolarizabilities.

Intelligent Molecular Design (IMD) of NLO molecules (NL-OMs)

Any material in gaseous/liquid/solid state exhibits nonlinear optical (NLO) characteristics when illuminated by high intensity electromagnetic light of 200-2500 nm. But, the extent of non-linear response for fabrication of devices is a function of intrinsic electronic properties of the compound. The optimum factors of an NLO material needed to develop an efficient device are crystals with better linear optical (LO) and NLO properties, large transparency range, phase-matching range, device functional characteristics and operation conditions. On the microscopic scale they are dimension, geometry, acceptable loss, response time, nonlinear conversion efficiency, wavelength, power, CW or pulse of laser source. Thus, the choice of material is a multi-conflicting-object -task and thus, there is no one ideal material for all applications. Further, theories are also not developed encompassing complete understanding optimal NLO materials and even design protocols from molecules to polymeric structures through nano dimensions. Electro Optical (EO) activity has long been known to functionally depend upon chromophore. However, at the molecular level, the first order NLO properties (frequency doubling, Kerr effect, (EO) Pockels effect etc.) are driven by first hyperpolarizability (β), acentric order ($\langle \cos^3 q \rangle$),

number density (N) and their inter-dependence. The fact that quantum and statistical mechanics probe into details has only recently been appreciated.

Design of molecules and materials through CQC and experimental output: The quantum mechanical guidance opens new vistas to a large number of design possibilities to choose compounds with novel NLO chromophores (chart 45). The classes of materials include inorganic salts, semiconductors, organic compounds, metal complexes etc. The criteria in selecting molecules with prospecting groups to move towards higher β values are in KB. 5.

Chart 45: Characteristics NLO materials	KB. 5: Materials with NLO properties
<ul style="list-style-type: none">  Planar donor-π conjugated bridge-acceptor (D-π-A)  Extending the conjugated bridge conjugation path between the electron-donating and -withdrawing groups  D, A, heterocycle, bridges (Ac,N=N)  Bond length alternation (BLA)  Twisted π-electron moieties  Optimizing the D/A strengths  Delocalised π-electron system with donor and acceptor groups at the opposite ends of the molecule  Degree of π-conjugation, steric hindrance  Donor (D) and acceptor (A) substitution on the heterocycle/aromatic moiety of the molecule 	<p>If medium does not possess a center of symmetry</p> <p>Then it exhibits second-order nonlinear susceptibility</p> <p>If For a medium noncentrosymmetric</p> <p>Then it exhibits second-order nonlinear susceptibility</p> <p>If Material is centrosymmetric</p> <p>Then first hyperpolarizabilities = 0</p> <p>If any material can, that is,</p> <p>Then exhibit third-order response or exhibit nonlinear optical phenomena</p> <p>If material exhibits a high degree of nonlinearity at a reasonable intensity of light</p> <p>Then useful for a device application</p>
<p> The extension of the conjugation path also induces a bathochromic shift of the intramolecular charge transfer absorption band.</p> <p>— It is detrimental for the requirement of high transparency to visible light</p>	

Chemical moieties

Non-linear (2D-, 3D) organic molecules: The accentric molecules with highly delocalized pi-electron systems interacting with suitably substituted electron donor and acceptor groups exhibit high values of second order polarizability. The different aromatic delocalization energy/ charge density, the various orientation of the heterocycles, dipole moment, even the variable longitudinal charge-transfer interaction due to the auxiliary electron donor/acceptor nature of the heterocycles modulate the NLO. The optimum values of these properties play a key role in selecting good NLO materials. The multidimensional compounds with large off diagonal β tensor components are highly desirable to probe into details with experimental and theoretical methods. These materials exhibit ease of fabrication, relatively low cost and integration into devices. The tailorability permits to fine-tune the chemical structure to be within the limits of non-linear optical characteristics viz. high laser damage thresholds, low dielectric constants, large enrobe coefficients, fast nonlinear optical response times and off-resonance nonlinear optical susceptibility.

Hybrid metal-organic systems: Under this category, organo-metallic compounds, coordinated metal complexes, organic salts have greater design flexibility, intense electronic transitions and low energy.

Inorganic molecules: They are available as large single crystals and lattice distortions cause electronic NLO effects (chart 46).

Chart 46a: Pros and cons of materials for use in NLO materials

- + Large transparency range
 - + Robust
 - + Single crystals have several advantages over poled polymers
 - + High chromophore packing density
 - + Orientation stability
- Pure electronic NLO effects deteriorated by lattice distortions like
- Slow response times
 - Non-synchronization of the phase of the interacting optical fields

Chart 46b: Non-linear NLO compounds

- + Large enrobe coefficients
 - + Structural diversity or flexibility
-
- Low thermal stability
 - Poor physico chemical stability
 - Low mechanical strength
 - Facile relaxation to random orientation in poled guest-host systems,
 - Low optical transparency in the UV-vis region result from low-energy transitions

Limitations of 1D-NLO materials

- It is difficult to construct large bulk NLO materials,
- In the crystal, problems arise from the phase-matching orientations of 1-D molecules

Semiconductors: NLO response of semiconductors originates from saturate absorption. Their third-order NLO responses are among the largest known

- NLO processes based on such resonant interactions are relatively slow

Organic molecules: The interest in organic moieties is now astounding.

1D- organic molecules as NLO materials

1D-Push-pull molecules: They possess a large permanent dipole moment, which would favor the formation of the centrosymmetric arrangement in the crystal. A molecule with a center of inversion has no hyperpolarizability. The dipole-dipole interaction also prevails. Thus, they were tried with a little success as NLO materials since they possess no bulk NLO response. Further, most of dipolar species, crystallize in centrosymmetric space groups, where the $\chi(2)$ macroscopic susceptibility vanishes. However, self-aggregation of 1-D organic compounds (for example PNA) results into an excellent NLO material.

Non-linear (2D-, 3D) organic molecules: The accentric molecules with highly delocalized pi-electron systems interacting with suitably substituted electron donor and acceptor groups exhibit high values of second order polarizability. The different aromatic delocalization energy/ charge density, the various orientation of the heterocycles, dipole moment, even the variable longitudinal charge-transfer interaction due to the auxiliary electron donor/acceptor nature of the heterocycles modulate the NLO.

The optimum values of these properties play a key role in selecting good NLO materials. The multidimensional compounds with large off diagonal β tensor components are highly desirable to probe into details with experimental and theoretical methods. These materials exhibit ease of fabrication, relatively low cost and integration into devices. The tailorability permits to fine-tune the chemical structure to be within the limits of non-linear optical characteristics viz. high laser damage thresholds, low dielectric constants, fast nonlinear optical response times and off-resonance nonlinear optical susceptibility. However, the limitations of organic molecules are low thermal stability, low mechanical strength and facile relaxation to random orientation in poled guest-host systems and low optical transparency in the UV-VIS region.

5. Characteristic Properties

Electrons are identical and degenerate in isolation. The chemical properties/characteristics of species arise because of rearrangements of electrons around the nucleus of an atom or their equilibrium positions in multi-atomic molecules.

► Ionization potential (IP)

Koopmans' only independent paper in theoretical physics/chemistry bridged theoretical QM and experimental chemistry. A simple approximation of a more general statement known as Koopmans' theorem identifies IP and EA as E_{LUMO} and E_{HOMO} respectively (Eqn. 2). Immediately afterwards, he turned his attention to economics and won Nobel Prize in 1975. If the functional is exact in DFT, eigenvalue of the highest KS orbital has been proven to be the IP.

Eqn. 2: Physico-chemical descriptors derived from E_{HOMO} and E_{LUMO}

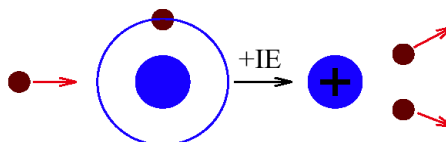
$$IP = E_{LUMO}$$

$$EA = E_{HOMO} \quad IP_{\Delta SCF} = E_{HF}(A^+) - E_{HF}(A)$$

$$\text{Electronegativity} = \frac{(E_{HOMO} + E_{LUMO})}{2}$$

$$\text{Electrophilicity} = \frac{(IP + EA)^2}{8 * (IP - EA)}$$

$$\text{Hardness} = \frac{(E_{HOMO} - E_{LUMO})}{2}$$



IP

- Koopmans' theorem is not applicable directly for DFT
- Koopman theorem ignores electronic relaxation in the ionized product
- In a cation remaining electrons redistribute after the removal of one electron from HOMO

► **Remedy:** The geometry is optimized separately for closed shell neutral and open shell cation

$$IP_{\Delta SCF} = E_{HF}(A^+) - E_{HF}(A)$$

- The neutral molecule is more destabilized compared to cation

EA

- EAs based Koopman theorem are more in error with experimental quantities

► Electron affinity (EA) and Electrophilicity

Koopmans' theorem identifies EA as E_{HOMO} . Here, the correlation and relaxation effects are additive in estimating EA. Thus, Electrophilicity is an important physico-chemical quantity by algebraic manipulation of IP and EA.

🌀 Atom in molecule analysis AIM

AIM shows the presence of bond critical points (BCPs).

🌀 HOMO, LUMO, Δ ($= E_{LUMO} - E_{HOMO}$), where Δ : Probable charge transfer (CT) within chromophore

🌀 Intramolecular charge by HOMO \rightarrow LUMO transition energy

► Electronegativity

Electronegativity of an atom (or a molecule) is the negative of its chemical potential.

🌀 Population Analysis (PA)

Population analysis deals with distribution of electrons in MOs of a molecule with its optimized 3D-structure. It is the QC explanation of classical chemical theory or in other words chemical concepts

projected into QC framework. Of the many types, NPA, Mullikan PA (MPA), Lowden, natural bond order (NBO), natural atomic orbital (NAO) and atoms in a molecule (AIM) are popular.

Mullikan PA: It is obtained based on overlapping AOs. Lowden PA is arrived at by systematically orthogonalising the BSs. The input for MPA and LPA are overlap (S) and density (P) matrix defined in terms of LCAO coefficients (Alg. 6). The diagonal of the final electron density matrix is (atom) the valence orbital electron population.

NBO: It is used to assess the extent of electron transfer from the donor (O1) atom to the acceptor (XSiC3).

NBO occupancies quantitatively evaluate the

occupation number given localized bonding orbital, which give information regarding the strength of interaction among different units within a molecule.

Wiberg bond indices and natural charges are recalculated from NBO. The derived charges and bond order etc. have classical chemical significance.

In addition, partial atomic charges, which cannot be experimentally measureable, are computable. Electron population charges are calculated using NBO.

The stability of the molecule arising from hyper-conjugative interaction and charge delocalization has been analyzed using NBO analysis.

Natural population analysis (NPA)

NPA a preferred method nowadays, employs one-electron density matrix to partition electron distribution. Another approach involves a fitting procedure and CHelp, CHelpG are coveted characteristics of species.

Charges on atoms of the molecule

The distribution of electrons in a molecule in absence of an external electric field (applied or another molecule) results in charges on atoms (Eqn. 3 and Eqn. 4). It may be positive, negative or negligible i.e. nearer to zero. Although fractional charges are present on each atom of a neutral molecule, they sum up to zero for the entire molecule respecting the principle of electro-neutrality. The QC based calculation of charges using the results of population analysis are Mullikan, ESP (=MAC), CHelp, CHelpG etc. MPA is a partition technique. The formulae for calculating charges using Mullikan population analysis (MPA) and the advantages/limitations are in chart 47. In MPA, wave function is partitioned in terms of basis function.

Eqn. 3: Partial charge

$$\text{Partial_charge_on_each_atom} = \text{Atomic_number} - \left\{ \text{sum_of_number_of_Core_electrons} + \text{valence_electrons} \right\}_{\text{SEMO(AMPAC)}}$$

Atom	Mulliken atomic charges	Hydrogen summed into
O	-0.81	0
H	0.40	0
H	0.40	0

Alg.6: MPA	
Step : 0	Final RHF wave function
Step : 1	Divide eigen vector matrix by square root of overlap matrix
Step : 2	Cal Coulson type density matrix (P)
Step : 3	Overlap population
Step : 4	Half the diagonal term; sum them into diagonal matrix

MPA	
+	Trend is good enough for closely related compounds
-	is sensitive to BS effect
-	overestimates dipole moment
	Remedy: Corrected Mullikan charge

Eqn. 4: charges from CQC

Charges on atoms from CQC

$$N_k = \sum_j^{\text{electrons}} \left(\sum_{r \in k} c_{jr}^2 + \sum_{r,s \in k, r \neq s} c_{jr} c_{js} S_{rs} + \sum_{r \in k, s \notin k} c_{jr} c_{js} S_{rs} \right)$$

$$q_k = Z_k - N_k$$

Z	Nuclear charge
r, s	Index AO basis function
c_{jr}	Coefficient of basis function r in MO
j, s	Usual overlap matrix element
r, s	Total number of basic functions
$S^{-1/2}$	Inverse of the square root of overlap matrix

Chart 47: Mullikan_charge

- + Trend is good enough for closely related compounds
 - It is not very reliable
 - Differs from those from Bader using topological approach
- 🔧 Remedy : Corrected Mullikan charge

Eqn. 4b: Corrected_Mullikan_charge

$$P_{YY}^{\alpha} = \text{Mullikan_charge} + \text{Element_of_overlap_tensor}$$

Y : Direction perpendicular to molecular plane

$$P_{YY}^{\alpha} = q_{\alpha}^M + \square_{y,\alpha}^{YY}$$

- + Reproduces calculated dipole moments for planar molecules in contrast to Mullikan charges
- + Similar to those from ESP charge

- Limited to planar molecules
 - It is not invariant to rotation
- Remedy: CHelpG charge

🔔 Atomic charges

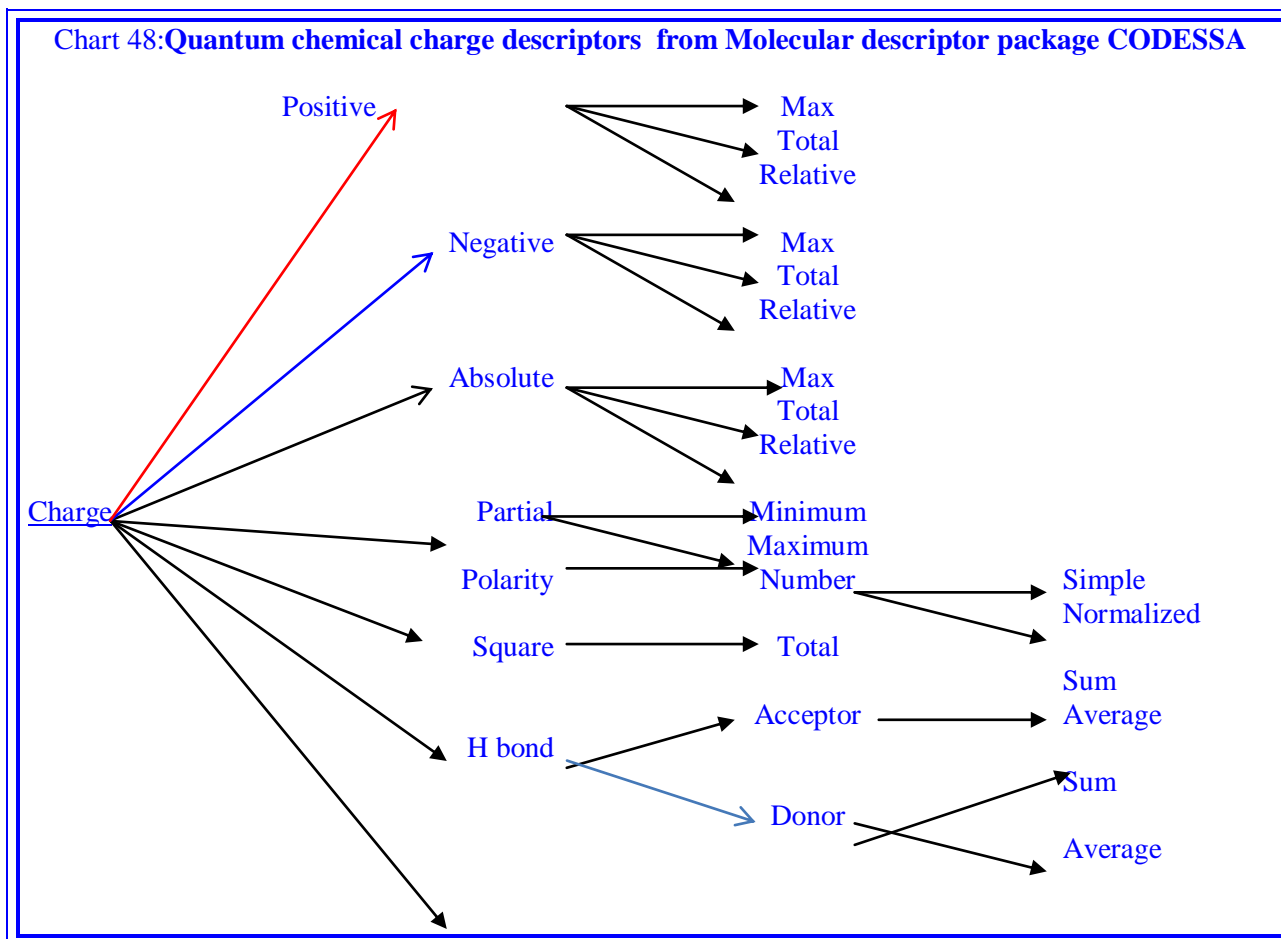
They cannot adequately explain the behavior and chemical reactivity of molecule. Electronic densities and molecular ESPs sometimes give contradictory results. Molecular descriptor packages (CODESSA, DRAGON etc) output large number of quantum chemical charge based descriptor from optimized geometry of any QC software (AMPAC, Gxx, etc.) (chart48). The trend in atomic charges is related to active site in electrophilic and nucleophilic reaction and charge based interactions between molecules. Complete picture of electronic charge density of the molecule is viewed through NPA and is useful to study the stability of the molecule

🔔 CHelpG charge

Breneman model of calculation of charges is popularly known as CHelpG (charge electrostatic point grid) (chart 47b). It fits point charges with ESP near Van der Waal surface grid and uses Breneman radii. Chart 48 incorporates charge-descriptors calculated by CODESSA, a molecular descriptor package.

Chart 47b: CHelpG charge

- + Superior to Mullikan charges
 - + Invariant to rotation
 - + Does not depend upon the orientation of the molecule in a coordinate system
- 👉 Reason: uniform grid of points used to sample ESP
- Assignment of grid points does not reach satisfactorily for buried atoms (SP3 hybridization)
 - 👉 Ex. sterically crowded environment in bulkier sec and tertiary ammonium ion
 - Does not sample points far away from vander waal surface



► Multi-pole moments

The dipole to hexadeca-pole moment and hyper-polarizabilities throw light on polarity and non-linear polarizability of the molecule in isolation and in presence of protein fold/bulk matrix (Eqn. 5). The change in energy from nonlinear effects is due to a change in the electron density, which creates an induced dipole moment and, to a lesser extent induced higher-order multipoles.

🔔 Dipole moment

An electrical field (E) induces a dipole in a molecule, which is considered as a perturbation. However, in QC the charge is a continuous distribution of distance. Dipole moment is an average over the wave function of the dipole moment operator. The difference in sign is due to different conventions of physics and chemistry. Dipole moment from MPA is called permanent molecular dipole moment. The relative magnitudes for comparison are acceptable. Non-quantum mechanical (classical) dipole moment is the sum of product of point charges located at positions r_i .

Eqn. 5: Multipole moments

Dipole_moment	
Classical	QC
$\sum q_i * r_i$	$\sum_i (-r_i) + \sum_A Z_A * R_A$
Z_A	Charge on nuclear core
R_A	Distance between origin and nucleus A

Dipole moment in CQC	
$H' = -e * X * E$	H : perturbation operator X: general Coordinates of atom E: Energy

Multipole				
#_pole	Components			Units
Di_pole	X	Y	Z	Debye/Ang
Quadru_pole	XX	YY	ZZ	Debye/Ang **2
	XY	XZ	YZ	
Octa_pole	XXX	YYY	ZZZ	Debye/Ang ** 3
	XYY	XXY	XXZ	
	XZZ	YZZ	YYZ	
	XYZ			
Hexadeca_pole				Debye/Ang ** 4

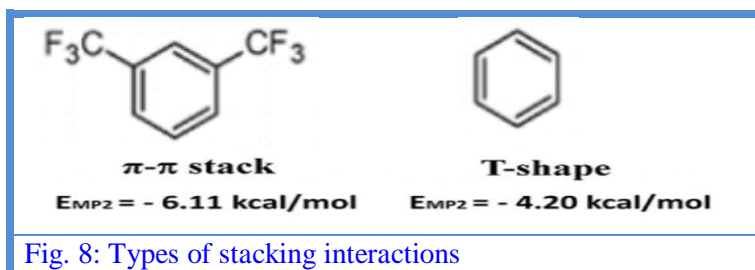
Multi_pole_moments

$$\langle \mathbf{x}^k \mathbf{y}^l \mathbf{z}^m \rangle = \sum_i^{\text{atoms}} Z_i x_i^k y_i^l z_i^m - \sum_j^{\text{electrons}} \int \psi_j(\mathbf{r}_j) (x_j^k y_j^l z_j^m) \psi_j(\mathbf{r}_j) d\mathbf{r}_j$$

k, l, m	0 : monopole, 1 : dipole 2 : quadrupole, 3 : Octapole 4 : hexadecapole	ψ_j	MO occupied by electron j
Z_i	nuclear charge on atom i	\mathbf{r}_j	jth Cartesian coordinates

🔔 Quadrupole moment

Body et al. [122] reported the nuclear quadrupole moment of ^{27}Al as $1.616 (\pm 0.024) \times 10^{-29} \text{ m}^2$ from the correlation of experimental and EFG (electric field gradients) tensor values. Combining complementary/supplementary/exclusive inferences from combining accurate NMR quadrupolar parameter measurements, DFT-based calculations of electric field gradients (EFG) and geometry optimizations (with WIEN2k package) result in more reliable structural information of fluoroaluminates. Mottishaw and Sun [114] employed MP2 and dispersion-corrected DFT (DFT-D) in studying π - π interactions of methylated, fluorinated and trifluoromethylated benzene, pyridine and bipyridine dimers. The molecular quadrupole moment and dispersion enhance these π - π interactions (Fig. 8).



Sedlak et al. [101] used B97-D3, M06-2X, DFT-SAPT, and CCSD(T) for dimers of halogen (F, Cl, Br, I) and nitrogen molecules (Inf.Bits. 9).

Inf.Bits. 9: Quadrupole moment

- ☞ Qzz component of quadrupole moment
- ⇒ Positive for dihalogens

Table 17: SCF values at Equilibrium bond length (= 1.8934 Å)

Quadrupole moment	1.0682 ea ₀ ²
Hexadecapole moment	-41.68 ea ₀ ⁴

Inf.Bits-dipole

<p>⇒ Negative for dinitrogen reflecting magnitude of the σ-hole</p> <p>☞ Dihalogen dimers</p> <p>☞ Most stable structure is LS</p> <p>☞ Dispersion energy > Coulomb energy</p>	Mean Alpha	51.16	<p>Dipole polarizabilities by DFT \approx CCSD(T)</p> <p>- DFT overestimate the second dipole hyperpolarizability</p>
	Anisotropy of dipole polarizability	$28.58 e^2 a_0^2 E_h^{-1}$	
	Mean second dipole	$16.5 \times 10^3 e^4 a_0^4$	
	hyperpolarizability	E_h^{-3}	

Maroulis and Xenides et al. [128] computed electric multi- (Quadru-, Hexadeca-) pole moments, dipole/quadrupole polarizabilities, second electric dipole hyperpolarizability for P2 with finite-field MPx, DFT and coupled cluster techniques (table 17). The near-HF values were with a very large (20s15p10d5f) uncontracted basis set consisting of 300 Gaussian-type functions. The best post-HF magnitudes were computed with a [9s7p5d3f] basis set at the CCSD(T) level.

► Octa polar molecules

Octupolar molecules lack ground state dipole moment and thus crystallize in non-centrosymmetric space groups. They exhibit broader transparency to UV_VIS light and possess higher NLO responses. The compounds with two dimensional frame and 3D-molecules possessing D2, D3, or Td symmetry have been investigated extensively. Some of the typical sets are trisubstituted (triphenyl, tricyano, trinitro, trimethoxy) benzenes hexasubstituted benzenes and phenylacetylene mesitylenes, and 1,3,5-triazines.

🌀 Polarisabilities and hyperpolarisabilities

🔔 If the external electric field is fixed at a definite (frequency) value, the response properties are termed static. For optimized geometries, HF and DFT are used in computation. β_{ijk} tensorial components (Eqn. 6) are calculable using HF/Finite-Field (FF), followed by DFT/CAM-B3LYP or M0x functionals. The third rank tensor of first hyper polarizability is a 3-way tensor of size $3 \times 3 \times 3$. This tensor reduces to 10 components due to Kleinman symmetry. The third rank tensor of first hyperpolarizability is a 3-way tensor of size $3 \times 3 \times 3$. The tensor is reduced to 10 components according to Kleinman symmetry.

🔔 Variation (derivatives) of energy with external electric field

On the other hand, if oscillating electric field (different frequencies) of electromagnetic radiation is applied the hyperpolarizability (response) also becomes dynamic. TD-DFT and TD-HF are the CQC approaches here. Ab initio methods viz. SCF, MCSCF, and Full CI obey Hellmann Feynman theorem rigorously.

Eqn. 6: Induced macroscopic polarization

$$P_i(E) = P_i(0) + \chi_{ij}^{(1)} E_j + \chi_{ijk}^{(2)} E_j E_k + \chi_{ijkl}^{(3)} E_j E_k E_l$$

$\chi^{(1)}$	linear (first order) susceptibility	$\chi^{(2)}$	nonlinear (second order) susceptibility
$P_i(0)$	Intrinsic (zero order) static dipole moment of	$\chi^{(3)}$	nonlinear (third order) susceptibility

1 a.u. = 8.3693×10^{-33} esu

$$\beta^T = 4 * \beta^x$$

output [G03;MOPAC] : atomic units

Software for hyperpolarizabilities: Hyperpolarizabilities seem to be relatively insensitive to the core electron description. Many a time, due to hardware limitations and size of the molecules, initial values are obtained with trodden basis sets or SEMO procedures. In such cases, the numerical values are not only

approximate but are even absurd. The usual practice is to calculate second/third order non-linear polarizabilities along with dipole and multipole moments with both ab initio and DFT paradigms. Ab initio methods viz. SCF, MCSCF, and Full CI obey Hellmann Feynman theorem rigorously. Thus, hyperpolarizabilities computed with these CQC procedures are accurate and reliable for small molecules. Champagne et al. have shown that traditional B3LYP functional in DFT overestimate the (hyper) polarizabilities of large systems especially where contribution of long range charge-transfer transition significantly. Higher basis sets with diffuse/high-angular-momentum polarization functions yield quantitatively correct values of NLO parameters for simple molecules. Also, explicitly correlated wave functions give very accurate results. However, the calculations are not tractable with MPx, TD-HF except for very small molecules. Good agreement is there between ECP basis sets and all electron basis sets. Recently, Coulomb-attenuated hybrid exchange-correlation functional (CAM-B3LYP) was introduced in to this bandwagon. It accurately predicts NLO properties of a large system (fullerene-dimers) and circumvents earlier limitations. In this decade, DFT with newer powerful exchange/correlation functionals viz. BMK, M0x [M05, M05-2X, M06], CAM-B3LYP is trust worthy approach for NLO parameters of comparable values with instrumental results. Even very small variations in the physico chemical characteristics, solvent cavity and/or solute-solute/solute-solvent interactions alter hyperpolarizabilities largely. They are partially accounted in computations by invoking dispersion effects either empirically or through new functional. Polarizabilities are calculated using analytical/numerical derivatives depending upon level of theory and functional.

material		Expt : β^T
$\beta_{tot}^2 = \beta_{xxx}^2 + \beta_{yyy}^2 + \beta_{zzz}^2 + 3\beta_{xyy}^2 + 3\beta_{xzz}^2 + \beta_{yzz}^2 + 3\beta_{yxx}^2 + 3\beta_{zxx}^2 + 3\beta_{zyy}^2 + 6\beta_{xyz}^2$		
Polarizability_G03	:	[Analytical derivatives, Numerical derivatives]
Analytical_derivatives	:	[HF (RHF, UHF), MP2 (RMP2, UMP2), CASSCF, DFT]
Numerical_derivatives	:	[MP3, MP4 (SDQ), CI [CID, CISD, PCISD], CCD]
Keyword	:	[polar] [CPHF = Rdfreq]

Electro-optics (EO)

While EO activity has long been known to functionally depend upon chromophore first hyperpolarizability, (b) acentric order ($\langle \cos 3q \rangle$) and number density (N), the inter-dependence of these parameters and the need to use quantum and statistical mechanics to understand this interdependence has only recently been appreciated.

► Derived NLO characteristics

The other NLO phenomenon includes Electro-optics Pockels effect (EOPE), Optical rectification (OptRect), two-wave mixing (TWM) in the case of second order, while third order one includes Intensity-dependent refractive index or degenerate four-wave mixing (IDRI), Optical Kerr effect (OKE), DC-induced optical rectification (DCOR), DC-induced second harmonic generation or electric-field-induced second harmonic (DC-SHG or EFISH), Electro-optic Kerr effect (EOKE), three-wave mixing, DC-induced two-wave mixing and Coherent anti-Stokes Raman scattering (CARS).

The ratio of off diagonal to the diagonal of second order hyper polarisability tensorial components ($r = \beta_{xyy} / \beta_{xxx}$), product of dipole moment and second order hyperpolarizability ($\mu^* \beta_0$), length (top)

and calculated $(N^2 * \langle \beta_{eff}^2 \rangle)$ where N is chromophore number density (bottom) and square of effective first hyperpolarizability and inplane non-linear anisotropy are a few typical derived quantitative measures of functional characteristics of NLO materials. The density-matrix renormalization group (DMRG) procedure is used to compute the dynamic NLO responses of p-conjugated systems. The static polarizabilities (zero to third order) differ from second/third order hyperpolarisabilities in that the exciting photon has same or different frequency from incoming radiation photons.

A set of organic chromophores with β values (30 to $120 * 10^{-30}$ esu) for application in non-linear optics with modulated thermal stability are reported. In an elongated molecule, electrons flow easily from one end to the other. It functions as a molecular wire, which is the simplest molecular electronic device. The electronic structure of substituted (-NH₂, -CH₃O, -CN and -NO₂) compounds containing three benzene rings with intervening acetylene moieties are prospecting candidates. Nitro group resulted in conducting HOMO and LUMO levels, which leads to the engineering of tailor made molecular devices with specific conducting characteristics.

Switching

An NLO material exhibits reversible switching of hyperpolarisability due to photochromic/thermochromic reactions in solutions/solid phases. The requirement for the binary/multiple switching components is that the molecules have multiple stable and independently addressable states. The outcome at utility level is smaller size devices. A number of two/multi-way (five/six) state switches are developed based on first order hyperpolarizability response. Although, conformation change is a means of developing switching material, yet the moment monitoring NLO response of conformers is difficult with the current hyperpolarizability measurement procedures. The unique advantages of 3D organic NLO compounds are high oscillator strength and low-lying energy excited states, increased stability of polar order in poled polymers and Langmuir-Blodgett (LB) films better nonlinearity/transparency tradeoff, larger macroscopic NLO responses under the phase-matching orientations and the off-diagonal β tensor component is larger compared to that of 1-D compounds.

Compound	α	γ
Flouro-diacetylene F-C=C-C=C-H	49	9626
Diacetylene H-C=C-C=C-C-H	47.8	11,450

Chemically significant descriptors derived from CQC

The number of quantum chemical descriptors now calculable with CODESSA, DRAGON etc exceeds 4000 in number. An in-depth analysis shows that QC output can be categorized as descriptors obtained by simple algebraic manipulation of FMO energies. The information obtained from derivatives of energy with respect to nuclear co-ordinates, external electrical/magnetic field, application of statistical mechanics, population analysis etc. is the basis.

Fuki Descriptors

Fuki descriptors are the difference between gross charges of the atoms in the neutral molecule and the corresponding cationic and anionic species. They distinguish electrophilic/nucleophilic/radical reaction sites (atoms) in the molecule without knowing the other reactant. These are also used as additional indicators to determine relative softness of each atom. In fact, for a set of analogous molecules, Fuki indices offer a good comparison.

Relative densities of FMOs and their relationships including condensed Fuki functions are most useful and consequently more laudable criteria to predict chemical reactivity. Condensed local softness indices are related to condensed Fuki values. For frontier orbital controlled soft-soft interactions, Fuki values are very large.

Softness and hardness

If a molecule is hard, it resists the changes in distribution of electron charge cloud in space or total amount of charge. The magnitude of hardness is thus a measure of the ease with which electrons are polarized or resists to deformation. Thus, hard-hard interactions are charge based (chart 49). On the other hand, soft molecule is easily susceptible to change in charge cloud density. The electrostatic and covalent interactions are reflected in hardness and softness of the molecule. The localized and delocalized FMOs provide information about orbital based interactions in addition to Woodward-Hoffman rules.

Chart 49: Chemically significant descriptors

Descriptor	Type of reaction
Total energy	Measure of stability
Electro negativity chemical hardness	$E_{\text{HOMO}} - E_{\text{LUMO}}$ gap
Fuki+	Nucleophilic
Fuki-	Electrophilic
FukiRad	Radical

Descriptor	Meaning
BE	Binding
CCE (core_core)	Core-Core
Ele_E	Electronic
IAE	Isolated atomic
LLE	Lowest level
NRE (nucl_repul)	Nuclear repulsion
Rel_ener	Relative
TE	Total
Tot_ener	

6. I/O of CQC (ICO)

Input

3D-structure of chemical compound represented in x,y,z axis is the basic chemical input information to any CQC software package. X-ray or NMR structures of many compounds are available in standard databases like Swiss-PDB, Cambridge crystallography database etc. G03 accepts PDB compound structure as input. When only 2D-information is available, programs like CORINA converts it into 3D-structure.

Co-ordinate system to represent structure of a molecule/atom

The quality of a co-ordinate system used in CQC package depends upon minimum of coupling between atoms. This correlation manifests primarily due to large partial derivative terms between different co-ordinates. The best representation has minimum impact of variation of one the co-ordinates on other co-ordinates. A brief description of different types of co-ordinate systems is as follows (Chart 50, KB. 6).

Chart 50: Co-ordinate systems in CQC

Cartesian (XYZ)

- + Gradient and Hessian calculated directly
- Heavily coupled

Z matrix (BL, BA, DH)

- + Efficiency (for acyclic)
- + Redundancy partially reduced
- BA, DH arbitrarily omitted
- Induces anharmonic coupling between coordinates

Natural internal co-ordinates (NIC) Pulay (1979)

- + Coupling reduced
 - o Harmonic & anharmonic
- + Optimum ensured
- + Approximate Hessian
- User input of coordinates
- Breakthrough Automatic generation of NIC from Cartesian

KB. 6: Co-ordinate systems

- | | | |
|------|------------------------------------|---|
| If | Medium size molecule | & |
| | Initial geometry reasonable | & |
| | Reliable Hessian | |
| Then | Cartesian coordinates good choice | |
| If | Long chain acyclic system | & |
| | No good Hessian | |
| Then | Cartesian coordinates insufficient | |

Delocalised internal co-ordinates (DIC)

❖ Basis: RCS + A complete non redundant set
--

For simple molecules (H_2 , ethylene, methyl alcohol, benzene ... etc) and substituent's ($-NO_2$, $-NH_2$, $-CONH_2$ etc.), Z-matrices method is viable from the inspection of connectivity of atoms in the molecule. It is prone to be erroneous to jot down Z-matrices for even 20-atom compounds with a paper and pencil technique followed by keying it into a computer readable file. GUI embedded into the packages (even low-end academic/commercial ones), relieves this drudgery and a chemist is comfortable to develop molecules of any complexity from the rings, groups etc. And, special provision is available to develop periodic (polymer) systems, crystal lattices and so on. AGUI of AMPAC, GaussianView of G03/G09, Chemcraft of GAMESS and built in features of Hyperchem are a few examples. The third party software modules are also available with tremendous portable characteristics. This front-end module contains meta-chemical bonding knowledge and cleaning option enables further refinement of chemical structure. The total charge on the chemical moiety (-4 to +4 through 0), multiplicity (singlet to sextet), solute phase and medium are other information needed. The level of theory (SEMO, ab initio, DFT), functional and basis sets are user chosen options. The task viz. geometry optimization, frequency calculation, properties etc are the input depending upon the provisions of the package. Meta knowledge is useful for expert mode package like in G1 to G4 models of G03/G09. The initial Hessian and output choice are optional. Abelian/framework group/subgroup information of the molecule is required in a few packages.

GUI: Although separate modules or packages are developed for input of chemical compounds and output of (2D-, 3D-) graphical display they are integrated with most of software. Gaussview released with G03 is a landmark in ab initio and DFT calculations. Earlier to this, the output files from other packages like MOPAC, AMPAC were used as input to Gaussian. The interface programs for a variety of third party tools were remarkable. Now GAMESS and Hyperchem also have GUI for I/O operations. The need of the hour is experts' knowledge bits for post-processing as well as for input choices. This guides inexperienced application users and a time relieving tool for experts. With exponential growth breadth wise of CQC literature for molecules and improvements/reports of new functionals and models in the solvent, ES approach is warranted.

Front end and backend MATLAB programs for G03

Front end and backend programs are developed in MATLAB to eliminative drudgery of editing input job-files, pooling up and preparing the tables of output for routine inspection and promoting automatic prototype tables. GIFT.m (pronounced as gift) is a front end module.

bcfs.m

In G03 suit of programs, any number (≥ 1) runs (.gjf) can be given and the system runs the jobs sequentially. It requires the preparation of a .gjf file for each molecule or for each model (chart 51).

In projects demanding scientific enquiry, a large number of small molecules each with different models and each model with a variety of (hither to available) functionals required. In such tasks, the run time is negligible, but job file editing is tedious. An automatic generation of .gjf files for each system and a batch file to run these jobs is contemplated and implemented in bcf.m. In these tasks, the molecular information remains same and if once checked, it is fool proof even for hundreds of runs. It further avoids cut and paste jargon for a set of .gjf files. A machine generated file is 100% reliable. For instance, when a quantum chemical run is to be repeated say for different functionals/methods/solvents a portion of the file is be edited. MATLAB m-function (h2oenergy.bcf) is developed to create a batch file compatible with G03 stipulations. It is an illustration for H_2O with different SEMO/ab initio/DFT. An abridge form of the results is in table. This approach is in the practice in this laboratory for over a decade. It hastened the development of hundreds to thousands of output files from which a few sets are selected in intensive

studies. Although a batch file with hundreds of jobs is created (G03 test data files), one can start running from any job (say 9) with a meta command, 'start=9'.

SEMO_packages

AMPAC performs semi empirical quantum chemical MO calculations for a given chemical structure in either Z-matrix or Cartesian coordinates format and outputs optimized geometry, numerical data for HOMOs/LUMOs and charge density. Agui is an add-on multi-dimensional graphics interface to draw the chemical structure, display optimized geometry, total electron density (TD), electrostatic potential (ESP) etc.

Input files for molecules with different Hamiltonians, convergence in SCF/ geometry and calculation of hyperpolarizabilities are generated from MATLAB (INPAMP.m) functions developed in our laboratory. In house programs are available for tabular and graphic display of output of Ampac for a set of runs (compounds/Hamiltonians/parameters etc).

Output

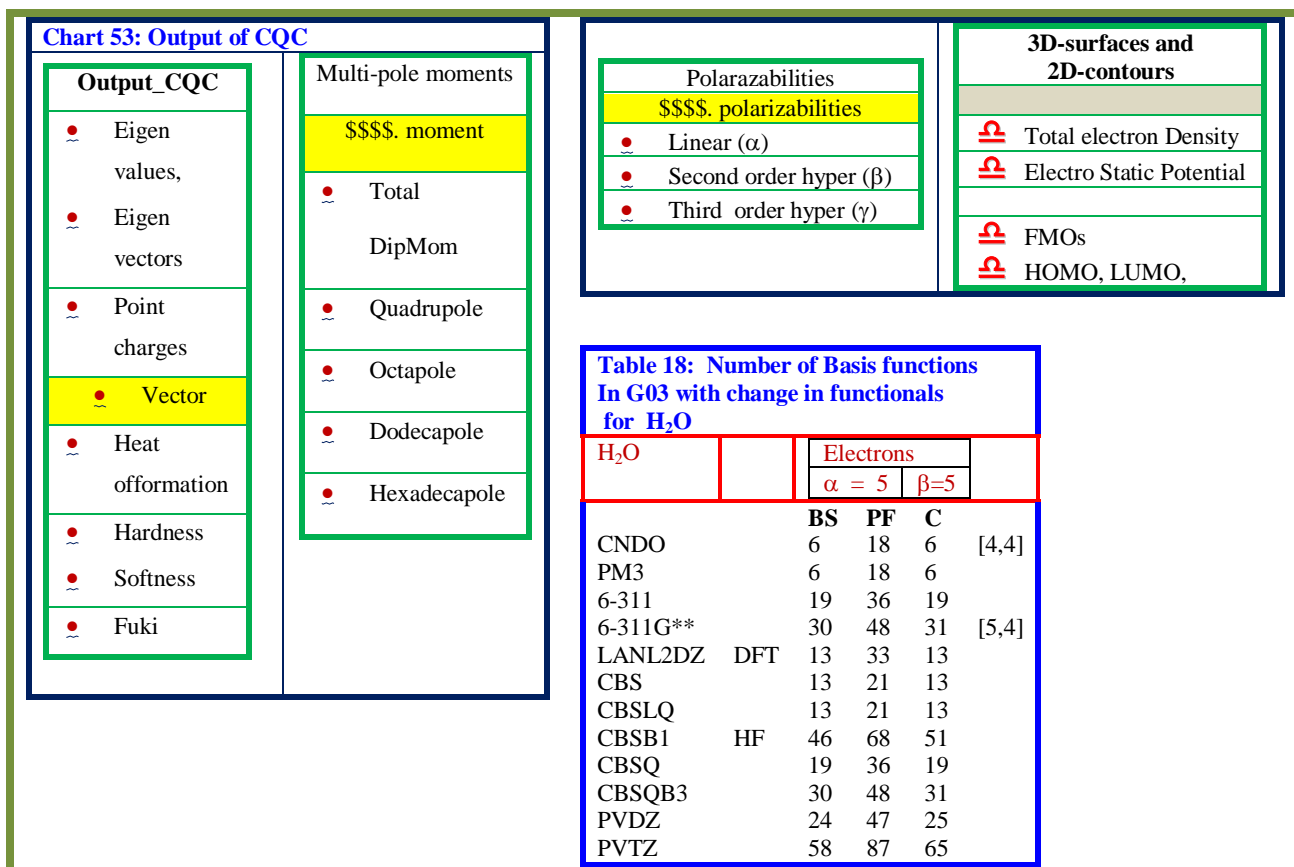
The primary output of CQC calculation (chart 52) based on solution of Schrodinger wave equation for a given geometry of a molecule is a set of MOs (FMOs) and corresponding energies in the gas phase for a chosen frame work [MM, SEMO, ab initio [[HF, post-HF], DFT[TD-DFT]]]. i.e. a valid (real chemical species). The types of derived descriptors are in chart 53. At any other geometry than at fully optimised geometry is undefined. Table 18 incorporates the increase in number of basis functions with change in functionals in CQC.

Chart 51: Batch file

```
D:\H2O\h2oenergy.bcf
!
!user created batch file list
!start=9
!
D:\H2O\h2o-CNDO.gjf, D:\H2O\h2o-CNDO.out
D:\H2O\h2o-cbs.gjf, D:\H2O\h2o-cbs.out
D:\H2O\h2o-cbs-4M.gjf, D:\H2O\h2o-cbs-4M.out
D:\H2O\h2o-cbs-LQ.gjf, D:\H2O\h2o-cbs-LQ.out
D:\H2O\h2o-cbs-q.gjf, D:\H2O\h2o-cbs-q.out
D:\H2O\h2o-cbs-qb3.gjf, D:\H2O\h2o-cbs-qb3.out
D:\H2O\h2o-G2.gjf, D:\H2O\h2o-G2.out
D:\H2O\h2o-G3.gjf, D:\H2O\h2o-G3.out
D:\H2O\h2o-G3B3.gjf, D:\H2O\h2o-G3B3.out
D:\H2O\h2o-G3MP2B3.gjf, D:\H2O\h2o-G3MP2B3.out
```

Chart 52: Output of CQC

```
Primary      : [optimized
                geometry,
                [{energy,MO}]
Auxillary    : Group [point,
                Ableian]
                Alpha_,Beta_
                electrons
                No_of_BFs,
                No_of_primary
                functions
```



Single point energy

A single point (Eqn. 6b, Fig. 9) corresponds to the co-ordinates of the molecule on potential energy surface (PES). The single point referred may be stationary point, TS, saddle point or any point (with no specific name). It outputs electronic energy derivatives viz. ESP, E_FMO. Some of typical energies in vogue in CQC are

Eqn. 6b: Energy from CQC

$$\text{Energy} : \left[\begin{array}{l} \left[\text{Nuclear, electronic} \right], \\ \left[\text{Translational, [vibrational, Rotational, Vibronic_rotational]} \right] \end{array} \right]$$

$$\text{Energy_vibrational} : \left[\text{ZPE}, \{ \text{vibronic_modes}(1, 2, \dots) \} \right]$$

$$\text{Energy_electron-electron} : \left[\begin{array}{l} \text{Coulomb_energy}, \\ \text{exchange_energy, Correlation_energy} \end{array} \right]$$

$$\text{Energy_AMPAC} : \left[\text{oc-eea oc-eer tc-eea tc-eer thc-eer thc-eer} \right]$$

oc : one center, tc : two center; thc : three center; e: electron ;
c : center; a : attraction; r: repulsion

<p>Chart 6c: Energy terms</p> <table border="1"> <tr><td></td><td>\$\$_Energy</td></tr> <tr><td>BE</td><td>Binding</td></tr> <tr><td>CCE</td><td>Core-Core</td></tr> <tr><td>(core_core)</td><td></td></tr> <tr><td>Ele_E</td><td>Electronic</td></tr> <tr><td>IAE</td><td>Isolated atomic</td></tr> <tr><td>LLE</td><td>Lowest level</td></tr> <tr><td>NRE</td><td>Nuclear repulsion</td></tr> <tr><td>(nucl_repul)</td><td></td></tr> <tr><td>Rel_ener</td><td>Relative</td></tr> <tr><td>TE</td><td>Total</td></tr> <tr><td>Tot_energ</td><td></td></tr> </table>		\$\$_Energy	BE	Binding	CCE	Core-Core	(core_core)		Ele_E	Electronic	IAE	Isolated atomic	LLE	Lowest level	NRE	Nuclear repulsion	(nucl_repul)		Rel_ener	Relative	TE	Total	Tot_energ		<p>Chart 6d: Partitioning of energy terms</p> <table border="1"> <tr><td>oc</td><td>One center</td><td>e</td><td>Electron</td></tr> <tr><td>tc</td><td>Two center</td><td>c</td><td>Center</td></tr> <tr><td>A</td><td>Attraction</td><td>r</td><td>Repulsion</td></tr> <tr><td>NPI</td><td>Neighboring pair interaction</td><td>OCE</td><td>One electron core-electron attraction</td></tr> <tr><td>NNI</td><td>Non-neighbor interaction</td><td>TCE</td><td>Two center core-electron attraction</td></tr> </table>	oc	One center	e	Electron	tc	Two center	c	Center	A	Attraction	r	Repulsion	NPI	Neighboring pair interaction	OCE	One electron core-electron attraction	NNI	Non-neighbor interaction	TCE	Two center core-electron attraction
	\$\$_Energy																																												
BE	Binding																																												
CCE	Core-Core																																												
(core_core)																																													
Ele_E	Electronic																																												
IAE	Isolated atomic																																												
LLE	Lowest level																																												
NRE	Nuclear repulsion																																												
(nucl_repul)																																													
Rel_ener	Relative																																												
TE	Total																																												
Tot_energ																																													
oc	One center	e	Electron																																										
tc	Two center	c	Center																																										
A	Attraction	r	Repulsion																																										
NPI	Neighboring pair interaction	OCE	One electron core-electron attraction																																										
NNI	Non-neighbor interaction	TCE	Two center core-electron attraction																																										
<p>Chart 6e: Relationship between analytical derivatives of energy with electric field and magnetic properties</p> <table border="1"> <tr> <td>Permanent dipole moment</td> <td>First derivative of energy (E) wrt external electric field (EF)</td> <td>$\frac{\partial E}{\partial EF_a}$</td> </tr> <tr> <td>Polarizability</td> <td>Second derivative of energy (E) wrt external electric field (EF)</td> <td>$\frac{\partial^2 E}{\partial EF_a \partial EF_b}$</td> </tr> <tr> <td>Hyperpolarizability</td> <td>Third and higher order derivatives of energy (E) wrt external electric field (EF)</td> <td>$\frac{\partial^3 E}{\partial EF_a \partial EF_b \partial EF_c}$</td> </tr> </table>	Permanent dipole moment	First derivative of energy (E) wrt external electric field (EF)	$\frac{\partial E}{\partial EF_a}$	Polarizability	Second derivative of energy (E) wrt external electric field (EF)	$\frac{\partial^2 E}{\partial EF_a \partial EF_b}$	Hyperpolarizability	Third and higher order derivatives of energy (E) wrt external electric field (EF)	$\frac{\partial^3 E}{\partial EF_a \partial EF_b \partial EF_c}$	<p>Chart 6f: Relationship between vibrational frequencies and analytical derivatives of energy with nuclear co-ordinates</p> <table border="1"> <tr> <td>Forces on nuclei</td> <td>$\frac{\partial E}{\partial R_x}$</td> <td rowspan="3"> <table border="1"> <tr><td>R</td><td>Nuclear co-ordinates</td></tr> <tr><td>x,y,z</td><td>directions</td></tr> </table> </td> </tr> <tr> <td>Harmonic vibrational frequency</td> <td>$\frac{\partial^2 E}{\partial R_x \partial R_y}$</td> </tr> <tr> <td>Fundamental vibrational frequencies</td> <td>$\frac{\partial^3 E}{\partial R_x \partial R_y \partial R_z}$</td> </tr> </table>	Forces on nuclei	$\frac{\partial E}{\partial R_x}$	<table border="1"> <tr><td>R</td><td>Nuclear co-ordinates</td></tr> <tr><td>x,y,z</td><td>directions</td></tr> </table>	R	Nuclear co-ordinates	x,y,z	directions	Harmonic vibrational frequency	$\frac{\partial^2 E}{\partial R_x \partial R_y}$	Fundamental vibrational frequencies	$\frac{\partial^3 E}{\partial R_x \partial R_y \partial R_z}$																								
Permanent dipole moment	First derivative of energy (E) wrt external electric field (EF)	$\frac{\partial E}{\partial EF_a}$																																											
Polarizability	Second derivative of energy (E) wrt external electric field (EF)	$\frac{\partial^2 E}{\partial EF_a \partial EF_b}$																																											
Hyperpolarizability	Third and higher order derivatives of energy (E) wrt external electric field (EF)	$\frac{\partial^3 E}{\partial EF_a \partial EF_b \partial EF_c}$																																											
Forces on nuclei	$\frac{\partial E}{\partial R_x}$	<table border="1"> <tr><td>R</td><td>Nuclear co-ordinates</td></tr> <tr><td>x,y,z</td><td>directions</td></tr> </table>	R	Nuclear co-ordinates	x,y,z	directions																																							
R	Nuclear co-ordinates																																												
x,y,z	directions																																												
Harmonic vibrational frequency	$\frac{\partial^2 E}{\partial R_x \partial R_y}$																																												
Fundamental vibrational frequencies	$\frac{\partial^3 E}{\partial R_x \partial R_y \partial R_z}$																																												
<p>Chart 6g: Relationship between analytical derivatives of energy with magnetic moment, susceptibility and magnetic field</p> <table border="1"> <tr> <td>Magnetic dipole moment</td> <td>$\frac{\partial E}{\partial B_x}$</td> <td rowspan="3"> <table border="1"> <tr><td>B</td><td>Magnetic field</td></tr> <tr><td>$\mu_{nuclear}$</td><td>Nuclear magnetic moment</td></tr> </table> </td> </tr> <tr> <td>Magnetic susceptibility</td> <td>$\frac{\partial^2 E}{\partial B_x \partial B_y}$</td> </tr> <tr> <td>NMR chemical shielding</td> <td>$\frac{\partial^2 E}{\partial B_x \partial \mu_{nuclear}}$</td> </tr> </table>	Magnetic dipole moment	$\frac{\partial E}{\partial B_x}$	<table border="1"> <tr><td>B</td><td>Magnetic field</td></tr> <tr><td>$\mu_{nuclear}$</td><td>Nuclear magnetic moment</td></tr> </table>	B	Magnetic field	$\mu_{nuclear}$	Nuclear magnetic moment	Magnetic susceptibility	$\frac{\partial^2 E}{\partial B_x \partial B_y}$	NMR chemical shielding	$\frac{\partial^2 E}{\partial B_x \partial \mu_{nuclear}}$																																		
Magnetic dipole moment	$\frac{\partial E}{\partial B_x}$	<table border="1"> <tr><td>B</td><td>Magnetic field</td></tr> <tr><td>$\mu_{nuclear}$</td><td>Nuclear magnetic moment</td></tr> </table>		B	Magnetic field	$\mu_{nuclear}$	Nuclear magnetic moment																																						
B	Magnetic field																																												
$\mu_{nuclear}$	Nuclear magnetic moment																																												
Magnetic susceptibility	$\frac{\partial^2 E}{\partial B_x \partial B_y}$																																												
NMR chemical shielding	$\frac{\partial^2 E}{\partial B_x \partial \mu_{nuclear}}$																																												

The electronic energies computed from G4, G4_MP2, G3B3, G3_MP2, G3, CBS etc are in good agreement with the experimental values obtained from accurate (instrumental) measurements. It enables one to compute energies and geometry for a large set of molecules well before synthesis.

Energies of FMOs

In HF theory, the eigen-value associated with each MO is the energy of an electron in that MO. The energy of the molecule in the ground state computed from SWE is the electronic energy. The two important

components deserve utmost attention in moving from single electron to multi-electron moieties are correlation and exchange energies.

The progress of levels of theory, functionals, BSs of the atom, multiple convergence criteria by quantum chemists and optimization algorithms, parallelization of computation increased the accuracy of electronic energy of even large molecular systems in gas as well as in condensed phases. The evolution of Hamiltonians, projection of classical physico-chemical procedures into QC framework endorsed that CQC is another tool competing with a century old instrumental methods of analysis. The noteworthy feature of CQC-software (QC-instrument) is it outputs all descriptors even for molecules not yet synthesized i.e. virtual (brainchild) molecules. The iterative advances of experimental, CQC-algorithms are competitive finding a niche and they are in no comparison with those of even mid twentieth century.

The summation model to calculate the total energy is used with nuclear repulsion energy, vibrational components from first derivative of energy with respect to nuclear co-ordinates translational, rotational and vibronic-rotational energy components calculated by non-quantum mechanical methods. In SEMO, the components used are OC-CEA, CC-eer etc to decompose the energy into constituent parts. Statistical thermodynamic principles are used to calculate G, H and S of the molecule. The figurative representation of energies of FMOs is called energy diagram separating HOMOs from LUMOs (KB.7, Fig. 9) and is useful to explain photochemistry, transition metal chemistry and energetics of excited states (table 19). The energy gap between HOMO and LUMO is a measure of aromaticity of the organic molecule. It is obvious that it is related to chemical hardness, redox potential and electrical resistivity. The electronic spectrum of 2,3- trifluoromethyl-INH calculated using TD-DFT at 6-311G level is in the table. 19b.

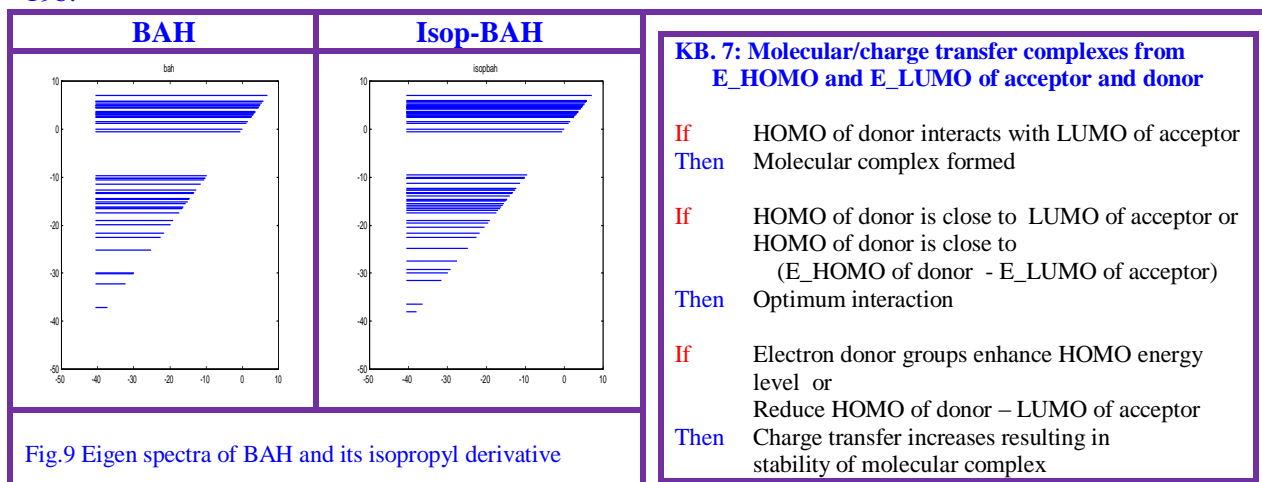
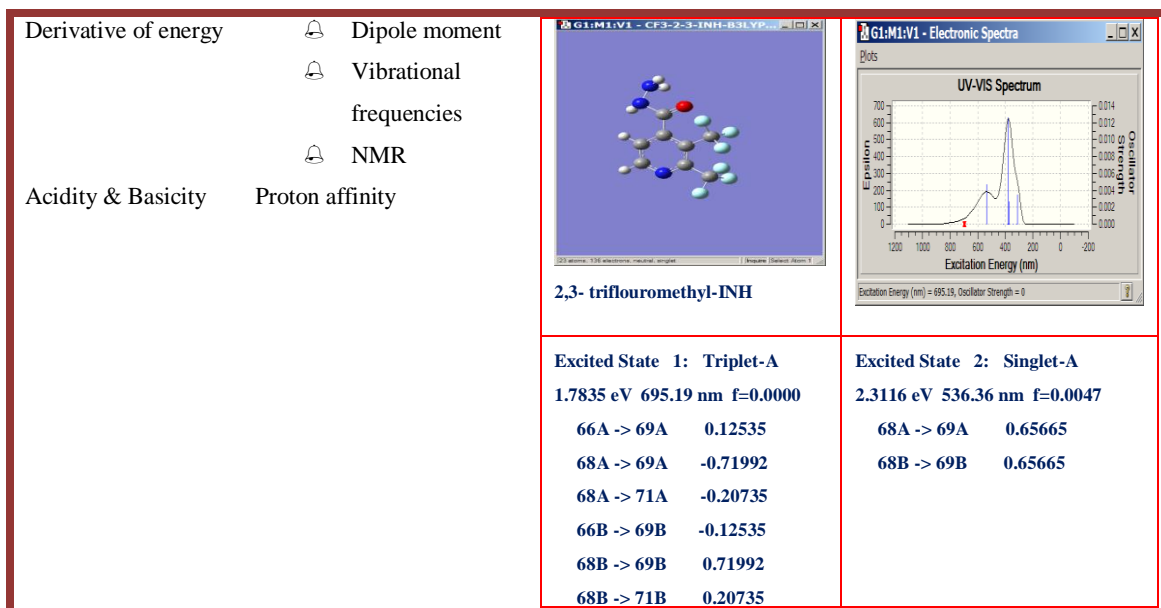


Fig.9 Eigen spectra of BAH and its isopropyl derivative

Table 19: Descriptors and UV-Vis spectrum from CQC

Type of energy	Physico-chemical descriptor
Energy	Enthalpy of formation
Orbital energy levels	HOMO, LUMO, others
Electron distribution	Electron density
HOMO energy	Ionization energy
LUMO energy	Electron affinity
UV-Vis spectra	HOMO-LUMO gap

Table 19b: Electronic transitions and for excited states



Gradient, Hessian and higher order derivatives of energy

In HF theory, the eigen-value associated with each MO is the energy of an electron present probabilistically in that MO. The variation of quantum chemical energy is the key to obtain vibrational characteristics, NMR chemical shifts, dipole moments and/or (linear/non-linear) polarizabilities of a real/virtual moiety with chemical validity. The formulae and heuristics are useful in pedagogy and expert system driven software. These meta rules form the basis as a front end to warn amateur users of the packages.

Hyper.m

This m-file (om_hyper.m) calculates anisotropic polarizabilities viz. linear and non-linear second order from polar and bivectors. Hyper.m program outputs α , β and γ for a series of compounds (KB.8, table 20). The input consists of compound name, polar and hyper polar vectors (chart 54).

Chart 54: Matlab program for Hyperpolarizability

```

%
% om_hyper.m      ver 2 06/5/11 ; Ver.1: 2006
%
% (Om : Object function module, Object m-file, a + e + u + m)
%
function [alpha,delalpha, beta_au,beta_esu]=om_hyper(polar,b)
if nargin == 0
    polar = [5.5031611,0.0000021,2.4079671,-1.3285897,-0.000003,6.4426222]';
    b= [24.2541891,-0.0039745,2.4887686,0.,-
6.7652237,0.000343,1.7598252,3.6767058,0.0024724,26.5224571]';
    %[alpha,delalpha, beta_au,beta_esu]=om_hyper(polar,b);
end
a =polar;
beta_au= [-12.808528];
beta_esu = beta_au * 8.6393e-33/1e-30;

```

```

axx = a(1);
axy = a(2);
ayy = a(3);
axz= a(4);
ayz= a(5);
azz = a(6);
disp('Linear polarizability
(Alpha)')
disp(a')
alpha = (axx+ayy+azz)/3;

```

KB. 8: Hyperpolarizability and NLO property

If Hyper polarizabilities of a microscopic molecule is large ($\beta > 30$ or 40) $\gamma > 300$

Then Macroscopic molecules have non-linear optical properties

Expert opinion: substituent, branches may increase NLO characteristics

```

% anisotropy of polarizability

```

```

delalpha = ((axx - ayy).^2 + (axx - azz).^2 + (ayy - azz).^2)/2;
bxxx = b(1 );
bxyy = b(2 );
bxyy = b(3 );
byyy = b(4 );
bxxz = b(5);
bxyz = b(6 );
byyz = b(7 );
bxzz = b(8 );
byzz = b(9 );
bzzz = b(10 );

```

Table 20: Polarizability of As_4

$e^2 a_0^2 E h^{-1}$	
Expt ⁽¹⁾	CQC ⁽²⁾
116.7 ± 1.1	119.5 ± 3.6
⁽¹⁾ Refractivity measurements in arsenic vapor	
⁽²⁾ ab initio finite-field many-body perturbation + coupled-cluster	

```

beta_au = ((bxxx+bxyy+bxzz).^2 + (byyy+byzz+bxyy).^2 + (bzzz+bxxz+byyz).^2)^0.5;
beta_esu = beta_au * 8.6393e-33/1e-30;
disp('Second order hyper polarizability (Beta)')
disp(b')
disp('alpha,delalpha, beta_au,beta_esu')
disp([alpha,delalpha, beta_au,beta_esu])

```

```

% gamma pol/03/20
% gama_av = (gxxxx + gyyyy + gzzzz + 2 * gxxxy + 2 * gxxzz + 2 * gyyzz)/5

```

```

%
% inh_hyper ver 2.0 06/5/11 ;
%
% (Om : Object function module, Object m-file, a + u + m)
%
clean
level = ' RB3LYP/6-311G'
name1 = 'BAH'
n = 1
Polar=[94.7176724,3.4066889,42.2723933,2.7421619,1.4505011,125.6734235];
HyperPolar=[-6.6746043,-2.2101354,10.6746678,3.1341474,-92.6898251,-
32.0947475,6.02059,-30.3811687,-6.894522,103.011786];

[alpha(n,1),delalpha(n,1), beta_au,beta_esu(n,1)]=om_hyper(Polar,HyperPolar)

name2 = 'INH'
.....
name6 = 'isop-PAH'
n = n+1
Polar=[133.6616149,2.6800391,88.3388982,13.7792836,16.2726099,133.4938733]
HyperPolar=[22.9074608,-30.743575,-23.3860724,-115.7484845,-50.9228626,-4.0916948,-
3.280071,11.5084081,38.4804155,32.864346]

```

```
[alpha(n,1),delalpha(n,1), beta_au,beta_esu(n,1)]=om_hyper(Polar,HyperPolar)

[alpha,beta_esu]
comp= str2mat(name1,name2,name3,name4,name5,name6)
gap = ', '
disp('Table #: Linear and Hyperpolarizabilities')
disp('-----')
disp('          Alpha          DelAlpha          Beta ')
disp('          (esu *1e-30)')
disp('-----')
for i = 1:6
    disp( [comp(i,:),gap, num2str(delalpha(i)),gap,
num2str(alpha(i)),gap,num2str(beta_esu(i))] )
end
disp('-----')
break
```

Static dipole polarizability: Hohmet al. [134] found experimental and CQC output are in close agreement for As₄(table 20).

fuki.m

From the three input vectors containing charges on cation, neural and anion moieties of the molecule, Fuki descriptors are calculated and outputted in a tabular form for all the atoms of the molecule (chart 55). dem_fuki.m is a demonstration program for three atoms. The m-files and the output follows.

Chart 55: Fuki descriptors

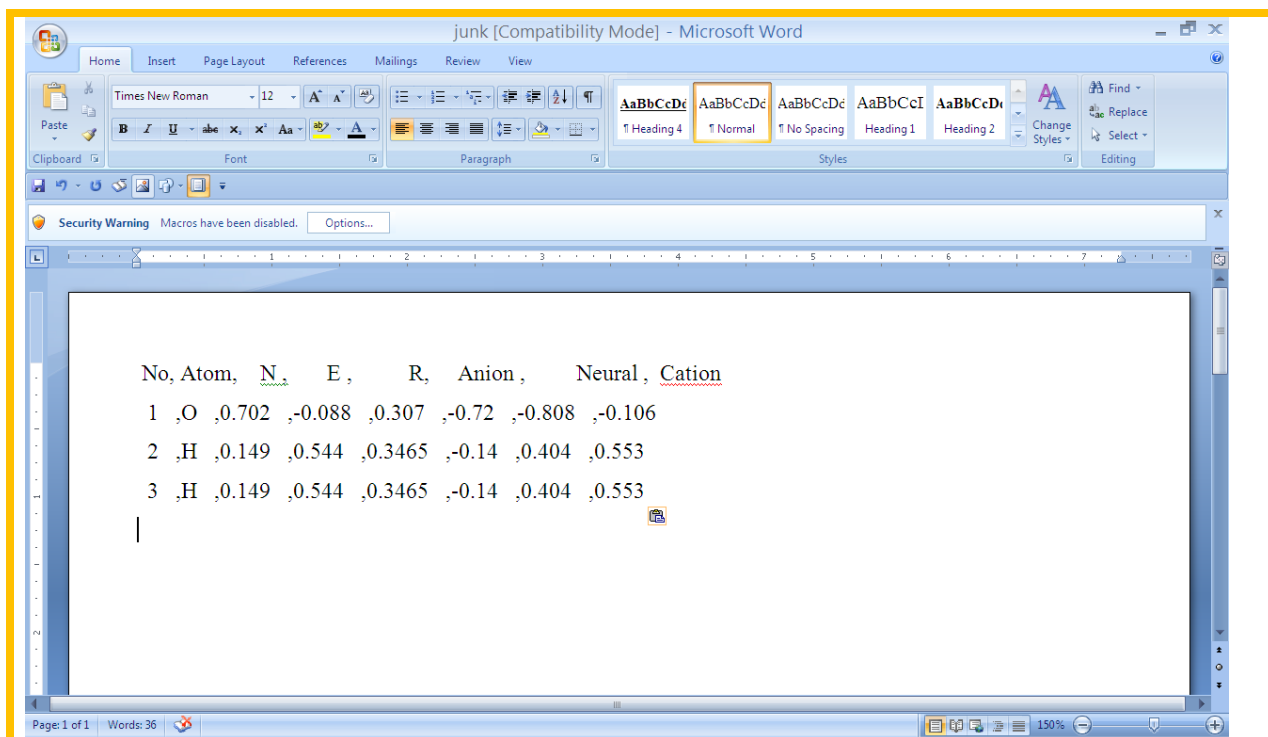
In MATLAB window

```
>> dem_fuki
```

```
-----
No, Atom, N, E, R, Anion, Neural, Cation
1 ,O ,0.702 , -0.088 ,0.307 , -0.72 , -0.808 , -0.106
2 ,H ,0.149 ,0.544 ,0.3465 , -0.14 ,0.404 ,0.553
3 ,H ,0.149 ,0.544 ,0.3465 , -0.14 ,0.404 ,0.553
-----
```

```
>>
```

copy output to word file



insert → table

Convert text to table

choose commas
click OK

No	Atom	N	E	R	Anion	Neural	Cation
1	O	0.702	-0.088	0.307	-0.72	-0.808	-0.106
2	H	0.149	0.544	0.3465	-0.14	0.404	0.553
3	H	0.149	0.544	0.3465	-0.14	0.404	0.553

Autofit → contents							
No	Atom	N	E	R	Anion	Neural	Cation
1	O	0.702	-0.088	0.307	-0.72	-0.808	-0.106
2	H	0.149	0.544	0.3465	-0.14	0.404	0.553
3	H	0.149	0.544	0.3465	-0.14	0.404	0.553

1	O	0.702	-0.088	0.307	-0.72	-0.808	-0.106
2	H	0.149	0.544	0.3465	-0.14	0.404	0.553
3	H	0.149	0.544	0.3465	-0.14	0.404	0.553

```
%
% dem_fuki.m 16/4/11
%

clear all, clc, format short g

charge0=[-0.808,0.404,0.404];
chargep1=[-0.106,0.553,0.553];
chargem1=[-0.720,-0.140,-0.140];

[nucleophilicity, electrophilicity, radical]
=fuki(chargem1, charge0, chargep1);
```

```
%
% fuki.m 1/6/11 v2. ; 17/4/06 v1
%
function [nucleophilicity, electrophilicity, radical]
=fuki(chargem1, charge0, chargep1, ATOM)

[r, c]=size(chargep1);
for i = 1:r
    qp1= chargep1(i);
    q0 = charge0(i);
    qm1= chargem1(i);
    nucleophilicity(i,1) = qp1-q0;
    electrophilicity(i,1) = q0-qm1;
    radical(i,1) = (qp1-qm1)/2;
end
```

```
n= [1:r]';

disp('-----')
disp('          Atom          Anion          Neural          cation'),
disp('-----')
disp(' '), disp([n, chargem1, charge0, chargep1])
disp('-----')

if nargin ==3
disp('~~~~~')
disp('          Atom          N          E          R'),
disp('~~~~~')
disp([n, nucleophilicity, electrophilicity, radical])
disp(' ')
disp('~~~~~')
end

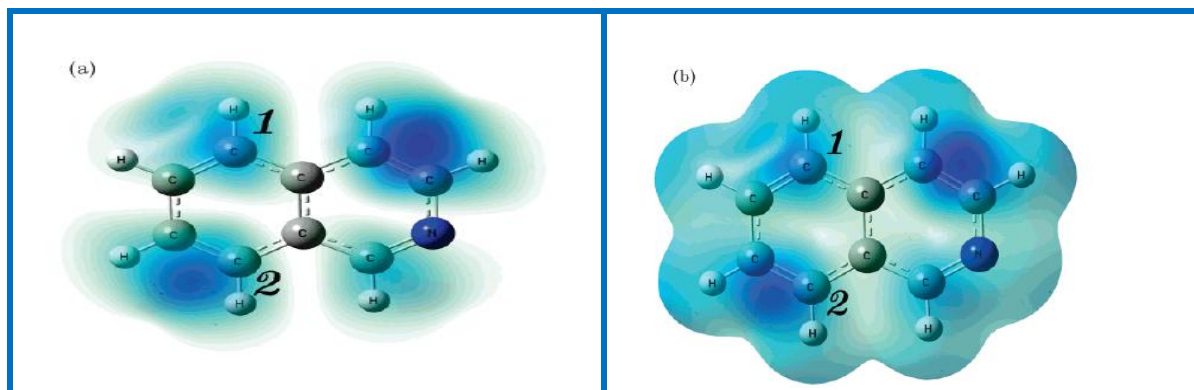
if nargin ==4
[r, c]=size(chargem1);
disp('-----')
disp('-----')
```



```

disp('No, Atom, N, E, R, Anion, Neural,
cation '),
% disp('-----')
disp('-----')
for i = 1:r
    zz= [' ',int2str(n(i)), ' ',ATOM(i,:), '
',num2str(nucleophilicity(i)), ' ',num2str(electrophilicity(i)), '
',num2str(radical(i)) ....
',num2str(chargem1(i)), ' ',num2str(charge0(i)), ' ',num2str(chargep1(i))
];
    disp(zz)
end
end
disp(' ')
disp('-----')
disp('-----')

```



(a) Square magnitude of the HOMO orbital, $\text{HOMO}(r)$,
(b) Fukui function from below, plotted on the 0.0004 isodensity surface

James S. M. Anderson, Junia Melin, and Paul W. Ayers, *J. Chem. Theory Comput.* 2007, 3, 375-38

- Conceptual Density-Functional Theory for General Chemical Reactions, Including Those That Are Neither Charge- nor Frontier-Orbital-Controlled. 2. Application to Molecules Where Frontier Molecular Orbital Theory Fails

It is reported isoquinoline molecule should be most reactive where Fuki functions are the largest. The numbers denote the experimentally observed reactivity preferences.

7. Software evolution (Se) in CQC

GUASSIAN XX: GUASSIAN70 by John Pople et al. (chart 56) and GAMESS an academic endeavor, running on today's laptops to peta-scale hardware, are life time contributions and evolutionary in nature. Even though more than a hundred commercial and freely downloadable software packages are available, MOPAC/AMPAC HYPERCHEM, ADF etc. are the sought after ones.

Chart 56: Evolution of Gaussian CQC package into Gaussian09

Gaussian70	Gaussian76	Gaussian77	Gaussian78	
Gaussian80	Gaussian82	Gaussian83	Gaussian85	Gaussian86
Gaussian88	Gaussian90	Gaussian92	Gaussian93	Gaussian94
Gaussian95	Gaussian96	Gaussian98	Gaussian03	

Gaussian80 : First version published on Quantum Chemical Program Exchange (QCPE) running on IBM mainframe

The software implementable components of computational chemistry are so complex to develop in terms of man-hours and fool proof character. Even in CQC, it is hard to mimic a small module in G09, GAMESS, ADF or Hyperchem. However, development of select modules is for pedagogical purposes. It is not viable to fabricate an instrument (say NMR 900MHz, MS-MS, excited-emission-flourescence) to study the spectra even for thousands of compounds. It is equally not a pragmatic venture to think of in house software for CQC to probe into biochemical/ physics/chemical/physical chemistry/chemical physics/PCCP research. In this decade, the output of computational science (Neuralware Professional II for artificial intelligence,AI) is also called response with equal status to that of experimental (in) direct observations (data). The modules are known as probes of the instrument. The computations and/or simulations (emulations, virtual objects/scenes) are refereed as experiments.

Q-Chem: The postdocs and students of Pople developed the initial code of Q-Chem (chart 57)and the first commercial version was available in 1997. Over two decades, the code grew to 3.3 million lines by more 170 of which 1.5 million is machine generated.

Hartree-Fock	DFT	IQMol <ul style="list-style-type: none"> ▶ Hierarchical input generator ▶ Molecular builder ▶ General visualization capabilities (MOs molecular vibrations etc.)
MP2	TDDFT	
CC		
Equation-of-motion (EOM-CC)	QM/MM	
CI	GI	

☎ Interfaced with WebMO

- ▶ Computing engine in [Spartan](#)
- ▶ Back-end to
 - 🔔 [CHARMM](#)
 - 🔔 ChemShell

GAMESS: It is a freeware for academic institutes with almost equivalent features of the commercial packages like Gxx, HYPERCHEMx etc. The input can be prepared through the structure entry (generic or IUPAC) in CHEMDRAW followed by CHEM 3D package. The output of GAMESS is exportable to CHEM-3D to visualize 3D surface and 2D-contour of FMOs, TD, ESP, solvent accessible volumes etc. A few typical software packages for quantum chemical computations are given in [table 1](#).

Optimization methods: Derivative, direct search and nature inspired methods are in vogue for optimization tasks ([KB. 9](#)).The methods like Powell, Bartel, and McIver-Komornicki of AMPAC toolbox can be activated by specific key words. BFGS and Beryny algorithm ([KB. 9b](#)) widely employed and successful ones follow.

BFGS (Broyden, Fletcher, Goldberg and Shannon):A quasi Newton optimization algorithm capable of arriving at the minimum even in pseudo flat surfaces, unlike other gradient-based techniques operates in AMPAC along with DFP (Davidon, Fletcher and Powell) procedure. It ensures optimization of geometry of a stable conformer. But, it fails for a molecule corresponding to a higher order saddle point and sometimes for a geometric structure corresponding to a transition state (TS).

Beryny algorithm: G03 implements Beryny algorithm ([KB.9b](#)) with options Tight, VeryTight, Expert, Eigentest and EstmFC.

KB.9: Choice of training methods

If Object function has derivatives
 Then Gradient methods are used
 Else Direct search methods

If Derivatives are not calculable &
 Function value is not available
 Then simplex

KB. 9b: Typical steps in Beryny algorithm in Knowledge format

If First step then, Hessian is estimated
 Elseif Analytic Hessian is computed
 Then Hessian is updated

If A minimum is sought
Then Perform a linear search between the latest point and the best previous point which lowest energy

If Second derivatives are available at both points and a minimum is sought
Then Quintic polynomial fit attempted first

If It does not have a minimum in the acceptable range or if second derivatives are not available
Then A constrained quartic fit is attempted
 (+) This fits a quartic polynomial to the energy and first derivative (along the connecting line) at the two points with the constraint that the second derivative of the polynomial just reach zero at its minimum, thereby ensuring that the polynomial itself has exactly one minimum

If This fit fails or if the resulting step is unacceptable
Then A simple cubic is fit is done

If All fits fail and the most recent step is the best so far
Then No linear step is taken.

If All fits fail &
 Most recent step is not the best &
Then The linear step is taken to the midpoint of the line connecting the most recent and the best previous points.

If Latest point is the best so far or transition state is sought
Then a quadratic step is determined using the current (possibly approximate) second derivatives

If A linear search was done
Then Quadratic step is taken from the point extrapolated using the linear search and uses forces at that point estimated by interpolating between the forces at the two points used in the linear search.

If quadratic step exceeds the trust radius and a minimum is sought,
Then Step is reduced in length to the trust radius by searching for a minimum of the quadratic function on the sphere having the trust radius

If a transition state is sought or if **NRScale** was requested,
Then the quadratic step is simply scaled down to the trust radius

Acceptance of polynomial fit

If latest point is the best so far
Then Any quintic or quartic step acceptable

If Two points are in between or
 not larger than the previous step
Then Cubic steps are accepted
 H. B. Schlegel, *J. Comp. Chem.* **3**, 214 (1982)

► Berny geometry optimisation

Convergence

Finally, convergence is tested against criteria for the maximum force component, root-mean square force, maximum step component, and root-mean-square step (KB11, table 21). The step is the change between the most recent point and the next to be computed (the sum of the linear and quadratic steps).

Table21: Convergence output in G03

Item	Value	Threshold	Converged?
Maximum Force	0.000105	0.000450	YES
RMS Force	0.000103	0.000300	YES
Maximum Displacement	0.000418	0.001800	YES
RMS Displacement	0.000387	0.001200	YES
Predicted change in Energy=-4.787633D-08			
Optimization completed.			

```
-- Stationary point found.
```

KB11: CONVERGENCE CRITERIA BEGINNING WITH GAUSSIAN 98

If Forces < 1/100th cutoff value
Then Geometry is considered converged even if the displacement is larger than the cutoff value








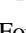

+ Facilitates optimizations of large molecules, which may have a very flat potential energy surface around the minimum.

8. State-of-knowledge-of-CQC













The literature grew exponentially, research papers are around 16,000 in Science Direct and 27,000 research papers in ACS since 2000 onwards (chart 10). Still we hear the positive slogan, 'The trends from computed QC fall in line with experimental results and hence useful for prediction without performing costly/time consuming experiments.

















SWE is milestone in the annals of science of chemistry. It is a chemical laboratory with a mathematical eye to know characteristics of chemicals without using real chemicals. This is the earliest virtual chemical laboratory before computer era. During nearly nine decades of clock time, yet millions of (man) brain hours of effort in writing, correcting, erasing, rewriting, updating on white board of science resulted into a mature CQC paradigm (chart 58, table 22).























Table 22: Computer languages, BSs used in typical quantum chemical packages

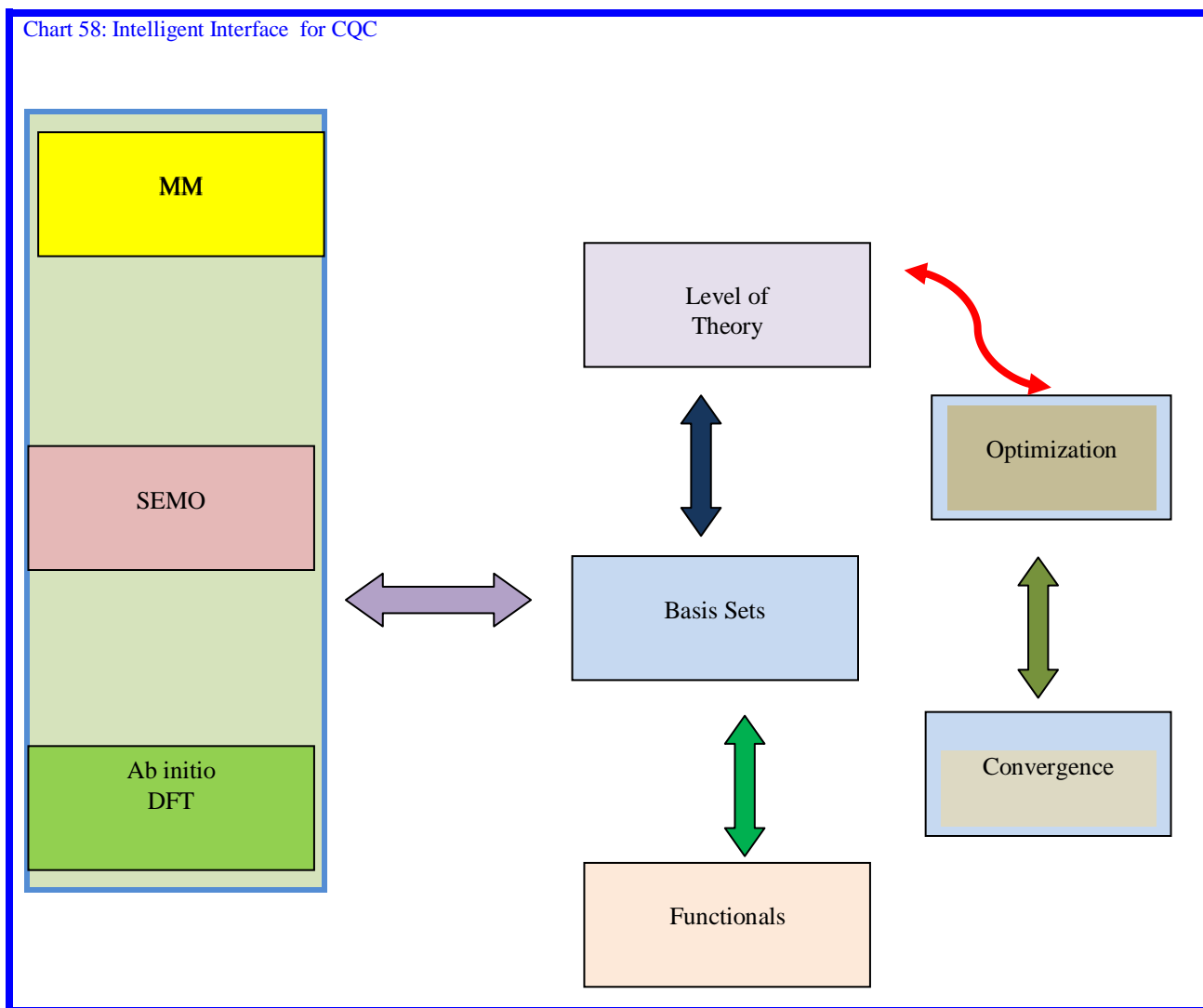
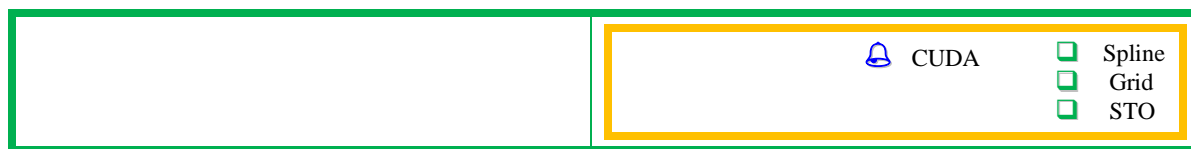
Academic	Language	Basis Set	Academic (UK) / Commercial	Language	Basis Set
Priroda-06	C	GTO	TERACHEM ⁸	 CCUDA	GTO
ORCA	C++	GTO		 C++	
OpenAtom	Charm++ (C++)	PW		 C	GTO
CADPAC	Fortran	GTO	SCIGRESS	 Java	
CFOUR	Fortran	GTO		 Fortran	
COLUMBUS	Fortran	GTO	Atomistix ToolKit (ATK)	 C++	 NAO
DALTON	Fortran	GTO		 Python	 EHT
GAMESS (US)	Fortran	GTO	CRYSTAL	Fortran	GTO
TB-LMTO	Fortran	LMTO	GAMESS (UK)	Fortran	GTO
SIESTA	Fortran	NAO	Quantemol-N	Fortran	GTO
CPMD	Fortran	PW	Gaussian	Fortran	GTO
	Fortran 77		MOLCAS	Fortran	GTO
DIRAC	Fortran 90	GTO	MOLPRO	Fortran	GTO
	C		TURBOMOLE	Fortran	GTO
CONQUEST	Fortran 90	NAOSpline	MOPAC	Fortran	Minimal GTO
FLEUR	Fortran 95	FP-(L)APW+lo	Empire	Fortran	Minimal STO
		GTO	FHI-aims	Fortran	NAO
		PW	CASTEP	Fortran	PW
CASINO(QMC)	Fortran 95	Spline	ONETEP	Fortran	PW
		Grid			
		STO			

LOWDIN	Fortran 95 Fortran 03	GTO
RSPt	Fortran C	FP-LMTO
Firefly PC GAMESS	Fortran C Assembly	GTO
PLATO	Unknown	NAO

VASP	Fortran	PW
ADF	Fortran	STO
DMol3	Fortran 90	NAO
DFTB+	Fortran 95	NAO
WIEN2k	 Fortran  C	FP-(L) APW+lo
Jaguar	 Fortran  C	GTO
Spartan	 Fortran  C  C++	GTO
Q-Chem	 Fortran  C++	GTO
PyQuante	 Python	GTO
PySCF	 Python	GTO
PQS	 Unknown	Unknown

	Language	Basis Set
NWChem	 Fortran 77  C	<input type="checkbox"/> GTO <input type="checkbox"/> PW
ABINIT	 Fortran	PW
ACES II	 Fortran	GTO
ACES III	 Fortran  C++	GTO
BigDFT	 Fortran	Wavelet
CP2K	 Fortran 95	<input type="checkbox"/> HybridGTO <input type="checkbox"/> PW
DFT++	 C++	<input type="checkbox"/> PW <input type="checkbox"/> Wavelet
ELK	 Fortran 95	<input type="checkbox"/> FP-LAPW
ErgoSCF	 C++	<input type="checkbox"/> GTO
ERKALE	 C++	<input type="checkbox"/> GTO
EXCITING	 Fortran 95	<input type="checkbox"/> FP-LAPW
FreeON	 Fortran 95	<input type="checkbox"/> GTO
GPAW	 Python  C	<input type="checkbox"/> Grid <input type="checkbox"/> NAO <input type="checkbox"/> PW

JDFTx	 C++  CUDA	PW
MADNESS	 C++	Wavelet
MISSTEP	 C++	PW
MolDS	 C++	<input type="checkbox"/> STO <input type="checkbox"/> GTO
Octopus	 Fortran 95,  C,  OpenCL	Grid
OpenMX	 C	NAO
PSI	 C  C++	GTO
PUPIL	 Fortran  C	GTO PW
PWscf ⁶	 Fortran	PW
Quantum ESPRESSO	 Fortran	PW
RMG	 C  C++	Real space grids
Siam Quantum	 C	GTO
Yambo Code	 Fortran	PW
DACAPO	 Fortran	PW
MPQC	 C++	GTO
QMCPACK(QMC)	 C++	<input type="checkbox"/> GTO <input type="checkbox"/> PW



Similarities between CQC experiments_with_instruments: The diverse approaches and functionals are similar to different apparatus in a laboratory aimed for diverse tasks viz. separation, sieving, combination and decomposition. Special equipment is to do chemistry in varying environments viz. low pressure, air, harsh media and so on. In CQC, the parallel situation is computations in vacuum, solvent, solid state materials, interfaces etc. The scaling up is routine in translating laboratory procedure to an industrial level. Here, the number atoms in a molecule are scale of requirement of hardware and time resources.

Like in any new discipline, it should be able to reproduce earlier results in toto if not better. The real acceptance increases only if it does what earlier methods could not do. In this perspective, almost few decades from early fifties were in reproducing thermodynamic energies, properties of atoms, molecules in vacuum. The growth story of CQC was the embracing different types of compounds. The detection of TS and stability order of conformers not synthesized/available were the highlights and success stories of the

field. The processes in solvent, interfaces, solid surfaces and macromolecules added a feather in the cap of CQC.

The higher-end suite is a mixture of methods, so inter-oven that to a naked eye that it appears as a valid/dependable tool without real chemicals. The truth is SWE is in the core and so mathematical tool. Here, it is a black box powerful computational tool. It does not create any white box impression, but amateur user is in the dream of white box. At the same time the caution to amateur package user is not create his own lullabies about it and best way is to probe into details through white box approach.

Now, QC bagged the merits of 'exact solution of an approximate equation' and 'approximate solution of exact equation' and smoothing procedures (by additive compensate terms based on many experimental/ theoretical calculation) and CQC as a whole now an admixture of mathematical approach, indirect use of experimental data, statisticalparametric approach, empirical methodology and interpolating NNs.

Chronological developments in CQC: In the first four decades after the introduction of Schrodinger wave equation (SWE) in 1927, core of quantum mechanics, methods, study of perturbation by electrical and magnetic fields and applications to hydrogen like atoms were developed. The later four decades of concerted efforts were for better and better numerical solutions for single atom to macromolecules in all phases and effect of solvents. The initial attempts of improvisation were based on comparison of quantum chemical computed values of structure parameters (BL, BA and DH), properties (IP, EA, dipole moments), energies (ΔG , enthalpy, Bond dissociation energies), with experimental ones and reduce the discrepancy to smaller and smaller magnitudes, sometimes beyond experimental accuracy. The last decade has seen the success of CQC in thermal/photochemical reactions, transition states, and excited state reactions, resolving the alternative mechanisms, explaining why a reaction (hydration, weak interactions) takes place, also predicting the feasibility of experimentally unexplored systems, and even correcting the experimental derived values.

Chronological developments in experimental chemistry: Five-element paradigm was macroscopic view of micro-systems and paved way to alchemy era. The arguably systematic chemistry of 20th century unequivocally explained covalent, electrostatic and co-ordinate bonds. It dumped the unexplained factors as non-covalent interactions and assumed the additivity of electro-static and non-electrostatic interactions for classical thermodynamic free energy changes. The coveted but difficult gas phase experiments and easy, yet difficult to understand reactions in non-aqueous solvents/ water/ water miscible solvents emerged interesting solution phase theories are a consequence of efforts of elite chemists, chemical physicists and physical chemists.

The electrometric, spectrophotometric quantitation in first half of 20th century laid a firm ground of chemical science. The instrumental accuracy, hyphenation, computerization and application to complicated real life samples (environment, in vivo, deep ocean, moon) dominated in the second half. The stacking interactions, $\sigma \longrightarrow \sigma^*$, $\pi \longrightarrow \pi^*$ etc., explicit and implicit solvation effects, multiple moments, their derivatives were more a mental exercise and using theoretical physics formalism. The physical reality however was to produce materials of exciting applications targeted in defense, industry and comfortable civil life and to drive away the ill effects of natural calamities.

In this decade, the free and commercial software packages, instrumental data services, inexpensive large amount of literature availability on WWW and generosity of prime commercial publishers and easy to go attitude are a few but important factors for exploding breadthwise research results (plug and play) difficult even to monitor. Further, it is a fact that each compound and sets of them have application/importance and at the same time limitations, disadvantages, and it is ones' choice to highlight or find fault.

Major research directions of CQC:

In yesteryears, most of contributions dealt with calculating a set of QC-output either with latest or little older methods (implemented in packages) and showing that the experimental data supports the CQC and

rarely it differs. A few others deal that the present CQC is inadequate for a set of properties, mechanism, matrix and positive results with suggested modification.

The sole objective of CQC remains to compute chemistry in a computational box at least as accurately as the time old experimental approach (chart 59), if not more nearer to the true values. This is comparable to bat's shrewd long and short distance vision and adaptive speed with a single goal of catching the moving prey on the ground. CQC is an indispensable computational tool; it is accepted now as an experimental (instrumental) probe. It is inadequate to state that it plays a dual role, but evolved with right fusion of experimental techniques, theories, mathematical models, solution methods and accumulated information/knowledge/intelligence of many inter- intra-cross-disciplines.

The software development with noteworthy improvements in Gaussian (from 80 to 09), Q-Chem, GAMESS, etc. is the corner stone of today's implementation of CQC. Nevertheless, the industry brought more than hundred packages necessitating another software package to speak about them and to compare their unique features and pitfalls.

It is informative to probe into backend processes in parametric models (AM1, PM3, PM6 etc.), development of DFT functional in explaining newer and newer properties/interactions, improvements in BSs and orbitals (GTO, STO etc.) account for decay in energy/electron density/potential or influence of electrons on others and ever growing deep-level solvent models.

Chart 59: Typical objectives of CQC

⊕	Different means to improve representation of orbitals ⊕ Slater Fn, Gaussian Fn, plane waves etc.
⊕	Functionals (local, global) for DFT
⊕	Basis sets accounting for exchange and correlation
⊕	Incorporating even small (but cumulatively significant) factors in DFT, Ab-initio separately
⊕	Reaching nearer to accurate experimental (spectroscopic, thermal, kinetic) data available with newer/ modified terms

Post-(geometric-)optimization processes: After optimizing geometries, charges of different kind (ChelpG, APT, ESP, Mullikan), dipole/multipole moments, linear/non-linear polarisabilities (α , β and γ), Fukui parameter, hardness, etc. can be calculated using HF/Finite-Field (FF), followed by DFT/CAM-B3LYP or M0x functionals.

3D surfaces and 2D contours of TED and ESP: Data for 3-D surface/ 2-D contour plots of electron density, ESP, and HOMO/ LUMO are calculable from G09 and visual outputs from GAUSSVIEW software. Central composite and uniform designs help in selecting the basis sets.

The total electron density maps reflect the shape including cavities that indicate the size of the compound and scope for the penetration or even weak interaction including handshake mode.

ESP surface: It characterizes site of attack by an electrophile or nucleophile. It is a quantitative treatment when a unit charge approaches the molecule. The ESP maps are preferred to the numeric atomic or ESP charges.

HOMO and LUMO energies: HOMO and LUMO analysis is used to determine the charge transfer within the molecule. The functions of HOMO and LUMO energies pave way to many physical/chemical parameters and throw light in probing into micro-/nano-/molecular processes. The electron affinity, hardness, Chattaraj and condensed Fukui functions are laudable criteria to predict chemical reactivity both in gaseous and in solution phases.

Charges: Apart from experimental methods, computational techniques employ MPA, NPA or Lowdin procedures to calculate atomic charges. Electrical indices throw light on the reactivity, H-bonding and nature of electronic excitation.

Multipole moments: The di-/ multi-pole moment and molecular ESP represent static molecular indices. The numerical values and the associated sign arise due to intra-molecular interaction or electronic excitation.

Polarizabilities: The calculation of polarizabilities is routinely at a single frequency as implemented in AMPAC, MOPAC etc. However, frequency dependent values are calculable from G03 and ADF.

Spectra: The Transparency characteristics indicated by UV-Vis, IR spectra are quantum mechanically computable by ZINDO, CIS-, TD-DFT calculations. ^1H and ^{13}C NMR spectra of the compounds are obtainable using TD-DFT and HF approach using CSGT, GIAO, IGAIM options.

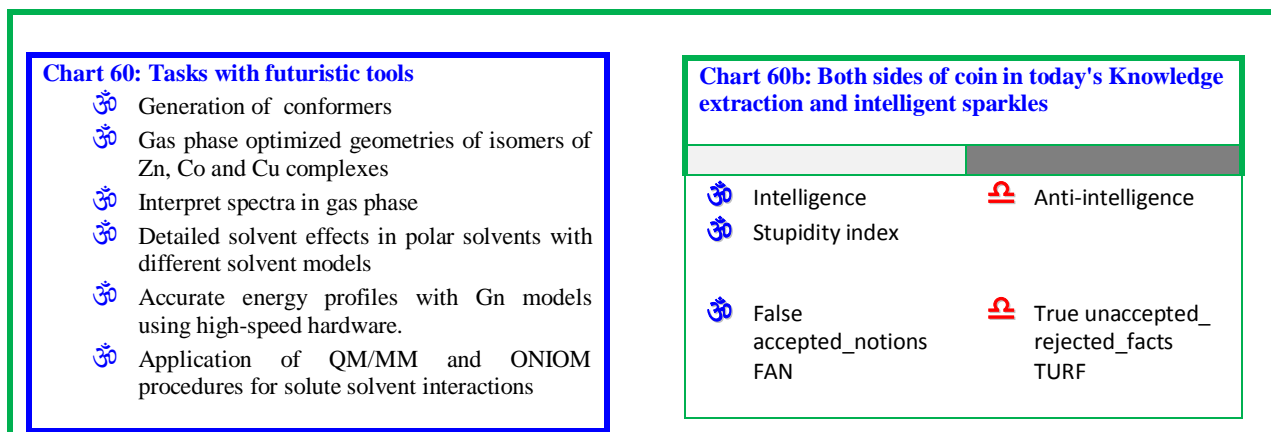
Quantum topological properties: Popelier and Aicken [47] derived quantum topological properties from partitioning the molecular electron density of optimized geometry of amino acids and derived molecules totaling to 57 at B3LYP/6-311+G(2d,p)//HF/6-31G(d) level.

The activity of the drugs (psycho activity of cannabinoids, analgesic activity and cyto toxicity of paracetamol) and function of estrogen are explained successfully based on the ESP, charge on the atoms, IP, TD, EHOMO, ELUMO, and molecular volume of the molecule.

9. Future outlook of CQC

Quantum chemistry although not a panacea, its role and impact in each phase of experimental, simulation and predictive activity is significant. The focus of next two decades of effort in research mode compendium (first in white box software paradigm and then on upgradable hardware/firmware chip) for deep level developers opens new vistas in CQC (chart 60). Implanting nature-inspired algorithms, heuristic and meta rules based numerical expert systems, evolving machine intelligence generated sparkles in the integration of knowledge/information. It fuels the takeoff of computational science with jet speed into a new computational world similar or excelling brain of a child prodigy. The quest into new untrodden path explores 'what happens? What does not happen? Then, 'what to discover?' 'what to invent?' and 'when and how to probe into a new paradigm?'. The consequence is a future torch in the unexplored scientific arena.

The utopian goal of CQC is to examine accurate energies of all conformers and predict the properties. Further, it is interesting to probe into and predict chemical structure for desired range of properties before synthesis of material.



Further, there is a need for fine-tuning the approach, as instances of disagreement with ever developing (accurate/sophisticated) experimental techniques accumulate! The penultimate goal (which changes with time) is emergence of computational/computation science replaceable with experimental (direct/indirect) tools and vice versa. Just like artificial brain is a far off realization, computational tools to understand real life dynamic bio/ environment/ terrestrial/ inter stellar ongoing processes/ prediction of the future or looking back (hind cast) in time awaits sparkles of research outcome. For devices with nanowires/nanofibers, physisorbed water is not negligible. Thus, CQC (at ab initio level) and DFT with newer functionals as well as high tech experimental probes enable to extract (physical/ chemical) process knowledge.

The experts' knowledge in the choice of optimization algorithm, convergence and input checking are included in some of the packages. The intelligent problems solver approach and task dependent expert solution methodology implemented in neural nets will revolutionize QC paradigm for inter disciplinary research. A white box approach of algorithms, source code and plug and play type of inter-faces on one side and database including multidimensional surfaces will give a boost in pedagogy of CQC.

Hands-on-tutorials (Hot-) in computational chemistry (Hot.CQC): With profound developments, learning while assisting in execution of research project with high tech methods, intelligent software on high-end hardware platforms lead to awareness and repeatability for another prototype. This is as expert screwdriver operation to screw and unscrew bolts of varying dimensions and what so ever machine is. The other side of coin is the appraising terminology viz. transfer-of-technology, on-site-learning and knowledge transfer etc. However, the real life challenges are to sail alone and make oneself self-sufficient-efficient/confident for a sail on rough sea and face calamities. To this end, one should undergo rigorous long-term-formal training and solve different toy-problems, large-scale-ones with known solutions and arrive at conclusive results for open ended riddles and wait for an experts' solution for fixing coordinates. This demands research pedagogy, a new paradigm beyond formal education in cross-disciplinary areas.

The tutorials in CQC will comprise tasks practicable by an undergraduate with software on a laptop/smart phone. However, it gives impetus to become conversant with state-of-art protocols at research level. Secondly, the method bases with necessary conditions, failure tags and remedial measures with relevant formulae without derivations make non-majors in mathematics feel at home about what it is? How and when can be safely used? What are the pitfalls and methods to surmount/avoid the hurdles? Another focal point of Hot_CQC is to train researchers entering into CQC to familiarize what happens 'behind the computer software packages' in outpouring a variety of information bits from simple input. The toil is not repeat standard class room courses in a new form or molding trainee into an expert overnight per se, but making aware of what is the optimum and righteous path, learning tricks of trade to pick up suitable tools to master later.

Acknowledgements

Dr. G. Narahari sastry, scientist, IICT asked RSR to contribute a manuscript for the special issue of Ind.J.Chem in 2003 and my immediate response was to agree for a review paper in computational quantum chemistry. But, his soft-force made me acceptable for a research communication in gas phase studies, although all my past experience was with chemical reactions in aquo-organic mixtures and chemometrics and of course quantum chemical/hybrid descriptors in structure response relationships. I do relish storing in my deep memory the unstinted support of Dr. V Anantha Ramam and also sparing long hours of time during and after university schedule for many futile attempts before arriving each bit of knowledge in a foreign discipline for both of us. The consequence was SEMO study of hydrazides in gas phase with follow-up publications in Ind. J Chem. and dissertations. I appreciate Dr. G. Narahari sastry, Bhatnagar awardee for his confidence in our research group to probe into new ventures. This review summarily is an outcome of invited lectures, summer school/staff college programs and quest for broadening our understanding of computational intricacies and their synergistic positive march in chemical sciences in fusing experimental and computational knowledge.

My mother tongue in research was co-ordination chemistry and quantitation in solution phase. I learnt another language 'chemometrics' and a fast number crunching tool namely 'software' paving way to publish in chemical equilibrium, kinetics and calibration/prediction. The seed of interest in quantum chemistry calculations were sown in my brain in early nineteen eighties. It happened primarily from the information of Fortran programs in Quantum chemistry program exchange (QCPE), Indiana Univ, propagation of vibrational spectroscopy with CNDO/PPP procedures by Dr. Surjit Singh, IIT Madras and on-going teaching programs by Prof P.V. Krishna Rao and Prof. L.S.A. Dikshitulu (my teachers) in Andhra university. Later, Prof M S Prasada Rao and Prof P V Ramana continued the saga of pedagogy for post-graduation students.

The first leap into practice of AMPAC was during execution of DRDE project in the calculation of molecular descriptors of organo-phosphorous compounds (nerve agents) during 1999-2001. My experience in computer augmented instruction, artificial intelligence and optimizations had influence in probing into another field. The idea of putting a temporary stop of continuing the sure-to-work-tools-on-hand and diverting focus on a different discipline of research made possible to arrive at newer results like injecting expert system approach into CQC for method selection, input/output and analysis. The partial realization of translation of CQC into pedagogy started with invited lecture programs at Aurangabad on fundamentals of object oriented computations with high performance tools and graphics in QC. During 2005-2006, DFT and ab initio computations were carried out for chemically and biologically relevant descriptors for anti-tubercular drugs, anti-HIV compounds and effect of explicit/implicit solvation of small bio-molecules. I was interested in the role of water in proteins and the literature reports in seventies and eighties formed the base of how to view and enter into field. The effective dielectric constant concept of Helmut Sigel is Professor Emeritus, University of Basel is a sparkle in interfacing in-vitro and in-vivo chemical investigations. The knowledge now is mature in protein chemistry, CQC, solvent models, interfaces and intricate matters of brain functioning, atmospheric reactions and even geo-chemical processes. Our contribution are in study of water-miscible solvents with varying coordinating properties, dielectric constants, non-covalent interactions of a single molecule, polymers, nano clusters, macro-clusters and bulk of both solute and solvent. It is apt to say that still one should march long before a rest state to integrate knowledge of these cross-innovative technologies.

Dr. Ramakrishna's primary research focus was in micellar kinetics and pharmaceutical quantitation. During Indian Academy Science' program, he had advanced training in CQC from Prof Satyamruti, IIT, Kanpur. Later he published quantum chemistry of drugs, clusters of small exotic molecules using SEMO, ab initio and DFT methods.

Kameswara Rao had MPhil degree in CQC of anti-tubercular drugs and now pursuing research in quantum molecular descriptors.

REFERENCES

- [1] S. Li, W. Li, and J. Ma, *Acc. Chem. Res.*, **2014**, 47, (9),2712–2720.
[Generalized Energy-Based Fragmentation Approach and Its Applications to Macromolecules and Molecular Aggregates](#)
- [2] O. Marsalek, F. Uhlig, J. V. Vondele, and P. Jungwirth, *Acc. Chem. Res.*, **2012**, 45, (1),23–32.
[Structure, Dynamics and Reactivity of Hydrated Electrons by Ab Initio Molecular Dynamics](#)
- [3] G. Schreckenbach and G. A. Shamov, *Acc. Chem. Res.*, **2010**, 43, (1),19–29.
[Theoretical Actinide Molecular Science](#)
- [4] K. Świderek, I. Tuñón, V. Moliner and J. Bertran, *ACS Catal.*, **2015**, Just Accepted.
[Protein Flexibility and Preorganization in the Design of Enzymes. The Kemp Elimination Catalyzed by HG3.17](#)
- [5] R. E. Patet, N. Nikbin, C. L. Williams, S. K. Green, C. C. Chang, W. Fan, S. Caratzoulas, P. J. Dauenhauer, and D. G. Vlachos, *ACS Catal.*, **2015**, Just Accepted.
[Kinetic Regime Change in the Tandem Dehydrative Aromatization of Furan Diels-Alder Products](#)
- [6] X. Liu, O. Coutelier, S. Harrisson, T. Tassaing, J. D. Marty, and M. Destarac, *ACS Macro Lett.*, **2015**, 4, (1),89–93.
[Enhanced Solubility of Polyvinyl Esters in scCO₂ by Means of Vinyl Trifluorobutyrate Monomer](#)
- [7] I. Y. Stein, N. Lachman, M. E. Devoe, and B. L. Wardle, *ACS Nano*, **2014**, 8, (5),4591–4599.
[Exohedral Physisorption of Ambient Moisture Scales Non-monotonically with Fiber Proximity in Aligned Carbon Nanotube Arrays](#)
- [8] J. V. Vermaas, A. T.Taguchi, S. A. Dikanov, C. A.Wraight, and E. Tajkhorshid, *Biochemistry*, **2015**, Just Accepted.
[Redox Potential Tuning Through Differential Quinone Binding in the Photosynthetic Reaction Center of Rhodobacter sphaeroides](#)

- [9] K. Tan, S. Zuluaga, Q. Gong, Y. Gao, N. Nijem, J. Li, T. Thonhauser, and Y. J. Chabal, *Chem. Mater.* **2015**.
ASAP Competitive Co-adsorption of CO₂ with H₂O, NH₃, SO₂, NO, NO₂, N₂, O₂, and CH₄ in M-MOF-74 (M = Mg, Co, Ni): The Role of Hydrogen Bonding
- [10] Ao. Yu, Y. Liu, Y. Wang, *Chemical Physics Letters*, **2007**, 436, 276–279.
Ab initio calculations on pK_a values of benzo-quinuclidine series in aqueous solvent
- [11] R. B. Viana, A. B.F. da Silva, *Comput. Theoret. Chem.*, **2015**, 1059, 35-44.
Interaction between PH₃ and small water clusters: Understanding the electronic and spectroscopic properties
- [12] A. K. Baron, *Comput. Theoret. Chem.*, **2015**, 1057, 7-14.
Theoretical study of the complexes of tyrosine and tryptophan with biologically important metal cations in aqueous solutions
- [13] D. J. Bigler, L. W. Peterson, M. Cafiero, *Comput. Theoret. Chem.*, **2015**, 1051, 79-92.
Effects of implicit solvent and relaxed amino acid side chains on the MP2 and DFT calculations of ligand–protein structure and electronic interaction energies of dopaminergic ligands in the SULT1A3 enzyme active site
- [14] C. J. Brala, I. Fabijanić, A.K. Marković, V. Pilepić, *Comput. Theoret. Chem.*, **2014**, 1049, 1-6.
The average local ionization energy and Fukui function of L-ascorbate, the local reactivity descriptors of antioxidant reactivity
- [15] F. Puerto, A. M. Losa, M. E. Martín, M. A. Aguilar, *Comput. Theoret. Chem.*, **2014**, 1040–1041, 287-294.
Theoretical study of the absorption and emission spectra of the anionic p-coumaric methyl ester in gas phase and in solution
- [16] A. Vagánek, J. Rimarčík, K. Dropková, J. Lengyel, E. Klein, *Comput. Theoret. Chem.*, **2014**, 1050, 31-38.
Reaction enthalpies of OH bonds splitting-off in flavonoids: The role of non-polar and polar solvent
- [17] T. Etienne, H. Gattuso, A. Monari, X. Assfeld, *Comput. Theoret. Chem.*, **2014**, 1040–1041, 367-372.
QM/MM modeling of Harmane cation fluorescence spectrum in water solution and interacting with DNA
- [18] M. C. Pichardo, R. L. C. Mendoza, L. A. Z. Hernandez, J. C. Borbolla, C. A. G. Ramírez, T. Pandiyan, N. Jayanthi, *Comput. Theoret. Chem.*, **2014**, 1047, 47-54.
Activation of Pt–O and Pt–H bonds: DFT studies on adsorption of [Gd(H₂O)_n]³⁺ (n = 8–9) with Ptn (n = 3–7) cluster
- [19] D. E.C. Ferreira, I. S. Boldt, W. B. De Almeida, W. R. Rocha, F. Nome, *Comput. Theoret. Chem.*, **2014**, 1043, 5-12.
Quantum mechanical/effective fragment potential (QM/EFP) study of phosphate diester cleavage in aqueous solution
- [20] E. D. Raczyńska, *Comput. Theoret. Chem.*, **2014**, 1031, 56-63.
Effects of positive and negative ionization for 2-aminopyrimidine in the gas phase and in water solution
- [21] F. Momany, U. Schnupf, *Comput. Theoret. Chem.*, **2014**, 1029, 57-67.
DFT optimization and DFT-MD studies of glucose, ten explicit water molecules enclosed by an implicit solvent, COSMO
- [22] P. Li, Wei-hua Wang, Hai-tao Sun, Si-wei Bi, *Comput. Theoret. Chem.*, **2013**, 1006, 127-132.
A DFT study on the electron affinity of tetrachloro-p-benzoquinone: Toward to understanding its electron-accepting ability in solution
- [23] A. L. Tessaro, V. R. Batistela, D. S. Pellosi, W. Caetano, L. T. Ueno, A. E. da H. Machado, M. G. van der Linden, N. Hioka, *Comput. Theoret. Chem.*, **2013**, 1020, 173-179.
Electronic structures and spectroscopic properties of benzoporphyrin protolytic species: A TD-DFT study
- [24] T. Lukmanov, S. P. Ivanov, E. M. Khamitov, S. L. Khursan, *Comput. Theoret. Chem.*, **2013**, 1023, 38-45.
Relative stability of keto-enol tautomers in 5, 6-substituted uracils: Ab initio, DFT and PCM study
- [25] S. R. Pruitt, S. S. Leang, P. Xu, D. G. Fedorov, M. S. Gordon, *Comput. Theoret. Chem.*, **2013**, 1021, 70-83.

- Hexamers and witchamers: Which hex do you choose?
- [26] P. Grancic, R. Bylisma, H. Meekes, and H. M. Cuen, *Cryst. Growth Des.*, **2015**, Just Accepted.
[Evaluation of all-atom force fields for anthracene crystal growth](#)
- [27] D. E. Braun, M. Orlova, and U. J. Griesser, *Cryst. Growth Des.*, **2014**, 14, (10),4895–4900.
[Creatine: Polymorphs Predicted and Found](#)
- [28] W. W. Rudolph, D. Fischer, G. Irmer and C. C. Pye, *Dalton Trans.*, **2009**, 6513–6527.
[Hydration of beryllium \(II\) in aqueous solutions of common inorganic salts. A combined vibrational spectroscopic and *ab initio* molecular orbital study](#)
- [29] K. R. Koch, M. R. Burger, J. Kramer and A. N. Westra, *Dalton Trans.*, **2006**,3277–3284.
[Pt NMR and DFT computational methods as tools towards the understanding of speciation and hydration/solvation of \[PtX₆\]²⁻ \(X = Cl⁻, Br⁻\) anions in solution](#)
- [30] W. Han, C. Zhong, L. Liang, Y. Sun, Y. Guan, L. Wang, X. Sun, J. Li, *Electrochim. Acta*, **2014**, 130, 179-186.
[Electrochemical degradation of triazole fungicides in aqueous solution using TiO₂-NTs/SnO₂-Sb/PbO₂ anode: Experimental and DFT studies](#)
- [31] M. L. Souza, E. E. Castellano, J. Telser, and D. W. Franco, *Inorg. Chem.*, **2015**, 54, (4),2067–2080.
[Secondary Coordination Sphere Effects in Ruthenium \(III\) Tetraammine Complexes: Role of the Coordinated Water Molecule](#)
- [32] K. M. N. Burgess, Y. Xu, M. C. Leclerc, and D. L. Bryce, *Inorg. Chem.*, **2014**, 53, (1),552–561.
[Alkaline-Earth Metal Carboxylates Characterized by ⁴³Ca and ⁸⁷Sr Solid-State NMR: Impact of Metal- Amine Bonding](#)
- [33] M. G. Mavros, T. Tsuchimochi, T. Kowalczyk, A. McIsaac, Lee-Ping Wang, and T. V. Voorhis, *Inorg. Chem.*, **2014**, 53, (13), 6386–6397.
[What Can Density Functional Theory Tell Us about Artificial Catalytic Water Splitting?](#)
- [34] A. S. Petit, R. C. R. Penniford, and J. N. Harvey, *Inorg. Chem.*, **2014**, 53, (13), 6473–6481.
[Electronic Structure and Formation of Simple Ferryl-oxo Complexes: Mechanism of the Fenton Reaction](#)
- [35] A. C. Tsipis and A. V. Stalikas, *Inorg. Chem.*, **2013**, 52, (2),1047–1060.
[Face-to-Face Stacks of Trinuclear Gold \(I\) Trihalides with Benzene, Hexafluorobenzene, and Borazine: Impact of Aromaticity on Stacking Interactions](#)
- [36] S. F. A. Kettle, G. L. Aschero, E. Diana, R. Rossetti, and P. L. Stanghellini, *Inorg. Chem.*, **2006**, 45, (13),4928–4937.
[The Vibrational Spectra of the Cyanide Ligand Revisited: Terminal Cyanides](#)
- [37] S. Sinnecker, L. D. Slep, E. Bill, and F. Neese, *Inorg. Chem.*, **2005**, 44, (7),2245–2254.
[Performance of Nonrelativistic and Quasi-Relativistic Hybrid DFT for the Prediction of Electric and Magnetic Hyperfine Parameters in ⁵⁷Fe Mössbauer Spectra](#)
- [38] B. J. Drouin, J. J. Dannemiller, and S. G. Kukolich, *Inorg. Chem.*, **2000**, 39, (4),827–835.
[Structural Characterization of anti- and syn-Allyltricarbonyliron Bromide: Rotational Spectra, Quadrupole Coupling, and Density Functional Calculations](#)
- [39] Z. Benkova, Sadlej A J, Oakes RE, Bell SE, J. Comput. Chem.,**2005**,26,145–153.
[Reduced-size polarized basis sets for calculations of molecular electric properties. I. The basis set generation](#)
(b) R. E. Oakes, S. E. J. Bell, Z. Benkova, A. J. Sadlej, J. Comput. Chem.,**2005**,26,154–159.
[Reduced-size polarized basis sets for calculations of molecular electric properties. II. Simulation of the Raman spectra](#)
- [40] F. Buchner, A. Nakayama, S. Yamazaki, Hans-Hermann Ritze, and A. Lübcke, *J. Am. Chem. Soc.*, **2015**, 137 (8),2931–2938.
[Excited-State Relaxation of Hydrated Thymine and Thymidine Measured by Liquid-Jet Photoelectron Spectroscopy: Experiment and Simulation](#)
- [41] A. Petrone, G. Donati, P. Caruso, and N. Rega, *J. Am. Chem. Soc.*, **2014**, 136, (42),14866–14874.
[Understanding THz and IR Signals beneath Time-Resolved Fluorescence from Excited-State *Ab Initio* Dynamics](#)

- [42] T. A. Pham, D. Lee, E. Schwegler, and G. Galli, *J. Am. Chem. Soc.*, **2014**, 136, (49),17071–17077.
[Interfacial Effects on the Band Edges of Functionalized Si Surfaces in Liquid Water](#)
- [43] P. Slavíček, B. Winter, L. S. Cederbaum, and N. V. Kryzhevoi, *J. Am. Chem. Soc.*, **2014**, 136, (52),18170–18176.
[Proton-Transfer Mediated Enhancement of Nonlocal Electronic Relaxation Processes in X-ray Irradiated Liquid Water](#)
- [44] J. Sun, G. Niehues, H. Forbert, D. Deck, G. Schwa, D. Marx, and M. Havenith, *J. Am. Chem. Soc.*, **2014**, 136, (13),5031–5038.
[Understanding THz Spectra of Aqueous Solutions: Glycine in Light and Heavy Water](#)
- [45] S. E. Wheeler, *J. Am. Chem. Soc.*, **2011**, 133, (26),10262–10274.
[Local Nature of Substituent Effects in Stacking Interactions](#)
- [46] D. L. Bryce, E. B. Bultz and D. Aebi, *J. Am. Chem. Soc.*, **2008**, 130, (29),9282–9292.
[Calcium-43 Chemical Shift Tensors as Probes of Calcium Binding Environments. Insight into the Structure of the Vaterite CaCO₃ Polymorph by ⁴³Ca Solid-State NMR Spectroscopy](#)
- [47] P. L. A. Popelier and F. M. Aicken, *J. Am. Chem. Soc.*, **2003**, 125, (5),1284–1292.
[Atomic Properties of Selected Biomolecules: Quantum Topological Atom Types of Carbon Occurring in Natural Amino Acids and Derived Molecules](#)
- [48] L. Capoferri, A. Lodola, S. Rivara, and M. Mor, *J. Chem. Inf. Model.*, **2015**, ASAP.
[Quantum Mechanics/Molecular Mechanics Modeling of Covalent Addition between EGFR–Cysteine 797 and N-\(4-Anilinoquinazolin-6-yl\) Acrylamide](#)
- [49] G. Leonis, A. Avramopoulos, R. E. k. Salmas, S. Durdagi, M. Yurtsever, and M. G. Papadopoulos, *J. Chem. Inf. Model.*, **2014**, 54, (8),2294–2308.
[Elucidation of Conformational States, Dynamics, and Mechanism of Binding in Human \$\kappa\$ -Opioid Receptor Complexes](#)
- [50] Y. Tawada, T. Tsuneda, S. Yanagisawa, T. Yanai and K. Hirao, *J. Chem. Phys.*, **2004**, 120,8425.
[A long-range-corrected time-dependent density functional theory](#)
- [51] H. Takahashi, D. Suzuoka, and A. Morita, *J. Chem. Theory Comput.*, **2015**, 11, (3),1181–1194.
[Why is Benzene Soluble in Water? Role of OH/ \$\pi\$ Interaction in Solvation](#)
- [52] E. M. Sproviero, *J. Chem. Theory Comput.*, **2015**, 11, (3),1206–1219.
[Opsin Effect on the Electronic Structure of the Retinylidene Chromophore in Rhodopsin](#)
- [53] S. Fatehi and R. P. Steele, *J. Chem. Theory Comput.*, **2015**, 11, (3),884–898.
[Multiple-Time Step Ab Initio Molecular Dynamics Based on Two-Electron Integral Screening](#)
- [54] P. Sokkar, E. Boulanger, W. Thiel, and E. Sanchez-Garcia, *J. Chem. Theory Comput.*, **2015**.
Just Accepted.
[Hybrid Quantum Mechanics/Molecular Mechanics/Coarse Grained Modeling: A Triple-Resolution Approach for Biomolecular Systems](#)
- [55] Q. Li, B. Mennucci, M. A. Robb, L. Blancafort, and C. Curutchet, *J. Chem. Theory Comput.*, **2015**, ASAP.
[Polarizable QM/MM Multi configuration Self-Consistent Field Approach with State-Specific Corrections: Environment Effects on Cytosine Absorption Spectrum](#)
- [56] I. Viciano, P. González-Navarrete, J. Andrés, and S. Martí, *J. Chem. Theory Comput.*, **2015**, ASAP.
[Joint Use of Bonding Evolution Theory and QM/MM Hybrid Method for Understanding the Hydrogen Abstraction Mechanism via Cytochrome P450 Aromatase](#)
- [57] P. Li, L. F. Song, and K. M. Merz, Jr *J. Chem. Theory Comput.*, **2015**, ASAP.
[Systematic Parameterization of Monovalent Ions Employing the Non-bonded Model](#)
- [58] J. Sauter and A. Grafmueller, *J. Chem. Theory Comput.*, **2015**, Just Accepted.
[Solution Properties of Hemicellulose Polysaccharides with Four Common Carbohydrate Force Fields](#)
- [59] Y. Yin, A. K. Sieradzan, A. Liwo, Yi He, and H. A. Scheraga, *J. Chem. Theory Comput.*, **2015**,
Just Accepted.

- Physics-based potentials for coarse-grained modeling of protein-DNA interactions
- [60] S. Ruiz-Barragan, K. Morokuma, and L. Blancafort, *J. Chem. Theory Comput.*, **2015**, Just Accepted.
Conical Intersection Optimization Using Composed Steps Inside the ONIOM (QM: MM) Scheme: CASSCF: UFF Implementation with Microiterations
- [61] M. Faheem and A. Heyden, *J. Chem. Theory Comput.*, **2014**, 10, (8),3354–3368.
Hybrid Quantum Mechanics/Molecular Mechanics Solvation Scheme for Computing Free Energies of Reactions at Metal–Water Interfaces
- [62] J. Liu, R. I. Cukier, Y. Bu, and Y. Shang, *J. Chem. Theory Comput.*, **2014**, 10, (10),4189–4197.
Glucose-Promoted Localization Dynamics of Excess Electrons in Aqueous Glucose Solution Revealed by Ab Initio Molecular Dynamics Simulation
- [63] S. Fritsch, R. Potestio, D. Donadio, and K. Kremer, *J. Chem. Theory Comput.*, **2014**, 10, (2),816–824.
Nuclear Quantum Effects in Water: A Multi-scale Study
- [64] S. Schenker, C. Schneider, S. B. Tsogoeva, and T. Clark, *J. Chem. Theory Comput.*, **2011**, 7, (11),3586–3595.
Assessment of Popular DFT and Semiempirical Molecular Orbital Techniques for Calculating Relative Transition State Energies and Kinetic Product Distributions in Enantioselective Organocatalytic Reactions
- [65] P. G. Karamertzanis, P. Raiteri and A. Galindo, *J. Chem. Theory Comput.*, **2010**, 6, (5),1590–1607.
The Use of Anisotropic Potentials in Modeling Water and Free Energies of Hydration
- [66] M. L. Hall, J. Zhang, A. D. Bochevarov, and R. A. Friesner, *J. Chem. Theory Comput.*, **2010**, 6 (12),3647–3663.
Continuous Localized Orbital Corrections to Density Functional Theory: B3LYP-CLOC
- [67] B. A. Bauer, G. L. Warren and S. Patel, *J. Chem. Theory Comput.*, **2009**, 5, (2),359–373.
Incorporating Phase-Dependent Polarizability in Nonadditive Electrostatic Models for Molecular Dynamics Simulations of the Aqueous Liquid–Vapor Interface
- [68] L. Turi, *J. Chem. Theory Comput.*, ASAP.
Hydrated Electrons in Water Clusters: Inside or Outside, Cavity or Noncavity?
- [69] L. Gurzynski, A. Puszko, M. Makowski, J. Makowska, L. Chmurzynski, *J. Chem. Thermodynamics*, **2006**,38,1584–1591.
Potentiometric and ab initio studies of acid–base interactions of substituted 4-halo(Cl, Br)pyridine N-oxide systems
- [70] D. M. Elking, G. A. Cisneros, Jean-Philip Piquemal, T. A. Darden and L. G. Pedersen, *J. Chem. Theory Comput.*, **2010**, 6, (1),190–202.
Gaussian Multipole Model (GMM)
- [71] S. Kerisit, D. J. Cooke, D. Spagnoli and S. C. Parker, *J. Mater. Chem.*, **2005**, 15, 1454–1462.
Molecular dynamics simulations of the interactions between water and inorganic solids
- [72] P. Lazar, S. Kim, Y. Lee, K. W. Lee, *J. Mol. Graphics Model.* **2010**, 29,573–580.
Computational approach to ensure the stability of the favorable ATP binding site in *E. coli* Hfq
- [73] A. Ramraj, R. K. Raju, Q. Wang, I. H. Hillier, R. A. Bryce, M. A. Vincent, *J. Mol. Graphics Model.*, **2010**, 29,321–325.
An evaluation of the GLYCAM06 and MM3 force fields, and the PM3-D* molecularorbital method for modelling prototype carbohydrate–aromatic interactions
- [74] M. P. Gleeson, S. Hannongbua, D. Gleeson, *J. Mol. Graphics Model.*, **2010**, 29,507–517.
QM methods in structure based design: Utility in probing protein–ligand interactions
- [75] P. K. Naik, A. Dubey, K. Soni, R. Kumar, H. Singh, *J. Mol. Graphics Model.*, **2010**, 29,546–564.
The binding modes and binding affinities of epipodophyllotoxin derivatives with human topoisomerase II
- [76] Li Yu, Jing-Min Shi, Yi-Quan Zhang, Yu-Qing Wang, Ya-Nan Fan, Gui-Qiu Zhang, Wei Shi, P. Cheng, *J. Mol. Struct.*, **2011**, 987,138–143.

- p-p Stacking and magnetic coupling mechanism on a mono-nuclear Mn(II) complex
- [77] Furer V.L, I. I. Vandyukov, A.E. Vandyukov, S. Fuchs, J. P. Majoral, A. M. Caminade, V.I. Kovalenko, *J. Mol. Struct.*, **2011**, 987,144–151.
- DFT study of structure, IR and Raman spectra of the first generation Dendron built from cyclotriphosphazene core
- [78] Sudha S, N. Sundaraganesan, M. Kurt, M. Cinar, M. Karabacak, *J. Mol. Struct.*, **2011**, 985,148–156.
- FT-IR and FT-Raman spectra, vibrational assignments, NBO analysis and DFT calculations of 2-amino-4-chlorobenzonitrile
- [79] Kariduraganavar M.Y, S. M. Tambe, R. G. Tasaganva, A.A. Kittur, S.S. Kulkarni, S.R. Inamdar, *J. Mol. Struct.*, **2011**, 987,158–165.
- Studies on nonlinear optical polyurethanes containing heterocyclic chromophores
- [80] Gang Fu, R. J. Doerksen, P. Xu, *J. Mol. Struct.*, **2011**,987,166–173.
- Assignment of absolute configuration of sulfinyl dilactones: Optical rotations and ¹H NMR experiment and DFT calculations
- [81] Hao-Hong Li, Jun-Xiong Wu, Hai-Jun Dong, Yan-Ling Wu, Zhi-Rong Chen, *J. Mol. Struct.*, **2011**, 987,180–185.
- A combined experimental and theoretical study of an semi-conductive iodoargentate hybrid induced by large conjugate cation
- [82] J. R. Durig, H. Dee, I. D. Darkhalil, J. J. Klaassen, T. K. Gounev, A. Ganguly, *J. Mol. Struct.*, **2011**, 985,202–210.
- The r0 structural parameters, conformational stability, barriers to internal rotation, and vibrational assignments for trans and gauche ethanol
- [83] Li Yi, M. Yang, Y. Liu, R. Wei, X. Liu, F. gshi Li, *J. Mol. Struct.*, **2011**, 987,206–213.
- Synthesis, characterization and structural aspects of new haptens for PAHs
- [84] S. F. Tayyari, F. Naghavi, S. Pojhan, R. W. McClurg, R. E. Sammelson, *J. Mol. Struct.*, **2011**,987,241–254.
- Conformational analysis, tautomerization, IR, Raman, and NMR studies of benzyl acetoacetate
- [85] B. V. Cunning, G. A. Hope, P. C. Healy, C. L. Brown, *J. Mol. Struct.*, **2011**, 987,25–33.
- Vibrational and crystal structure analysis of a phenylenedioxydiacetic acid derivative
- [86] S. Yaz, Ç. Albayrak, I. Gumrukcuog, I. Senel, O. Buyukgungor, *J. Mol. Struct.*, **2011**,985,292–298.
- Experimental and density functional theory (DFT) studies on (E)-2-Acetyl-4-(4-nitrophenyldiazenyl) phenol
- [87] K. Chruszcz-Lipska, K. K. Zborowski, E. Podstawka-Proniewicz, S. Liu, Y. Xu, L. M. Proniewicz, *J. Mol. Struct.*, **2011**, 986,49–56.
- Phosphonic drugs: Experimental and theoretical spectroscopic studies of fosfomycin
- [88] N. Veiga, J. Torres, G. González, K. Gómez, D. Mansell, S. Freeman, S. Domínguez, C. Kremer, *J. Mol. Struct.*, **2011**,986, 75–85.
- Insight into the protonation and K (I)-interaction of the inositol 1, 2, 3-trisphosphate as provided by ³¹P NMR and theoretical calculations
- [89] D. M. Denning and D. E. Falvey, *J. Org. Chem.*, **2014**, 79, (10),4293–4299.
- Solvent-Dependent Decarboxylation of 1,3-Dimethylimidazolium-2-Carboxylate
- [90] X. Yang and Y. Xue, *J. Org. Chem.*, **2014**, 79, (11),4863–4870.
- Medium Effects on the 1,3-Dipolar Cycloaddition of Pyridazinium Dicyanomethanide with Ethyl Vinyl Ketone in Pure and Mixed Solvents from QM/MM Simulations
- [91] V. Barone, R. Arnaud, P. Y. Chavant, and Y. Vallée *J. Org. Chem.*, **1996**, 61, (15),5121–5129.
- Substituent Effects in the Hetero-Diels–Alder Reaction of Thiocarbonyl Compounds with Butadiene
- [92] Z. Kan, X. Yan, and J. Ma, *J. Phys. Chem. A*, **2015**, 119, (9),1573–1589.
- Conformation Dynamics and Polarization Effect of α , α -Trehalose in a Vacuum and in Aqueous and Salt Solution

- [93] R. Kania, J. K. Malongwe, D. Nachtigallová, J. Krausko, I. Gladich, M. Roeselová, D. Heger, P. Klán, *J. Phys. Chem. A*, 2014, (118), 35, 7535–7547.
[Spectroscopic Properties of Benzene at the Air–Ice Interface: A Combined Experimental–Computational Approach](#)
- [94] H. Ke, Christian van der Linde, and J. M. Lisy, *J. Phys. Chem. A*, **2015**, 119, (10), 2037–2051.
[Insights into the Structures of the Gas-Phase Hydrated Cations \$M^+\(H_2O\)_nAr\$ \(\$M = Li, Na, K, Rb, \text{ and } Cs; n = 3–5\$ \) Using Infrared Photo dissociation Spectroscopy and Thermodynamic Analysis](#)
- [95] P. Delcroix, M. Pagliai, G. Cardini, D. Bégué, and B. Hanoune, *J. Phys. Chem. A*, **2015**, 119, (2), 290–298.
[Structural and Spectroscopic Properties of Methanediol in Aqueous Solutions from Quantum Chemistry Calculations and Ab Initio Molecular Dynamics Simulations](#)
- [96] G. M. Chaban, D. Wang, W. M. Huo, *J. Phys. Chem. A*, **2015**, 119, (2), 377–38.
[Ab Initio Study of Guanine Damage by Hydroxyl Radical](#)
- [97] Z. Zeng, Cheng-Wen Liu, Gao-Lei Hou, G. Feng, Hong-Guang Xu, Yi Qin Gao, and Wei-Jun Zheng, *J. Phys. Chem. A*, **2015**, ASAP.
[Photoelectron Spectroscopy and ab initio Calculations of \$Li\(H_2O\)_n-\$ and \$Cs\(H_2O\)_n-\$ \(\$n = 1–6\$ \) Clusters](#)
- [98] A. Petrone, J. Cerezo, F. J. A. Ferrer, G. Donati, R. Improta, N. Rega, and F. Santoro, *J. Phys. Chem. A*, **2015**, ASAP.
[Absorption and Emission Spectral Shapes of a Prototype Dye in Water by Combining Classical/Dynamical and Quantum/Static Approaches](#)
- [99] P. Jankowski, G. Murdachaew, R. Bukowski, O. Akin-ojo, C. Leforestier, and K. Szalewicz, *J. Phys. Chem. A*, **2015**, Just Accepted Manuscript.
[Ab Initio Water Pair Potential with Flexible Monomers](#)
- [100] A. A. Freitas, F. H. Quina, and A. A. L. Maçanita, *J. Phys. Chem. A*, **2014**, 118, (45), 10448–10455.
[Femtosecond and Temperature-Dependent Picosecond Dynamics of Ultrafast Excited-State Proton Transfer in Water–Dioxane Mixtures](#)
- [101] R. Sedlak, P. Deepa, and P. Hobza *J. Phys. Chem. A*, **2014**, 118, (21), 3846–3855.
[Why Is the L-Shaped Structure of \$X_2 \cdots X_2\$ \(\$X = F, Cl, Br, I\$ \) Complexes More Stable Than Other Structures?](#)
- [102] S. Riikonen, P. Parkkinen, L. Halonen, and R. B. Gerber *J. Phys. Chem. A*, **2014**, 118, (27), 5029–5037.
[Ionization of Acids on the Quasi-Liquid Layer of Ice](#)
- [103] R. Hatz, V. Hänninen, and L. Halonen *J. Phys. Chem. A*, **2014**, 118, (30), 5734–5740.
[Dispersion Interactions in Small Zinc, Cadmium, and Mercury Clusters](#)
- [104] T. Sommerfeld, K. M. Dreux, and R. Joshi *J. Phys. Chem. A*, **2014**, 118, (35), 7320–7329.
[Excess Electrons Bound to Molecular Systems with a Vanishing Dipole but Large Molecular Quadrupole](#)
- [105] F. Uhlig, J. M. Herbert, M. P. Coons, and P. Jungwirth, *J. Phys. Chem. A*, **2014**, 118, (35), 7507–7515.
[Optical Spectroscopy of the Bulk and Interfacial Hydrated Electron from Ab Initio Calculations](#)
- [106] P. Xu and M. S. Gordon, *J. Phys. Chem. A*, **2014**, 118, (35), 7548–7559.
[Renormalized Coupled Cluster Approaches in the Cluster-in-Molecule Framework: Predicting Vertical Electron Binding Energies of the Anionic Water Clusters \$\(H_2O\)_n-\$](#)
- [107] R. Chaudret, N. Gresh, C. Narth, L. Lagardère, T. A. Darden, G. A. Cisneros, and Jean-Philip Piquemal, *J. Phys. Chem. A*, **2014**, 118, (35), 7598–7612.
[S/G-1: An ab Initio Force-Field Blending Frozen Hermite Gaussian Densities and Distributed Multipoles. Proof of Concept and First Applications to Metal Cations](#)
- [108] X. Liu, A. L. Sobolewski, and W. Domcke, *J. Phys. Chem. A*, **2014**, 118, (36), 7788–7795.
[Photoinduced Oxidation of Water in the Pyridine–Water Complex: Comparison of the Singlet and Triplet Photochemistries](#)
- [109] X. Guo, Y. Zhao, and Z. Cao, *J. Phys. Chem. A*, **2014**, 118, (39), 9013–9020.

- Ab Initio Study on Ultrafast Excited-State Decay of Allopurinol Keto-N9H Tautomer from Gas Phase to Aqueous Solution
- [110] S. Wang, J. Liu, C. Zhang, Li Guo, and Y. Bu, *J. Phys. Chem. A*, **2014**, 118, (39),9212–9219.
Crucial Role of Solvent-Impacted Molecular Anionic Resonances in Controlling Protonation Modes in the Acetonitrile–Water Anionic Cluster Revealed by ab Initio Molecular Dynamics Simulations
- [111] M. Wońska and P. M. Dominiak, *J. Phys. Chem. A*, **2013**, 117, (7),1535–1547.
Transferability of Atomic Multipoles in Amino Acids and Peptides for Various Density Partitions
- [112] P. I. Nagy, *J. Phys. Chem.A*, **2013**, 117, (13),2812–2826.
Are the Intramolecular O–H···F and O–H···Cl Hydrogen Bonds Maintained in Solution? A Theoretical Study
- [113] A. P. Charmet, G. Quartarone, L. Ronchin, C. Tortato, and A. Vavasori, *J. Phys. Chem. A*, **2013**, 117, (31),6846–6858.
Quantum Chemical Investigation on Indole: Vibrational Force Field and Theoretical Determination of Its Aqueous pKa Value
- [114] J. D. Mottishaw and H. Sun, *J. Phys. Chem.A*, **2013**, 117, (33),7970–7979.
Effects of Aromatic Trifluoromethylation, Fluorination, and Methylation on Intermolecular π – π 621 Interactions
- [115] A. Paul, M. Kubicki, A. Kubas, C. Jelsch, K. Fink, and C. Lecomte, *J. Phys. Chem. A*, **2011**, 115, (45),12941–12952.
Charge Density Analysis of 2-Methyl-4-nitro-1-phenyl-1*H*-imidazole-5-carbonitrile: An Experimental and Theoretical Study of C \equiv N···C \equiv N Interactions
- [116] G. F. Mangiatordi, J. Hermet, and C. Adamo, *J. Phys. Chem.A*, **2011**, 115, (12),2627–2634.
Modeling Proton Transfer in Imidazole-like Dimers: A Density Functional Theory Study
- [117] G. Anders and I. Borges, Jr, *J. Phys. Chem.A*, **2011**, 115, (32),9055–9068.
Topological Analysis of the Molecular Charge Density and Impact Sensitivity Models of Energetic Molecules
- [118] M. Devereux, N. Plattner and M. Meuwly, *J. Phys. Chem. A*, **2009**, 113, (47),13199–13209.
Application of Multipolar Charge Models and Molecular Dynamics Simulations to Study Stark Shifts in Inhomogeneous Electric Fields
- [119] Y. Kitagawa, T. Saito, Y. Nakanishi, Y. Kataoka, T. Matsui, T. Kawakami, M. Okumura and K. Yamaguchi, *J. Phys. Chem. A*, **2009**, 113, (52),15041–15046.
Spin Contamination Error in Optimized Geometry of Singlet Carbene (1A1) by Broken-Symmetry Method
- [120] P. K. Nandi, N. Panja, T. K. Ghanty and T. Kar, *J. Phys. Chem.A*, **2009**, 113, (11),2623–2631.
Theoretical Study of the Effect of Structural Modifications on the Hyperpolarizabilities of Indigo Derivatives
- [121] C. S. P. Gamage, K. Ueno-Noto and D. S. Marynick, *J. Phys. Chem.A*, **2009**, 113, (35),9737–9740.
Computational Studies of Gas-Phase Ca3P2 and Ca6P4
- [122] M. Body, C. Legein, J.-Y. Buzaré, G. Silly, P. Blaha, C. Martineau, and F. Calvayrac, *J. Phys. Chem. A*, **2007**, 111, (46),11873–11884.
Advances in Structural Analysis of Fluoroaluminates Using DFT Calculations of 27Al Electric Field Gradients
- [123] C. Lepetit, H. Chermette, M. Gicquel, Jean-Louis Heully, and R. Chauvin, *J. Phys. Chem. A*, **2007**, 111, (1),136–149.
Description of Carbo-oxocarbons and Assessment of Exchange–Correlation Functionals for the DFT Description of Carbo-mers
- [124] M. H. Karimi-Jafari and A. Maghari, *J. Phys. Chem. A*, **2007**, 111, (27),6077–6083.
An Ab Initio Intermolecular Potential Energy Surface for the F2 Dimer
- [125] G. Corongiu, *J. Phys. Chem. A*, **2006**, 110, (40), 11584–11598.
Hartree–Fock–Heitler–London Method. 2. First and Second Row
- [126] A. V. Fishchuk, P. E. S. Wormer, and Ad van der Avoird, *J. Phys. Chem.A*, **2006**, 110, (16),5273–5279.
Ab Initio Treatment of the Chemical Reaction Precursor Complex Cl (2P)–HF. 1. Three-Dimensional Diabatic Potential Energy Surfaces

- [127] R. Ponec and G. Yuzhakov, *J. Phys. Chem.A*, **2003**, 107, (12),2100–2105.
[Electron Reorganization in Chemical Reactions. Structural Changes from the Analysis of Bond Order Profiles](#)
- [128] G. Maroulis and D. Xenides, *J. Phys. Chem. A*, **2003**, 107, (5),712–719.
[Electric Quadrupole and Hexadecapole Moment, Dipole and Quadrupole Polarizability, Second Electric Dipole Hyperpolarizability for P2, and a Comparative Study of Molecular Polarization in N2, P2, and As2](#)
- [129] L. Carballeira, I. Pérez-Juste, and C. V. Alsenoy, *J. Phys. Chem.A*, **2002**, 106, (15),3873–3884.
[Theoretical Study of Pyrrolidine: Revised Conformational Energies and Vibrational Assignments](#)
- [130] H. Huang and M. T. Rodgers, *J. Phys. Chem.A*, **2002**, 106, (16),4277–4289.
[Sigma versus Pi Interactions in Alkali Metal Ion Binding to Azoles: Threshold Collision-Induced Dissociation and ab Initio Theory Studies](#)
- [131] G. Talarico, V. Barone, P. H. M. Budzelaar, and C. Adamo, *J. Phys. Chem.A*, **2001**, 105, (39),9014–9023.
[Modeling Polymerization Reactions at Aluminum-Based Catalysts: Is DFT a Reliable Computational Tool?](#)
- [132] S. S. C. Ammal and P. Venuvanalingam, *J. Phys. Chem. A*, **2000**, 104, (46),10859–10867.
[Origin and Nature of Lithium and Hydrogen Bonds to Oxygen, Sulfur, and Selenium](#)
- [133] G. Wu, A. Hook, S. Dong, and K. Yamada, *J. Phys. Chem.A*, **2000**, 104, (17),4102–4107.
[A Solid-State NMR and Theoretical Study of the ¹⁷O Electric Field Gradient and Chemical Shielding Tensors of the Oxonium Ion in p-Toluenesulfonic Acid Monohydrate](#)
- [134] U. Hohm, D. Goebel, P. Karamanis, G. Maroulis, *J. Phys. Chem. A*, **1998**, 102, (8),1237–1240.
[Electric Dipole Polarizability of As4, a Challenging Problem for Both Experiment and Theory](#)
- [135] V. Barone and M. Cossi, *J. Phys. Chem. A*, **1998**, 102, (11),1995–2001.
[Quantum Calculation of Molecular Energies and Energy Gradients in Solution by a Conductor Solvent Model](#)
- [136] M. P. Hodges and A. J. Stone, *J. Phys. Chem.A*, **1998**, 102, (14),2455–2465.
[Analytical Potentials for HF Dimer and Larger HF Clusters from ab Initio Calculations](#)
- [137] C. Trindle and K. Romberg, *J. Phys. Chem. A*, **1998**, 102, (1),270–273.
[Reactions of HSCH2 Radical with O2, NO, and NO2: Ab Initio Calculations of Enthalpies of Reaction](#)
- [138] R. Kaschner and D. Hohl, *J. Phys. Chem.A*, **1998**, 102, (26),5111–5116.
[Density Functional Theory and Biomolecules: A Study of Glycine, Alanine, and Their Oligopeptides](#)
- [139] A. M. Brouwer, *J. Phys. Chem.A*, **1997**, 101, (19),626–3633.
[Ab Initio Study of the Structures and Vibrational Spectra of Some Diamine Radical Cations](#)
- [140] C. Calero, J. Martí, and E. Guàrdia, *J. Phys. Chem. B*, **2015**, 119, (5),1966–1973.
[¹H Nuclear Spin Relaxation of Liquid Water from Molecular Dynamics Simulations](#)
- [141] H. Wang and N. Agmon, *J. Phys. Chem. B*, **2015**, 119, (6),2658–2667.
[Protonated Water Dimer on Benzene: Standing Eigen or Crouching Zundel?](#)
- [142] R. K. Zenn, E. Abad, and J. Kastner, *J. Phys. Chem. B*, **2015**, 119, (9),3678–3686.
[Influence of the Environment on the Oxidative Deamination of p-Substituted Benzylamines in Monoamine Oxidase](#)
- [143] M. L. Laury, Lee-Ping Wang, V. S. Pande, T. Head-Gordon, and J. W. Ponder, *J. Phys. Chem. B*, **2015**, ASAP.
[Revised Parameters for the AMOEBA Polarizable Atomic Multipole Water Model](#)
- [144] L. K. Tolonen, M. Bergenstråhle-Wohlert, H. Sixta, and J. Wohlert, *J. Phys. Chem. B*, **2015**, Just Accepted.
[The Solubility of Cellulose in Supercritical Water Studied by Molecular Dynamics Simulations](#)
- [145] L. Cao, G. Dong, and W. Lai, *J. Phys. Chem. B*, **2015**, Just Accepted.
[Reaction Mechanism of Cobalt-Substituted Homoprotocatechuate 2, 3-Dioxygenase -A QM/MM Study](#)
- [146] M. Kumari, S. Kozmon, P. Kulhanek, J. Stepan, I. Tvaroska, and J. Koča, *J. Phys. Chem. B*, **2015**, Just Accepted.
[Exploring Reaction Pathways for O-GlcNAc Transferase Catalysis. A String Method Study](#)
- [147] Ya Gao, Y. Li, L. Mou, W. Hu, Jun Zheng, John Z. H. Zhang, and Ye Mei, *J. Phys. Chem. B*, **2015**, Just Accepted.

- Coupled Two-Dimensional Main-Chain Torsional Potential for Protein Dynamics II: Performance and Validation
- [148] A. Carof, M. Salanne, T. Charpentier, and B. Rotenberg, *J. Phys. Chem. B*, **2014**, 118, (46),13252–13257.
- Accurate Quadrupolar NMR Relaxation Rates of Aqueous Cations from Classical Molecular Dynamics
- [149] S. Riahi and C. N. Rowley, *J. Phys. Chem. B*, **2014**, 118, (5), 1373–1380.
- Solvation of Hydrogen Sulfide in Liquid Water and at the Water–Vapor Interface Using a Polarizable Force Field
- [150] J. Cuny and Ali A. Hassanali, *J. Phys. Chem. B*, **2014**, 118, (48),13903–13912.
- Ab Initio Molecular Dynamics Study of the Mechanism of Proton Recombination with a Weak Base
- [151] R. Cisek, D. Tokarz, S. Krouglov, M. Steup, M. J. Emes, Ian J. Tetlow, and V. Barzda, *J. Phys. Chem. B*, **2014**, 118, (51),14785–14794.
- Second Harmonic Generation Mediated by Aligned Water in Starch Granules
- [152] A. Bhattacharjee, A. K. H. Weiss, V. Artero, M. J. Field, and T. S. Hofer, *J. Phys. Chem. B*, **2014**, 118, (20),5551–5561.
- Electronic Structure and Hydration of Tetramine Cobalt Hydride Complexes
- [153] M. Galib and G. Hanna, *J. Phys. Chem. B*, **2014**, 118, (22),5983–5993.
- The Role of Hydrogen Bonding in the Decomposition of H₂CO₃ in Water: Mechanistic Insights from Ab Initio Metadynamics Studies of Aqueous Clusters
- [154] P. Musto, M. Galizia, M. Pannico, G. Scherillo, and G. Mensitieri, *J. Phys. Chem. B*, **2014**, 118, (26),7414–7429.
- Time-Resolved Fourier Transform Infrared Spectroscopy, Gravimetry, and Thermodynamic Modeling for a Molecular Level Description of Water Sorption in Poly(ϵ -caprolactone)
- [155] Z. Ma, D. Anick, and M. E. Tuckerman, *J. Phys. Chem. B*, **2014**, 118, (28),7937–7945.
- Ab Initio Molecular Dynamics Study of the Aqueous HOO– Ion
- [156] Yong-Lei Wang, F. U. Shah, S. Glavatskih, O. N. Antzutkin, and A. Laaksonen, *J. Phys. Chem. B*, **2014**, 118, (29),8711–8723.
- Atomistic Insight into Orthoborate-Based Ionic Liquids: Force Field Development and Evaluation
- [157] T. T. Duignan, D. F. Parsons, and B. W. Ninham, *J. Phys. Chem. B*, **2013**, 117, (32), 9412–9420.
- A Continuum Solvent Model of the Multipolar Dispersion Solvation Energy
- [158] P. Troster, K. Lorenzen, M. Schwörer, and P. Tavan, *J. Phys. Chem. B*, **2013**, 117, (32),9486–9500.
- Polarizable Water Models from Mixed Computational and Empirical Optimization
- [159] T. Hasegawa and Y. Tanimura, *J. Phys. Chem. B*, **2011**, 115, (18),5545–5553.
- A Polarizable Water Model for Intramolecular and Intermolecular Vibrational Spectroscopies
- [160] A. Avramopoulos, M. G. Papadopoulos, and H. Reis, *J. Phys. Chem. B*, **2007**, 111, (10),2546–2553.
- Calculation of the Microscopic and Macroscopic Linear and Nonlinear Optical Properties of Liquid Acetonitrile. II. Local Fields and Linear and Nonlinear Susceptibilities in Quadrupolar Approximation
- [161] L. Lo Presti, R. Soave and R. Destro, *J. Phys. Chem. B*, **2006**, 110, (12),6405–6414.
- On the Interplay between CH...O and OH...O Interactions in Determining Crystal Packing and Molecular Conformation: An Experimental and Theoretical Charge Density Study of the Fungal Secondary Metabolite Austdiol (C₁₂H₁₂O₅)
- [162] K. M. Bulanin and R. F. Lobo, M. O. Bulanin, *J. Phys. Chem. B*, **2000**, 104, (6),1269–1276.
- Low-Temperature Adsorption of N₂, O₂, and D₂ on LiX, NaX, and NaLiX Zeolites Studied by FT-IR Spectroscopy
- [163] R. Koitz, M. Iannuzzi, and J. Hutter, *J. Phys. Chem. C*, **2015**, 119, (8),4023–4030.
- Building Blocks for Two-Dimensional Metal–Organic Frameworks Confined at the Air–Water Interface: An Ab Initio Molecular Dynamics Study
- [164] E. Benassi, G. Granucci, M. Persico, and S. Corni, *J. Phys. Chem. C*, **2015**, Just Accepted.
- Can Azobenzene Photoisomerize When Chemisorbed on a Gold Surface? An Analysis of Steric Effects Based on Nonadiabatic Dynamics Simulations

- [165] Z. Shen, Y. Liu, P. E. Brown, I. Szlufarska, and H. Xu, *J. Phys. Chem. C*, **2014**, 118, (29),15716–15722.
[Modeling the Effect of Dissolved Hydrogen Sulfide on Mg²⁺–Water Complex on Dolomite Surfaces](#)
- [166] A. N. Rudenko, S. Bendt, and F. J. Keil, *J. Phys. Chem. C*, **2014**, 118, (29),16218–16227.
[Multiscale Modeling of Water in Mg-MOF-74: From Electronic Structure Calculations to Adsorption Isotherms](#)
- [167] A. Ambrosetti and P. L. Silvestrelli, *J. Phys. Chem. C*, **2014**, 118, (33),19172–19179.
[Gas Separation in Nanoporous Graphene from First Principle Calculations](#)
- [168] P. Li, G. Henkelman, J. A. Keith, and J. K. Johnson, *J. Phys. Chem. C*, **2014**, 118, (37),21385–21399.
[Elucidation of Aqueous Solvent-Mediated Hydrogen-Transfer Reactions by ab Initio Molecular Dynamics and Nudged Elastic-Band Studies of NaBH₄ Hydrolysis](#)
- [169] C. Butchosa, P. Guiglion, and M. A. Zwijnenburg, *J. Phys. Chem. C*, **2014**, 118, (43),24833–24842.
[Carbon Nitride Photocatalysts for Water Splitting: A Computational Perspective](#)
- [170] M. A. Brown, M. Arrigoni, F. Héroguel, A. B. Redondo, L. Giordano, J. A. van Bokhoven, and G. Pacchioni, *J. Phys. Chem. C*, **2014**, 118, (50),29007–29016.
[pH Dependent Electronic and Geometric Structures at the Water–Silica Nanop Interface](#)
- [171] I. Unger, S. Thürmer, D. Hollas, E. F. Aziz, B. Winter, and P. Slavíček, *J. Phys. Chem. C*, **2014**, 118, (50),29142–29150.
[Ultrafast Proton and Electron Dynamics in Core-Ionized Hydrated Hydrogen Peroxide: Photoemission Measurements with Isotopically Substituted Hydrogen Peroxide](#)
- [172] A. Bankura, A. Karmakar, V. Carnevale, A. Chandra, and M. L. Klein, *J. Phys. Chem. C*, **2014**, 118, (50),29401–29411.
[Structure, Dynamics, and Spectral Diffusion of Water from First-Principles Molecular Dynamics](#)
- [173] G. K. Lockwood and S. H. Garofalini, *J. Phys. Chem. C*, **2014**, 118, (51),29750–29759.
[Proton Dynamics at the Water–Silica Interface via Dissociative Molecular Dynamics](#)
- [174] J. Cheng, J. VandeVondele, and M. Sprik, *J. Phys. Chem. C*, **2014**, 118, (10),5437–5444.
[Identifying Trapped Electronic Holes at the Aqueous TiO₂ Interface](#)
- [175] S. Sanna, W. G. Schmidt, and P. Thissen, *J. Phys. Chem. C*, **2014**, 118, (15),8007–8013.
[Formation of Hydroxyl Groups at Calcium-Silicate-Hydrate \(C-S-H\): Coexistence of Ca–OH and Si–OH on Wollastonite](#)
- [176] P. Maldonado, L. Z. Evins, and P. M. Oeneer, *J. Phys. Chem. C*, **2014**, 118, (16), 8491–8500.
[Ab Initio Atomistic Thermodynamics of Water Reacting with Uranium Dioxide Surfaces](#)
- [177] K. Abderrafi, R. G. Calzada, M. B. Gongalsky, I. Suárez, R. Abarques, V. S. Chirvony, V. Yu. Timoshenko, R. Ibáñez, and J. P. Martínez-Pastor, *J. Phys. Chem. C*, **2011**, 115, (12),5147–5151.
[Silicon Nanocrystals Produced by Nanosecond Laser Ablation in an Organic Liquid](#)
- [178] J. M. Bowman, Y. Wang, H. Liu, and J. S. Mancini, *J. Phys. Chem. Lett.*, **2015**, 6, (3),366–373.
[Ab Initio Quantum Approaches to the IR Spectroscopy of Water and Hydrates](#)
- [179] H. Iglev, S. K. Kolev, H. Rossmadl, P. St. Petkov, and G. N. Vayssilov, *J. Phys. Chem. Lett.*, **2015**, 6,986–992.
[Hydrogen Atom Transfer from Water or Alcohols Activated by Presolvated Electrons](#)
- [180] K. Z. Sumon, A. Henni, and A. L. L. East, *J. Phys. Chem. Lett.*, **2014**, 5, (7),1151–1156.
[Molecular Dynamics Simulations of Proposed Intermediates in the CO₂+ Aqueous Amine Reaction](#)
- [181] E. Pluhařová, M. D. Baer, C. J. Mundy, B. Schmidt, and P. Jungwirth, *J. Phys. Chem. Lett.*, **2014**, 5, (13), 2235–2240.
[Aqueous Cation-Amide Binding: Free Energies and IR Spectral Signatures by Ab Initio Molecular Dynamics](#)
- [182] Q. Wan, L. Spanu, F. Gygi, and G. Galli, *J. Phys. Chem. Lett.*, **2014**, 5, (15),2562–2567.
[Electronic Structure of Aqueous Sulfuric Acid from First-Principles Simulations with Hybrid Functionals](#)
- [183] G. Cui and W. Thiel, *J. Phys. Chem. Lett.*, **2014**, 5, (15),2682–2687.

- Intersystem Crossing Enables 4-Thiothymidine to Act as a Photosensitizer in Photodynamic Therapy: An Ab Initio QM/MM Study
- [184] J. Savage and G. A. Voth, *J. Phys. Chem. Lett.*, **2014**, 5, (17),3037–3042.
[Persistent Subdiffusive Proton Transport in Perfluorosulfonic Acid Membranes](#)
- [185] U. Rivard, V. Thomas, A. Bruhacs, B. Siwick, and R. Iftimie, *J. Phys. Chem. Lett.*, **2014**, 5, (18),3200–3205.
[Donor–Bridge–Acceptor Proton Transfer in Aqueous Solution](#)
- [186] Tocci and A. Michaelides, *J. Phys. Chem. Lett.*, **2014**, 5, (3),474–480.
[Solvent-Induced Proton Hoing at a Water–Oxide Interface Gabriele](#)
- [187] Yu Liu, Jia Fu, and J. Wu, *J. Phys. Chem. Lett.*, **2013**, 4, (21),3687–3691.
[High-Throughput Prediction of the Hydration Free Energies of Small Molecules from a Classical Density Functional Theory](#)
- [188] V. B. Oyeyemi, J. A. Keith, M. Pavone, and E. A. Carter, *J. Phys. Chem. Lett.*, **2012**, 3,(3),289–293.
[Insufficient Hartree–Fock Exchange in Hybrid DFT Functionals Produces Bent Alkynyl Radical Structures](#)
- [189] P. Jiang, Ke Deng, D. Fichou, Si-Shen Xie, A. Nion, and C. Wang, *Langmuir*, **2009**, 25, (9),5012–5017.
[STM imaging ortho- and para-Fluorothiophenol Self-Assembled Monolayers on Au \(111\)](#)
- [190] F. Rittner, B. Boddenberg, R. F. Fink, and V. Staemmler, *Langmuir*, **1999**, 15, (4),1449–1455.
[Adsorption of Nitrogen on Rutile \(110\). 2. Construction of a Full Five-Dimensional Potential Energy Surface](#)
- [191] M. Segall, P. Lindan, M. Probert, C. Pickard, et al., *Materials Studio CASTEP Version 4.1. 2006*.
[Code for exchange–correlation functional](#)
- [192] G. Tocci, L. Joly, and A. Michaelides, *Nano Lett.*, **2014**, 14, (12), 6872–6877.
[Friction of Water on Graphene and Hexagonal Boron Nitride from Ab Initio Methods: Very Different Sliage Despite Very Similar Interface Structures](#)
- [193] D. D. Lovingood and G. F. Strouse, *Nano Lett.*, **2008**, 8 (10),3394–3397.
[Microwave Induced In-Situ Active Ion Etching of Growing InP Nanocrystals](#)
- [194] B. Siboulet, C. J. Marsden and P. Vitorge, *New J. Chem.*, **2008**,32, 2080–2094.
[What can quantum chemistry tell us about Pa\(V\) hydration and hydrolysis?](#)
- [195] C. Garau, D. Quiñonero, A. Frontera, P. Ballester, A. Costa, and P. M. Deyà, *Org. Lett.*, **2003**, 5,(13),2227–2229.
[Dual Binding Mode of s-Triazine to Anions and Cations](#)
- [196] J. P. Gallivan and D. A. Dougherty, *Org. Lett.*, **1999**, 1, (1),103–106.
[Can Lone Pairs Bind to a \$\pi\$ System? The Water–Hexafluorobenzene Interaction](#)
- [197] D. Banerjee, P. K. Verma and S. K. Pal, *Photochem. Photobiol. Sci.*, **2009**, 8, 1441–1447.
[Temperature-dependent femtosecond-resolved hydration dynamics of water in aqueous guanidinium hydrochloride solution](#)
- [198] A. I. Borodicha and G. M. Ullmann, *Phys. Chem. Chem. Phys.*, **2004**, 6, 1906–1911.
[Internal hydration of protein cavities: studies on BPTIy](#)
- [199] W. Dzwolak, R. Ravindra and R. Winter, *Phys. Chem. Chem. Phys.*, **2004**, 6, 1938-1943.
[Hydration and structure—the two sides of the insulin aggregation process](#)
- [200] S. B. Rempe, D. Asthagiri and L. R. Pratt, *Phys. Chem. Chem. Phys.*, **2004**, 6, 1966-1969.
[Inner shell definition and absolute hydration free energy of Kp\(aq\) on the basis of quasi-chemical theory and ab initio molecular dynamics](#)
- [201] L. M. Ricardo, M. Chalaris, K. Refson and J. Samios, *Phys. Chem. Chem. Phys.*, **2004**, 6, 94-102.
[Molecular dynamics simulation of dilute aqueous DMSO solutions. A temperature-dependence study of the hydrophobic and hydrophilic behaviour around DMSO](#)
- [202] F. Ramondo, L. Tanzi, M. Campetell, L. Gontrani, G. Mancini, A. Pieretti and C. Sadun, *Phys. Chem. Chem. Phys.*, **2009**, 11,9431–9439.

- Hydration of diazoles in water solution: pyrazole. A theoretical and X-ray diffraction study
- [203] W. Cai, T. Sun, X. Shao and C. Chipot, *Phys. Chem. Chem. Phys.*, **2008**, 10, 3236–3243.
[Can the anomalous aqueous solubility of \$\beta\$ -cyclodextrin be explained by its hydration free energy alone?](#)
- [204] P. O. Momoh and M. S. El-Shall, *Phys. Chem. Chem. Phys.*, **2008**, 10, 4827–4834.
[Gas phase hydration of organic ions](#)
- [205] D. Russo, J. Ollivierb and J. Teixeira, *Phys. Chem. Chem. Phys.*, **2008**, 10, 4968–4974.
[Water hydrogen bond analysis on hydrophilic and hydrophobic biomolecule sites](#)
- [206] T. Suzuki, *Phys. Chem. Chem. Phys.*, **2008**, 10, 96–105.
[The hydration of glucose: the local configurations in sugar–water hydrogen bonds](#)
- [207] K. Leung and S. B. Rempe, *Phys. Chem. Chem. Phys.*, **2006**, 8, 2153–2162.
[Ab initio rigid water: Effect on water structure, ion hydration, and thermodynamics](#)
- [208] T. Yamaguchi, T. Matsuoka and S. Koda, *Phys. Chem. Chem. Phys.*, **2006**, 8, 737–745.
[Mode-coupling study on the dynamics of hydrophobic hydration II: Aqueous solutions of benzene and rare gases](#)
- [209] A. Tongraar and B. M. Rode, *Phys. Chem. Chem. Phys.*, **2003**, 5, 357–362.
[The hydration structures of F₋ and Cl₋ investigated by ab initio QM/MM molecular dynamics simulations](#)
- [210] G.T. Castro, F.H. Ferretti, S.E. Blanco, *Spectrochim. Acta Part A*, **2005**, 62, 657–665.
[Determination of the overlapping pK_a values of chrysin using UV–vis spectroscopy and ab initio methods](#)
- [211] S.E. Blanco, M.C. Almandoz, F.H. Ferretti, *Spectrochim. Acta Part A*, **2005**, 61, 93–102.
[Determination of the overlapping pK_a values of resorcinol using UV-visible spectroscopy and DFT methods](#)
- [212] M. Noguera, R. Rios-Font, L. Rodriguez-Santiago, X. Solans-Monfort, A. Oliva, J. Bertran, M. Sodupe, *Theor. Chem. Acc.*, **2009**, 123, 105–111.
[Influence of p-stacking on the N7 and O6 proton affinity of guanine](#)
- [213] B. G. Luigi, A. Monari, S. Evangelisti, *Theor. Chem. Acc.*, **2009**, 123, 265–272.
[A numerical method for computing dispersion constants](#)
- [214] C. Pisani, L. Maschio, S. Casassa, *Theor. Chem. Acc.*, **2009**, 123, 327–335.
[A local-MP2 approach to the ab initio study of electron correlation in crystals and to the simulation of vibrational spectra: the case of Ice XI](#)
- [215] A.C. Ghi, *Theor. Chem. Acc.*, **2009**, 123, 337–346.
[Stepwise versus concerted mechanisms in the Wittig reaction in vacuo and in THF: the case of 2,4-dimethyl-3-pyrrol-1-ylpentanal and triphenylphosphonium ylide](#)
- [216] P. Stefano, A. E P. Lazzeretti, R. Zanasi, *Theor. Chem. Acc.* **2009**, 123, 353–364.
[Topological models of magnetic field induced current density field in small molecules](#)
- [217] K. Ramakrishna, R. Sambasiva Rao, *Journal of Applicable Chemistry*, **2015**, 4, 2, 355–449.
[OmniMetrics Part II: Applications of neural networks \(Ma_NN\) in Environmetrics](#)
- [218] K. Ramakrishna, R. Sambasiva Rao, *Journal of Applicable Chemistry*, **2015**, 4, 1, 1–98.
[OmniMetrics Part I: Applications of neural networks \(Ma_NN\) in Medicinometrics and pharmacometrics](#)
- [219] K. RamaKrishna, V. A. Ramam, R. Sambasiva Rao, *Journal of Applicable Chemistry*, **2014**, 3, 6, 2209–2311.
[Mathematical Neural Network \(MaNN\) Models Part VI: Single-layer perceptron \[SLP\] and Multi-layer perceptron \[MLP\] Neural networks in ChEM- Lab](#)
- [220] K. RamaKrishna, Ch. V. K. Rao, V. A. Ramam R. Sambasiva Rao, *Journal of Applicable Chemistry*, **2014**, 3, 1, 6–29.
[Mathematical Neural Network \(MaNN\) Models, Part I: Data-driven Soft-models for ozone in air quality](#)
- [221] Ch. V. Kamewara Rao, M.Phil thesis, **2012**, Acharya Nagarjuna University, Nagarjuna Nagar, AP
[Computational quantum chemistry \(CQC\) models of isonicotinic acid hydrazide, its valence isomers and their isopropyl derivatives](#)
- [222] K. RamaKrishna, Ch.V. Kameswara Rao, V. Ananta Ramam, R. Sambasiva Rao & M. Venkata Subba Rao, *Ind. J. Chem.*, **2012**, 51A, 571–579.

- Model chemistries of hydrazides III: SEMO computations of isonicotinic acid hydrazide, its valence isomers and their isopropyl derivatives
- [223] I. Suryanarayana, V. Ananta Ramam, K.M.M.Krishna Prasad and R.Sambasiva Rao, Ind. J. Chem., **2008**,47A, 199-206 .
- Model chemistries of hydrazides I. Electronic parameters of aliphatic hydrazides with AM1 and PM3 Hamiltonians
- [224] V Ananta Ramam, V.V. Panakala Rao, K Rama Krishna and R. Sambasiva Rao, Ind J Chem, **2006**, 45A, 100-105 (Special issue).
- Model chemistries of hydrazides II. Electronic structure of five membered aromatic hydrazides
- [225] K. Ramakrishna, R. Sambasiva Rao, *Manuscript under preparation*.
Impact of experimental design and NNs in CQC

**Appendix-1 Quantum mechanics (QM) evolving into an
Instrumental probe through
Computational quantum chemistry (CQC)**



Origin of Quantum mechanics: Max plank, in 1900, used the phrase 'quantum' of Latin origin (meaning 'how much?') both as noun and adjective. The plural form of quantum is quanta, in the context of constrained amounts/quantities of matter, which emit or absorb energy. In 1924, Born appears to have used the term quantum mechanics in the context of particles for the first time. It is in contrast to classical mechanics, dealing with large quantities of matter one comes across in daily life (Chart A1-1). The efforts during 1925 in matrix algebra and differential equations (DEs) enabled precise way of representation of long algebraic formulae. Algebra is, in fact, symbolic representation of geometric figures and their manipulation.

Chart A1-1: Popular analogies for quantum effects

- 🔔 Cats which are simultaneously alive and dead
- 🔔 Objects which are both particles and waves
- 🔔 Subatomic particles that know whether you are looking at them or not

Quantum mechanics (Qu.Mech., QM) - A physicists' mathematical model of electron(s)

Electrons are too small to apply laws of classical mechanics. Light and sound propagate in waveform. With the fundamental assumption that electrons also behave like waves, Schrodinger put forward the wave equation as mathematical model of an electron. SWE is a second order PDE in nuclear/geometric axis (x,y,z). An analytical solution exists only for one electron system i.e. H atom, H₂⁺, He⁺ and Li⁺⁺ ions. If the atomic number exceeds one (from helium atom onwards) or hydrogen and other galaxy of molecules, the equation is similar but scales up. Further, system is more complicated for mathematical solution and relative potential energy is intractable. ψ is deemed as electronic road map. The solution of DE results in a set of equations and 3D-surfaces/ 2D-contours of their output show electron density (called orbitals of electrons).

QM applied to hydrogen atom: The application of QM was first to hydrogen atom (Eqn. A1-1).

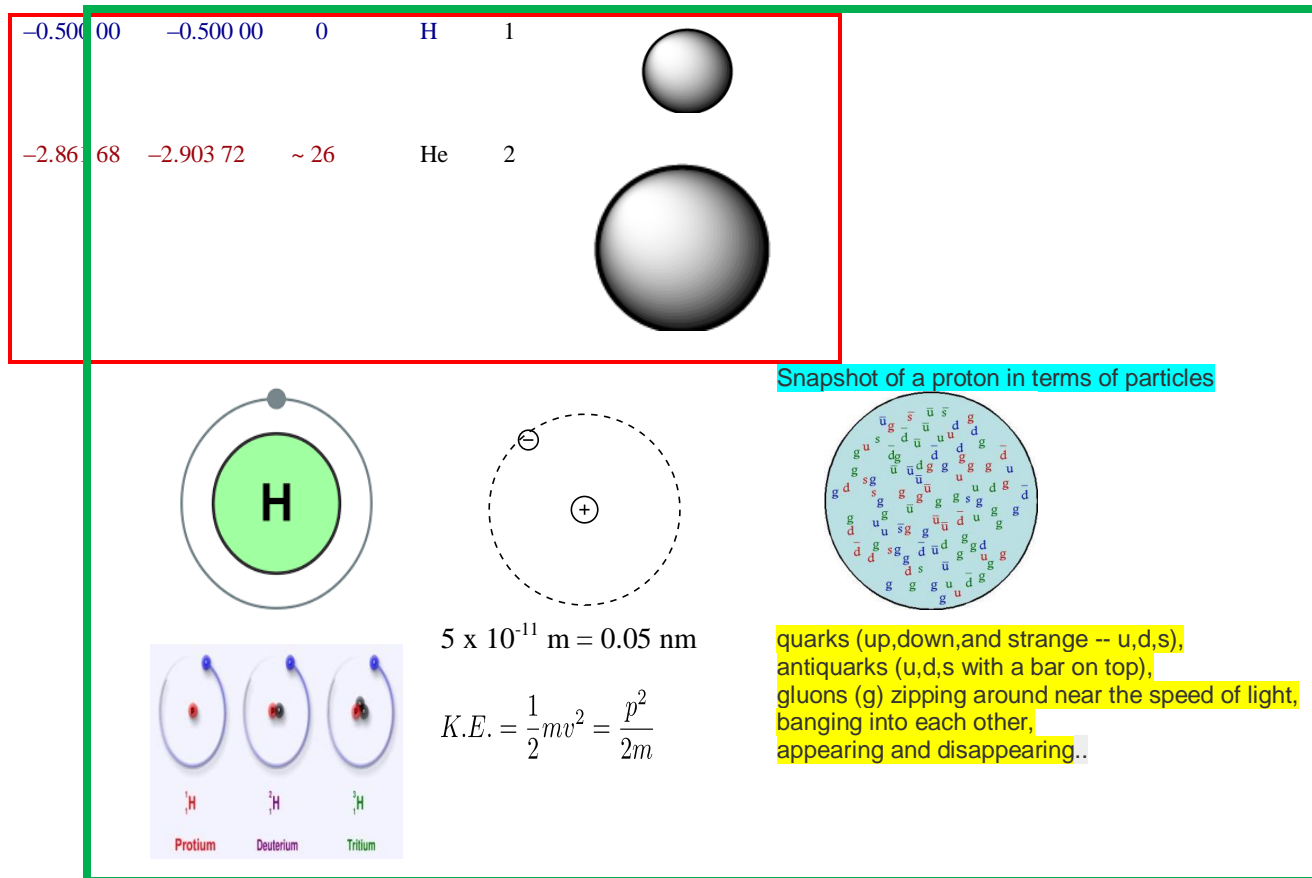
Eqn. A1-1: SWE for one electron system.

$$\frac{\delta^2 \psi}{\delta x^2} + \frac{\delta^2 \psi}{\delta y^2} + \frac{\delta^2 \psi}{\delta z^2} + \frac{8\pi^2 m}{h^2} (E - V) \psi = 0$$

Hamiltonian_QM: $\nabla^2 = \frac{\partial^2}{\partial x^2} + \frac{\partial^2}{\partial y^2} + \frac{\partial^2}{\partial z^2}$

m	:	Electron mass
E	:	Total energy
V	:	Potential energy
h	:	Planck's constant

a.u.	kcal mol ⁻¹	Atom	#el	Shape
Exact	Error			



Evolution of Quantum Chemistry (Qu.Chem., QC)

Quantum mechanics, a physicist tool, revolutionized chemistry. Its' initial application of course was restricted to one-electron systems. Yet, QM remained to be a discipline of theoretical impetus in chemistry curriculum with particle in 1D-, 3D- boxes, perturbation, variation principle, effect of magnetic and electric field for hydrogen like atoms. The axiom here is that energy cannot go lower than the "true" one. The popular form $H\Psi = E\Psi$ is understood with implicit implications. $E\Psi$ is read as product of energy (a scalar term) and wave function.

Eqn. A1-2: Hamiltonian operator

$$\text{operator}(\text{function}(x)) = \text{eigen_value} * \text{function}(x)$$

$$\text{Hamiltonian}(\Psi) = \text{Energy} * \Psi$$

abbreviated as

$$H(\Psi) = E * \Psi$$

The LHS term $H\Psi$ is comprehended as Hamiltonian operator (H) operates on ψ , the wave function (Eqn. A1-2). In this information era, $H(\Psi) = E * \Psi$ format is preferable for pedagogy and trivial translation into even object code. The wave function, ψ in Schrodinger wave equation has only mathematical relevance and does not signify anything in the physical world, although the square of it is probability of electron density. The fictitious particles (appendix-04) with no real existence are the basis of DFT. However, it adequately represents the physically significant electron density.

A philosophical question arises for the choice of two different worlds (viz. a paradigm with mathematically sound foundation without physical significance or physically significant particles with no exact mathematical solution) equally adaptable with trust worthy results at ones' disposal. Now, both are acceptable keeping in view of the tremendous success in computing (without experiment), a huge set of physico-chemical parameters and characteristics of chemical reactions. The units of wave function are chosen such that its square is number of electrons per unit volume. However, electrons are quantum

particles with non-point distributions. Electron density or probability density is used in CQC instead of electrons per volume. This arises as a result of indistinguishability of quantum particles, here electrons.

The advances in solution algorithms widened the scope of applications in chemical and biological sciences. QM comprises of ab initio and semi empirical (SEMO) methods (Fig. A1-1). Ab initio now can be viewed to comprise of Hart-Fock (HF) [+post_HF] (Eqn. A1-3) and density functional theory (DFT) paradigms. The progress of QC is in fact evolution of operators (Hamiltonian), functionals and approximation of variation of electron density with know-how of combination of primitive mathematical basis functions (appendix-05). Evolution of operator is to account for the effect of external electrical/magnetic fields, solvent, condensed phase artifacts and so on. Hamiltonian operator becomes more and more complicated in this systematic improvisation.

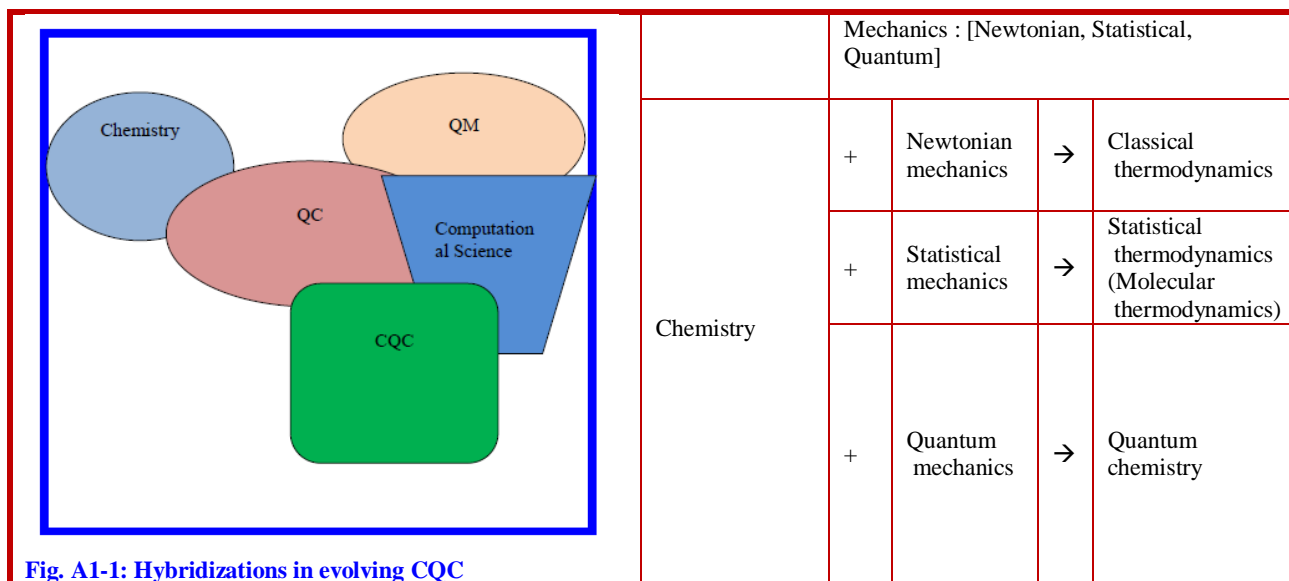


Fig. A1-1: Hybridizations in evolving CQC

Eqn. A1-3: Components of Molecular Hamiltonian

$$\begin{array}{l}
 \mathbf{H} = \\
 \text{Molecular Hamiltonian}
 \end{array}
 =
 \begin{array}{l}
 [\text{KE_nuclei} + \text{KE_electrons}] \\
 + [\text{Repulsion_nuclei_nuclei}] \\
 + [\text{Repulsion_electron_electron}] \\
 + [\text{attraction_nuclei_electrons}]
 \end{array}
 =
 \begin{array}{l}
 \text{KE_N} + \text{KE_el} + \\
 \text{Rep_N_N} + \\
 \text{Rep_el_el} + \\
 \text{Attr_el_N}
 \end{array}$$

ab-initio Hamiltonian of the coupled electron-nucleus system

Kinetic energy	Potential interaction
$\hat{T}_n = \sum_{\alpha=1}^K \frac{(-i\hbar\nabla_{\mathbf{R}_\alpha})^2}{2M_\alpha}$	$\hat{V}_{n-n} = \sum_{\alpha,\beta=1; \alpha<\beta}^K \frac{Z_\alpha Z_\beta e^2}{ \mathbf{R}_\alpha - \mathbf{R}_\beta }$
$\hat{T}_e = \sum_{i=1}^N \frac{(-i\hbar\nabla_i)^2}{2m}$	$\hat{V}_{n-e} = - \sum_{\alpha=1}^K \sum_{i=1}^N \frac{Z_\alpha e^2}{ \mathbf{R}_\alpha - \mathbf{r}_i }$
	$\hat{V}_{e-e} = \sum_{i,j=1; i<j}^N \frac{e^2}{ \mathbf{r}_i - \mathbf{r}_j }$

T_{ni} : Kinetic energy of non-interacting electrons
 V_{ne} : Nuclear-electron interaction
 V_{ee} : Classical electron-electron repulsion
 Δ : Correction to kinetic energy
 ΔV_{ee} : All non-classical corrections due to el.-el. repulsion_energy

Eqn. A1-3b: Schrodinger wave equation

Hamiltonian Neutron

$$H_n = (\text{Kinetic energy})_n + (\text{attraction})_{n-e} + (\text{repulsion})_{n-n}$$

$$\hat{H} = \hat{T}_n + \hat{V}_{n-n} + \hat{H}_e (+\hat{V}_{n\text{-field}})$$

Hamiltonian electron

$$H_e = (\text{Kinetic energy})_e + (\text{attraction})_{n-e} + (\text{repulsion})_{e-e}$$

$$\hat{H}_e = \hat{T}_e + \hat{V}_{n-e} + \hat{V}_{e-e} (+\hat{V}_{e\text{-field}})$$

$$H\Psi = E\Psi = \sum_{i=1}^N \left(\frac{-\hbar^2}{2m} \nabla_i^2 \Psi - Z e^2 \sum_{\mathbf{R}} \frac{1}{|\mathbf{r}_i - \mathbf{R}|} \Psi \right) + \frac{1}{2} \sum_{i \neq j} \frac{e^2}{|\mathbf{r}_i - \mathbf{r}_j|} \Psi$$

Time dependence of Hamiltonian

Treating the motion of the nuclei in classical frame, introduces time dependence into electronic H. In a single atom not exposed to electrical/magnetic field, the system is transformed into the center of mass frame. Now H separates into two components

$$H = H_{\text{translational motion of the atom}} + H_{\text{motion of electron relative to center of mass}}$$

The origin of center of mass frame is identified with the position of nucleus. So, the nucleus is considered as a static external source. However, for multi-atomic molecules, the degrees of freedom cannot be factorized for nucleus and electrons. Thus, for coupled dynamics of electrons and nuclei SWE is in Eqn. A1-3c.

Eqn. A1-3c: SWE with coupled dynamics

$$\hat{H}\Psi_a(\mathbf{R}_1, \dots, \mathbf{R}_K; r_1\sigma_1, \dots, r_N\sigma_N)$$

$$= E_a \Psi_a(\mathbf{R}_1, \dots, \mathbf{R}_K; r_1\sigma_1, \dots, r_N\sigma_N)$$

σ_i : spin-orientation of electron i with respect to some chosen axis

N =

Kinetic energy of electrons	+
Kinetic energy of nuclei	+
Coulombic attraction between electrons	+
Coulombic attraction between nuclei	+
Repulsion terms between electrons	+
Repulsion terms between nuclei	

- The order of equation is very high.
- Solution of this PDE is an exceedingly complicated issue
- Remedy:** Partial decoupling of electrons from nucleus (Born-Oppenheimer approximation)

Born-Oppenheimer approximation

The mass of an electron is three orders smaller than that a proton. During a very small interval of time, the movement of nucleus of a multi-electron moiety is negligible. Electrons move very fast resulting in smooth distribution. Thus, kinetic energy (KE) of nucleus is negligible. Further, in the case of molecules with higher nuclear masses of nuclei, the relative motion is negligible compared to that of electrons whereby a KE_{nucleus} becomes zero. For a molecule of fixed orientation of atoms, (conformer) nuclear-nuclear repulsion is constant. It tantamounts to apparently stationary nuclei move on a potential energy surface (PES) with instantaneous adjustments of electrons to changes in nuclear positions. In other words, motion of electron is in a static field of nucleus. The result of different time scales of the motion of electrons and nucleus implies decoupling of electronic and nuclear components is a valid proposition.

The nuclei are at rest in a common Lorentz frame and it is applicable for ground state properties. ψ^{electron} depends parametrically on the position of nuclei. Thus, SWE for electronic component is given Eqn. A1-3d. It is a stationary eigen value task for a given set of R_k . The Eigen values acts as potentials in which nuclei are moving. The solution of this Eigen equation is a formidable task.

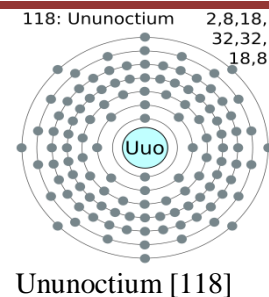
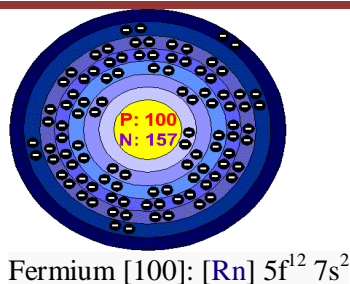
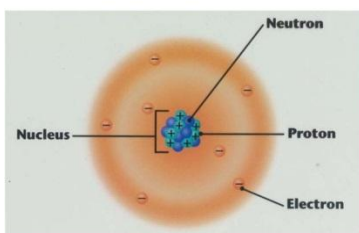
Hamiltonian

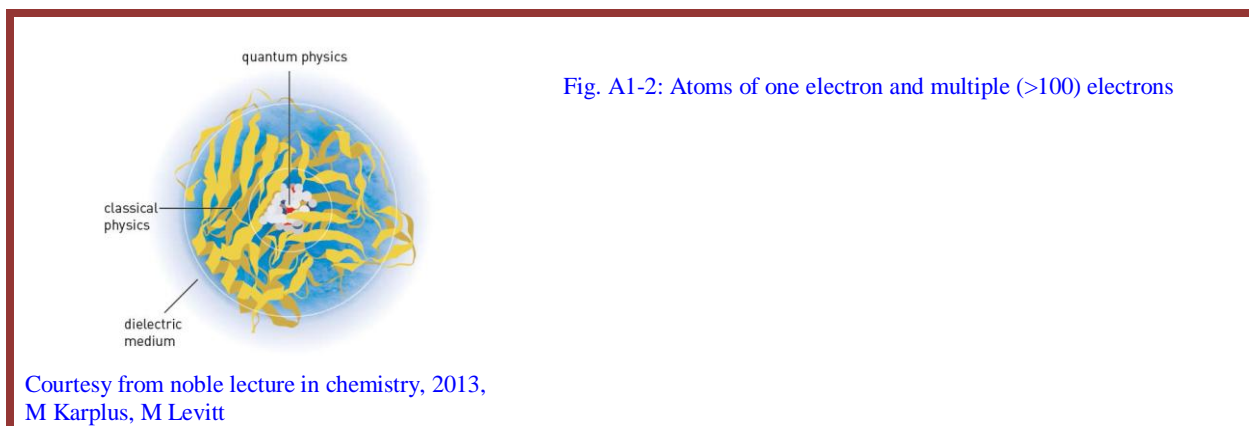
The electronic Hamiltonian includes kinetic energy, nuclear attraction, even for one electron moieties viz. Hydrogen atom, H^{2+} , He^+ (Fig. A1-2). In the case of multi electron systems (H_2 , He , Li , Na etc), one more term corresponding to electron-electron repulsion is also present. The e-e repulsion term renders it to be a hard problem, which is not solvable even for classical tasks. A pragmatic way is to ignore correlated motion of electrons. In other words, each electron is independent of others. But, it is untrue. However, HF approach achieves it through Slater determinant, which is anti-symmetric product of one electron MOs and molecular orbital-based methods offer approximate solutions of SWE.

Eqn. A1-3d: Wave function components

$$H_{el} \quad \psi_{total} = \psi_{ik}^{nuclear} + \psi_k^{electron}$$

- The complexity increases with number of nuclei, quantum nature of electrons, complexity of geometry, meta-stable arrangements etc.
- ▶ **Remedy** : HF approximation



**Chart A1-2: Difficulties in relativistic theory**

- Relativistic corrections for KE of electrons (spin-orbit interactions) for heavy atom are very high. It modifies the structure of electronic Hamiltonian to a noticeable extent reflected in bonds.
- The interaction between charged particles in Hamiltonian ignores transverse nature of light (photons and its finite speed). The manifestation is in-built interaction. Instantaneous and spin independent coulomb interaction is considered
- Spin-orbit interaction is more critical compared to Breit phenomenon

Chart A1-3: Positive features of CQC

- + CQC does not require information about the location or geometry of bonding of the molecule
- + Calculate coefficients for BSs are from experimental data.

Non-relativistic treatment: The potential energy at a point on the surface is calculated as $V_{\text{PES}} = E_{\text{el}} + (\text{repulsion})_{\text{n-n}}$. The motion of electrons and the nuclei are treated non-relativistically in equations of KE and PF. Further, it implied that nuclei are point particles. But, they have mass, charge and dipole moment sounding that relativistic treatment is appropriate (chart A1-2). The non-relativistic treatment is acceptable for calculation at first level only.

Self-consistent field (SCF)

It gives a configuration describing the occupancy of MOs with electrons. In HyperChem the iterations are stopped when coefficients of occupied orbitals or computed energy does not change.

Solution of Schrodinger equation multi-electron system

The concept of an exact solution is the focus of mathematical science. It was realized that it is not possible to solve SWE exactly for a multi-electron system. Therefore, a fully interacting many body problem is to be mapped onto an effective single particle problem in a more complete fashion. The two popular approaches are ab initio and DFT methods.

The solution of Schrodinger equation was not possible even for methane. The only choice was resorting to approximate methods. Pople enunciated in 1960s the revolutionary concept of CNDO in ab initio computations, a Nobel Prize winning contribution. Ab initio methods viz. HF and post-HF are computationally intensive and the computer power in 1970s was low. This paved way Dewar and his group to resort to a battery of SEMO calculations making use of accurate and reliable experimental data of organic compounds. Pople's ab initio and Kohn's DFT approaches widened the scope of the application of Schrodinger wave equation that was initially applied to hydrogen and hydrogen like species. During the last three decades, molecules with a single digit to hundreds of atoms are comfortably studied with QC methods in gas phase. The effect of solvent requires additional inclusion of the solvent models.

Computational quantum chemistry

Computational quantum chemistry is all-pervading in diverse disciplines of scientific research and received acceptance as a super instrument outputting physicochemical data. Computational quantum chemists are

now no different from experimentalists both in practice and in generating information. The three facets are to validate a QC procedure by comparing with other experimental techniques, predicting physico-chemical data before synthesis of a compound (comprising of many virtual laboratory instruments) and to investigate in provocative areas leading to opening new vistas/concepts. With CQC, electronic structure and properties of an optimized geometry of a molecule in ground/excited states in gas/solution phase is a major area of interest. The conformers of different energies, intermediates and transition states are detected with frequency analysis. The mechanism of transformation of (as simple as) an isomer into another, or complex multipath/multi step reactions is analyzable through intermediate reaction coordinate (IRC). With any of good software packages, CQC for many of the elements in the periodic table even in molecules containing 2 to 200 atoms is feasible. It is now the heart of multi-disciplinary paradigm viz., chemistry, theoretical biology, drug discovery and development (D³).

The purview of modern CQC ranges from large proteins down to hydrogen atom. The state of art of QM encompasses relativistic Schrodinger wave equation (SWE), sub-particle (boson, positron, Freon etc.) interactions to account for subtle energies and low energy emissions/absorptions in condensed matter.

CQC not only adequately explains, but quantitatively outputs numerical data for many chemical reactions (chart A1-3). It also generated huge amount of physico-chemical data and paves way to compute derived QC descriptors, broadening the scope of interpretation. The activity of computational quantum chemists is multifold. Newer procedures are developed to combat with the increasing the accuracy of experimental data and harness in software with hardware demands. Yet, CQC is not a panacea. Both experimental and computational science complements each other with continuous uplift and integration of knowledge to achieve the changing real life tasks. The object oriented perspective of CQC models are briefed in chart A1-4.

Chart A1-4a. Object oriented view (OOV) of CQC_models

Mechanics	: [Newtonian_Mechanics, Molecular_mechanics, Quantum_mechanics, Wave_mechanics,]
CQC_Models	: [Single_paradigm, multiple_paradigm]
CQC_Models_Single_paradigm	: [SEMO, ab_initio, DFT]
SEMO	: [CNDO, [NDO[MNDO[MNDO/3], INDO]], [AM1], [PM3, PM6],]
ab_initio	: [HF, post_HF]
post_HF	: [CC, CI, MPn]
DFT	: [[DFT, TD_DFT,], Conceptual_DFT]
TD_DFT	: [TDHF, TDDFT]
[MM]	: [MM3, AMBER]



Chart A1-4b: OOV of MM



[MM]	: [MM3, AMBER, MM2, MM3 (Allinger), MMX (Gilbert, in PCModel), MMFF (Merck Pharm.), Amber (Kollman), OPLS (Jorgensen), BIO+ (Karplus, part of CHARMM)]
------	--























Chart A1-4c: OOV of Hybrid Paradigms

Hybrid	: [SEMO+MM, SEMO+ab_initio, DFT+ab_initio, DFT+Dispersion]
[SEMO+MM]	: [PM3MM]
	Ex: [PM3MM]: [PM3+MM]
[SEMO+ab_initio]	: [SAM1]
	Ex: [SAM1]: [PM3+ab_initio]
[DFT+ab_initio,]	: [Gn]
[DFT+Dispersion]	: [Empirical]

Chart A1-4d: Typical research journals for CQC_models

Quantum chemistry journals	
	Advances in Molecular Modeling
	Advances in Quantum Chemistry

Computational Chemistry	
	Reviews in Computational Chemistry
	Structural Chemistry

<ul style="list-style-type: none">  Computational and Theoretical Polymer Science  International Journal of Quantum Chemistry  J. Computational Chemistry  J. Computer-Aided Materials Design  J. Computer-Aided Molecular Design  J. Molecular Graphics and Modelling  J. Molecular Modeling  J. Molecular Structure  J. Molecular Structure: THEOCHEM  J. Physical organic chemistry  Journal of Biomolecular Structure and Dynamics  Macromolecular Theory and Simulations  Molecular Simulation 	<ul style="list-style-type: none">  Theoretical Chemistry Accounts: Theory, Computation, and Modeling (formerly Theoretica Chimica Acta)  QSAR Quantitative Structure-Activity Relationships SAR and QSAR in Environmental Research  Chemometrics Computers and Chemistry  J. Mathematical Chemistry  J. Chemical Information and Computer Science  J. Chemometrics  Chemical Informatics Letters  Chemical Modelling: Applications and Theory  Chemometrics and Intelligent Laboratory systems
---	---

Appendix-02: SEMO-methods

Ab initio approach

It employs fundamental constants (velocity of light, Plank constant). The input characteristics of a compound are atomic number of each element, connectivity of other atoms, charge and multiplicity. The addition of determinants improves the quality of HF model. Nevertheless, it scales up to 4th power of BS due to the number of two electron integrals necessary to construct Fock matrix. It finally leads towards the exact solution. Thus, Hartree-Fock (HF) model of Schrodinger equation is the branching point for the surge of different approaches and approximations.

Valence shell approximation: In this approximation approach, electrons in the valence shell play a dominant role in chemical bonding and other chemical phenomenon. Thus, the nuclear core subsumes the core electrons and only valence electrons are considered in the model.

SEMO: SemiEmpiricalMolecularOrbital methods result from additional approximations. The conspectus of this approach is in [chart A2-1](#).












-  Consider only valence electrons with independent practical approximation
-  Employ experimental parameters to simplify the solution of Schrodinger wave equation.
-  CPU (central processing unit) intensive explicit evaluation of one-center repulsion and resonance integrals are replaced by a curve fitting procedure employing experimental values of heat of formation (HoF), dipole moment, ionization potential, bond length and bond angle for typical sets of compound.
-  Diminish two electron integrals by neglecting some or all of them. It is equivalent to Valence shell approximation.
-  Basis set comprising of Slater type s, p orbitals (STOs) and some times d-orbitals are used in SEMO. The orthogonality of these STOs results in further simplification made (applicable) to Roothan-Hall equations.

Chart A2-1: Evolution of SEMO calculations

<table border="1"> <thead> <tr> <th>Abbreviation</th> <th>Acronym</th> </tr> </thead> <tbody> <tr> <td>DO</td> <td>Differential overlap</td> </tr> <tr> <td>ZDO</td> <td>Zero DO</td> </tr> <tr> <td>NDO</td> <td>Neglect of</td> </tr> </tbody> </table>	Abbreviation	Acronym	DO	Differential overlap	ZDO	Zero DO	NDO	Neglect of	<table border="1"> <thead> <tr> <th colspan="2">Parametric models</th> </tr> </thead> <tbody> <tr> <td> AM1</td> <td>Austin model1</td> </tr> <tr> <td> PM3</td> <td>Parametric</td> </tr> </tbody> </table>	Parametric models		 AM1	Austin model1	 PM3	Parametric	<table border="1"> <thead> <tr> <th rowspan="2">Year</th> <th rowspan="2">Method</th> <th colspan="2"># compounds used for parameterization</th> </tr> <tr> <th>experimental</th> <th>ab initio</th> </tr> </thead> <tbody> <tr> <td>1977</td> <td>MNDO</td> <td>39</td> <td>----</td> </tr> </tbody> </table>	Year	Method	# compounds used for parameterization		experimental	ab initio	1977	MNDO	39	----
Abbreviation	Acronym																									
DO	Differential overlap																									
ZDO	Zero DO																									
NDO	Neglect of																									
Parametric models																										
 AM1	Austin model1																									
 PM3	Parametric																									
Year	Method	# compounds used for parameterization																								
		experimental	ab initio																							
1977	MNDO	39	----																							

CNDO Complete NDO INDO Intermediate NDO MINDO Modified INDO	DO	model # PM6 PM7	1985 AM1 ~200 ---- 1989 PM3 ~500 ---- 2007 PM6 > 9,000 yes 2012 PM7 > 9,000 Yes
RM1 (Recife Model 1) SAM1 SCC-DFTB		Hybrid models PDDG/PM3 PM3MM	

Chart A2-1b: SEMO

Level	Semi empirical methods
Axiom	<ul style="list-style-type: none"> ❖ All valence electrons considered ❖ Independent particle approximation
Basis	<p>Introduction of empirical parameters instead of explicit evaluation of integrals</p> <ul style="list-style-type: none"> 🔔 One center repulsion integrals 🔔 Resonance integrals substituted by parameters
Method	Parameters fitted as close as possible to experimental data
Speed	N^3 where N: Number of basis functions
Predictions	<ul style="list-style-type: none"> ▶ Relative stabilities of electrons in atomic energy level ▶ Special character of all bonding orbitals ▶ Electrostatic repulsion between electrons
Advantage	Parameters against experimental results, which include effects of electron correlation. Thus some allowance for the effect is implicit
Limitation	<ul style="list-style-type: none"> - Ignored <ul style="list-style-type: none"> - Core electrons - Di atomic differential overlap (NDDO) - Instantaneous correlation of motion of electrons neglected
Remedy	Ab initio or DFT

Applicability -- CNDO

- 🔔 Closed shell (fully paired electrons in [molecular orbitals](#)) and open shell (radicals with unpaired electrons) molecules
- 🔔 solid state and nanostructures calculations

Chart A2-1c: CNDO

Level of theory	SEMO
Hamiltonian	CNDO
Basis	☐ ZDO
Speed	+Faster than MNDO/3, MNDO, AM1, PM3
Memory	+Requires less memory
Empirical parameters	+Employs fewer number
Advantage	+Easier interpretability to understand the results
Applicability	Even for molecules that are too large for MNDO/3, MNDO, AM1, PM3
Not applicable	For molecules where electron spin is critically important
Remedy	INDO

🔔 CNDO does not require knowledge about [chemical bonds](#)

🔔 Uses quantum [wavefunctions](#) information

If closed shell

Output	Then HOMO,LUMO reported
+ Good results for partial atomic charges and molecular dipole moment .	
+ Total energy and binding energy	

Zero differential overlap (ZDO): It means two electron repulsions are neglected (ignored or made equal to zero). Obviously three/ four center integrals become zero. The overlap integrals (corresponding) $S_{\mu\nu}$ are neglected. The chemical consequences are

- 🔔 Bonds on adjacent atoms are allowed
- 🔔 Complete Neglect of Differential Overlap (CNDO)

Complete Neglect of differential overlap (CNDO/1, CNDO/2): The basis of CNDO approximation of solution of Schrodinger wave equation for multi-electron systems ($n > 2$) is ZDO. Here, all two-electron repulsions are set equal to zero i.e. neglected. The consequence is coulomb type of integrals reduce to a single value $\gamma_{AB} = f$ (Nature of atoms A & B with which ϕ & ϕ are associated – not actual type of orbitals that overlap)

Neglect of diatomic differential overlap (NDDO): Pople was the initiator of NDDO and based on this foundation, not only successful but also competing CQC procedures are developed for large molecules and of course at the cost of accuracy. NDDO retains all one-center differential overlap terms when Coulomb and exchange integrals are computed. Products of orbitals and differential overlap products of orbitals on different atoms neglected in electron repulsion integrals. All two-electron integrals are neglected. These depend on overlapping of charge densities of basis orbitals. NDO methods (like CNDO, MNDO_x, INDO) include electron repulsion and consider terms for pairs of electrons. Another feature is inclusion of nuclear repulsion. However, it is at the cost of reducing the charge on each of the nucleus by the number of core electrons shielding it.

Intermediate NDO (INDO). Modified INDO (MINDO) considers core-core repulsion as a function of electron-electron (e-e) repulsion and has seven parameters ([chart A2-2](#)).

Chart A2-2a: INDO		Chart A2-2b: MINDO	
Theory level	Semi-empirical	Theory level	Semi-empirical
Hamiltonian	INDO	Hamiltonian	MINDO
Basis	CNDO	Axiom	▶ Exponents of Atoms determining BSs are allowed to vary
Method	▶ Two electron integrals centered on the same atom are calculated explicitly ▶ Adds spin effects not accounted by CNDO		▶ Core integrals β_{AB}^0 are not taken as average of limited no of atom specific parameter
Features	+ Faster than MNDO/3, MNDO, AM1 and PM3 + More accurate than CNDO	Basis	Energy expression as adjustable parameter
Applicability	+ Improves molecular geometry	Parameters	🔔 Number of parameters: 7 🔔 Orbital exponents 🔔 Resonance integral 🔔 Core integral 🔔 Core-core repulsion is treated as function of electron-electron repulsion
Limitation	= Interpretability is lost	Parameters available	Li,F,S,Zn,I
	If UHF and open shell molecules Then INDO is a method of choice	Features	+ Improvement over MINDO/3
		Applicability	+ qualitative agreement with

	<p>Limitation</p> <ul style="list-style-type: none"> - experimental measurement - H-bonding pattern not reproduced - Over estimation of interactive repulsion when atoms are separated by distances greater than those of chemical bonds <p>Remedy AM1, PM3</p>
<p>Chart A2-2c: MNDO</p> <p>Theory level Semi-empirical</p> <p>Hamiltonian MNDO</p> <p>Axiom</p> <ul style="list-style-type: none"> ❖ NDO approximation <ul style="list-style-type: none"> ◆ [Electron-electron repulsion is negligible] <p>Features To overcome problems of MNDO/3</p> <p>Applicability Properties</p> <ul style="list-style-type: none"> 🔔 HOF, Geometry, Dip Mom., IE, Ea <p>Limitation Compounds</p> <ul style="list-style-type: none"> <input type="checkbox"/> Unstable compounds <input type="checkbox"/> Hypervalent <input type="checkbox"/> Sterically crowded <input type="checkbox"/> 4-membered ring <input type="checkbox"/> Non-existent <input type="checkbox"/> H-bond <p>Failure</p> <ul style="list-style-type: none"> - Overestimates repulsions between atoms separated by distances approximately equal to the sum of their van der waals radii <p>Remedy AM1 Hamiltonian</p> <p>Contradiction MNDO gives better results than AM1</p>	<p>Chart A2-2d: MNDO/3</p> <p>Theory level Semi empirical</p> <p>Hamiltonian MNDO/3</p> <p>Objective Remedial measures to circumvent limitations of INDO</p> <p>Features</p> <ul style="list-style-type: none"> + More accurate geometries & HOF compared to CNDO or INDO + Better than MNDO and AM1 + Compounds good for carbo cations, polynitro organic compounds <p>Limitation</p> <ul style="list-style-type: none"> - Accuracy decreases for molecules with hetero atoms <div style="border: 1px solid blue; padding: 5px; margin-top: 10px;"> <p>If NDO approximation is false [Electron-electron repulsion is negligible]</p> <p>Then MNDO fails</p> </div>

MNDO: [29-34] with seven parameters is an improvement over MNDO/3. The QC parameters are in qualitative agreement with experimental values. It overestimates the interactive repulsion. Further, results of H-bonded systems are in error.

Parametric SEMO methods

Austin method 1 (AM1) and PM_x (x: 3, 6, 7) algorithms are widely employed low cost (CPU time) semi quantum chemical computational methods and still in vogue for large (atoms >50) molecules, or for set of large (>50) number of even small moieties (size<20) or in presence of a solvent.

AM1: In 1985, Dewar proposed Austin method (AM1), a second parametrization of MNDO with 13 to 16 empirical parameters derived from experimental data. It modifies core-core repulsion using spherical Gaussian functions and is applicable for atoms C, H, N, O, F, P, and I. It takes into consideration core-core repulsion using Gaussian function. It is a method of choice for organic molecules and reductions in errors in this procedure are to an extent of 40% compared to MNDO. This is really a great achievement over CNDO. However, results of AM1 are in error for molecules containing peroxide and P-O bonds.

PM3: Stewart in 1989 put forward third parametrization of MNDO and continued saga for two decades in raising the status of SEMOs. The result is innovative PM6 and PM7 incorporated in MOPAC2012. PM4 and PM5 were internal versions without release to users. MNDO adopted automatic procedure in reparametrization of AM1. Here, larger numbers of compounds are used. AM1, PM3 are available in Gaussian 03, but the output gives the energy difference between the final and pre-final iterations. Thus, one should be cautious to draw quantitative conclusions.

PM6

SEMO, the contributions of Dewar and Stewart in the initial phase, was like a poor man's apple in quantum chemistry and wide spread use was mainly due to low computational time on desktops. Stewart continued his march with vigor holding the torch. The outcome is PM6 in 2008 and later PM7 is a landmark in SEMO_CQC. It generates quantum chemical data of accuracy comparable with more expensive techniques viz. DFT.

MOPAC2012: The package, free for academic researchers, is a trustworthy tool to get hands on experience with SEMO calculations of simple molecules to large macro-structures. Dewar and Thiel's NDDO approximations are at the core. The open source code is another boon to inculcate scientific software development, maintenance for a variety of hardware platforms and to enter the new era of adaptive, intelligent problem solving approach.

SAM1: It belongs to a new paradigm of quantum chemical computations involving hybridization of semi-empirical and ab initio philosophies. It uses STO-3G basis set unlike SEMO methods. The number of parameters is less compared to PM3 and considers electron repulsion integrals. The general expectation is that reliability of model chemistries should increase from MNDO to SAM1 through AM1 and PM3. However, a perusal of literature indicates diverse conclusions regarding the quality, of course based on specific objective (protonation, property etc.) of a small set of compounds, substituents, moieties etc. Specific reports indicate the inadequacy of the very semi-empirical methods for specific sets of compounds. However, SEMO algorithms are in use as a preamble to investigate with higher levels of theory viz. ab initio and DFT.

Chart A2-3a: AM1		Chart A2-3b: PM3	
Theory level	Semi-empirical	Theory level	Semi-empirical
Hamiltonian	AM1 (Austin Method) Second parameterization of MNDO	Hamiltonian	PM3 Third parameterization of MNDO
Proposed by	Dewar 1985		
Parameters	13 to 16		
Available for	C, H, N, O, F, I, P		
Basis	<ul style="list-style-type: none"> Assumptions of MNDO Chemical knowledge intuition 	Basis	AM1 Many molecular properties depend upon valence electrons of corresponding atoms
Method	<ul style="list-style-type: none"> Modified MNDO <ul style="list-style-type: none"> Additional terms for core-core repulsion containing more adjustable parameters Spherical Gaussian functions— a, b & c are adjustable parameters Modifies core-core repulsion using Gaussian form 	Method	<ul style="list-style-type: none"> Reparameterization of AM1 Parameters (from larger number of compounds) obtained by automatic procedure
Features	<ul style="list-style-type: none"> Non bonded interactions are more repulsive than PM3 Offers significant enhancement over 	Features	Non bonded interactions are less repulsive in PM3 than AM1
		Applicability	<ul style="list-style-type: none"> Compounds <ul style="list-style-type: none"> Organic molecules Main group elements

earlier SEMO like CNDO/2
 ► Surmounts problems of MNDO

Applicability Improvement capability in

Compounds

- H-bonds
- Activation barrier of reaction
- HOF

🔔 Error is 40% smaller than MNDO

- Correct excessive interatomic repulsion

Parameters available H B C N O F Al Si P S Cl Zn, Ge Br Sn

Original AM1
 Both attractive & repulsive Gaussians

4 C
 3 H
 3 N
 2 O

Limitations of AM1

Parameter	Compound	Comment
Bond	Peroxide	Too short
Bond	P-O	Inaccurate
Energy	Nitro-compound	Too positive

Chart A2-3c: ZINDO/1

Theory level	Semi-empirical
Hamiltonian	ZINDO/1
Applicability	<ul style="list-style-type: none"> ► Compounds <ul style="list-style-type: none"> ☐ First & second row transition metals ► Energy ► Geometry
Improvement in capability	Success for metals; MolcularMechanics fails
Limitation	<ul style="list-style-type: none"> – Less reliable results compared to those for organic compounds – Reasons Valencies, Oxidation states, spin multiplicities, unusual bonding (dpi-p_pi back bonding) – Non directional metallic bonding – Less amenable for ball and spring interpretation

Chart A2-3g: PM7, MOPAC2012

Method	Based on				
MOPAC2012	MOPAC-9	+	PM7	+	PM7_TS
PM7	PM6	+	Errors in PM6 removed		
<ul style="list-style-type: none"> + Intel Math Kernel Library and paralleelizaion of codes + CPU time reduction ; in some cases by 99% 					

Chart A2-3d: ZINDO/s

Theory level	Semi-empirical
Hamiltonian	ZINDO/s
Applicability	<ul style="list-style-type: none"> ► Parameterized for spectroscopic properties ► Single point energy for Geometric from model building
Limitation	Not applicable for geometry optimization
If	Uv-Vis spectra
Then	Perform CI single calculations

Chart A2-3e: SAMI

Theory level	Hybrid of Semi-empirical and ab-initio
Hamiltonian	SAMI
Basis set	STO-3G
Basis	Electron repulsion integrals
Number of parameters	NparSAM1 ≅ NoParAM1 < NoParAM1

Chart A2-3f: PM6

- + Reduction of average errors of organic compounds by 10%
- + Significant lowering of errors for large organics and solids
- A few errors affecting NDDO theory for large systems
- Diatomic parameters reoptimized

Chart A2-3h: PM7, MOPAC2012

Hamilton	BS	Error#
PM7		4.01
PM6		4.42
B3LYP	6-31G(d)	5.14
HF	6-31G(d)	7.34
PM3		6.23
AM1		10.0
# : Average unsigned error (kcal/mol) 1,366 compounds --heats of formation		

H	#	Element
PM7	83	H, He, Li, Be, B, C, N, O, F, Ne, Na, Mg, Al, Si, P, S, Cl, Ar, K, Ca, Sc, Ti, V, Cr, Mn, Fe, Co, Ni, Cu, Zn, Ga, Ge, As, Se, Br, Kr, Rb, Sr, Y, Zr, Nb, Mo, Tc, Ru, Rh, Pd, Ag, Cd, In, Sn, Sb, Te, I, Xe, Cs, Ba, La, Lu, Hf, Ta, W, Rh, Os, Ir, Pt, Au, Hg, Tl, Pb, Bi +15 lanthanide sparkles4 uses PM6 sparkles
PM6	83	H, He, Li, Be, B, C, N, O, F, Ne, Na, Mg, Al, Si, P, S, Cl, Ar, K, Ca, Sc, Ti, V, Cr, Mn, Fe, Co, Ni, Cu, Zn, Ga, Ge, As, Se, Br, Kr, Rb, Sr, Y, Zr, Nb, Mo, Tc, Ru, Rh, Pd, Ag, Cd, In, Sn, Sb, Te, I, Xe, Cs, Ba, La, Lu, Hf, Ta, W, Rh, Os, Ir, Pt, Au, Hg, Tl, Pb, Bi +15 lanthanide sparkles4
PM3	57	H, He, Li, Be, B, C, N, O, F, Ne, Na, Mg, Al, Si, P, S, Cl, Ar, K, Ca, Zn, Ga, Ge, As, Se, Br, Kr, Rb, Sr, Cd, In, Sn, Sb, Te, I, Xe, Cs, Ba, Hg, Tl, Pb, Bi, + 15 lanthanide sparkles4
AM1	57	H, He, Li, Be, B, C, N, O, F, Ne, Na, Mg, Al, Si, P, S, Cl, Ar, K, Ca, Zn, Ga, Ge, As, Se, Br, Kr, Rb, Sr, Mo, In, Sn, Sb, Te, I, Xe, Cs, Ba, Hg, Tl, Pb, Bi, + 15 lanthanide sparkles4
MNDO	17	H, B, C, N, O, F, Na, Al, Si, P, S, Cl, Zn, Br, Cd, I, Hg
RM15	10	H, C, N, O, P, S, F, Cl, Br, I

#Compounds	Property	Units	Error					Ref
			MNDO/3	MNDO	AM1	PM3	SAM1	
138	HOF		11.0	63				Dewar 1972
228	BL	A ⁰	0.022	0.04				
91	BA		5.6	2.80				
57	Dip Mom	D	0.49	0.78				
----		----		----		----		
58	HOF	Kcal/mol	9.7	5.87	5.07			1985
80	HOF	N and O donors	11.69	6.64	5.84			
46	Dip Mom	D	0.54	0.32	0.26			
29	IE	Ev	0.31	0.39	0.29			
----		----		----		----		
406	HOF				8.82	7.12	5.21	Dewar 1993
196	Dip Mom				0.35	0.40	0.32	

MNDO/3	MINDO	AM1
3.5	34.5	13.7

<ul style="list-style-type: none"> Stewart, J. J. P. (1989). J. Comp. Chem. 10(2): 209-220; 221-264. Stewart, J. J. P. (2004). J. Mol. Modelling 10: 6-12. Stewart, J. J. P. (2004). J. Phys. Chem. Ref. Data 33(3): 713-724. Rocha, G. B. et al (2006). J. Comp. Chem. 27(10): 1101-1111

Appendix-03: Post-HF methods

Raleigh-Schrodinger perturbation theory: It maps an inexact operator with known eigen functions to an exact operator with increasing orders of accuracy. Fock operator is a sum of one-electron mean field operators. The lacuna is that it counts the sum of HF occupied Eigen values two times.

Møller-Plesset (MP) perturbation theory

Rayleigh–Schrödinger perturbation theory (RSPT) is the basis of MP perturbation method (Eqn. A3-1) and accounts for the correlation energy not accounted by HF method.

Eqn. A3-1: Second-order MP-type expression for exchange correlation energy

$$E_{xc} = (1 - a_x) E_x^{GGA} + a_x * E_x^{HF} + b * E_c^{GGA} + c * E_c^{PTq}$$

$$E_c^{PT2} = \frac{1}{4} \sum_{ia} \sum_{jb} \frac{[(ia|jb) - (ib|ja)]^2}{\epsilon_i + \epsilon_j - \epsilon_a - \epsilon_b}$$

spin-orbital form

indices <i>ia, jb</i>	Represent single occupied-virtual replacements
<i>a_x</i>	HF-exchange mixing parameter
<i>c</i>	Scale perturbative correlation contributions
<i>b</i>	Scale GGA_contributions
terms in brackets	Denote regular two-electron integrals over the KS orbitals

It mapped zeroth order Fock operator to the correct Hamiltonian. The zeroth-order Hamiltonian (H₀, for known Eigen function and Eigen values) and perturbation forms the total Hamiltonian MP corrects for the entire electron repulsion energy which is counted second time. The extra computation is only calculation of electron repulsion integrals over MOs with the available λs in HF computation. It includes some electron correlation. In G03, there is an option for MP2, MP3, MP4, MP5, MP6 models. HyperChem software supports both frozen core (inner shell orbitals omitted) approximation and melted core options for MP2.

In Hartree Fock (HF) approximation, Coulomb potential is modeled. As exchange energy (potential) is not considered, the solution for other molecules results in a systematic deviation in frequency and ΔG values. The geometric optimization even fails for metal complexes.

Configuration interaction (CI)

Other configurations can be generated from SCF reference configuration by exciting electrons from the set of occupied MOs to unoccupied MOs. CI matrices consist of a number of blocks corresponding to excited configurations. The size of block is equal to the size of the basis set. In order to capture electron correlation the size of CI matrix should be larger and larger. The implementation is through increasing basis set size (increasing the size of block) or including more excited configurations (increasing the number of blocks). Chart A3-1 incorporates applications and pitfalls of CI. The components viz. exchange, correlations, Coulomb etc. taken care by different levels of theory are given in Chart A3-2.

Chart A3-1: Configuration interaction

If	Closed shell singlet ground state & SEMO/ab initio
Then	CI
If	Half electron (excited singlet shell) & SEMO
Then	CI
If	Half electron/doublet/singlet & open shell ground state and SEMO
Then	CI

- CI is more sensitive to BS incompleteness compared to HF
 - **Remedy:** inclusion of single and double excited states (CISD)
 - + A viable compromise as it is not size extensive

CI_applications

- 👉 UV-Vis spectra
- 👉 Energy of excited states
- 👉 Making/breaking of bonds
- 👉 Change of spin coupling (dissociation of N₂)



Captures effects of London dispersion forces
Accurate description of singlet-triplet spinning

Chart A3-2: Different interactions considered in SEMO, DFT and ab initio procedures

Paradigm	Level	Coul(omb)	eXch(ange)	Corr(elation)	Stack(ing)	Disp(ersion)	Exp(erimental)
SEMO	Classical	y	y	N	N	N	N
	Advanced	Y	Y	N	N	N	N

Paradigm	Level	Coul(omb)	eXch(ange)	Corr(elation)	Stack(ing)	Disp(ersion)	Exp(erimental)
Ab initio	HF	Y	N	N	N	N	N
	Post HF	Y	Y	Y	N	N	N
DFT	original	Y	Y	Y	N	N	N
	Empirical	Y	Y	Y	N	Y	Y
	SIESTA	Y	Y	Y	N	Y	Y

Appendix-04: DFT

First generation density function theory (DFT)

The total energy is expressed as a functional of electron density. The many electron (body) problems are reduced to the variational equation. It requires explicit representation of T_s in terms of density. Only Thomas-Fermi type functionals are available.

Second generation DFT

T_s is implicitly represented by KS orbitals. Here a many electron problem is recasted in the form of KS equations. What is required here is explicit representation of exchange_ correlation_ energy (E_{xc}) in terms of density. Kohn-Sham proposed the equation for electron density in terms of KE, nuclear attraction energy, Coulomb and exchange ($E_{xc} = E_{ex} + E_{corr}$). KS equations are fundamental to modern DFT. The working principle is to find good expressions for E_{xc} .

- Even atomic shell structure was not represented with these functionals
▶ **Remedy** : KS orbitals of second generation DFT

Third generation DFT

A system with many electrons is represented by simultaneous solution of KE equations and integral equations (chart A4-1), which gives V_x .

DFT paradigm looks how E_{el} varies with electron density while HF probes into the change of E_{el} with wave function (ψ). Exchange-correlation functional of electron-density replaces HF potential of ab initio method. Thus, DFT is comparable to HF plus MP2 (post-HF) correlation. The basic assumptions of DFT and its limitations are briefed in Fig. A4-1 and chart A4-2. Each MO has a uniquely defined orbital energy. E_{FMO} allows interpreting molecular geometry (Walsh's rule) and chemical reactivity (Woodward-Hoffman's rule).

- Explicit representation has limitations
▶ **Remedy** : Representation of E_{xc} or E_{ex} in terms of KS orbital

- Computationally expensive
▶ **Remedy** : Generalized KS orbitals

Generalized KS orbitals

HF type orbital equations replace KS equations. They arise from optimization of TE functional with respective orbitals.

Local density approximation (LDA)

If there is an overlap of atomic electronic densities, then E_{corr} includes inter atomic interactions. Binding energy (E_{bind}) results from non-linear density dependence of $E_{\text{corr_LDA}}$. The $E_{\text{corr_density}}$ is obtained from that of homogeneous electron gas evaluated with local density. The region with non-vanishing density contributes to correlation energy. Helium molecule (He_2) is an example of a diatomic molecule with two neutral closed-sub shell atoms. They are far apart and thus the densities do not overlap. For this molecule there is no electrostatic interaction between the two atoms and also bonding orbitals are not formed. The virtual (dipole) excitations lead to be together (binding vs. London dispersion forces). The exchange correlation energies are described in [Eqn. A4-1](#) along with recent M06 functional ([chart A4-3](#))

Relativistic homogeneous electron gas (RHEG) consists of an infinite electron gas with density n_0 plus a neutralizing positive background charge $n_+ = n_0$. The similarities and differences between HF and DFT are incorporated in [Chart A4-4](#).

RHEG

- + It suppresses long-range Coulomb divergence. Now electrons and their interactions are treated on the level of quantum electro dynamics (QED)

Chart A4-1: Flow chart of KS SCF procedure

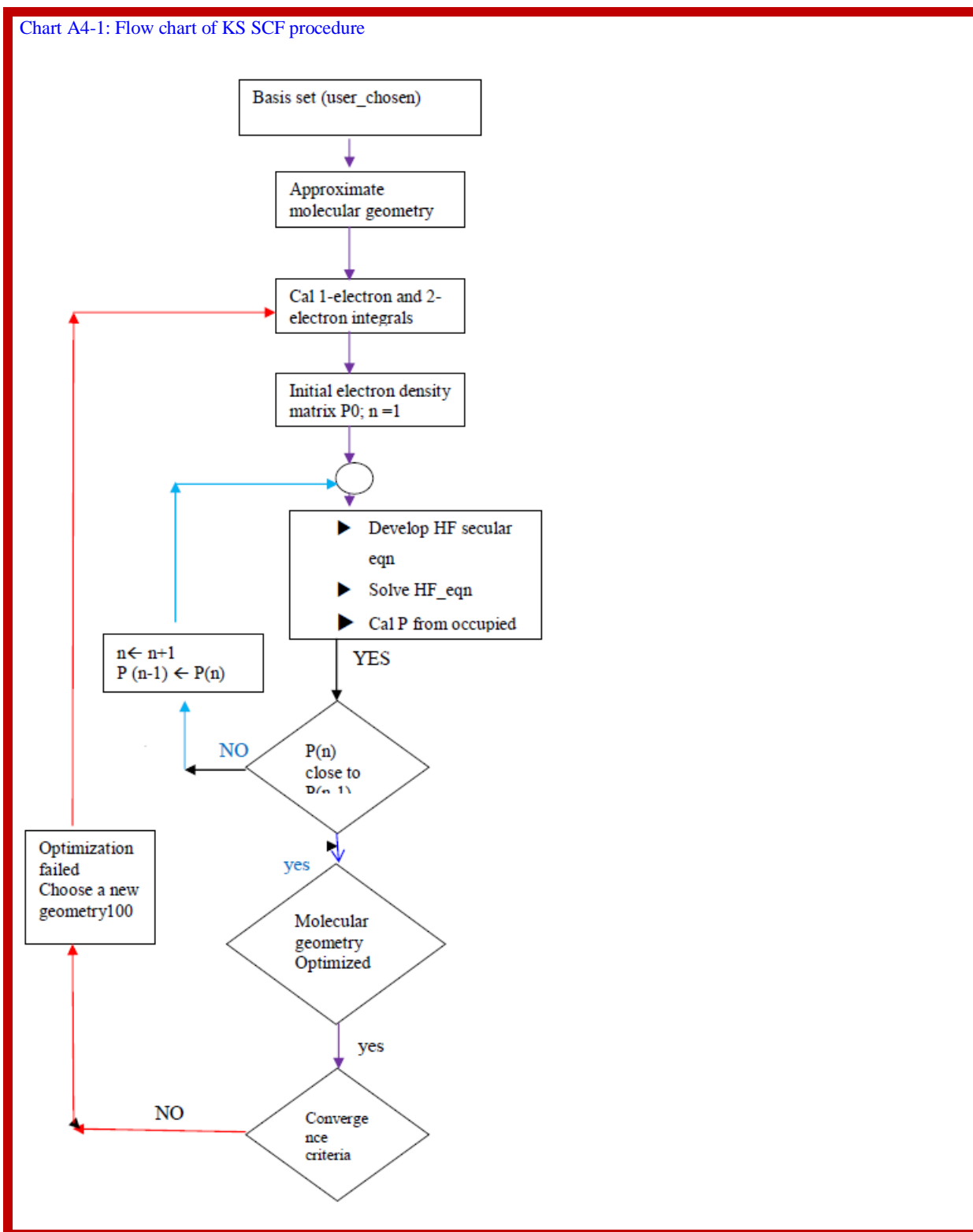




Fig. A4-1: Philosophy of DFT

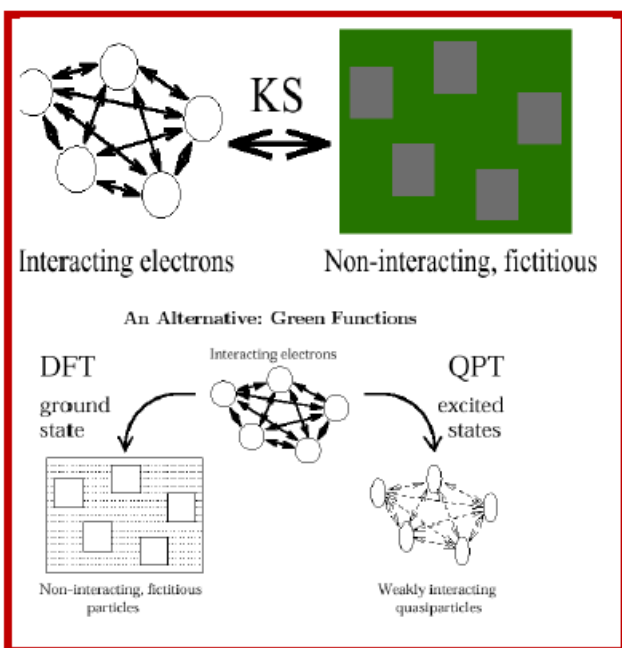


Chart A4-2: Limitations of DFT

DFT	
-	HK theorem breaks for dielectrics (infinite insulating solids) in presence of electric field
-	KS equations are not for very large (100 to 1000 atoms) systems
-	KS orbitals do not satisfy 'Bruener theorem', but HF orbitals do
-	LDA and GGA fail to model London dispersion forces
	Remedy: Empirical DFT
Don'ts	KS orbitals should not be used to perform CI calculations like HF orbitals
DOs	Hyperchem allows the user to use KS orbitals in the same way as HF orbitals.

Eqn. A4-1: Exchange and correlation energies by hybrid components

$$E_x^{\text{hyb}} = a_0 E_x^{\text{exact}} + a_1 E_x^{\text{GGA}} + (1 - a_0 - a_1) E_x^{\text{LDA}}$$

$$E_c^{\text{hyb}} = b_1 E_c^{\text{GGA}} + (1 - b_1) E_c^{\text{LDA}} .$$

Chart A4-3: Recent MO6 functional

M06-2X and w97Bxd

+ Include dispersion implicitly or explicitly

Size based

- 1) RICC2/TZVP//M06-2X/TZVP
- 2) RI-MP2/TZVP// M06-2X/TZVP
- 3) M06-2X/TZVP// M06-2X/TZVP

Chart A4-4a: Key similarities and differences between HF and KS

	HF	KS
Variational principle	<-----	Common ----->
Kinetic energy and nuclear attraction	component matrix_elements_F ≡ matrix_elements_K	

If density in the classical interelectronic repulsion operator is expressed in the same basis functions used for the KS orbitals Then computation of secular matrix elements	Four index electron-repulsion integrals same K & F Density required orbitals obtained from solution of the secular equation are used
Density determination	

Chart A4-4b: Key similarities and differences between HF and DFT

	HF	DFT
Exact/approximate	HF approximate theory	DFT exact theory:
Solution	solve the relevant equations exactly	solve the relevant equations approximately because the form of the operator is unknown.
NC	Knowledge of Exc as a function of density	Functional of ψ must exist No guidance, though, as to what the functional should look like
Difficulty	No true functional known	No set procedure
Remedy (pragmatic)	Several approximate, but useful functional developed	MOs of increasing quality Linear combination

- + Exact DFT is variational.
- If approximations of Exc are introduced, then DFT_variability is no longer true
- Both exact and approximate DFT are size extensive

KB.A4-1: Comparison of function of DFT with HF and post-HF

If DFT exchange-correlation (XC) functionals <~22% Hartree-Fock (**HF**) exchange or >25% or more **HF** exchange.
Then structures predicted are qualitatively different from *ab initio* **HF** and **post-HF** CQC

Advanced applications of DFT

DFT models plasmas [Dharma-Wardana (1982,1995), Perrot (1984,1995)], freezing process [Senatore (1990)] and multi-component systems [Sander(1973), Kalia(1978), Capitani(1982), Gidopoulos(1998), Kreibich(2001,2008)]. By adding a density variable [Oliveira (1988), Capelle(1997)] to DFT, superconductivity is also modelled. It is based on anomalous (off-diagonal) density term, which is added to the conventional DFT. A TD-version is also available in this context. Here, the coupling of electrons to nuclei in the sense of multi-component DFT is included with application [Suvasini (1992,1993), Temmerman (1996), Gyroffy (1998), Marques (2005), Profeta (2006), Sanna (2006,20007), Floris (2007), Cudazzo (2008), Bersier(2009), Sharma(2009)] . The foundations of DFT for nuclei are of recent study [Engel (2007), Barnea (2007), Messud (2009)]. DFT based on 2-particle density pair [Ziesche

(1994,1996), Gonis(1996), Levy (2001) Furche(2004)] and reduced to particle density metric [Mazziotti (2004,2006)]. The foundations of DFT for bosons [Griffin (1995), Nunes(1999)], mixture of fermions and bosons [Albus(2003)] is of interest and TDDFT is used for Bosons [Kim(2003)]. Typical references of DFT for advanced physics are in Chart A5-5.

Chart A4-5: Ref_ Advanced applications of DFT**Output of om_ref_JAVATYP.m**

- Albus A.P., F. Illuminati, M. Wilkens, \$Phys. Rev. A **67**, 063606 (2003)
Barnea N., \$Phys. Rev. C **76**, 067302 (2007)
Bersier C., A. Floris, A. Sanna, G. Profeta, A. Continenza, E.K.U. Gross, S. Massida, \$ Phys.Rev. B **79**, 104503 (2009)
Capelle K., E.K.U. Gross, \$Int. J. Quantum Chem. **61**, 325 (1997)
Capitani J.F., R.F. Nalewajski, R.G. Parr, \$ J. Chem. Phys. **76**, 568 (1982)
Cudazzo P., G. Profeta, A. Sanna, A. Floris, A. Continenza, S. Massida, E.K.U. Gross, Phys.Rev. Lett. **100**, 257001 (2008)

Dharma-Wardana M.W.C., F. Perrot, Phys. Rev. A **26**, 2096 (1982)
Dharma-Wardana M.W.C., in *Density Functional Theory, NATO ASI Series B*, vol. 337, ed. by E.K.U. Gross, R.M. Dreizler (Plenum, New York, NY, 1995), p. 625

Engel J., Phys. Rev. C **75**, 014306 (2007)
Floris A., A. Sanna, S. Massida, E.K.U. Gross, Phys. Rev. B **75**, 054508 (2007)
Furche F., Phys. Rev. A **70**, 022514 (2004)
Gidopoulos N., Phys. Rev. B **57**, 2146 (1998)
Gonis A., T.C. Schulthess, J. van Ek, P.E.A. Turchi, Phys. Rev. Lett. **77**, 2981 (1996)
Griffin A., Can. J. Phys. **73**, 755 (1995)
Gyorffy B.L., Z. Szotek, W.M. Temmerman, O.K. Andersen, O. Jepsen, Phys. Rev. B **58**, 1025 (1998)

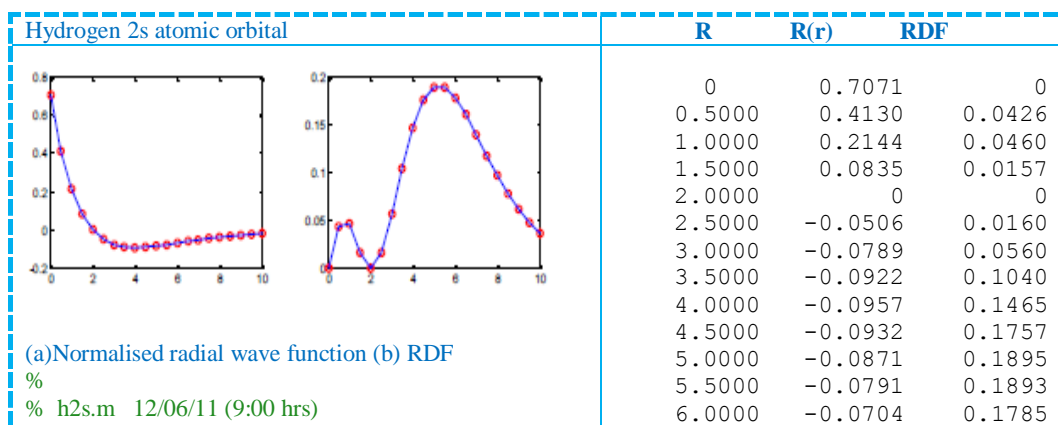
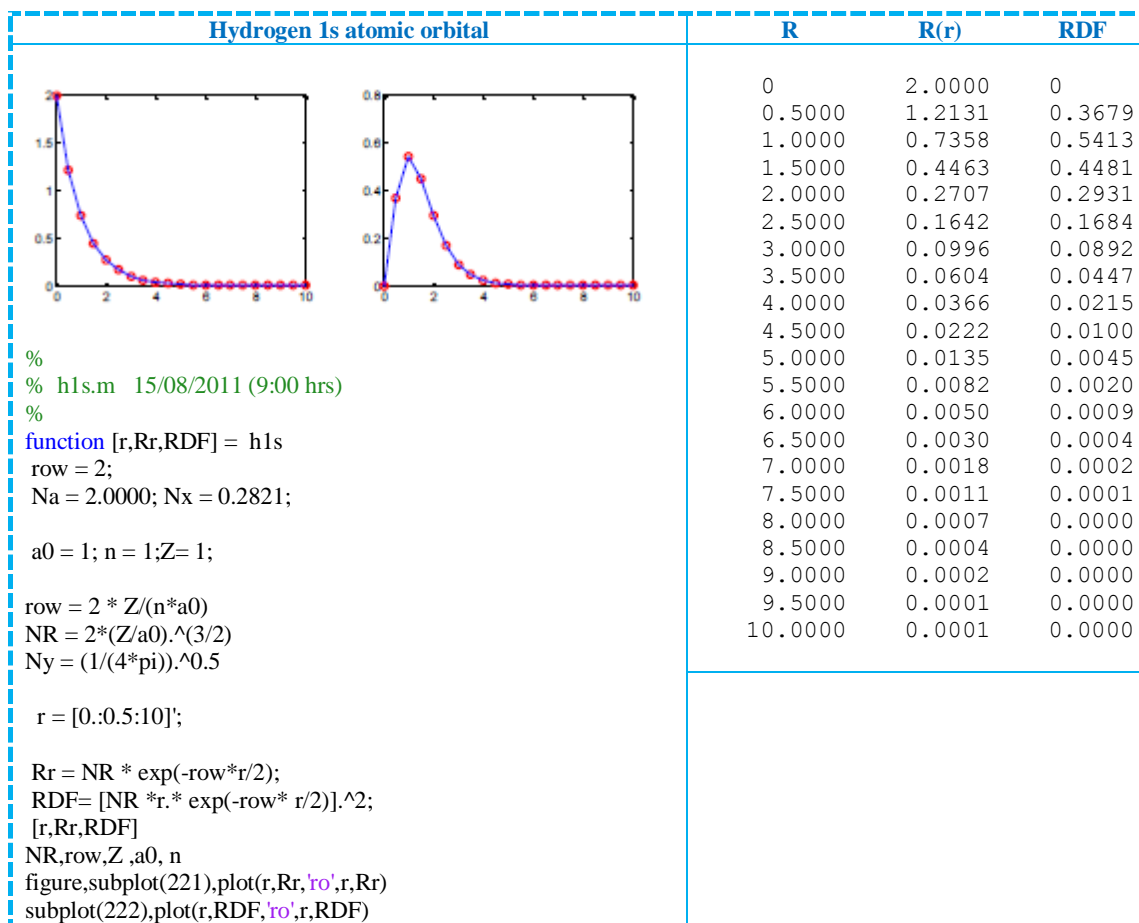
Kalia R.K., P. Vashishta, Phys. Rev. B **17**, 2655 (1978)
Kim Y.E., A.L. Zubarev, Phys. Rev. A **67**, 015602 (2003)
Kreibich T., E. Gross, Phys. Rev. Lett. **86**, 2984 (2001)
Kreibich T., R. van Leeuwen, E.K.U. Gross, Phys. Rev. A **78**, 022501 (2008)
Levy M., P. Ziesche, J. Chem. Phys. **115**, 9110 (2001)
Marques M.A.L., M. L'uders, N.N. Lathiotakis, G. Profeta, A. Floris, L. Fast, A. Continenza, E.K.U. Gross, S. Massida, Phys. Rev. B **72**, 024546 (2005)

Mazziotti D.A., Phys. Rev. Lett. **93**, 213001 (2004)
Mazziotti D.A., Phys. Rev. Lett. **97**, 143002 (2006)
Messud J., M. Bender, E. Suraud, Phys. Rev. C **80**, 054314 (2009)
Nunes G.S., J. Phys. B: At. Mol. Opt. Phys. **32**, 4293 (1999)
Oliveira L.N., E.K.U. Gross, W. Kohn, Phys. Rev. Lett. **60**, 2430 (1988)
Perrot F., M.W.C. Dharma-Wardana, Phys. Rev. A **29**, 1378 (1984)
Perrot F., M.W.C. Dharma-Wardana, Phys. Rev. B **52**, 5352 (1995)
Profeta G., C. Franchini, N.N. Lathiotakis, A. Floris, A. Sanna, M.A.L. Marques, M. L'uders, S. Massida, E.K.U. Gross, A. Continenza, Phys. Rev. Lett. **96**, 047003 (2006)
Sander L.M., H.B. Shore, L.J. Sham, Phys. Rev. Lett. **31**, 533 (1973)
Sanna A., C. Franchini, A. Floris, G. Profeta, N.N. Lathiotakis, M. L'uders, M.A.L. Marques, E.K.U. Gross, A. Continenza, S. Massida, Phys. Rev. B **73**, 144512 (2006)
Sanna A., G. Profeta, A. Floris, A. Marini, E.K.U. Gross, S. Massida, Phys. Rev. B **75**, 020511R (2007)
Senatore G., G. Pastore, Phys. Rev. Lett. **64**, 303 (1990)
Sharma S., S. Shallcross, J.K. Dewhurst, A. Sanna, C. Bersier, S. Massida, E.K.U. Gross, Phys. Rev. B **80**, 184502 (2009)
Suvasini B., B.L. Gyorffy, Physica C **195**, 109 (1992)
Suvasini B., W.M. Temmerman, B.L. Gyorffy, Phys. Rev. B **48**, 1202 (1993)
Temmerman W.M., Z. Szotek, B.L. Gyorffy, O.K. Andersen, O. Jepsen, Phys. Rev. Lett. **76**, 307 (1996)

Ziesche P., Phys. Lett. A **195**, 213 (1994)
Ziesche P., Int. J. Quantum Chem. **60**, 1361 (1996)

Appendix-05: State-of-the-art-of basis sets

John Pople, noble prize winner, was a mathematician by training and profession. His passion to find solution for the then impossible Schrodinger wave equation for multi-electron system opened new vistas in quantum chemistry. The three decades of untiring and concerted efforts made CQC what it is today. Atomic orbitals (AOs) are functions of XYZ co-ordinates of electron. They closely resemble the valence orbitals of the isolated atoms. These AOs (also called STOs) are a simplification of SWE for H-atom. The matlab programs, h1s_AO.m and h2s_AO.m output graphic display of normalized radial wave function and radial distribution function of 1s and 2s atomic orbitals of hydrogen atom. The module AO_MO.m of the toolbox_CQC generates 2D- figures for second row and other elements.



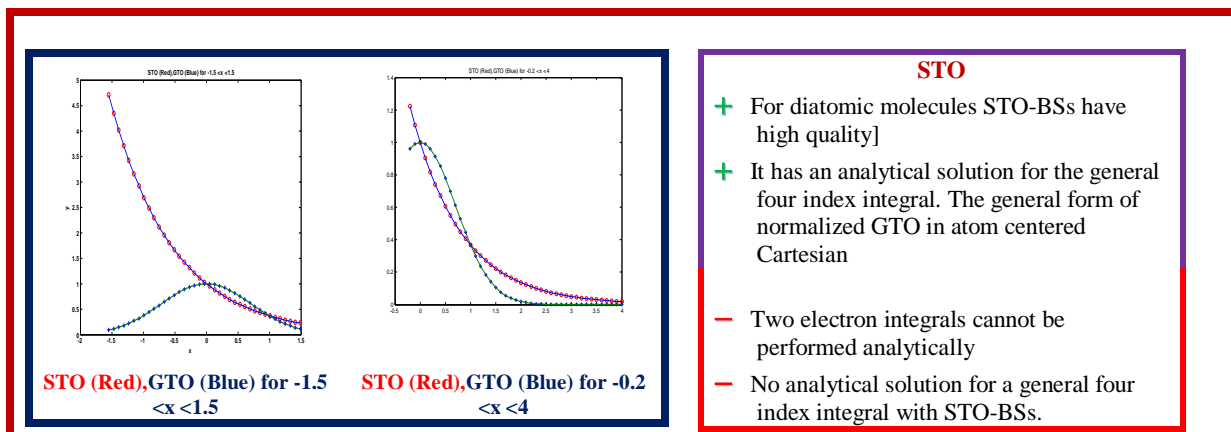
%	6.5000	-0.0617	0.1608
function [r,Rr,RDF] = h2s	7.0000	-0.0534	0.1396
row = 2;	7.5000	-0.0457	0.1176
Na = 2.0000; Nx = 0.2821;	8.0000	-0.0389	0.0966
a0 = 1; n = 2; Z = 1;	8.5000	-0.0328	0.0776
row = 2 * Z / (n * a0)	9.0000	-0.0275	0.0612
	9.5000	-0.0229	0.0475
	10.0000	-0.0191	0.0363
r = [0:.05:10]';			
%			
% Hydrogen 2s			
%			
[rows,col] = size(r); one = ones(rows,1);			
NR = (1/[2*sqrt(2)]) * (Z/a0).^(3/2)			
row,a0			
Rr = NR*(2*one - row *r).* exp(-row*r/2);			
RDF = [NR * r.* (2*one - row *r).* exp(-row*r/2)].^2;			
[r,Rr,RDF]			
figure,subplot(221),plot(r,Rr,'ro',r,Rr)			
subplot(222),plot(r,RDF,'ro',r,RDF)			

Molecular orbital (MO) is a one electron wave function and the energy of an electron is called orbital (also frontier MO) energy. A molecular orbital is represented as a linear combination of AOs.

$$\psi = c_1 * \phi_1 + c_2 * \phi_2 + c_3 * \phi_3 + \dots c_n * \phi_n$$

{ c_i } : coefficients depending upon the system, { ϕ_i } molecular orbitals which are fixed. The more the number of AOs (basis functions, BFs), the more accurate approach is needed to represent realistic electron movement. This is due to variational degrees of freedom. In the first phase, basis sets considered are s', 'p', 'd', 'f', ... atomic orbitals. Although those basis sets are good approximations, latter incorporation of influence of higher-level orbitals on the lower ones became necessary.

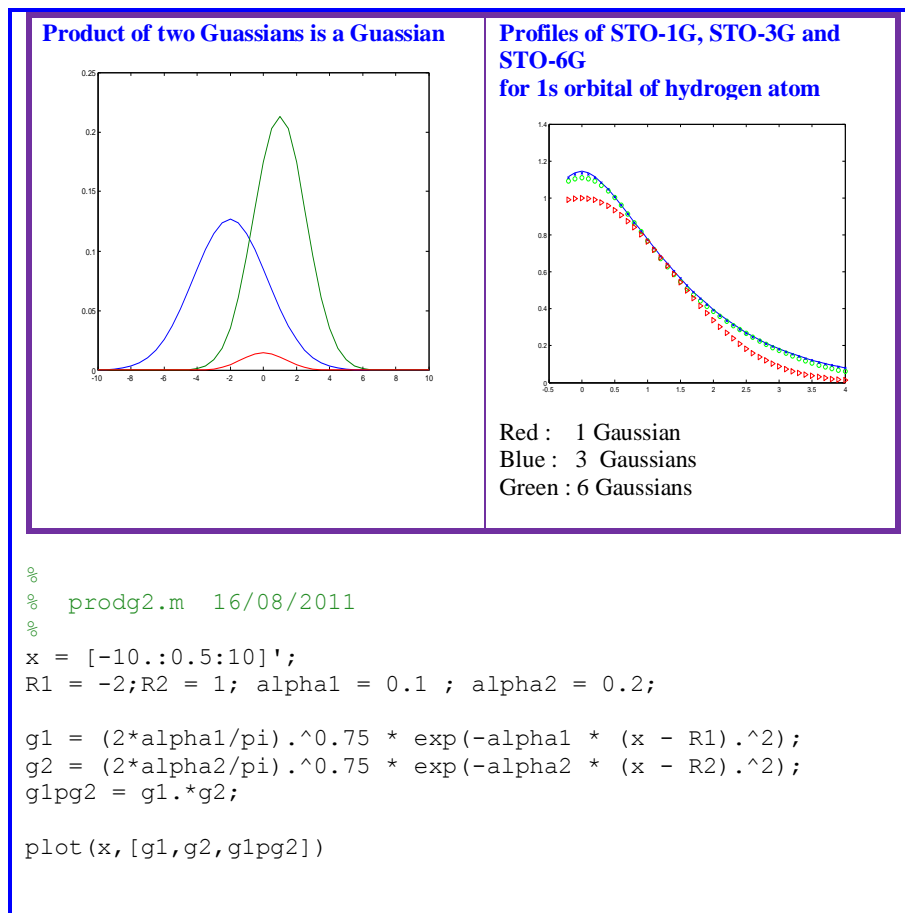
STO: The basis function ($e^{-\alpha * x}$) represents 1s-orbital of hydrogen atom. It is referred as Slater-type-orbital (STO). In extended Huckel theory, STOs are used. All MOs are combination of some set of atomic orbitals. They differ only in their LCAO expansion coefficients STO-3G is the minimal basis set and called single zeta BS. The nomenclature single ψ refers to one and only one BS for each type of core orbital through valence.



Basis set

It is a set of mathematical functions from which a wave function is developed by combination. Each MO in HF theory is expressed as a linear combination of basis set functions (BSF). The coefficients are determined from iterative solution of HF-SCF equations. The full HF wave function is expressed as Slater determinant formed from individual occupied MOs. It is not pragmatic to employ an infinite BS and most of the efforts in the few decades are to identify mathematical BFs which allow ψ representing HF limit as closely as possible. Further, functional form and computational efficiency are also considered.

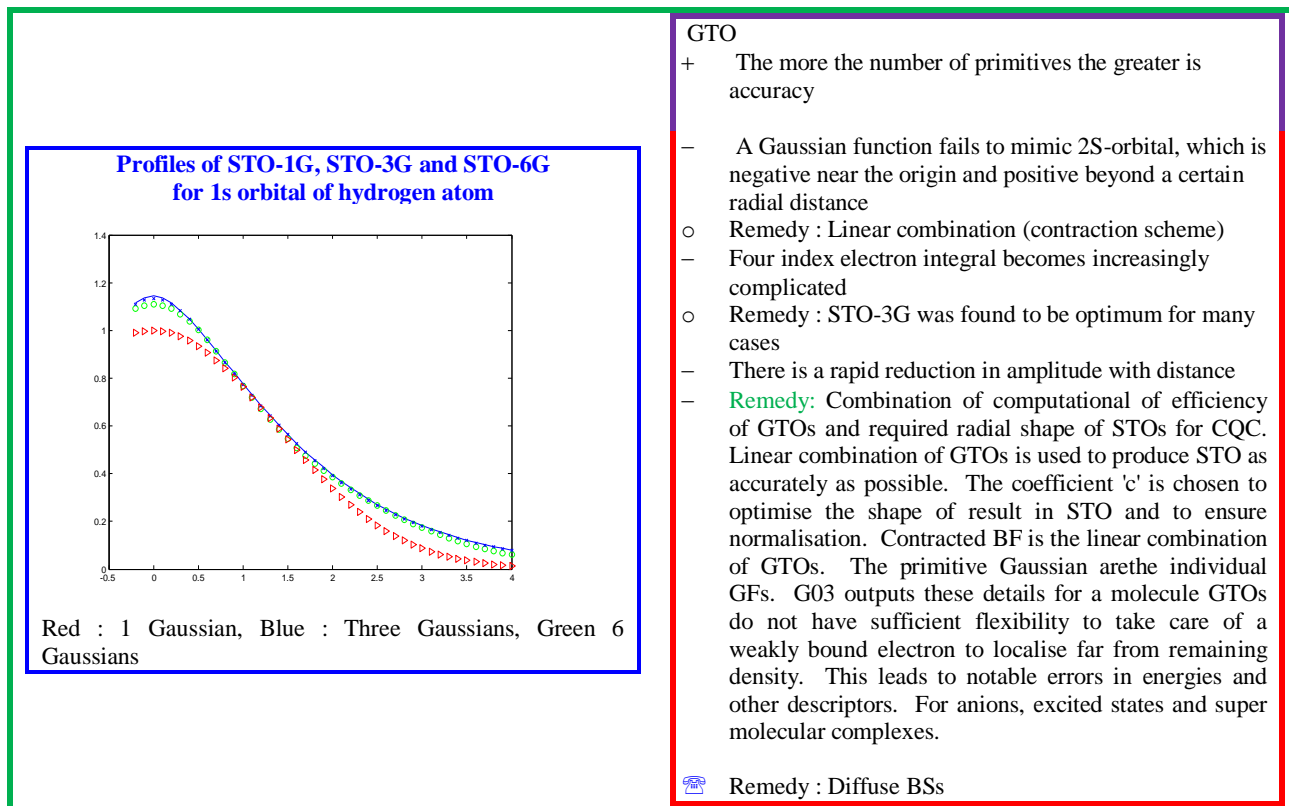
The BF form should be a meaningful and possess chemical sense. In other words, the value of the function should be very large amplitude in regions of space with high electron probability density (ψ^2). It should be of small amplitude at points with low PDF. The simultaneous adherence of the multi-objectives is not easy and the available BSF are a result of sparkling outcome from archive of mathematical functions. The number of computations and thus CPU time increase in calculating 2- and 3-electron integrals with STOs. In 1950s, STO is replaced with a Gaussian function, but the differences in the profile are significant and the end result is of no value. In contracted basis function approach, linear combination of n-number of Gaussians ($n = 3$ to 6) are used to approximate STO. The advantage is taken from the fact that the product of two Gaussians is again a Gaussian. Boys showed that an integral over a product of 1 s Gaussians centered about two positions, reduces to a single integral over a third Gaussian about an intermediate position. This fundamental result has impetus in evaluating multi-center integrals required in solving Schrodinger equation.



GTO

Pople in 1969, and other groups systematically determined optimal values of exponents. The contraction coefficients are linear sum of GTOs to mimic STOs for a large number of atoms in the periodic table.

STO-nG stands for Slater type orbital (STO) approximated by 'n' Gaussians. With increase in number of Gaussians, the profile coincides with that of STO. But, STO-1G (red) is inadequate while STO-6G is an adequate linear combination.



The limitation of Contracted Gaussian function is that GTOs are smooth and differential at the nucleus $\gamma = 0$. It is inadequate to model hydrogen AOs that have a cusp.

Decontracted BS

Each BF is the sum of three Gaussians in STO-3G. Instead, two BFs can be taken for each AO. The first is a contraction of the first two primitive Gaussians and the second is a normalized primitive. A basis set with two functions for each AO is called a double zeta BS.

Decontracted BS	General contraction <i>BF</i>
<ul style="list-style-type: none"> + It will not double its size of BS + Increases flexibility + Tend to be closer to HF limit - Size of secular equation increases 	<ul style="list-style-type: none"> + The integrals with the same primitives are calculated only once Ex. cc-pCVDZ and cc-pCVTZ + Correlation consistent implies that exponents and contraction coefficients are optimised variationally for HF and also for methods including electron correlation.

Triple zeta is a result of further decontraction. The continuation of this process can be done indefinitely. Some of recent examples are cc-pCVDZ and cc-pCVTZ of Denning BSs. The acronym is correlation-consistent-(cc)_polarized(p)_core-and-valence(CV)_[Double (D),Triple for T]_zeta BSs. Raffanetti in 1993 proposed general contraction where in there is a single set of primitives that are used in all contracted BFs. However, the coefficients are different.

Pople split valence BSs

The core orbitals are represented by a single contracted BS (with $n = 3, 4,$ or 6 GTOs). The hyphen (-) represents the core orbitals and valence orbitals. If there two numbers (ij), it is valence-double zeta BS (generally $i = 2$ or 3 and $j = 1$). For the three numbers (ijk), it is valence-triple zeta BS ($k = 1$). Multiple functions are used for the same AO. In double zeta one loose and one tight BS are employed which increase flexibility. In triple zeta, one loose, one medium and one tight BSs are in practice for valence electrons. The general formula is n -ijk G.

For example, 6-311G means there are six GTOs for core (He, Ne, or Ar) electrons, and three-valence triple zeta set. This is the current notation in practice in all CQC publications. The split valence sets uses p-BFs with common exponents. The seminal contribution of Pople et al is in optimizing the exponents and coefficients with test set of energies of atoms and/or molecules. Here, there are no primitives between 2s and 3s BFs of (say phosphorous) atom. It is referred as segmented contraction. Recent examples are partially polarized BSs, MIDI and MAXI BSs of Huzinaga. MIDI is pronounced as 'Bang'. Crammer and Truhlar proposed MIDIX. The optimized geometries of neutral, cationic and anionic molecules are used to design BSs.





MIDIX

+ overcomes wrong geometry for hypervalent second row atoms

MIDIX	d functions
MIDI-(6d)	6 Cartesian d functions
MIDI-!	5 spherical functions

MIDI-1	MAXI-1
MIDI-2	MAXI-2

6-31G*	6-31G(d)
6-31G**	6-31G(3d,2f,g,2p d)

 Expert Opinion (EO)
 4-31G is inferior to 3-21G
 6-21G is obsolete
 i function is not necessary

Complete Basis Set (CBS)

It is an extrapolation of BSs for accurate estimation of total correlation energies applicable to first and second row elements

- Not designed for TS_{energy} calculations
- Not well tested for chemical dynamics calculation for instance barrier height

Diffuse functions

The loosely bound electrons of an atom in an anion or in an excited state are much more important for the energy in the tail of the wave function. However, in traditional chemistry, the valence electrons which interact with other molecules are of utmost concern. Hitherto many of the basis sets concentrate on the main energy located in the inner shell electrons. This is the main area under the wave function curve. The diffuse functions with very small exponents to account for the properties of the tail are introduced. BSs of Pople use the notation 6-311+G and 6-311++G. One '+' means correction is for the 'p' orbitals. A BS with double diffusion i.e. two '++', applies tail correction for both 'p' and 's' orbitals. The plus sign denotes that heavy atoms are augmented with an additional 1s and one set of p-functions, but with small exponents. A second plus in 6-311++G means that p-functions are used for H-atoms. The exponents for diffuse functions are variationally optimized for BH2⁻. The exponents are same

If	Low lying excitation energies & Large molecule
Then	Diffuse function has little effect
If	Hyperpolarizability & Small molecule
Then	Diffuse function is essential
If	Diffuse BS used or Diffuse functions are used for atoms that are not apart
Then	The numerical dependence in BS or hence numerical problems
	→ Remedy : ADF and keyword DEPENDENCY

for 3-21G, 6-31G and 6-311G. The heuristic is that the exponents of diffuse function are 25% of smallest valence exponent.

Diffuse functions are essential as they allow distant interactions and are useful for

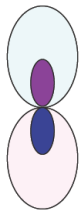
- Smaller molecules compared to larger species
- Hyper- and multi-pole polarizabilities compared to linear polarizabilities
- High lying excitation energies than low-lying excitations.

BS	Diffused	Comment	BS_Polarized		
			Heavy	Hydrogen	
n-ijkG	n-ijk+G		6-31G	p-functions d-functions	-- --
	n-ijk++G		6-31G*		
MIDIX	MIDIX+		6-31G**	d-functions	p-functions
MIDIY	MIDIY+		Balanced double zeta	d-functions	p-functions
cc-pVnz	Aug-cc-pVnz	One set of diffuse function is added for each angular momentum already present	Balanced double zeta	One set of f & Two sets of d	One set of d Two sets of p
	Aug-cc-pVTz	f,d,p and s functions on heavy atoms	cc-pVnZ (n = 6)	One set of Two sets of Three sets of Four sets of Five sets of Six sets of	I functions h functions g functions f functions d functions s & p (valence) functions
		Diffuse d,p and s functions on H and He			


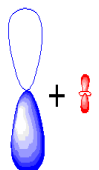




Polarisation function

As different atoms approach each other, the positive charge is drawn to one side while the negative charge is drawn to the other. Thus, their charge distribution causes a polarization effect, which distorts the shape of the atomic orbitals. It is reasonable to conceive that 's' orbitals begin to have a little of the 'p' shape and 'p' orbitals begin to have a little of the 'd' flavor. People refers polarization function as '*' (pronounced as 'star'). One asterisk (*) at the end of a basis set (6-31G*) denotes that polarization has been taken into account in the 'p' orbitals. The polarized basis set represents the orbital as more than just 'p', by adding a little 'd'. The second star (6-31G**) indicates that 's' orbital also has a little of 'p' shape. The difference between the representation of the 'p' orbital for the 6-31G and the 6-31G* basis sets viewed in mathematical form is also enchanting.

Consider NH₃ where s and p functions are centered on atoms. They do not provide adequate mathematical variation to describe the wave function for a pyramidal geometry. The required flexibility is added considering one quantum number higher than valence orbitals and thus adding corresponding BFs. The polarisation function in practice for a first row atom is d GTOs. For hydrogen p-GTOs have the same effect. The d-function on oxygen polarizes the p-function. Thus, OH bond in water is better described compared to the model without polarization. Similarly, addition of d-functions to nitrogen BS results in pyramidal structure of NH₃. The geometry optimization of hypervalent moieties like phosphates, sulphoxides, siliconates etc. require polarized BSs.

$$\phi(x, y, z; Z) = \frac{\sqrt{2}Z^{5/2}}{81\sqrt{\pi}} \left(6 - Z\sqrt{x^2 + y^2 + z^2} \right) ye^{-Z\sqrt{x^2 + y^2 + z^2} / 3}$$


normalization factor radial phase factor cartesian directionality (if any) ensures square integrability

 = 6-31G	 +  = 6-31G*
Original 'p' orbital	Modified 'p' orbital (p +d)
 = 6-31G	 +  = 6-31G**
Original 's' orbital	Modified 's' orbital (s +p)

Floating GTOs

- Geometry optimization becomes more complicated

The polarization functions, in a nut shell, mixes d,p with p,s orbitals. It is also introduced by not concentrating BF on the center of atoms like in floating GTOs (FLOGOs). Thus, the shapes of MOs share qualities of 's' and 'p' orbitals or 'p' and 'd', etc. and not necessarily have characteristics of only one or the other.

In a p-orbital, the positive or negative signs do not refer to charges in the conventional sense. Both lobes of electron cloud are negatively charged. The signs in fact are of wave function. A node (zero electron density) separates the two parts of orbital; naturally, the two lobes have opposite signs viz. positive and negative. Further, according to Pauli exclusion principle, not more than two electrons are present in any orbital justifies that they should have opposite spins.

Knowledge base for i,k,j characteristics	
Antecedent	THEN (Consequent)
If each of three indices are zero (sum = 0)	GTO has spherical symmetry and called an s-type GTO
If one of the indices (m) is one and the other two are zero (sum = 1)	function has axial symmetry about a single (m) Cartesian axis {p-type GTO} [pxpy and pz orbitals]
	<div style="border: 1px solid purple; padding: 5px; display: inline-block;"> $\begin{matrix} i+j+k=2 \\ i & j & k \end{matrix}$ </div>

$$\begin{matrix} 1 & 1 & 0 & xy \\ 0 & 1 & 1 & yz \\ 1 & 0 & 1 & xz \end{matrix}$$

If the sum of the indices =2

orbital is d-type GTO

If $l = 2$

then five functions are xy , xz , yz , $x^2 - y^2$, and $3z^2 - r^2$.

Components : x^2, y^2, z^2
 Binary d-orbitals Ternary combination
 combination
 $x^2 - y^2$ $dx^2 - y^2$ $x^2 + y^2 + z^2$,
 $3z^2 - r^2$ $d3z^2 - r$

i+j+k=2			d-orbitals	
i	j	k		
2	0	0	x^2	$dx^2 - y^2$
0	2	0	y^2	
0	0	2	z^2	$3z^2 - r^2$

- ▶ $x^2 - y^2$, and $3z^2 - r^2$. are derived as linear combinations of the Cartesian d functions.
- ▶ $x^2 + y^2 + z^2$, is an s-type GTO & has spherical symmetry

Improvement in BS and Gn vs Kitchen floor cleaning

Step 1	With Minimal BS, gross energy terms are calculated	Sweep to get all big pieces of dirt
Step 2	Split valence BS	Go back & mop to get little bits of grime
Step 3	Diffusion effect	High vacuum cleaning
Step 4	Polarization effect	Wax to make sure that everything is cleaned off
Step 5	G3 and G4 models for accurate energy	High intensity lights
Step 6	Near exact solution All energy terms (electrostatic to weak vander waals taken care)	The floor is shining All dirt of different size is removed

I row

Atom	#el	[core]	1s	2s	2px	2py	2pz	3s2	3p6	4s2	3d10	4p6
H	1	[zero]	1	0	0	0	0	0	0	0	0	0
He	2	[zero]	2	0	0	0	0	0	0	0	0	0

2_el : [He_core] : [zero][1s2]

II row

	#el	[core] [1s2]	2s	2px	2py	2pz
Li	3	[He]	1	0	0	0
Be	4	[He]	2	0	0	0
B	5	[He]	2	1	0	0
C	6	[He]	2	1	1	0
N	7	[He]	2	1	1	1
O	8	[He]	2	2	1	1
F	9	[He]	2	2	2	1
Ne	10	[He]	2	2	2	2

III row

			Valence electrons			
	#el	[core]	3s	3px	3py	3pz
Na	11	[Ne]	1	0	0	0
Mg	12	[Ne]	2	0	0	0
Al	13	[Ne]	2	1	0	0
Si	14	[Ne]	2	1	1	0
P	15	[Ne]	2	1	1	1
S	16	[Ne]	2	2	1	1
Cl	17	[Ne]	2	2	2	1
Ar	18	[Ne]	2	2	2	2

10_el : [Ne_core] : [He] [2s2, 2p6] : [2+8]	18_el : [Ar_core] : [Ne] [3s2, 3p6] = [10 +8]

IV_row_elements: [non-transition , transition]
 [non-transition] : [[K,Ca], [Ga, ...,Kr]]
 [transition] : [Sc, ..., Zn]

IV row, non-transition metals (K, Ca)									
	#el	[core]	Valence electrons						
			4s	3d1	3d2	3d3	3d4	3d5	4p
K	19	[Ar]	1	0	0	0	0	0	0
Ca	20	[Ar]	2	0	0	0	0	0	0

IV row, Transition metals									
	#el	[core]	Valence electrons						
			4s	3d1	3d2	3d3	3d4	3d5	4p
Sc	21	[Ar]	2	1	0	0	0	0	0
Ti	22	[Ar]	2	1	1	0	0	0	0
V	23	[Ar]	2	1	1	1	1	0	0
Cr	24	[Ar]	2	1	1	1	1	0	0
Mn	25	[Ar]	2	1	1	1	1	1	0
Fe	26	[Ar]	2	2	1	1	1	1	
Co	27	[Ar]	2	2	2	1	1	1	0
Ni	28	[Ar]	2	2	2	2	1	1	0
Cu	29	[Ar]	2	2	2	2	2	1	0
Zn	30	[Ar]	2	2	2	2	2	2	0

IV row, non-transition metals (Ga to Kr)							
	#el	[core]	4s	3d10	4px	4py	4pz
Ga	31	[Ar]	2	10	1	0	0
Ge	32	[Ar]	2	10	1	1	0
As	33	[Ar]	2	10	1	1	1
Se	34	[Ar]	2	10	2	1	1
Br	35	[Ar]	2	10	2	2	1
Kr	36	[Ar]	2	10	2	2	2

36_el : [Kr_core] : [Ar] [4s2, 3d10,4p6] = [18 +18]

EMSL Basis Set Exchange Library		
H	0	STO-2G
S	2	1.00
	1.309756377	0.430128498
	0.233135974	0.678913531
H	0	6-311++G**
S	3	1.0
	33.8650000	0.0254938
	5.0947900	0.1903730
	1.1587900	0.8521610
S	1	1.00.
	0.3258400	1.0000000
S	1	1.00
	0.1027410	1.0000000
S	1	1.00
	0.0360000	1.0000000
P	1	1.00
		3.0000000
P	1	1.00
H	0	STO-6G
S	6	1.00
	35.52322122	0.00916359628
	6.513143725	0.04936149294
	1.822142904	0.16853830490
	0.625955266	0.37056279970

0.243076747	0.41649152980	0.7500000	1.0000000
0.100112428	0.13033408410	P	1.
			1.00
			0.1875000
		D	1.
			1.00
			1.0000000
			1.0000000

C	0.	6-311G**	
S	6	1.00	
	4563.2400000	0.00196665	
	682.0240000	0.0152306	
	154.9730000	0.0761269	
	44.4553000	0.2608010	
	13.0290000	0.6164620	
	1.8277300	0.2210060	
SP	3	1.00	
	20.9642000	0.1146600	0.0402487
	4.8033100	0.9199990	0.2375940
	1.4593300	-0.00303068	0.8158540
SP	1	1.00	
	0.4834560	1.0000000	1.0000000
SP	1	1.00	
	0.1455850	1.0000000	1.0000000
D	1	1.00	
	0.6260000	1.0000000	

S : Core SP: Split D: Diffuse P:polarisation

	EMSL Basis Set Exchange Library		
	STO-2G		
H-He	W.J. Hehre, R.F. Stewart and J.A. Pople	J. Chem.Phys.	2657(1969)
Li-Ne Na-Ar K-Kr	W.J. Hehre, R. Ditchfield, R.F. Stewart, J.A. Pople	J. Chem.Phys.	52, 2769 (1970)

	STO-6G		
H-Ne	W.J. Hehre, R.F. Stewart and J.A. Pople	J.Chem.Phys.	51, 2657(1969)
Na-Ar	W.J. Hehre, R. Ditchfield, R.F. Stewart and J.A. Pople	J.Chem.Phys.	52, 2769 (1970)

	6-311++G(3df,3pd)		
H, Li - Ne	R. Krishnan, J.S. Binkley, R. Seeger and J.A. Pople	J. Chem. Phys.	72, 650 (1980)
Na - Ar	A.D. McLean and G.S. Chandler	J. Chem. Phys	72, 5639(1980)
K - Ca	J-P. Blaudeau, M. P. McGrath, L.A. Curtiss and L. Radom,	J. Chem. Phys.	107, 5016(1997)
Ga - Kr	L. A. Curtiss, M. P. McGrath, J-P. Blandeau, N. E. Davis! R. C. Binning, Jr. L. Radom	J. Chem. Phys.	103, 6104(1995)
H-Ne:	! M.J. Frisch, J.A. Pople and J.S. Binkley,	J. Chem. Phys.	80, 3265 (1984)

I	M.N. Glukhovstev, A. Pross, M.P. McGrath, L. Radom,	J. Chem. Phys.	103, 1878 (1995)
H, Li-Cl:	T. Clark, J. Chandrasekhar, G.W. Spitznagel, P.V.R. Schleyer	J. Comp. Chem.	4, 294 (1983)

Appendix 6: Gn models

G1 (Theory) model [Pople89, Curtiss90]

The core philosophy of G1 model is to calculate energy at MP4 level, but by performing CQC at lower levels adopting approximation theory. The initial geometry optimization and frequency calculations are performed at ab initio level (HF/6-31G*) to arrive at the chemically valid structure with a minimum on PES. Further, refinement of geometry is done with expensive post-HF model, MP2(full) /6-31G*. Adapting the trend, MP4SDTQ/6-31G** is the CQC model used in computing energies. The accuracy of energy at this level is increased by applying corrections for diffuse-sp/higher polarization functions on non-hydrogen atoms, correlation beyond fourth-order perturbation theory, higher-level correction, to make electronic energy (E_{el}) exact for hydrogen atom and hydrogen molecule. The accurate_Energy_at_G1_model is finally obtained by adding ZPE and the modes operndi are depicted. The data pertaining to Na to Cl are used in this G1 model.

Computation of accurate_Energy_at_G1_model

Equilibrium geometry & Vibrational frequency		Single point_energy_initial_G1	
CQC computation	@ (level, BS)	MP4SDTQ(FC)/6-31G**	
Initial equilibrium geometry	HF/6-31G*	FU	Full
Harmonic frequencies			Includes inner shell (core) electrons
Scaling factor	0.8929	FC	Frozen
			Only valence electrons considered i.e. core electrons frozen
Equilibrium geometry	MP2(FULL) /6-31G*		

MP4SDTQ(FC)/6-31G**// MP2(FULL) /6-31G* read as

Energy calculated at higher (MP4SDTQ(FC)/6-31G**) level while Geometry optimised only at a (lower) MP2(FULL) /6-31G* level and BSs

Corrections for (SP) Energy_G1		
diffuse-sp functions on non-hydrogen atoms	$\Delta E(+)$	$E[\text{MP4}/6-311+G^{**}] - E[\text{MP4}/6-311 G^{**}]$
Higher polarization functions on non-hydrogen atoms	$\Delta E(2df)$	$E(\text{MP4}/6-311G(2df)) - E[\text{MP4}/6-311G^{**}]$
Correlation beyond fourth-order perturbation theory using quadratic configuration interaction	$\Delta E(\text{QCI})$	$E[\text{QCISD}(T)/6311G^{**}] - E[\text{MP4} /6-311G^{**}]$

Higher level correction to make E_{el} exact for hydrogen atom and

$$E_{\text{HLC}} = -0.19 * n_{\alpha} - 5.95 * n_{\beta}$$

hydrogen molecule

$$E_{\text{corrections}} = \begin{array}{l} \Delta E(+), \\ + \Delta E(2df), \\ + \Delta E(QCI) \end{array}$$

Accurate Energy	=	MP2(full) /6-31G*	
Energy_G1_model	+	$\Delta E(+)$	
$E_{\text{[MP4]}}$	+	$\Delta E(2df)$	
	+	$\Delta E(QCI)$	
	+	E_HLC	
	+	E_ZPE	

G2 (Theory) model [Curtiss91]

G2 theory further applies corrections to G1 model to obtain still accurate energies through CQC. In the first phase, corrections for nonadditivity caused by the assumption of separate basis set extensions for diffuse-sp functions and higher polarization functions (2df in G1 theory) are applied. A weightage to number of valence pairs is given to obtain still accurate energies.

Computation of accurate Energy at G2 model

Corrections for (SP) Energy (G2)

Diffuse functions	$\Delta E(+,2df)$	$E(\text{MP2}/6-311+\text{G}(2df,p)] - E[\text{MP2}/6-311\text{G}(d,p)]$
Higher polarization functions on non-hydrogen atoms and p-functions on hydrogen atoms	$\Delta E(+)$	$E(\text{MP2}/6-311+\text{G}(d,p)] - E[\text{MP2}/6-311\text{G}(d,p)]$
Addition of a third d function to the non-hydrogen atoms and a second p function to the hydrogens	$\Delta E(2df)$	$E(\text{MP2}/6-311\text{G}(2df,p)] - E[\text{MP2}/6-311\text{G}(d,p)]$
	$\Delta E2$	$E(\text{MP2}/6-311+\text{G}(3df,2p)] - E[\text{MP2}/6-311+\text{G}(2df,p)]$

$$\Delta E(G2) = \Delta E(+,2df) + \Delta E(+), + \Delta E(2df) + \Delta E2$$

$$\text{Energy0}(G2) = E0(G1) + \Delta E + 1.14 * \text{number_of_valence_pairs}$$

Free energy from QC is based on application of statistical thermodynamics with in QC paradigm. When trends in ΔG obtained from experimental equilibrium constants or from single ion free energy changes, compensation effects of ΔH and ΔS mask the true picture. This emphasized the need for improvements in enthalpy and entropy values both experimentally and by theoretical calculations. Further, the separation of gross effects into electrostatic and non-electrostatic components, especially of neutral molecules in polar solvents continues to be fertile area of research in QC.

Expert Opinion	
If	First or second row elements Thermodynamic properties
Then	G2 method gives excellent results Exception : ΔH_f for PF_3 , PF_5 G2 method underestimates by 5 to 6 Kcal/mole
If	High accuracy methods like G2 and CBS are used
Then	Small errors for small molecules

G2_z			
Zero-point-corrected electronic energy (0K) $E_{0el} = E_{elec} + ZPE$			
Thermal-corrected energy:		$E = E_0 + E_{trans} + E_{rot} + E_{vib}$	
Enthalpy computed using the G2 predicted energy:		$H = E + RT$	
Gibbs Free Energy computed using the G2 predicted energy:		$G = H - TS$	
Temperature	298.15K	Pressure	1.0
E(ZPE)	0.020511	E(Thermal)	0.023346
E(QCISD(T))	-76.276078	E(Empiric)	-0.024560
DE(Plus)	-0.010827	DE(2DF)	-0.037385
G1(0 K)	-76.328339	G1 Energy	-76.325503
G1 Enthalpy	-76.324559	G1 Free Energy	-76.303182
E(Delta-G2)	-0.008275	E(G2-Empiric)	0.004560
G2(0 K)	-76.332054		
G2_output for H2O			
G2 Energy	-76.329219		
G2 Enthalpy	-76.328274		
G2 Free Energy	-76.306897		

G3 (Theory) model [Curtiss98]

In 1998, Pople et al brought out G3 theory with inclusion of different BSs, spin orbit correction for atoms and a term for correlation for single point energy. Baboul (1998) optimized geometry with DFT instead post-HF (MP2). Curtiss (2000) employed multiplicative scale factors in place of additive higher level corrections. Pople (2001) proposed G3X and G3SX series and tested with 376 energies (G3/99 test set of species). The highlight of this series is addition of g-polarization function to the G3Large BS for second row atoms. The other features are geometry optimization at B3LYP/6-31G(3df,p) and calculation of ZPE through frequency. It is applied to third row non-transition elements viz. Ca, K, Ga to Kr.

Computation of accurate_Energy_at_G3_model	
G3 JChemPhys_109_7764-G3	
CQC computation	@ (level. BS)

Initial equilibrium geometry	HF/6-31G(d)
Equilibrium geometry	MP2(full) /6-31G(d)
Harmonic frequencies	HF/6-31G*
Geometry opt_refinement	MP2(full)/6-31G(d)
Scaling factor	0.8929

Single point energy MP4/6-311G(d,p).

Corrections for (SP) Energy		
Diffuse functions	$\Delta E(+)$	$E[\text{MP4}/6-31+G(d)] - E[\text{MP4}/6-31 G(d)]$
Higher polarization functions on non-hydrogen atoms and p -functions on hydrogen atoms	$\Delta E(2df, p)$	$E[\text{MP4}/6-31 G(2df, p)] - E[\text{MP4}/6-31 G(d)]$
Correlation effects beyond fourth order MP	$\Delta E(\text{QCI})$	$E[\text{QCISD}(T)/6-31G(d)] - E[\text{MP4}/6-31G(d)]$

Correction for larger basis set effects

$$\Delta E_{\text{G3Large}} = E_{[\text{MP2_full} / \text{G3Large}]} - E_{[\text{MP2} / 6-31 G(2df, p)]} - E_{[\text{MP2} / 6-31+ G(d)]} + E_{[\text{MP2} / 6-31 G(d)]}$$

$$E_{\text{corrections}} = \Delta E(+) + \Delta E(2df, p) + \Delta E(\text{QCI}) + \Delta E(\text{G3large}) + \Delta E(\text{Spin_orbit_atoms})$$

Higher level correction (HLC) to compensate other (not accounted for) terms

$$E_{\text{HLC}} =$$

$$\begin{aligned} \text{Accurate_Energy_G3_model} &= E_{\text{MP4}/6-31G(d)} \\ &+ E_{\text{corrections}} \\ &\approx E_{[\text{QCISD}(T, \text{FULL})/\text{G3large}]} + E_{\text{HLC}} + E_{\text{ZPE}} \end{aligned}$$

Geometry optimization and SP in different models of G3

	Model 1	Model 2	Model 3	Model 4
Geometry	MP2~FU/6-31G(d)	B3LYP/6-31G.d.	MP2~FU/6-31G(d)	B3LYP/6-31G.d.

Single-Point energies	MP4~FC/6-31G(d) MP4~FC/6-311G(d) MP4~FC/6-31G(2df,p) QCISD~T,FC/6-31G(d) MP2~FU/G3large	MP4~FC/6-31G(d) MP4~FC/6-311G(d) MP4~FC/6-31G(2df,p) QCISD~T,FC/6-31G(d) MP2~FU/G3large	QCISD~T,FC/6-31G(d) MP2~FC/G3MP2large	QCISD~T,FC/6-31G(d) MP2~FC/G3MP2large
-----------------------	---	---	--	--

The results of comparative study of G3 with earlier model G2 and modified G3 are depicted in [table zzz](#). It is clear G3 >> G2 (and G1). Further, G3X is computationally less intensive but with less errors with respect to experimental values. Thuseven for larger set (376) of a variety properties (IP,EA, PA etc) of atomic and molecular species.

G3X > G3 >> G2 (>>G1)

Comparison of performance of G2,G3 and G2 MP2 with different data sets						
	#	Average absolute deviation, kcal/mol		#	Mean absolute deviation, kcal/mol	
		G2	G3		G3	G3_MP2
Enthalpies of formation	14					
• Nonhydrogen	8	1.56	0.94	22	1.05	0.88
• Hydrocarbons	35	2.44	1.72	2		
• Subst. hydrocarbons	22	1.29	0.68	47	2.11	1.9
• Inorganic hydrides	47	1.48	0.56	38	0.69	0.56
• Radical	15	0.95	0.87	91	0.75	0.75
Ionization energies	85	1.16	0.84	1	0.87	0.81
Electron affinities	29	1.41	1.13	31	0.8	0.7
Proton affinities	8	1.41	1	88	1.14	1.07
	29	1.08	1.34	58	0.98	0.98
All	9	1.48	1.02	8	1.34	1.21
				37	1.07	0.95
				6	(1.5)	(1.35)

	#	G2	G3
K, Ca, Ga to Kr	47	1.43	0.94
G3/99 test set + 47	423		1.06

Snapshot of post-HF procedures, BSs and phase wise refinement of SP energy in G3 model using G03 package

Phase I : Geometry optimization with HF;
Phase II : Frequency at HF level;
Phase VII : SP energy at G3 level + Frequency
[NImag] : 0 in Frequency calculation

	III	IV	V
4HF	-76.009808	-76.009808	-76.016743
MP2	-76.1992442	-76.1968478	-76.209702
MP3		-76.2027024	-76.2137491
MP4D		-76.20612	-76.2174994
MP4DQ		-76.2048784	-76.2162534
MP4SDTQ		-76.2073266	-76.2175887
MP4SDQ		-76.2055009	-76.2203046
QCISD		-76.2060602	
QCISD(T)		-76.2078917	
RMSD	3.160e-009	4.040e-010	6.869e-009

VI	VI	VII	VII
HF	-76.0277249	MP2/6-31G(d)	-76.1968478
MP2	-76.2670957	QCISD(T)/6-31G(d)	-76.2078917
MP3	-76.2747832	MP4/6-31G(d)	-76.2073266
MP4D	-76.2787939	MP2/6-31+G(d)	-76.209702
MP4DQ	-76.2756414	MP4/6-31+G(d)	-76.2203046
MP4SDQ	-76.276368	MP2/6-31G(2df,p)	-76.2670957
MP4SDTQ	-76.281815	MP4/6-31G(2df,p)	-76.281815
RMSD	2.445e-009	MP2/GTLarge	-76.3616032
		G3	-76.3820445

```
Phase G03 instruction
1 # G3 MaxDisk=40GB
2 #N Geom=AllCheck Guess=Read SCRF=Check HF/6-31G(d) Freq
3 #N Geom=AllCheck Guess=Read SCRF=Check MP2(Full)/6-31G(d) Opt=RCFC
4 #N Geom=AllCheck Guess=Read SCRF=Check QCISD(T,E4T)/6-31G(d)
5 #N Geom=AllCheck Guess=Read SCRF=Check MP4/6-31+G(d)
6 #N Geom=AllCheck Guess=Read SCRF=Check MP4/6-31G(2df,p)
7 #N Geom=AllCheck Guess=Read SCRF=Check MP2=Full/GTLarge
```

G3B3		NImag=0			
Level	BS				Energy
	n-pqr	Dif		Pol	
MP2	6-31		G	(d)	-76.1968451
QCISD(T)	6-31		G	(d)	-76.2078898
MP4	6-31		G	(d)	-76.2073246
MP2	6-31	+	G	(d)	-76.2096739
MP4	6-31	+	G	(d)	-76.220278
MP2	6-31		G	(2df,p)	-76.2671088

MP4	6-31	G (2df,p)	-76.2818268
MP2	GTLarge		-76.3615986
G3B3			-76.3837249
Normal termination of Gaussian 03			

G4 (Theory) model [Curtiss07]

In continuation of concerted efforts of obtaining accurate energies with higher level basis sets and hybrid (ab initio and DFT) models, Curtiss, Redfern and Raghavachari proposed G4 set during 2006 and 2007. The unique features include use of 4d and 3d polarization sets on second and first row atoms of periodic table, higher level corrections etc. with a test sets of 376 and 456 species. The additional computational steps and changes made in G4 are described. The performance of G4 is undoubtedly excelled G3 and earlier G-series. A less expensive G4_MP2 is also worth trying.

G4 >> G3
[G4_MP2 > G4_MP3]
 >>[G2_MP2] >> G1

Where > indicates performance superiority

Additional features of Gaussian_4 (G4) (Larry 2007)

- ▶ Extrapolation procedure is used to obtain Hartree-Fock limit for inclusion in total energy calculation
 - + *d*-polarization sets are increased to
 - ◆ 3*d* on the first-row atoms
 - ◆ 4*d* on the second-row atoms, with re optimization of the exponents for latter.
- ▶ QCISD_T_ method is replaced by the CCSD_T_ method
 - + highest level of correlation treatment
- ▶ Optimized geometries and zero-point energies are obtained with the B3LYP
 - ▶ Two new higher level corrections are added
 - + Accounts for deficiencies in the energy calculations

Supremacy of G4 models for energy and properties over G3

	G4	G4_ MP3	G4_ MP2	G3
Enthalpies of formation (270)	0.80	1.04	0.99	1.19
Nonhydrogens (79) Hydrocarbons (38)	1.13	1.61	1.44	2.10
Subst. hydrocarbons (100)	0.48	0.69	0.63	0.69
Inorganic hydrides (19)	0.68	0.78	0.83	0.82
Radicals (34)	0.92	1.06	0.94	0.95
	0.66	0.89	0.86	0.83
Ionization energies (105)	0.91	1.01	1.07	1.09
Atomic (26)	0.65	0.83	1.13	1.03
Molecular (79)	0.99	1.07	1.05	1.12
Electron affinities (63)	0.83	0.97	1.23	0.97
Atomic (14)	0.91	1.37	1.84	1.32
Molecular (49)	0.81	0.85	1.06	0.87
Proton affinities (10)	0.84	0.91	0.67	1.14
Hydrogen bonded complexes (6)	1.12	1.31	1.28	0.60
All (454)	0.83	1.03	1.04	1.13
G3/99 (376)	0.80	0.99	1.01	1.06
	Root mean square deviation kcal/mol			
All_454	1.19	1.52	1.49	1.67

aug-cc-pVQZ Basis sets used in single point HF energy calculations in G4 model

Atoms	Literature		G4 modified	
		Diffuse		Diffuse
H,He	➤ 4s 3p 2d 1f	➤ spdf	➤ 4s 2p d	➤ NO
➤ Li-Ne	➤ 5s 4p 3d 2f 1g	➤ spdfg	➤ 5s 4p 3d 2f 1g	➤ sp
➤ Na,Mg	➤ 6s 5p 3d 2f 1g	➤ ---	➤ 6s 5p 3d 2f 1g	➤ ---
➤ Al-Ar	➤ 6s 5p 3d 2f 1g	➤ spdfg	➤ 6s 5p 3d 2f 1g	➤ sp
➤ K,Ca	➤ 7s 6p 4d 2f 1g	➤ ---	➤ 7s 6p 4d 2f 1g	➤ ---
➤ Ga-Kr	➤ 7s 6p 4d 2f 1g	➤ spdfg	➤ 7s 6p 4d 2f 1g	➤ sp

Output of om_ref_JAVATYP.m
Gaussian_n_models

- Larry A. Curtissa, Krishnan Raghavachari, Paul C. Redfern, Vitaly Rassolov and **John A. Pople** J Chem Phys., **109**,1998_18_7764
 ➤ **Gaussian-3 .G3.theory for molecules containing first and second-row atoms**
- Larry A. Curtissa, Paul C. Redfern, Krishnan Raghavachari, Vitaly Rassolov and **John A. Pople** J. Chem. Phys. **110**,10_1999_4703
 ➤ **Gaussian-3 theory using reduced Moller-Plesset order**

Anwar G. Baboul, Larry A. Curtissa, Paul C. Redfern, Krishnan Raghavachari, ▶ Gaussian-3 theory using density functional geometries and zero-point energies	J. Chem. Phys. 110 ,16_1999_7650
Larry A. Curtissa, Krishnan Raghavachari, Paul C. Redfern, , and John A. Pople ▶ Gaussian-3 theory using scaled energies	J. Chem. Phys. 112 _3_2000_1125
Larry A. Curtissa, Paul C. Redfern, Krishnan Raghavachari, , and John A. Pople ▶ Gaussian-3X .G3X.theory: Use of improved geometries, zero-point energies, and Hartree-Fock basis sets	J. Chem. Phys. 114 _1_2001_108
Larry A. Curtissa, Paul C. Redfern, Vitaly Rassolov, Gary Kedziora, and John A. Pople ▶ Extension of Gaussian-3 theory to molecules containing third-row atoms K, Ca, Ga-Kr	J. Chem. Phys. 114 _21_2001_9287
Curtiss L. A., P. C. Redfern, and K. Raghavachari, ▶ Gaussian-4 theory	J. Chem. Phys. 123 , 124107_2006
Curtiss L A, Paul C. Redfern, K Raghavachari,	J. Chem. Phys. 126 , 084108, 2007
Curtiss L. A., P. C. Redfern, and K. Raghavachari ▶ Gaussian-4 theory using reduced order perturbation theory	J. Chem. Phys. 127 , 124105_2007
om_ref_JAVATYP.m	
object module (om_) reference (ref_) Journal Author Volume And (JAVATYP) Title Year Pages matlab function(m)	

G3MP2B3 and DFT models of uracil:Lukmanov[24] applied G3MP2B3 and DFT(TPSS) for stability order of uracil and its derivatives (chart A6-1).

Chart A6-1: G3MP2B3 model of uracil and its derivatives	Inform.Bits
X-uracil	5 water molecules in primary solvation shell
◆ 5-fluoro	Tautomers have varying hydration energy
◆ 5-chloro	
◆ 5-amino	NBO analysis,
◆ 5-hydroxy	Diketo tautomer
◆ 5-methyl	◆ stability due to the nN → π* (or σ*) interaction
◆ 6-methyl	
X Y-uracil	Enol form
◆ 5-hydroxy-6- methyl	■ nN → π* (or σ*) energy is
◆ 5-amino-6- methyl	

	lost <ul style="list-style-type: none"> ▪ Conjugation length partially compensates the lost energy
--	---

Appendix-07: I/Ofiles

Automatic search of optimized geometry and generation of an ASCII file from G03 output

A manual search for optimized geometry followed by cut-paste procedure of the optimized BL, BA, and DA is a routine but indispensable practice. In this laboratory m-files for a single/multiple G03 – output files (xx.out) has been in use to check the success of optimization of a run (om_xyz.m, om_zmatrix.m) and if so creating an ASCII file containing optimized geometry. Further, search for success of frequency analysis is also available. The modules for spectra, reaction characteristics and rotation constants are under development. The input for CQC computations is given in [chart A7-1](#).

Chart A7-1: software independent input form for CQC calculations in object oriented program format

Z-matrix

- Ground state
- Excited states
- TS
- Saddle point

- Single Point energy
- PES
- Higher order SP
- Conformers

Input	Default	Range
Charge	0	[-1 to -4 +1 to +4]
Multiplicity	1	<div style="border: 1px solid blue; padding: 2px; display: inline-block;"> Doublet Triplet Quartet Quintet Sextet </div>
Symmetry	C1	[...]
Solute Phase	gas	[Liquid, solid]
Medium	Vacuum	[solvent]
Periodicity	1	[>1]

Functional	STO-nG
	3-mnqG
	6-mnq++G(*,*)
	Default : B3LYP /6-311++G(*,*)

Level of theory	<input type="checkbox"/> SEMO
<input type="checkbox"/> Ab initio	<input type="checkbox"/> DFT
<input type="checkbox"/> Force fields	

Approximate Hessian

Output choice

```

%
% om_xyz.m (R S Rao) 23/10/05 ; 27/6/11
%
function om_xyz(fileName)
if nargin == 0
    fileName = 'PAh-6-31G.out';
    disp('***** USAGE : om_xyz(fileName)')
end

property = 'XYZ';
match1 = ' -- Stationary point found';
match2 = '          Input orientation';
over1 = '          Distance matrix (angstro');

scrch_props (fileName,property,match1,match2,over1);

```

```

h2o-6-311.out      XYZ  g03_output_g03_output_g03_output_g03_output_
                  -- Stationary point found.
                  Input orientation:
-----
Center  Atomic  Atomic      Coordinates (Angstroms)
Number  Number  Type        X        Y        Z
-----
  1     8       0    0.013566  0.000000  0.009593
  2     1       0   -0.006568  0.000000  0.954900
  3     1       0    0.898099  0.000000 -0.324493
-----

```

```

%
% om_zmatrix.m (R S Rao) 23/10/05 ; 27/6/11
%
function om_zmatrix(fileName)
if nargin == 0
    fileName = 'PAh-6-31G.out';
    disp('***** USAGE : om_zmatrix(fileName)')
end

property = 'Z-Matrix';
match2 = ' -- Stationary point found';
match1 = ' Gaussian 03';
over1 = ' GradGradGradGradGradGradGradGradGradGradGradGradGradGradGradGrad';

scrch_props (fileName,property,match1,match2,over1);

```

GOA.m

With user choice or in summary phase, a brief summary of generally relevant derived QC parameters viz. IP, μ , hyper polarisabilities (α , β , γ), microwave parameters etc. are printed. It is developed keeping in contingency of G03 options of output display. The limitation is one should rerun G03 to obtain detailed output.

Gout.m is a post processing suit of m-files for a set of GO3 output files. From GOA.m one or more properties can be chosen for a single compound and a tabular summary is outputted.

SHEAIP.m

From CQC software output, the energies of HOMO and LUMO are inputted to SHEAIP.m. The values of IP, EA, energy gap, hardness, softness and electronegativity are outputted with comma (',') as delimiter. This subsequently results in a tabular form conforming to a publication standard results (Table A7-1).

Dem_ .m

clean

```
hl = [26,-9.79 -0.53
      26 -9.99 -0.88 ];
chesi(hl)
```

```
hl = [26 -7.483 5.907
      26 -8.206 5.558
      26 -7.878 5.764
      35 -7.483 6.095
      35 -7.920 5.589
      35 -7.415 6.179];
chesi(hl)
```

Table A7-1: Physico-chemical parameters derived from CQC of energies of HOMO and LUMO

```
-----
## HOMO, IP, EA, Egap, Hardness, Softness, Chem Pot, Electronegativity
-----
```

```
26, 9.79, -0.53, -9.26, 10.32, 4.63, 9.26, -5.16
26, 9.99, -0.88, -9.11, 10.87, 4.555, 9.11, -5.435
#####
```

Table ##: Physico-chemical parameters derived from CQC of energies of HOMO and LUMO

```
-----
## HOMO, IP, EA, Egap, Hardness, Softness, Chem Pot, Electronegativity
-----
```

```
26, 7.483, 5.907, -13.39, 1.576, 6.695, 13.39, -0.788
26, 8.206, 5.558, -13.764, 2.648, 6.882, 13.764, -1.324
26, 7.878, 5.764, -13.642, 2.114, 6.821, 13.642, -1.057
35, 7.483, 6.095, -13.578, 1.388, 6.789, 13.578, -0.694
35, 7.92, 5.589, -13.509, 2.331, 6.7545, 13.509, -1.1655
35, 7.415, 6.179, -13.594, 1.236, 6.797, 13.594, -0.618
#####
```

```
%
% SHEAIP.m (R S Rao) 15-05-11
% Chemical Potential, Hardness, EA, Softness, IP

function chesi(hl)
    disp(' ')
    disp('Table ##: Physico-chemical parameters derived from CQC of energies of
HOMO and LUMO')
    Orbital_HOMO = hl(:,1);
    HOMO = hl(:,2);
    LUMO = hl(:,3);
    IP = -HOMO;
    EA = LUMO;
    H = (HOMO-LUMO)/2;
    H = (IP-EA);
```

```

S = (LUMO-HOMO)/2;
Egap = HOMO-LUMO;
Electronegativity = (HOMO+LUMO)/2;
CP = (LUMO-HOMO);
gap = ', ' ;
[r,c] = size(h1);
disp( '-----' )
disp(['## HOMO, IP, EA, Egap, Hardness, Softness, Chem Pot,
Electronegativity'])
disp( '-----' )
for i = 1 : r
    disp([' ',int2str(Orbital_HOMO(i)),gap, num2str(IP(i)),gap,
num2str(EA(i)),gap, num2str(Egap(i)),gap, ...
num2str(H(i)),gap, num2str(S(i)),gap, num2str(CP(i)),gap,
num2str(Electronegativity(i))])
end
disp(
'#####'
#####')

```

dip02.m

A chosen g03-output file is checked whether 'stationary point is found. If the optimized geometry corresponds to a valid chemical structure, it searches for dipole moment, octapole etc in the output file. The values are copied into a sequential file. Here, choice is available to get only dipole moment or all other multi-pole moments.

tab_dip.m

For a series of compounds a tabular summary of total dipole moments and its XYZ components are outputted in a text file with a delimiter(',') for easy preparation of tables.

eig02.m

This program picks up Eigen values for HOMO (occupied) and LUMO (virtual) MOs for optimized geometry of a chemical species. A 2D-plot representing each eigen value by a horizontal line indicates the energy gap between HOMO and LUMO and inter-orbital distance qualitatively. The quantitative picture is also available from tabular summary.

Similar object modules are written in MATLAB for charges (monopoles), ChelpG charges, hyper polarizabilities and the first six frequencies of vibrational analysis.

```

%
% g03_properties.m ver 2.0, 27/6/11
%
function g03_properties(fileName)
if nargin == 0
    fileName ='PAh-6-31G.out';
    disp('***** USAGE : g03_properties(fileName)')
end

om_xyz(fileName)
om_zmatrix(fileName)

om_eigenvalues(fileName)
om_rotconst(fileName)

```

```

om_monopole(fileName)
om_dipole(fileName)
om_multipole(fileName)
om_energy(fileName)

```

```

%
% om_eigenvalues.m 27/6/11
%
function om_eigenvalues(fileName)
if nargin == 0
    fileName = 'PAh-6-31G.out';
    disp('***** USAGE : om_eigenvalues(fileName)')
end

property = ' Eigenvalues';
match1 = ' -- Stationary point found';
match2 = ' Alpha';
over1 = ' Condensed';

scrch_props (fileName,property,match1,match2,over1);

```

```

h2o-6-311.out          Eigenvalues      g03_output_g03_output_g03_output_g03_output_
-- Stationary point found.
Alpha occ. eigenvalues -- -20.54526 -1.35693 -0.73130 -0.55169 -0.50130
Alpha virt. eigenvalues --  0.14516  0.21389  0.58283  0.58285  1.00217
Alpha virt. eigenvalues --  1.02047  1.15364  1.43224  2.45174  2.51901
Alpha virt. eigenvalues --  5.30958  5.41104  5.58188  51.43748

```

```

%
% om_energy.m 27/4/11
%
function om_energy(fileName)
if nargin == 0
    fileName = 'PAh-6-31G.out';
    disp('***** USAGE : om_energy(fileName)')
end

match1 = 'SCF Done: ';
match2 = 'SCF Done: ';
over1 = ' S**2 ';
property = 'Energy';

scrch_props (fileName,property,match1,match2,over1);

```

```

h2o-6-311.out          Energy      g03_output_g03_output_g03_output_g03_output_
SCF Done: E(RHF) = -76.0104553035
A.U. after 10 cycles
SCF Done: E(RHF) = -76.0104553035      A.U. after 10 cycles
Convrg = 0.2809D-08                    -V/T = 1.9993
SCF Done: E(RHF) = -76.0109454406
A.U. after 9 cycles
SCF Done: E(RHF) = -76.0109454406      A.U. after 9 cycles
Convrg = 0.2725D-08                    -V/T = 1.9986

```

```

%
% om_monopole.m (R S Rao) 23/10/05 ; 27/8/11
%
function om_monopole(fileName)
if nargin == 0
    fileName ='PAh-6-31G.out';
    disp('***** USAGE :
om_monopole(fileName)')
end

property = ' Mulliken Charges';
match1 = ' -- Stationary point found';
match2 = ' Mulliken atomic charges.';
over1 = ' Sum of Mulliken charges';

scrch_props (fileName,property,match1,match2,over1);

h2o-6-311.out          Mulliken Charges
g03_output_g03_output_g03_output_g03_output_
-- Stationary point found.
Mulliken atomic charges:
      1
  1  O   -0.816379
  2  H    0.408190
  3  H    0.408190

```

```

%
% om_dipole.m ; 27/6/11
%
function om_dipole(fileName)
if nargin == 0
    fileName ='PAh-6-31G.out';
    disp('***** USAGE : om_dipole(fileName)')
end

property = 'Dipole moment';
match1 = ' -- Stationary point found';
match2 = 'Dipole moment';
;over1 = 'Quadrupole';

scrch_props (fileName,property,match1,match2,over1);

```

```

h2o-6-311.out          Dipole moment      g03_output_g03_output_g03_output_g03_output_
-- Stationary point found.
Dipole moment (field-independent basis, Debye):
  X=    0.0000    Y=    0.0000    Z=   -2.4875    Tot=    2.487

```



```

%
% om_multipole.m (R S Rao) 23/10/05 ; 27/8/11
%
function om_multipole(fileName)
if nargin == 0
    fileName = 'PAh-6-31G.out';
    disp('***** USAGE : om_multipole(fileName)')
end

zz2=' Quadrupole';
zz3=' Octapole ';
zz4= ' Hexadecapole';
zz5 = ' N-N=';
match1=' -- Stationary point found';

%
% Quadrupole moment
%
    property =' Quadrupole';
match2 = zz2; over1 = zz3;
scrch_props (fileName,property,match1,match2,over1);
%
% Octapole moment
%
    property =' Octapole';
match2 = zz3; over1 = zz4;
scrch_props (fileName,property,match1,match2,over1);
%
% Hexadecapole moment
%
    property =' Hexadecapole';
match2 = zz4; over1 = zz5;
scrch_props (fileName,property,match1,match2,over1);

```

```

h2o-6-311.out          Quadrupole      g03_output_g03_output_g03_output_g03_output_
-- Stationary point found.
Quadrupole moment (field-independent basis, Debye-Ang):
  XX=   -7.2757   YY=   -3.8642   ZZ=   -6.3656
  XY=    0.0000   XZ=    0.0000   YZ=    0.0000
Traceless Quadrupole moment (field-independent basis, Debye-Ang):
  XX=   -1.4405   YY=    1.9710   ZZ=   -0.5304
  XY=    0.0000   XZ=    0.0000   YZ=    0.0000

h2o-6-311.out          Octapole      g03_output_g03_output_g03_output_g03_output_
-- Stationary point found.
Octapole moment (field-independent basis, Debye-Ang**2):
  XXX=    0.0000   YYY=    0.0000   ZZZ=   -1.4788   XYY=    0.0000
  XXY=    0.0000   XXZ=   -0.4290   XZZ=    0.0000   YZZ=    0.0000
  YYZ=   -1.3013   XYZ=    0.0000

h2o-6-311.out          Hexadecapole      g03_output_g03_output_g03_output_g03_output_
-- Stationary point found.
Hexadecapole moment (field-independent basis, Debye-Ang**3):
  XXXX=   -5.3835   YYYY=   -5.3130   ZZZZ=   -6.1814   XXXY=    0.0000
  XXXZ=    0.0000   YYYY=    0.0000   YYYZ=    0.0000   ZZZX=    0.0000
  ZZZY=    0.0000   XXYY=   -2.0638   XXZZ=   -1.9601   YYZZ=   -1.7032
  XXYZ=    0.0000   YYXZ=    0.0000   ZZXY=    0.0000

```

```

%
% om_rotconst.m (R S Rao) 23/10/05 ; 27/6/11
%
function om_rotconst(fileName)
if nargin == 0
    fileName = 'PAh-6-31G.out';
    disp('***** USAGE : om_rotconst(fileName)')
end

property = ' Rotational Constants';
match1 = ' -- Stationary point found';
match2 = ' Rotational constants';
over1 = '*****';

scrch_props (fileName,property,match1,match2,over1);

```

```

h20-UMP3.out           Rotational Constants      g03_output_g03_output_g03
-- Stationary point found.
Rotational constants (GHZ):      612.4379412      428.9988208      252.2814290

```

```

%
% scrch_props.m 27/6/11
%
function scrch_props (fileName,property,match1,match2,over1)
if nargin == 0
    fileName = 'PAh-6-31G.out';
    property = 'Dipole moment';
    match1 = ' -- Stationary point found';
    match2 = 'Dipole moment'; over1 = 'Quadrupole';
    disp('***** USAGE : scrch_props (fileName,property,match1,match2,over1)')
end
disp(' '), disp(' '); b51 = blanks(51);
H1 = ' g03_output_g03_output_g03_output_g03_output_';
disp([fileName, ' ', property, H1])
begin = 0; start = 0;

fid = fopen(fileName, 'r');
start2 = 0;

while 1
    tline = fgetl(fid);
    begin = strmatch(match1, tline);
    % if st, start=1; end
    % begin = strmatch(begin2, tline);
    if begin == 1, disp([b51, tline]), start = 1; end
    over = strmatch(over1, tline); ; if over == 1, start = 0; start2 = 0; end

    if start == 1
        begin2 = strmatch(match2, tline);
        if begin2 == 1, start2 = 1; end
        if start == 1 & start2 == 1
            disp(tline)
        end
    end
end

```

```
cputime= ' Job cpu time';  
cpu=strmatch(cputime,tline);  
if cpu  
    % disp(tline)  
end  
  
    if ~ischar(tline), break, end  
end  
fclose(fid)
```

Appendix-08: Exchange and correlation

Interaction between electrons

The electrons interact with each other by the exchange of photons and experience a static external potential (Eqn. A8-1).

Eqn. A8-1: Calculation of External potential

External potential = $V_i(x) =$
 Coulomb field of the nuclei +
 External electromagnetic (or)
 nuclear magnetic moments
 $Lagr(Fer) = Lagr_{Fer} + Lagr_{ph} + Lagr_{int} + Lagr_{ext}$

$Lagr(Fer)$: Lagrangian of noninteracting fermions	$Lagr(int)$: interaction between fermions & photons
$Lagr(Ph)$: Lagrangian of non-interacting photons	$Lagr(ext)$: interaction between fermions & static external potential V^3

Energy_(electron-electron interaction) :

$\begin{matrix} \text{e} \\ \text{e} \\ \text{e} \\ \text{e} \end{matrix}$
exchange energy (EX), $\begin{matrix} \text{u} \\ \text{u} \\ \text{u} \\ \text{u} \end{matrix}$
 $\begin{matrix} \text{e} \\ \text{e} \\ \text{e} \\ \text{e} \end{matrix}$
static_near-degeneracy (left-right), $\begin{matrix} \text{u} \\ \text{u} \\ \text{u} \\ \text{u} \end{matrix}$
 $\begin{matrix} \text{e} \\ \text{e} \\ \text{e} \\ \text{e} \end{matrix}$
dynamic electron correlations (Dyn_Ele_Corr) $\begin{matrix} \text{u} \\ \text{u} \\ \text{u} \\ \text{u} \end{matrix}$

The exact representation of exchange and correlation effects for molecules in quantum chemistry remains to be a challenging task. The pioneering proposals in ab initio and DFT approaches are attempts to be nearer to the realistic picture of at least (gaseous) atoms of increasing number of electrons. From computational point of view, the consequent neglect of electron correlation in HF is the sole cause of inaccurate wave functions and obviously the descriptors calculated for real life multi-electron chemical elements/compounds. The solution of HF with infinite basis set (with no additional approximations) is called HF_limit and reflects electron correlation energy. Although, it is not pragmatic, extrapolation from definite large size BSs (cc-pVnZ and cc-pCVnZ) is employed. The probability of finding electrons (e1 and e2) close to each other drops to zero at distance r12. Here wave function is discontinuous. It results in e2 electron is farther away from e1 than predicted by HF.

$$E_{e2} \ll (E_{e2})_{HF} \rightarrow E_{e2} - (E_{e2})_{HF} < 0$$

The consequence is a coulomb hole and HF overestimates electron-electron repulsion

The correlation energy (Eqn. A8-2) is the difference between electronic energies obtained from exact solution of HF approximation of Schrodinger equation at SCF level versus exact solution of the non-relativistic energy equation. The different types are radial, angular, static and dynamic electronic correlations (chart A8-1). Static correlation refers to near degeneracy of a given state. Dynamic correlation corresponds to instantaneous avoidance of electrons with each other or dynamical character of electron-electron repulsion.

Eqn. A8-2: Correlation energy

$$E_{el-corr} = E_{true} - E_{HF-limit}$$

Remedy: Post_HF and DFT functionals correct for $E_{el-corr}$

Chart A8-1: Categories of electronic correlations

Dynamic correlation		Radial correlation	
Occurs in	✓ Closed Shell	Results in atoms with	✓ pair of electrons
	✓ No bonds		✓ Orbital closer to nucleus
	✓ No electrostatic interaction		
Example	Ne-Ne [1s ² 2s ² 2p ⁶]		

Angular correlation	
Occurs in	✓ Two electrons
HF prediction	✓ The electrons are nearer
Reality	✓ The electrons are far away as possible one side and the other side

Eqn. A8-3 shows the generation of HF, post-HF, BLYP from exchange correlation of electrons.

Eqn. A8-3: Evaluation with the Kohn-Sham orbitals with corresponding eigenvalues.

Condition	E_{xc} reduces to
If $ax=0, b=1, c=0$, Then pure B-LYP_GGA	$E_x^{GGA} + E_c^{GGA}$
If $ax=1, b=0, c=1$, Then MP2	$E_x^{HF} + E_c^{PTq}$
If $ax=0, b=0, c=0$, Then GGA	E_x^{GGA}
If $ax=1, b=0, c=0$, Then HF	E_x^{HF}

DFT → HF

If DFT &
Exchange function is HF &
Correlation function is omitted &
Then KS energy reduces to HF theory

Exchange repulsion

It is a quantum mechanical effect with no classical analog. It has to satisfy the constraint that wave function should be multi-symmetric. For example, if multiplicity >1, number of α electrons is not equal to β -electrons. Some of spins are paired. Hence, α electrons repel more than β -electrons. It throws light on

- ☞ Energy difference between electronic state of different spin symmetries (Ex: singlet-triplet)
- ☞ Nature of covalent bond
- ☞ The energy of two hydrogen atoms separated by infinity minus the energy of stable hydrogen molecule at its equilibrium bond length is referred as binding energy. In H₂ all binding energy is due to exchange only.

Functionals for exchange and correlation of electrons

Ab initio or DFT (B3LYP) procedures do not take into account of Non-covalent interaction energies, which are smaller compared to those of ionic/covalent bonds. But, they play a non-negligible role in the study of macromolecules/small-molecules in a medium [solvent, ions, micelles, proteins ... etc.] /interaction of macromolecules with small/another macromolecule, London dispersion and stacking interactions. The functional, X3LYP also completely failed for nucleobases and aromatic amino acids with stacking interactions. Zhao and Truhlar proposed new functionals MPW1B95, MPWB1K, PW6B95 and PWB6K in calculating energetics of thermal processes and thermo-kinetics. Later, these functionals are shown to be efficient in calculating stacking interactions, PWB6K being the best for DNA and large protein systems. Table A8-1 describes typical functionals in vogue.

Table A8-1: DFT Functionals			
Method	Reference	Method	Reference
LSDA		hybrid-GGA	
SVWN5	Slater(1974) Vosko (1980)	B1LYP	Adamo(1997) Becke(1988) Lee(1988)
SPL	Perdew(1992) Slater(1974)	B3LYP	Becke(1988) Lee(1988) Stephens(1994) Hertwig(1997)
c-SVWN5(0.3)	Slater(1974) Vosko (1980)	PBE1PBE	Perdew(1996)
GGA		B3P86	Perdew(1986) Becke(1988)
BLYP	Becke(1988) Lee(1988)	B3PW91	Perdew(1992) Becke(1988)
BPW91	Becke (1988) Perdew(1992)	B98	Schmider(1998)
PBELYP	Lee(1988) Perdew(1996)	meta-GGA	
PBEP86	Perdew(1986, 1996)	VSXC	Voorhis (1998)
PBEPW91	Perdew(1992,1996)	BB95	Becke(1988,1996)
PBEPBE	Perdew(1996)	MPWB95	Becke(1996) Adamo(1998)
PW91LYP	Lee(1988) Perdew(1992)	TPSS	Staroverov (2003) Tao (2003)
PW91P86	Perdew(1986,1992)	MPWK CIS	Becke(1996) Rey(1998) Krieger(1999) Toulouse (2002)
PW91PW91	Perdew(1992)	PBEK CIS	Perdew(1996) Rey(1998) Krieger(1999) Toulouse (2002)
MPWLYP	Perdew(1986) Adamo(1998) Lee(1988)	TPSSK CIS	Staroverov (2003) Tao (2003) Rey(1998) Krieger(1999) Toulouse (2002)
MPWP86	Perdew(1986) Adamo(1998)	Hybrid-meta-GGA	
MPWPW91	Perdew(1992) Adamo(1998)	BB1K	Becke(1988,1996) Zhao(2004)

MPWPBE	Perdew(1996) Adamo(1998)	B1B95	Becke(1988,1996)
G96LYP	Lee(1988) Gill(1996)	TPSS1KCIS	Staroverov (2003) Tao (2003) Rey(1998) Krieger(1999) Toulouse (2002) Zhao (2005)
G96P86	Gill(1996) Perdew(1986)	PBE1KCIS	Perdew(1996) Rey(1998) Krieger(1999) Toulouse (2002)
HCTH	Hamprecht (1998)	MPW1KCIS	Adamo(1997) Becke(1996) Rey(1998) Krieger(1999) Toulouse (2002)

Output of om_ref_JAVATYP.m
Ref_DFT functionals

Adamo, C.; Barone, V. *J. Chem. Phys. Lett.* **1997**, 274, 242-250.
 Adamo, C.; Barone, V. *J. Chem. Phys.* **1998**, 108, 664- 675.
 Becke, A. D. *J. Chem. Phys.* **1993**, 98, 5648-5652.
 Becke, A. D. *J. Chem. Phys.* **1996**, 104, 1040-1046.
 Becke, A. D. *Phys. Rev. A* **1988**, 38, 3098-3100.
 Gill, P. M. W. *Mol. Phys.* **1996**, 89, 433-445.
 Hamprecht, F. A.; Cohen, A. J.; Tozer, D. J.; Handy, N. C. *J. Chem. Phys.* **1998**, 109, 6264-6271.
 Hertwig, R. H.; Koch, W. *Chem. Phys. Lett.* **1997**, 268, 345-351.
 Krieger, J. B.; Chen, J.; Iafrate, G. J.; Savin, A. In *Electron Correlations and Materials Properties*; Gonis, A., Kioussis, N., Eds.; Plenum: New York, 1999; pp 463.
 Lee, C.; Yang, W.; Parr, R. G. *Phys. Rev. B* **1988**, 37, 785-789.
 Møller, C.; Plesset, M. S. *Phys. Rev.* **1934**, 46, 618.
 Perdew, J. P. *Phys. Rev. B* **1986**, 33, 8822-8824.
 Perdew, J. P.; Burke, K.; Ernzerhof, M. *Phys. Rev. Lett.* **1996**, 77, 3865-3868.
 Perdew, J. P.; Chevary, J. A.; Vosko, S. H.; Jackson, K. A.; Pederson, M. R.; Singh, D. J.; Fiolhais, C. *Phys. Rev. B* **1992**, 46, 6671-6687.
 Perdew, J. P.; Wang, Y. *Phys. Rev. B* **1992**, 45, 13244-13249.
 Rey, J.; Savin, A. *Int. J. Quantum Chem.* **1998**, 69, 581-590.
 Roothan. *Rev. Mod. Phys.* **1951**, 23, 69.
 Schmider, H. L.; Becke, A. D. *J. Chem. Phys.* **1998**, 108, 9624-9631
 Slater, J. C. *Quantum Theory of Molecular and Solids*; McGraw-Hill: New York, 1974; Vol. 4.
 Staroverov, V. N.; Scuseria, G. E.; Tao, J.; Perdew, J. P. *J. Chem. Phys.* **2003**, 119, 12129-12137.
 Stephens, P. J.; Devlin, F. J.; Chabalowski, C. F.; Frisch, M. J. *J. Phys. Chem.* **1994**, 98, 11623-11627.
 Tao, J.; Perdew, J. P.; Staroverov, V. N.; Scuseria, G. E. *Phys. Rev. Lett.* **2003**, 91, 146401
 Toulouse, J.; Savin, A.; Adamo, C. *J. Chem. Phys.* **2002**, 117, 10465-10473.
 Voorhis, T. V.; Scuseria, G. E. *J. Chem. Phys.* **1998**, 109, 400-410.
 Vosko, S. H.; Wilk, L.; Nusair, M. *Can. J. Phys.* **1980**, 58, 1200-1211.
 Zhao, Y.; Lynch, B. J.; Truhlar, D. G. *J. Phys. Chem. A* **2004**, 108, 2715-2719.
 Zhao, Y.; Lynch, B. J.; Truhlar, D. G. *Phys. Chem. Chem. Phys.* **2005**, 7, 43-52.

Kevin E. Riley,[†] Bryan T. Op't Holt,[†] and
 Kenneth M. Merz, Jr,

J. Chem. Theory Comput. **2007**, 3, 407-433

► [DFT Methods and Two Wave- Function Methods Used in This Work, with Appropriate References](#)